

CONSORTIUM MATERIALS TECHNOLOGY for demonstration and development of thermal energy processes

Fuel additives to reduce corrosion at elevated steam data in biomass boilers

Annika Stålenheim, Maria Jonsson, Michal Glazer, Elin Edvardsson, Anders Hjörnhede, Fredrik Niklasson, Patrik Yrjas, Daniel Lindberg, Johanna Nockert Olovsjö, Fernando Rave, Fredrik Olsson, Christer Forsberg, Sonja Enestam, Paul Cho, Mats Åbjörnsson, Anna Jonasson, Susan Weatherstone, Colin Davis

KME-512

Fuel additives to reduce corrosion at elevated steam data in biomass boilers

Bränsleadditiv för att minska korrosionen vid förhöjda ångdata i biomassaeldade pannor

Annika Stålenheim, Maria Jonsson, Michal Glazer, Elin Edvardsson, Anders Hjörnhede, Fredrik Niklasson, Patrik Yrjas, Daniel Lindberg, Johanna Nockert Olovsjö, Fernando Rave, Fredrik Olsson, Christer Forsberg, Sonja Enestam, Mats Åbjörnsson, Anna Jonasson, Susan Weatherstone, Colin Davis

Preface

The project has been performed within the framework the fifth stage of the material technology research programme KME.

KME, Consortium Materials technology for demonstration and development of thermal Energy processes, was established 1997 on the initiative of the Swedish Energy Agency. In the consortium, the Swedish Energy Agency, seven industrial companies and 18 energy companies participate. The programme stage has been financed with 60.2 % by participating industrial companies and with 39.8 % by Swedish Energy Agency. The consortium is managed by Elforsk.

The programme shall contribute to increasing knowledge to forward the development of thermal energy processes for various energy applications through improved expertise, refined methods and new tools. The programme shall through material technology and process technology developments contribute to making electricity production using thermal processes with renewable fuel more effective. This is achieved by

- Forward the industrial development of thermal processes by strengthening collaboration between industry, academy and institutes.
- Build new knowledge and strengthen existing knowledge base at academy and institutes
- Coordinate ongoing activities within academy, institutes and industry

KME's activities are characterised by long term industry relevant research and constitutes an important part of the effort to promote the development of new energy technology with the aim to create an economic, environmentally friendly and sustainable energy system.

Abstract

Five additives were selected and tested in a fluidised bed combustion test rig. As a result of these tests, two additives, digested sewage sludge and kaolin, were found to have a positive effect on waterwall corrosion as well as on superheater corrosion when burning waste wood.

Sammanfattning

Breda bränsleblandningar är av intresse för många energibolag, beroende på ökande priser och minskande tillgänglighet för rena biobränslen. Breda bränsleblandningar, t.ex. returträ (även kallat RT-flis), innehåller dock ämnen som orsakar korrosion i eldstaden och på överhettarna. Väggkorrosion i synnerhet orsakar problem i anläggningar idag med ångdata vid konventionella/kommersiella nivåer. För att möjliggöra ökade ångdata i en demonstrationsanläggning, vilket är målet för KME-programmet 2010-2013, behöver man kunna visa att korrosionen kan begränsas till nivåer som tillåter kostnadseffektiv drift av anläggningen.

Det finns lite information tillgänglig om användning av additiv eller bränsleblandningar för att minska eldstadskorrosion. Nyligen genomförda Värmeforsk-studier rörande eldstadskorrosion har huvudsakligen utvärderat olika material. Andra KME-projekt, till exempel KME 508, berör området additiv, men det är inte deras huvudfokus. Det finns alltså ett behov av att fokusera mer på användandet av additiv inom KME. Det skulle också vara av värde att identifiera additiv som kan minska både eldstadskorrosion och överhettarkorrosion.

Projektets mål har uppfyllts genom följande:

Projektet har identifierat fyra typer av additiv som skulle kunna förhindra eldstadskorrosion. Fem additiv, som representerar dessa typer, har valts ut och testats i en reaktor med fluidiserad bädd. Dessa tester visade att två additiv, rötat avloppsslam och kaolin, hade positiv effekt på eldstadskorrosion och överhettarkorrosion vid förbränning av returträ.

Användning av avloppsslam förväntas minska överhettarkorrosion. Det minskar också risken för bäddsintring och minskar mängden avlagringar på överhettare och economiser. Den höga askhalten hos avloppsslam resulterar i en ökning av askmängden. Användande av avloppsslam kan öka behovet av svavelreduktion i rökgasreningen för att undvika att överskrida gränserna för SO₂-utsläpp. Användande av kaolin förväntas minska överhettarkorrosion. Det kan också minska risken för bäddsintring och minska mängden avlagringar på överhettare och economiser.

Projektet rekommenderar att det företas vidare undersökningar av avloppsslam och kaolin som additiv för att minska eldstadskorrosion.

Termodynamiska jämviktsberäkningar har visat sig vara ett användbart redskap för att förutspå effekterna av additiv och variationer i driftparametrar i en panna. Detta verktyg måste dock användas med försiktighet och expertkunskaper krävs för att tolka resultaten.

Nyckelord: eldstadskorrosion, överhettarkorrosion, bränsleadditiv

Summary

Wide fuel mixes are of interest for many energy companies due to increasing prices and reduced availability of clean biomass. However, wide fuel mixes, including for example waste wood (demolition wood, recycled wood) contain components causing corrosion in the furnace and convective superheaters. Especially wall corrosion is a problem in plants that operate today at conventional / commercial steam data levels. Therefore, to be able to increase the steam data level in a demonstration plant, which is one goal for the KME programme in the period 2010-2013, it must be shown that the corrosion can be limited to levels that allow cost-effective operation.

There is little information available on the use of additives or fuel blends to reduce furnace wall corrosion. Recent Värmeforsk studies on wall corrosion have mainly evaluated different materials. Other KME projects (for example, KME-508) touch on the area of additives, but fuel additives are not their main focus. Thus, there is a need to focus more strongly on the use of additives within KME. Also, it would be useful to identify additives that reduce furnace wall and superheater corrosion.

The project goals have been fulfilled by the following achievements:

The project has identified four different types of additives that might reduce furnace corrosion. Five additives, representing these types were then selected and tested in a fluidised bed combustion test rig. As a result of these tests, two additives, digested sewage sludge and kaolin, were found to have a positive effect on waterwall corrosion as well as on superheater corrosion when burning waste wood.

Two additives have been found to be promising for reducing waterwall corrosion, sewage sludge and kaolin. These additives are also expected to reduce superheater corrosion, reduce the risk for bed sintering and reduce the amount of deposits on superheaters and economiser. The high ash content of sewage sludge will result in an increase in the amount of ashes. Addition of sewage sludge may increase the need for sulphur reduction in the flue gas cleaning to avoid exceeding SO_2 emission limits. The use of kaolin is expected to reduce superheater corrosion. It may also reduce the risk for bed sintering and reduce the amount of deposits on superheaters and economiser.

The project recommends that sewage sludge and kaolin (or some other aluminium silicate) should be further investigated for reduction of waterwall corrosion.

Thermodynamic equilibration calculations have been found to be a useful tool for predicting the effects of additives and variations in operation parameters in a boiler. However, this is a tool that must be used with some care and expert knowledge is needed for the interpretation.

Key words: furnace wall corrosion, superheater corrosion, additives to fuel

Table of contents

1	Intr	oductio		1
	1.1	Backgro	ound	
	1.2	Descrip	otion of the research area	2
	1.3	The res	search task and its role within the research area	3
	1.4	Goals		4
	1.5		execution	
		1.5.1	Project organisation	
		1.5.2	Project tasks	
		1.5.3	Project budget	
2	Inve	entory o	of possible additives	10
	2.1	Backgro	ound	10
	2.2	Waterw	vall corrosion	11
	2.3	Additiv	es	
		2.3.1	Additive requirements	
	2.4	Corrosi	on inhibiting mechanisms of additives	
		2.4.1	Sulphur containing additives	
		2.4.2	Silicon containing additives	
		2.4.3	Other additives	
		2.4.3	Previous experiences of additives	
	2.5		ate additivesate	
	2.5	2.5.1	Sulphur	
			Sewage sludge	
		2.5.2		
		2.5.3	Kaolin	
		2.5.4	Foundry sand	
		2.5.5	Lime	
		2.5.6	Marl / marlstone	
		2.5.7	ICA 5000	
		2.5.8	Waste brick from steel production	
		2.5.9	De-inking sludge	
		2.5.10	Peat fly ash	
		2.5.11	Tunnel furnace slag	24
		2.5.12	Hard coal fly ash	24
		2.5.13	Gypsum	25
	2.6	Conclus	sions	25
3	Ana	lysis of	composition of fuels and additives	27
	3.1		cal fractionation	
	3.2		s of fuel analyses and fractionation	
	3.3		sion - Implications of the analysis results	
	0.0	3.3.1	Sewage sludge	36
		3.3.2	Kaolin	
		3.3.3	Foundry sand	
		3.3.4	Sulphur	
		3.3.4	Limestone	
			Final remarks	
		3.3.6	FILIAL LEHIALKS	

4	Ther	rmodyn	amic equilibrium calculations	39
	4.1		tions performed by Åbo Akademi using FactSage	39
		4.1.1	Method	
		4.1.2	Results	41
		4.1.3	Summary	56
	4.2	Calcula	tions performed by Vattenfall using HSC Chemistry	
		4.2.1	Method	
		4.2.2	Results	
		4.2.3	Summary	
	4.3	Discuss	sion	
		4.3.1	Comparing thermodynamic equilibrium calculations with	4.0
		122	experimental findings	
		4.3.2 4.3.3	Chemical equilibrium calculations – applicability and limitation Comparing the two calculation programmes	
	4.4		sions	
	4.4	Conciu	510115	19
5		oratory		81
	5.1		an	
	5.2		ls	
		5.2.1	Laboratory reactor	
		5.2.2	Fuels and additives	
		5.2.3	Test materials used in the laboratory tests	
		5.2.4	Test procedure	
		5.2.5	Measurement methods	
	5.3		S	
		5.3.1	Gas concentrations and temperatures	
		5.3.2	Fly ash	
		5.3.3	Bottom ash and wall deposits	
		5.3.4	Deposits	
		5.3.5	XRD analyses	
		5.3.6	Distribution of selected elements in ashes, deposits and gas	
		5.3.7	Corrosion analysis	
		5.3.8 5.3.9	BW comparison of additives (first set of tests)	119
			addition (second set of tests)	122
		5.3.10	Comparison between PbO spiked fuel with and without sewag sludge addition at the BW position (second set of tests)	
		5.3.11	• • • • • • • • • • • • • • • • • • • •	
			Comparison between reference case and sewage sludge addition in the SH position (second set of tests)	
		5.3.13	Comparison between PbO spiked fuel with and without sewag	e
		E 2 1 1	sludge addition at SH position (second set of tests)	
		5.3.14 5.3.15	Summary of corrosion analysis	
		_		4
6	-		d cost estimates of additives	153
	6.1		r	
	6.2		e sludge	
	6.3	Kaoiin.		156

7	Ana	lysis of the results	157	
	7.1		157	
	7.2	Kaolin		
	7.3	Lime	159	
	7.4	Sulphur	160	
	7.5	Sewage sludge	161	
8	Con	clusions	163	
9	Goa	165		
10	Prop	166		
11	1 References			

1 Introduction

1.1 Background

The vision for the KME programme period 2010-2013 is to improve the electrical and total efficiency by material technology development when utilising climate neutral fuels in thermal energy conversion processes. The long-term vision includes research for erection of a new full-scale demonstration CHP plant in 2017-2018, fired with renewable bio fuels and refuse fractions, with at least 3-4 % points higher electrical efficiency than commercial plants built today.

Wide fuel mixes are of interest for many energy companies due to increasing prices and reduced availability of clean biomass. However, wide fuel mixes, including for example waste wood (or demolition wood, recycled wood), contain components, for example chlorine, alkali, lead, and zinc, causing corrosion in the furnace and convective superheaters. Especially wall corrosion is a problem in plants that operate today at conventional / commercial steam data levels.

For the period 2010-2013, one goal for the KME programme is to report a technically and commercially viable process solution for a model plant concept that will provide the basis for a demonstration plant to be commissioned in 2017/2018. To be able to increase the steam data level in a demonstration plant using wide fuel mixes including waste wood, it must be shown that the furnace wall corrosion can be limited to levels that allow cost-effective operation of the plant. Different ways to solve the problem of furnace wall corrosion are, for example, more expensive materials, frequent change of heat transfer surfaces, wall cladding or additives or fuel blends to reduce the amount and/or corrosivity of deposits and slag on the furnace walls.

There is little or no information available on the use of additives or fuel blends to reduce furnace wall corrosion. Värmeforsk studies on wall corrosion [2], [4] have mainly evaluated different materials for the furnace wall.

The project KME-508 [1] will give recommendations about how to avoid furnace wall corrosion at increased steam data levels when burning biomass and waste wood mixes. The project includes an initial investigation (including tests in the Idbäcken plant) of additives that can reduce the furnace wall corrosion. However, the scope of KME-508 is wide (including materials, coatings, boiler design, operation, cleaning procedures, mechanisms for wall corrosion, chemical equilibrium calculations, test programme in the Idbäcken plant) so the work on additives will be limited. The HTC project 1a [5] also investigates furnace wall corrosion, but additives to reduce wall corrosion are not the main focus of that study.

1.2 Description of the research area

To reduce the corrosion rate, plants using wide fuel mixes usually have rather low steam data, for example, Vattenfall's Jordbro plant 470°C/80 bar (in operation 2010) and Söderenergi's Igelsta plant 540°C/90 bar (2009). There are examples of plants operating at higher steam data, for example Vattenfall's Idbäcken plant, where the fuel is mainly waste wood, at 540°C/140 bar. Here, the wall corrosion rates have been high and different measures have been tested to reduce the corrosion rate. Currently, Inconel 625 weld overlay of the furnace walls (installed in 2010) is evaluated. Idbäcken also uses the ChlorOut additive to achieve sulphation of alkali chlorides in the flue gas in order to reduce superheater corrosion. Flue gas additives such as ChlorOut are sprayed into the flue gas after combustion and therefore do not solve the problem of increased furnace corrosion rates during combustion of cheaper fuels.

The project KME-508 [1] will give recommendations about how to avoid furnace wall corrosion at increased steam data levels when burning biomass and waste wood mixes. The project includes an initial investigation (including tests in the Idbäcken plant) of additives that can reduce the wall corrosion. However, since the scope of KME-508 is wide (including materials, coatings, boiler design, operation, cleaning procedures, mechanisms for wall corrosion, chemical equilibrium calculations, test programme in the Idbäcken plant), there is a need to investigate the possibilities for using additives to reduce furnace wall corrosion in a separate project. The HTC project 1a [5] also investigates furnace wall corrosion. However, additives to reduce furnace wall corrosion are not the main focus of this study.

Fuel additives differ from flue gas additives in that they are fed into the boiler together with the fuel or, in the case of fluidised beds, possibly also with the bed material. They are co-fuels or materials containing elements or compounds that are beneficial to the ash chemistry in the furnace and the convective section of a boiler. One or more of the following effects could achieve this:

- Chemical reaction binding critical inorganics into the bottom ash or bed material in a form that does not melt at typical furnace temperatures
- Creation of particles with a porous structure, to which problematic inorganics such as alkali or heavy metal compounds can adsorb
- Addition of particles to the flue gas for abrasive blasting of the heat transfer surfaces, which keep deposits from growing
- Acting as an inert diluting agent in the fly ash or fluidised bed material

The effect of additives on deposits and corrosion on heat transfer surfaces and bed agglomeration in fluidised bed boilers was thoroughly studied within a recently finished Värmeforsk framework programme [8] and in the previous KME programme period [9]. In these projects, the impacts of different additives on the corrosiveness of superheater deposits were demonstrated in laboratory scale in the Chalmers 12 MW research boiler (bark and refusederived fuel, RDF, pellets) and in full-scale operation at the Händelö plant (household and industrial waste). Additives tested were ammonium sulphate, elemental sulphur, de-inking sludge and digested sewage sludge. The most

promising additive for reducing bed agglomeration, fouling and corrosion was found to be digested sewage sludge.

As in most studies on additives, the main objective in the above-mentioned tests was to reduce the superheater tube corrosion, and the average metal temperatures used were too high (450-550°C in [9] and 600-700°C in [8]) for the zinc and lead compounds to condense in any large amounts. However, these compounds (for example in metal chloride form) might very well cause corrosion at the lower metal temperatures of furnace walls. It would be of great interest to see if additives could be found that reduce both furnace and superheater corrosion at the same time, or to find a combination of additives that could minimise both problems.

1.3 The research task and its role within the research area

The aim of this project has been to evaluate, based on laboratory-scale combustion tests, the effectiveness of bed/fuel additives as a means to reduce furnace wall corrosion during combustion of wide fuel mixes/waste wood in CHP plants. The results add to the basis of information needed to compare different alternative measures to reduce furnace wall corrosion on a cost/benefit basis.

There is little or no information available on the use of additives or fuel blends to reduce wall corrosion, as described in the project proposal for KME-508 [1] and a Värmeforsk report [7]. Värmeforsk studies on wall corrosion [2] [4] have mainly evaluated different materials for the furnace wall. Other KME projects (like KME-508) touch on the area of additives, but fuel additives are not their main focus. Therefore, there is a need to focus more strongly on the use of additives within KME. Also, it would be useful to identify additives that reduce furnace wall corrosion and superheater corrosion.

Although the mechanisms of furnace wall deposits/slagging and corrosion are not yet clear, the fuel composition has a strong connection to the corrosion rate. The occurrence of zinc and lead, particularly in the presence of chlorides, is of interest when waste wood is part of the fuel mix. Work on theoretical corrosion mechanisms is done within KME-508 and especially in HTC project 1a. KME-508 presented their final results on wall corrosion mechanisms and methods to measure the wall corrosion in the beginning of 2014. To be able to perform project KME-512 before that, a working hypothesis was used, which meant looking for additives that minimise the deposits on the furnace walls and/or change the chemical composition of the deposits.

The focus of the present project has been practical/empirical, with focus on laboratory-scale combustion tests and analysis of results of these tests. Investigation of additive effectiveness must sooner or later include experimental tests. An iterative approach, where theoretical investigations and practical tests have been performed in parallel, has helped progress in the quest for solutions of the furnace corrosion problem. Close cooperation with projects KME-508 and HTC 1a has enabled interpretation of the results using the best available knowledge.

Full-scale tests with candidate additive materials in a boiler are not included in the project. One full-scale test with digested sewage sludge) was performed in the season 2012/2013 within the project KME-508.

1.4 Goals

The project will identify and then evaluate the use of additives and fuel blends to reduce furnace wall, and possibly also superheater, corrosion for wide biomass fuel mixes including waste wood. The expected effect of the additives on the rest of the boiler (uncooled components in the furnace, heat exchangers in the flue gas pass, flue gas cleaning equipment, emissions) will also be investigated.

The project will give a recommendation if the identified additives are a viable way to reduce furnace wall (and superheater) corrosion and, in that case, recommend some promising additive candidates for further evaluation. The most promising candidate/s/ from the evaluation will be proposed for pilot-scale or full-scale tests in a fluidised bed boiler in the next phase of the KME programme.

The project will evaluate the use of thermodynamic equilibrium calculations for predicting the chemical composition of the deposits formed at different temperatures, with different additives and under different combustion conditions.

1.5 Project execution

1.5.1 Project organisation

Table 1 gives an overview of the project performers.

Table 1. Project performers

Tabell 1. Projektutförare

Partner	Representatives	Tasks		Task					
			1	2	3	4	5	6	7
Vattenfall R&D	Maria Jonsson, Annika Stålenheim, Elin Edvardsson, Michal Glazer, Nader Padban, Linda Nylén (until Dec. 2012)	 Project management Test planning and support Coord. of additive inventory and evaluation Thermodyn. equilibrium calcs. with HSC Chemistry Coord. of report 	X ¹		X			X	X ¹
Vattenfall Heat Nordic	Christer Forsberg	 Participation in project working group Test planning and support Provide fuel for analysis and lab-scale tests Fuel analysis (standard lab analysis) Participation in project working group 		Х					
Metso Power	Sonja Enestam, Paul Cho (from Feb. 2013)	- Technical expertise, support to inventory and evaluation of additives, calcs. and lab-scale tests - Participation in project working group		Proj	ect v	vorki	ng gi	oup	
E.ON Värme Sverige	Mats Åbjörnsson, Anna Jonasson	- Contribute with experiences, e.g., from Händelö P14 (KME-411) on sludge as additive to CFB boiler - Participation in project working group			ect v			·	
E.ON Climate & Renewable s	Susan Weather- stone, Colin Davis	- Participation in project working group		Proj	ect v	vorki	ng gı	oup	
Sandvik Heating Technolog Y	Johanna Nockert Olovsjö, Fernando Rave	- Provision of materials for lab-scale testing (rings) - Material competence and support - Participation in project working group				X			
Outokump u	Fredrik Olsson, Rachel Pettersson (at project start)	- Provision of materials for lab-scale testing (rings) - Material competence and support - Participation in project working group				X			
Åbo Akademi	Patrik Yrjas, Daniel Lindberg	- Advanced fuel and fuel+additive analyses - Thermodyn. equil. calcs. using the chemical composition of the fuel – incl. additive - to validate assumptions regarding impact of the additive on corrosion mechanisms - Participation in project working group		X					X ¹
SP	Anders Hjörnhede, Fredrik Niklasson ort from all project part	- Tests in lab-scale fluidised bed reactor to study ash melting and sintering processes as well as deposit tendencies - Analysis of deposit rate and deposit chemistry, as well as initial corrosion, using appropriate methods (e.g., XRF, SEM/EDS, XRD) - Participation in project working group			Х	Х	Х		X ¹

The project working group included all project partners and reviewed results from the different project tasks and contributed with knowledge on different aspects and experiences from additives (for example, operation, handling, costs).

The performers of the KME-512 project would like to acknowledge the valuable input and comments from the reference group. Participants in the reference group:

- Jesper Liske, Chalmers, Department of Chemical and Biological Engineering, HTC
- Erik Skog, Skog Konsult
- Pamela Henderson, Vattenfall
- · Guocai Chai, Sandvik Materials Technology
- Eva-Katrin Lindman, Fortum
- Kenneth Lundkvist, Fortum

This project has been coordinated with:

- KME-508 ("Furnace wall corrosion in biomass-fired boilers at higher steam temperatures and pressures") [1]
- HTC project 1a ("Critical corrosion phenomena for combustion of biomass and waste") [5]
- KME-601 ("More Effective Power Production from Renewable Fuels –
 Reference Power Plant (RPP) Project") [6]. The aim of KME-601
 (Reference Power Plants, RPP) is to create and update RPP concepts in
 cooperation and dialogue with the steering group and the KME
 stakeholders. The RPP model concept(s) aim to be realised in
 demonstration project(s). Both virgin biomass fuels and a wide fuel
 mix (including waste wood) are investigated.

1.5.2 Project tasks

The work performed within the project was divided in 6 tasks. Below is a description of the work planned in the different tasks.

Task 1 Inventory of possible additives

An inventory of additives (to fuel and/or bed) that could reduce wall corrosion will be made. The impact of the additives on the rest of the boiler (uncooled components in the furnace, heat exchangers in the flue gas pass, flue gas cleaning equipment, emissions) will also be estimated.

Suggested additives are solid materials (wet or dry), added to the bed material or fuel. A more or less well established bed/fuel additive is elemental sulphur in granular form (will for example be used in Metso's wide fuel mix RPP concept as a means to reduce superheater corrosion). Elemental sulphur will therefore be included in this study as a reference additive, and also in order to study its influence in the furnace. Examples of other possible additive candidates are for example pyrite (FeS₂), waste materials from industrial processes, clay minerals such as kaolin or bauxite, de-inking sludge and digested sewage sludge.

The impact of the additive should be described (for example, reduced furnace wall slagging, fouling, corrosion) and how the additive works (by, for example, chemical reaction with compounds of alkali, lead, zinc or tin, or other mechanisms such as adsorption, dilution or sand blasting of alkali, binding alkali). The use of the additives in different types of boilers should be

considered (CFB, BFB, grate, PF). The main focus should be on the fuel components that cause wall corrosion (and superheater corrosion as well) when the RPP wide fuel mix (or waste wood) is fired at the target steam data levels defined in KME-601. When performing the inventory, available knowledge on wall corrosion mechanisms from the literature studies in projects KME-508 and HTC 1a should be used as far as possible. Discussion of candidate additives with participants in these projects is also suggested. Experiences from reference plants should be used if available.

Task 2. Analysis of composition of fuels and additives

- Vattenfall Heat Nordic provides the fuel to the tests
- Vattenfall Heat Nordic sends fuel samples to standard laboratory testing (proximate and ultimate/elementary analysis, maybe ash melting temperature)
- Åbo Akademi makes advanced analyses (for example, chemical fractionation) of composition of fuel and additive/s/ to be used in laboratory tests.

Task 3. Thermodynamic equilibrium calculations

- Thermodynamic equilibrium calculations using the chemical composition of the fuel – including additive and blending material – to validate assumptions regarding the impact of the additive on the deposit chemistry at different conditions (for example, oxidising/reducing, different CI concentrations).
- Two different calculation tools will be evaluated and compared. Åbo Akademi will use FactSage. Vattenfall will use HSC Chemistry.

Task 4. Laboratory tests

- Laboratory tests to study ash melting and sintering processes as well as deposit tendencies. For laboratory screening of additives, a 10 kW BFB combustion test rig at SP is proposed (including the appropriate probes and other measurement equipment for this rig). The fuel mix will be in accordance with KME-508 (for example RPP wide fuel mix with 75 % waste wood and 25 % forest residues, or waste wood).
- Task 4a. Deposit/corrosion probe measurements to evaluate the impact of the additive on composition of deposits and corrosion rate. The focus should be on temperature regions where Zn, Pb and Sn compounds (particularly chlorides) may play important parts in the corrosion. Materials and probe temperatures chosen in accordance with KME-601 and KME-508.
 - Furnace probe measurements (~200–400 °C)
 - Convection path probe measurements to simulate the colder part of the convective superheater (300-500 °C).
- Task 4b. Impactor measurements for particle size and chemistry.
- Task 4c. Gas phase measurements.

Task 5 Analysis of results

- Analysis of results of laboratory tests using appropriate methods (for example, SEM, XRD)
 - o Deposit rate and deposit chemistry
 - o Signs of initial corrosion
 - o Particle chemistry of impactor size fractions

Task 6. Impacts and cost estimates

- Task 6a. Impact on the classification of the fuel mix. If the additive is classified as a waste fraction, it must be used in a co-incineration classified boiler.
- Task 6b. Impact on the flue gas path after the furnace (for example, some additives to the furnace may have a positive or negative impact on the (higher-temperature) superheater corrosion rate or on the functioning of the flue gas cleaning equipment).
- Task 6c. Qualitative cost estimate. Cost for the additive. Investment (changes in the boiler, components for feeding the additive). Changes in boiler operation. Impact on ash quality. Impact on emission levels (need for more chemicals for flue gas cleaning and/or investment in flue gas cleaning equipment).

1.5.3 Project budget

This project was funded by the KME Materials Technology Consortium (project KME-512), which is financed by energy and materials companies and by the Swedish Energy Authority. Table 2 shows the project budget. The budget for the work performed at Åbo Akademi was 453 kSEK. The budget for the work performed at SP was 1 178 kSEK (from the Swedish Energy Authority) plus 400 kSEK (in-kind).

The project started in December 2011 and was finalised in March 2014.

Table 2. Project budget
Tabell 2. Projektbudget

Company	Mat	Bas	EPP		
(kSEK)	In-	Cash	In-	Cash	
	kind		kind		
Vattenfall (via VRD)	250		485	350	
Vattenfall (via Nordic Heat)			100		
Metso Power			100		
E.ON Värme Sverige			75		
E.ON Climate & Renewables			75		
Sandvik Heating Technology	40				
Outokumpu	60				
SP Technical Research Institute			400		
Sum industrial	350	0	1 235	350	
Swedish Energy Agency contribution	232	0	818	232	
(39.84 %)					
Sum industrial + Swedish Energy	582	0	2 053	582	
Agency contr.					
Sum ind. + SEA for MAT BAS and EPP,	582		2 635		
respectively					
Total industrial in-kind / SEA	1 585 / 1 050				
contribution (39.84 %)					
Total industrial cash / SEA contribution	350 / 232				
(39.84 %)					
Total project budget	3 217				
Total amount available for academic		1 6	531		
research					

2 Inventory of possible additives

2.1 Background

The effect of additives on deposits and corrosion on heat transfer surfaces and bed agglomeration in fluidised bed boilers was thoroughly studied within a recently finished Värmeforsk framework programme (Värmeforsk report 1167 [12]) and in the previous KME programme period [26]. In these projects, the impacts of different additives on the corrosiveness of superheater deposits were demonstrated in lab scale in the Chalmers 12 MW research boiler (bark and RDF pellets) and in full scale operation at the Händelö plant (household waste and industrial waste). Additives tested were ammonium sulphate, elemental sulphur, de-inking sludge and digested sewage sludge. The most promising additive for reducing bed agglomeration, fouling and corrosion was found to be digested sewage sludge.

As in most studies on additives, the main objective in the above-mentioned tests was to reduce the superheater tube corrosion, and the average metal temperatures used were too high (450-550°C in [26] and 600-700°C in [12]) for zinc and lead compounds to condense in any large amounts. However, these compounds (e.g. in metal chloride form) might very well cause corrosion at the lower metal temperatures of furnace walls. It would be of great interest to see if additives could be found that reduce both furnace and superheater corrosion at the same time, or to find a combination of additives that could minimise both problems.

An inventory of additives (to fuel and/or bed) that could reduce wall corrosion has been performed. The main focus has been on fluidised bed combustion of waste wood (representing both cases with 100% waste wood & KME-601 wide fuel mix), at target steam data levels defined in KME-601 (for wide fuel mix). The following issues are addressed in this report:

- Impact of additive (reduced e.g. furnace wall slagging, fouling, corrosion)
- How the additive works (by e.g. chemical reaction with compounds of alkali, zinc, lead or other mechanisms such as adsorption, dilution or abrasive blasting of alkali, binding alkali)

Available knowledge on wall corrosion mechanisms from the literature studies in KME-508 & HTC 1a has been used as far as possible. Alkali chlorides, Pb and Zn have been suggested as the main components causing furnace corrosion. Candidate additives were discussed with participants in KME-508 & HTC 1a. Experiences from reference plants have been used when available.

2.2 Waterwall corrosion

In parallel with this project, KME 508, a project investigating the causes of waterwall corrosion has been performed. For a deeper discussion on waterwall corrosion readers are referred to the report from KME 508. [2]

Corrosion of heat exchange surfaces in the furnace (mainly waterwalls) has long been a problem, but in comparison to superheater corrosion, the research about waterwall corrosion has been scarce. Regarding the superheaters it is well established that alkali chlorides are one of the main contributors to the corrosion attack. At superheater temperatures, the alkali chlorides are within their melting temperature range. However, as the material temperature of the waterwalls in the furnace is comparably lower, the corrosivity of alkali chlorides is expected to be smaller, as they exist predominantly in solid form at these temperatures.

Field studies have shown that the combustion of waste wood and other waste fractions can result in locally high concentrations of heavy metals (Pb and Zn), alkali (Na and K) and chlorine in waterwall deposits. [14], [27], [32], [33]

It is thought that heavy metal and alkali salts cause corrosion due to their low melting point. The melting point becomes especially low in mixtures of chloride salts, where the melting point can be as low as 230°C (KCI – ZnCl₂), i.e. lower than the material temperature. The aggressiveness of the melt is explained by its ability to dissolve the protective oxide layer of the metal. However, it does not seem as the presence of a molten phase is a requirement for a corrosion attack. [27], [33]

Corrosion has also been observed in areas with deposits containing chlorine but no heavy metal salts, indicating that chlorides associated with other species than heavy metals can cause corrosion as well. In addition to the corrosive environment caused by the presence of alkali chlorides and heavy metal salts, a reducing environment and/or large variations in the partial pressure of oxygen, p(O2), further increases the corrosion rate of the water walls. [34]

Thermodynamic equilibrium calculations indicate that zinc and lead are vaporised mainly as Pb(g) and Zn(g) in the lower, reducing part of the furnace; hence a major deposition mechanism in this part of the boiler is expected to be the condensation of metallic Zn and Pb. Both metals can condense in solid or liquid form, depending on the amount of metals in the fuel and on the temperature of the condensation surface. A part of the lead present in the fuel will form PbS(g), which can condense in solid form on the lower furnace walls. In the upper, oxidising part of the furnace, most of the zinc is oxidised to ZnO(s), but a small fraction remains in the gas phase as Zn(g) or ZnCl(g). While ZnO(s) may deposit on tube surfaces or stick to partially molten deposit surfaces and Zn(g) can condense on the furnace walls in the hottest part of the furnace, ZnCl(g) remains mainly in the gas phase because of its low condensation temperature. Lead is fully vaporised as PbO(g) in the upper part of the furnace, but condensation of PbO(s) can occur on cooled surfaces. [27]

Within KME 508, samples have been taken from the furnace walls of Idbäcken P3 and Steven's Croft. Both are fluidised bed boilers burning waste wood and experiencing problems with furnace corrosion. Several measurement campaigns have been performed in Idbäcken using deposit and corrosion probes as well as characterising the environment in the boiler. Test panels with different coatings are also installed in Idbäcken and samples have been taken from them in 2009, 2010 and 2011.

Deposits taken from the furnace wall were characterised by fairly high levels of alkali and chlorine and low levels of Pb and Zn. The deposit samples were all taken from a level between the secondary and tertiary air inlets.

Samples were also cut out from test panels with different metallic coatings in the furnace walls. The elemental composition of the oxide and reaction products near the unreacted metal of these samples (the "corrosion front") was analysed. On samples coated with Ni-based alloys, high levels of Pb were found close to the metal. S and K as well as some Zn were also found, but nearly no Cl. On the 16Mo3 sample, mainly O and Fe were found, but also some Cl.

A measurement campaign was also performed at Idbäcken with waste wood in November 2011. Flue gas composition, temperature, impactor and deposit probe measurements were made at the furnace wall and 0.8-1 m from the wall. Very low O_2 levels were detected, sometimes below 0.5%, and the fluctuation over time was large. The temperatures were lower close to the wall than 1 m into the furnace. The CO levels were high. K, Cl, Pb and Zn were found in the deposits.

Since the KME 508 project was performed in parallel to this project, many of the results from that project was not available when writing this report. However, the results available so far seem to verify previous observations that chlorine has a key role in corrosion and that alkali metals (Na and K) and heavy metals (Pb and Zn) also take part in the process. However, no final conclusions have yet been drawn concerning corrosion mechanisms.

The results from KME 508 indicate that for low alloyed steels, which are mostly used for furnace walls, chlorine is the main component in the deposits causing corrosion. For higher alloyed materials (austenitics and nickel based alloys) alkali and lead also seems to take part in the process. It is not known for either process yet in what form the corrosive species are deposited on the furnace walls, but a guess would be in the form of alkali chlorides and elemental lead.

2.3 Additives

Additives are not commonly used specifically for reduction of waterwall corrosion. Usually, when additives are fed into the boiler together with the fuel or with the bed material in FB boilers, the target is to reduce fouling and/or the defluidisation risk.

Additives fed into the boiler together with the fuel or, in the case of fluidised beds, possibly also with the bed material, may be co-fuels or materials containing elements or compounds that are beneficial to the ash chemistry in the furnace and convective section of a boiler. One or more of the following effects could achieve this:

- Chemical reactions, binding alkali or other critical inorganics into the bottom ash or bed material in a form that does not melt at typical furnace temperatures or converting them to some inert species that will not cause corrosion.
- Particles with a large specific surface (porous structure), to which problematic inorganics such as alkali, Pb and Zn can adsorb
- Addition of particles to the flue gas for abrasive blasting of the waterwalls and superheater tubes, which keeps deposits from growing
- The additive acts as an inert diluting agent in the fly ash or fluidised bed material

The effectiveness of the additive thus depends on properties such as particle size distribution (generally, the smaller the additive particles, the larger the surface area for reaction), reaction temperature and time, composition (active compounds in the additive), and stoichiometry (i.e. sufficient amounts of additive). [21]

One important factor is how the addition of the additive is carried out. In one case, where kaolin was added to the fuel in a grate boiler, the additive showed little effect, probably due to a poor contact between the additive and the flue gas, since most of the additive stayed in the fixed bed on the grate. One important conclusion is that, for a grate boiler, the additive most likely should be added directly above the bed, e.g., jointly with the secondary air. However, the optimum position for adding the additive will probably be different for different additives and for different boilers. [19]

2.3.1 Additive requirements

Fuel/bed additives intended to reduce ash-related problems during combustion of biomass and waste should meet the following requirements:

- Not contain high levels of volatile forms of alkali metals, heavy metals, or halogens.
- A particle fraction between 1-100 μ m (90% of the mass), although the required size also depends on the brittleness of the material. If it is to be used in BFB or CFB, the material could also be chosen for its capacity to form new bed material ($\sim 0.05-2$ mm, depending on density).
- A high ash-melting temperature, at least corresponding to silica sand (1700°C)
- The product should be easy to feed into the furnace. If to be fed into a fluidised bed, dry enough to be fed by a screw feeder alternatively a material in paste form, which can be pumped by a piston pump.
- Not be classified as waste unless intended for use in a boiler classified for waste combustion
- Not be hazardous to human health
- Have a satisfactory reliability of supply

The maximum price depends on several factors, such as the required amount, and need for refinement and transport. As a reference, the Swedish prices for natural (quartz) sand and kaolin are about 400 SEK/t and 2 000 SEK/t, respectively.

Before addition of an additive or co-firing fuel, possible side effects also need to be considered. Such effects are, e.g.

- Increased ash flows
- Increased moisture in the flue gas, which might require flue gas condensation
- Altering of the by-product quality (fly ash, effluent water)
- Impact on different by-products
- Health and safety issues
- Environmental concerns
- Public acceptance (although peat and hard coal would be good co-firing fuels from an ash perspective, it may be difficult to find public acceptance for adding fossil or semi-fossil fuels to dedicated biomass boilers, or in boilers where fossil fuels have already been phased out.)
- Agglomeration/sintering tendencies of the bed

2.4 Corrosion inhibiting mechanisms of additives

Since the corrosion is thought to be caused by chlorine, alkali chlorides, heavy metals or a combination of these, the aim has been to find additives that can reduce these components in the deposits on the walls and/or the flue gases in the furnace, either by chemical reactions or adsorption.

2.4.1 Sulphur containing additives

Sulphur containing additives (e.g. sulphur or ammonium sulphate) are commonly used to reduce the flue gas content of alkali chlorides with the purpose to reduce superheater corrosion.

The mechanism is a reaction with alkali chlorides forming alkali sulphates and HCl (g). This reaction, however, requires oxidising conditions to occur and might not take place in the furnace region, but further on in the flue gas path. Also, decreasing the amount of alkali in the flue gases will increase the amount of available chlorine in the flue gases, which will increase the heavy metal volatilisation. This in turn can increase the corrosion. [13], [18]

2.4.2 Silicon containing additives

Si-containing additives work by reaction of alkali chlorides with Si and, if present, Al, forming potassium silicates (K_2SiO_3) and also potassium-alumino silicates (K_2SiO_4). Common alkali-capturing fuel/bed additives are clay-type minerals such as kaolin and other layered alumino silicates. The active components of kaolin, ICA 5000 and foundry sand are porous aluminium silicates (layered). The mechanism of these additives should be similar. However, foundry sand also contains a large amount of sand (quartz or feldspar).

Si can be found in many different forms. Crystalline forms, such as quartz, are probably less reactive than amorphous forms, which can be found in e.g. bentonite, hard coal fly ash and ICA 5000. [17]

During fluidised bed combustion, potassium and calcium from biomass ash can react with quartz (SiO_2) from the bed sand already at the normal operation temperatures of $700-900^{\circ}C$, forming a layer of Ca,K silicate onto the bed particle. The layer becomes thicker in time, and the particle size increases. The layer is sticky, and the bed particles can agglomerate together increasing the bed particle size further. During unsteady operation of the boiler, or on an occasional excursion to high temperature, the whole bed can sinter. The bed agglomeration can be controlled by keeping the bed alkali contents low enough by regularly discharging the bed ash and feeding fresh sand into the bed. The chemistry of interactions between fuel ash and bed sand is however complicated. It is usually useful to minimise the quartz content in the make-up sand. [20]

2.4.3 Other additives

Ca and P in the bed, either from the fuel or from an additive, can form CaKPO₄, thus capturing alkali and reducing the presence of alkali chlorides in the flue gases. However, a deficiency in Ca can lead to the formation of low melting alkali phosphates and a surplus of Ca can lead to capture of sulphur that would otherwise have formed alkali sulphates and in turn lead to an increase of alkali chlorides in the flue gases. [17], [29]

Al- and Ca-based materials can serve as metal sorbents in fluidised beds. Heavy metals can be captured by sorbents, such as lime (CaO, CaCO₃) and kaolin by physical deposition and chemical adsorption. [35], [36]

2.4.4 Previous experiences of additives

A number of different additives to the fuel/bed material have been permanently used or tested in different plants during combustion of biomass or waste. Plants and additives are listed in Table 3.

Table 3. Plants where fuel /bed additives are used or have been testedTabell 3. Anläggningar där bränsle- / bäddadditiv använts eller har testats

Plant, boiler	Fuel	Additive	Comment		
Amager 2	Straw pellets	Chalk, bentonite, calcium phosphate, sand	Tests		
Idbäcken P3	Waste wood	Ammonium sulphate, de-inking sludge	Permanent use and tests		
Jordbro P34	Wood, peat	Elemental sulphur	Permanent use		
Myllykoski K7	Peat, bark, paper mill sludge, forest residues, waste wood	Kaolin	Tests		
Helsingborg	Wood pellets	Elemental sulphur	Tests		
Händelö P14	Industrial and household waste	Elemental sulphur	Tests		
Högdalen P6	RDF (paper, wood and plastics)	Elemental sulphur	Tests		
Nässjö	Forest residues	Kaolin	Tests		
Chalmers 12 MW research CFB	Various	Kaolin, de-inking sludge, elemental sulphur, zeolites, alternative bed materials (olivine, blast furnace slag, PFBC coal ash)	Tests		
Enstedværket	Wood chips	S, ammonium sulphate, bentonite, ICA 5000, coal fly ash, CaHPO ₄	Tests		

2.5 Candidate additives

Table 4. Candidate additives

Tabell 4. Möjliga additiv

Candidate	Comment			
Elemental sulphur (granular)	Will be used as reference. Simple to compare, extensive experience from use for reduction of superheater corrosion. Reacts with alkali chlorides forming alkali sulphates and HCl at oxidising conditions.			
Digested sewage sludge	Empirically shown to work for reduction of deposits, bed agglomeration/sintering, and superheater corrosion when using high-alkali fuels. Requires special feeding equipment.			
Kaolin	Captures alkali irreversibly as K/NaAlSiO ₄ in FB. Reduction of deposits, bed agglomeration/sintering, and superheater corrosion. Expensive (~2 kSEK/t).			
Foundry (casting) sand ("gjuterisand")	Quartz or feldspar sand grains covered with bentonite clay. Variable composition, should be tailored for waste wood. Reports of increased agglomeration risk for olive kernels but decreased risk for Ca-rich fuels.			
Lime	CaCO ₃ . Used for desulphurisation, mainly during coal combustion. Calcium has a high affinity for phosphorus, but in the absence of phosphorus, calcium will bind sulphur, thereby preventing sulphation of alkali chlorides.			
Marl / marlstone ("märgel / märgelsten")	Limestone with a higher mineral content than normal. (See "Lime")			
ICA 5000	An artificial aluminium silicate, probably similar to kaolin. Sold as additive for reduction of chlorine corrosion in the combustion chamber of waste fired grate boilers.			
Waste brick from steel production	Possibly abrasive and/or diluting effect, needs crushing.			
De-inking sludge	Contains CaCO ₃ and/or kaolin. Possibly reduces wall slagging according to tests.			
Fly ash from FB combustion of peat	Could sulphate alkali, adsorb heavy metals and/or have an abrasive effect.			
Fly ash from FB combustion of hard coal	Is expected to bind alkali mainly in the form of alkali alumino silicates. Would imply a share of fossil fuel.			
Tunnel furnace slag	Slag from sponge iron ("järnsvamp") production. Reduced slagging for high-alkali fuels, but contains unburnt coal from coke. Would imply a share of fossil fuel.			
Gypsum	Consists mainly of CaSO ₄ . By-product from flue gas cleaning in combustion processes.			

2.5.1 Sulphur

Elemental sulphur is used as means to reduce problems with fouling and corrosion in the convective section. The addition of elementary sulphur to the fuel has been shown to reduce superheater corrosion by reducing the content of alkali chlorides in the flue gases and deposits. When elementary sulphur is added to the fuel, SO_2 is formed and released into the flue gases. SO_2 is in equilibrium with SO_3 , and SO_3 reacts with alkali chlorides to form alkali sulphates and HCI. This reaction, however, requires oxidising conditions to occur and might not take place in the furnace region, but further on in the flue gas path.

Sulphur in the fuel or in additives is regarded as beneficial during combustion of fuels rich in alkali and chlorine. With an S/Cl ratio >4 in the fuel mix, the superheater corrosion risk may be regarded as low, while a ratio <2 indicates a high corrosion risk.

During addition of elemental sulphur in fluidised beds, sulphur granules are usually added to the bed material or fuel, and then fed into the furnace. Elemental sulphur in granular form may also be added to pulverised fuel boilers through the burners. This has been successfully practiced in Jordbro P34, but with the purpose to reduce CO emissions.

2.5.2 Sewage sludge

Digested sewage sludge is a residue generated from municipal wastewater treatment. It is considered a promising additive due to its high content of P, Al and Fe. The sludge is generated in urban areas, i.e. usually close to thermal power plants.

Sewage sludge addition has been shown to reduce bed agglomeration, deposit formation, and superheater corrosion in fluidised bed boilers, through tests in the Chalmers 12MW research CFB and in the E.ON waste-fired FB boiler P14 at the Händelö plant in Norrköping, Sweden, [12], [26].

Results from testing sewage sludge as an additive in Händelö P14 showed that the addition of digested sewage sludge decreased the corrosion rate by about 80% at 550°C material temperature. At lower temperatures (450°C and 500°C), the corrosion rates were much lower and the effect of adding digested sewage sludge was not as obvious. [26]

The mechanism behind the positive effects is not yet fully clarified, but it is believed to be conversion of alkali chlorides to alkali sulphates and alkali phosphates. [12] It is also possible that the addition of sewage sludge could be beneficial through other mechanisms, such as heavy metal adsorption.

The variation in the composition of sewage sludge is mainly caused by which precipitation chemicals have been used. This seems to influence the effect on bed agglomeration. Sludge that has been precipitated with aluminium sulphate seems to have somewhat better effect than sludge precipitated with

iron sulphate. Except for this, the content of sulphur and phosphorus and the fuel content of calcium seem to be the most important factors. [12] In some treatment plants, especially in the UK, sewage sludge is precipitated with chlorides instead of sulphates. This makes it unsuitable for use as additive.

Digested sewage sludge varies significantly in physical properties. Treatment and handling equipment needs to be adapted to the specific characteristics of the sludge in question. In particular, adhesion and clogging has to be considered in the design of equipment.

One conclusion from the tests in Händelö is that the quality of the sludge is very important for avoiding problems when feeding it into the boiler. On occasions when the sludge was too dry, it was not possible to pump it and there were also problems with contamination of the sludge with large stones. Also, when the sludge was mixed with the fuel, it made the fuel slippery, causing the fuel to slide on the conveyor belt. Another conclusion is that since the main component of digested sewage sludge is water, the boiler has to be controlled in a somewhat different manner than when not adding it. [25], [26]

A limitation when using digested sewage sludge is its classification as a waste product. The boiler used would need to be classified and follow the WID directives. Also green electricity certificates may be lost. For beneficial and approved use of digested sewage sludge as additive in combustion, the recycling of P as a nutrient is a critical question that needs to be solved. The Swedish environmental protection agency requires that 60 weight-% of P are returned to arable land in 2015. Work is going on to develop cost effective methods to separate and recover P from ash.

The sewage sludge used in the laboratory tests within KME 512 is dried sludge from Himmerfjärden. It has the same origin as the sludge that is used in the KME 508 full scale tests at Idbäcken. However, that sludge is only mechanically dewatered, which means that the water content is estimated to be 70-75%, whereas the sludge used in the lab tests has a water content of $\sim 6\%$.

2.5.3 Kaolin

Kaolin is the name of a group of clay minerals, whose most common mineral is kaolinite $(Al_2Si_2O_5(OH)_4)$. It has a large specific surface, allowing it to adsorb troublesome species in the flue gases. It is highly efficient in capturing gaseous alkali species from hot flue gases at fluidised bed combustion temperatures. Kaolin is the simplest and best-known technical solution to reduce bed agglomeration during combustion of difficult biomass fuels today. Kaolin has been shown to reduce fouling by binding alkali during combustion of lignite, especially if the fuel has a low mineral content. [22]

In Sweden, kaolin is sold by ACM AB. This is kaolin from England, supplied by the French company Imerys.

Kaolin will react with free sodium at a temperature above 850°C. The reaction will take place at temperatures down to 800°C, but comparably slowly. For a

high conversion efficiency, the kaolin should be added as a powder with a large specific surface area and be available in the final combustion zone, where the major part of the alkali is released. In this zone the temperature is usually high enough and the mixing vigorous, which will increase the chances of contact between free alkali and kaolin particles. This means that the position for addition of the additive is important and that the method for adding the additive will be different for different types of boilers. [19]

Kaolin captures gaseous NaCl irreversibly and very effectively, forming sodium alumina silicates. Solid KCl is captured by kaolinite at high temperatures to form compounds such as kalsilite (KAlSiO₄) and leucite (KAlSi₂O₆). Kaolin also irreversibly captures gaseous KCl and KOH. The overall adsorption process is proposed to include a reversible slow adsorption of KCl on the active sites of meta-kaolin, followed by an irreversible fast reaction between adsorbed KCl with water molecules in the gas phase. [22]

Kaolin has also been suggested for use for heavy metal capture in fluidised bed boilers.

2.5.4 Foundry sand

Foundry sand is used to make forms for iron casting, and contains quartz or feldspar sand grains covered with bentonite clay. Its composition may vary considerably depending on sand used (quartz, feldspar, olivine), clay mineral (bentonite, kaolin) and the metal used in the casting process. Foundry sand can also contain organic additives and kaolin. Bentonite is added to prevent surfaces from sintering during the casting, by increasing the thermal stability of the casting form. About 5-10 % of the foundry sand (~225 kton per year in Sweden) is not recyclable after the iron casting process. [28]

Sand from iron casting contains 3-9% bentonite and is usually made from Baskarp sand.

Bentonite is a geological term for soil materials with a high content of a swelling mineral, which usually is montmorillonite. High-quality commercial bentonites normally contain over 80% of montmorillonite. However, the other minerals in bentonite may vary substantially within, and especially between, different quarries.

Montmorillonite is hydrated sodium calcium aluminium magnesium silicate hydroxide (Na,Ca)0.33(AI,Mg)2(Si4O10)(OH)2·nH2O. One unit of montmorillonite consists of three layers, two layers of tetrahedral [SiO4] surrounding one layer of octahedral [AI/Mg(O5,OH)]. [28] Potassium, iron, and other cations are common substitutes, the exact ratio of cations varies with source.

According to tests in a bench-scale fluidised bed reactor at Umeå University, the behaviour of casting sand seems to depend on the composition of the fuel. The risk for agglomeration is lower with this material than with quartz sand for calcium-rich fuels such as bark, but it is higher for potassium-rich fuels such as olive kernels. The sand used in these tests was a by-product from

iron casting, based on Baskarp sand covered with a layer of bentonite. Baskarp sand is composed mainly of quartz (81 %) and feldspars (16 %). The sand used for the tests consisted of 7-8 % bentonite and 3 % carbon. [28]

Foundry sand could probably be used as bed material without previous sieving. Its composition may vary considerably depending on sand used (quartz, feldspar, olivine), clay mineral (bentonite, kaolin) and the metal used in the casting process.

The foundry sand used in this project is sand from iron casting (Volvo). It is a finer fraction with a higher content of bentonite than the main part of the foundry sand available. Its main constituent is Baskarp sand and it contains 17,4% active bentonite and 11,7% C.

2.5.5 Lime

Limestone is a sedimentary rock composed largely of the minerals calcite and aragonite, which are different crystal forms of calcium carbonate (CaCO₃).

Calcium oxide (CaO), commonly known as quicklime or burnt lime, is usually made by the thermal decomposition of limestone in a lime kiln. This is accomplished by heating the material to above 825 °C.

Calcium hydroxide $(Ca(OH)_2)$, traditionally called slaked lime, is obtained when calcium oxide is mixed, or "slaked" with water.

All these products are used as additives in boilers. Limestone or slaked lime is added into the furnace for reduction of SO_2 emissions by formation of $CaSO_4$. Slaked lime is fed into the flue gas channel for reduction of acid components, SO_2 , HCI and HF. [37]

Calcium has a high affinity for phosphorus, which is why lime might be a good choice as additive for such high-phosphorus fuels where phosphorus is expected to increase slagging and/or deposit corrosivity by lowering the melting point. However, when phosphorus is not available for reaction, calcium will instead bind sulphur, thereby preventing sulphation of alkali chlorides.

2.5.6 Marl / marlstone

Marlstone is a type of limestone containing more clay impurities than normal limestone. At the start of this project it was thought that the clay content of this product was much higher than it proved to be. As it is, this product is not much different from limestone and it has been excluded from further studies within this project.

A chemical analysis of marlstone from Nordkalk (average values) is given below. Table 5 and Table 6)

Table 5. Main constituents of marlstone, composition in %

Tabell 5. Sammansättning märgelsten i %

	Average	Std
		dev
CaO	50,9	1,6
SiO2	3	1,3
Al2O3	1,5	0,6
Fe2O3	0,6	0,3
MgO	1,5	0,7
K20	0,5	0,2
Sulphur, S	0,14	0,06
Glödförlust (950°C)	41,5	0,9

Methods: X-ray fluorescense spectrometry (XRF) for CaO, SiO_2 , Al_2O_3 , Fe_2O_3 , MgO och K_2O , Eltra for sulphur

Table 6. Trace elements of marlstone, composition in mg/kg

Tabell 6. Sammansättning spårämnen i märgelsten i mg/kg

	Average	Std
		dev
As	1	0,5
Cd	0,1	0,05
Со	1	0,4
Cr	3	1
Cu	2	0,5
Hg	<0,02	-
Ni	3	0,6
Pb	4	0,8
V	4	0,9
Zn	16	7

Method: AAS (Svensk Standard SS 028150)

2.5.7 ICA 5000

ICA 5000 is an additive developed for waste fired grate boilers that is injected with the secondary air with the purpose of reducing furnace corrosion and slagging caused by alkali chlorides.

ICA 5000 is an artificial aluminium silicate with highly active surfaces and with silanol groups on top which rigidly bind alkali and alkaline earth compounds at high temperatures forming metal silicates. The reaction products form melting liquid glasses under furnace temperature, acting as a protective barrier on the furnace walls. [15], [16]

2.5.8 Waste brick from steel production

Brick is assumed to be an inert material at normal combustion temperatures (<1000°C), as it has been burned at high temperatures. Waste brick from the steel industry is proposed as an alternative bed material when using high-alkali fuels. Crushed bricks could probably also provide a suitable particle loading in the convective section to achieve a soot-blowing effect and reduce deposit build-up on the heat transfer tubes.

The material would probably need pre-treatment (crushing and possibly magnetic separation) before use.

2.5.9 De-inking sludge

De-inking sludge is a by-product of paper recycling. Depending on the filler agent used in the paper production, it usually contains high levels of $CaCO_3$ or kaolin, or both. The greater the content of kaolin, the more pronounced positive effect is to be expected. However, kaolin is less common as filler agent due to its higher price. Tests with de-inking sludge in the Chalmers research CFB using wood and straw as fuel showed a positive effect on the defluidisation temperature [23]. As de-inking sludge usually contains high amounts of calcium, it decreases the SO_2 level in the flue gas, which in turn can have a negative effect on fouling and corrosion of superheater tubes, as shown in [24]. It is also known that finely ground Ca powders can increase the fouling of superheater tubes.

De-inking sludge has been tested as an additive for reduction of superheater corrosion in the waste fired FB boiler Händelö P14, Norrköping, owned and operated by E.ON Värme, Sweden. The de-inking sludge caused no reduction in alkali chlorides in the flue gases, but eliminated the sulphur in the flue gases. [26]

2.5.10 Peat fly ash

The chemistry of peat ash is complicated due to its complex and varying composition. Many studies, mainly from co-combustion of peat with problematic fuels show the many possible reactions between peat ash and other ash constituents. Peat also contains inert ash components like silicate and oxides which do not interact chemically with other components. The

physical effect of this inert ash may, however, be significant. It has been shown to have a cleaning effect on superheater deposits by mechanical wearing effects. Part of the oxide ash has been found to have an alkali absorbing ability and high calcium content may promote formation of Cacompounds which dissolve potassium and possibly also zinc and lead. Peat is also relatively rich in sulphur and promotes the formation of alkali sulphates instead of chlorides, which lowers both deposition and corrosion risks. [13]

The effect of addition of peat fly ash when firing waste wood has been investigated in a multi-fuel reactor. This was done in order to follow the fate of some of the problematic compounds in waste wood as a function of peatash addition and other combustion related parameters. The experiments showed that the reactions of potassium, zinc and lead were the most affected. This gave rise to higher concentrations of zinc and lead in the fly ash. The chlorine and potassium content in the fly ash decreased with increased peat ash addition. This will have an inhibiting effect on corrosion, but the higher Zn and especially Pb concentrations will lead to a lower first melting point of the fly ash particles. This may promote deposition and cause corrosion. It is thought that the binding of potassium in the bed material, retaining it in the bottom ash, gives rise to higher concentrations of zinc and lead in the fly ash. [13]

2.5.11 Tunnel furnace slag

Tunnel furnace slag is the slag from sponge iron production at Höganäs AB (in Swedish tunnelugnsslagg or TU-slagg). This by-product has been tested as an additive to agricultural residue in a pilot-scale burner at ETC in Piteå, Sweden. The results indicate that this additive could be used to reduce deposit build-up in the furnace and on superheaters and to reduce superheater corrosion. Addition of 5 and 20 weight % to the fuel was used in the tests. [30]

Tunnel furnace slag is a fine powder with $\sim 60\% < 100 \mu m$. The slag has high concentrations of C (s), CaO and ghelenite (Ca₂Al₂SiO₇). The production of TU slag at Höganäs yields ~ 17 -20 ktons per year. The origin of tunnel furnace slag is burnt lime and coke. Tunnel furnace slag is non-hazardous waste. Possible registration according to the chemical legislation REACH may change the classification and management. The content of fossil C in TU slag might affect the trade of CO₂ certificates for the plant. [30]

2.5.12 Hard coal fly ash

Hard coal fly ash is expected to bind alkali mainly in the form of alkali alumino silicates, much in the same manner as kaolin. For use with high-alkali fuels, fly ash from pulverised coal boilers is to be preferred due to its lower content of calcium. Fly ash from fluidised bed combustion is higher in calcium due to lime addition for flue gas desulphurisation. A high calcium content is probably not a drawback if the fuel is rich in phosphorus, provided phosphorus is the main reason for the ash-related problems (this is, however, only true for marginally used fuels such as e.g. rapeseed cake).

2.5.13 Gypsum

Gypsum is a sulphate mineral composed of calcium sulphate dihydrate, with the chemical formula $CaSO_4 \cdot 2H_2O$. It is a by-product of flue gas cleaning in combustion processes. It has been suggested to be used as an additive due to its content of sulphate. The idea is that alkali should be captured, forming alkali sulphate in the same manner as when using elemental sulphur. However, since sulphate has a higher affinity for Ca than for alkali, this will not happen to any large extent.

2.6 Conclusions

The results from KME 508 indicate that for low alloyed steels, which are mostly used for furnace walls, chlorine is the main component in the deposits causing corrosion. For higher alloyed materials (austenitics and nickel based alloys) alkali and lead also seems to take part in the process. It is not known for either process yet in what form the corrosive species are deposited on the furnace walls, but a guess would be in the form of alkali chlorides and elemental lead.

Since the corrosion is thought to be caused by chlorine, alkali chlorides, heavy metals or a combination of these, the aim has been to find additives that can reduce these components in the deposits on the walls and/or the flue gases in the furnace, either by chemical reactions or adsorption.

Sulphur containing additives (e.g. sulphur or ammonium sulphate) are commonly used to reduce the flue gas content of alkali chlorides with the purpose to reduce superheater corrosion. It is possible that a reduction of alkali chlorides in the flue gases also would reduce the corrosion in the furnace. The mechanism is a reaction with alkali chlorides forming alkali sulphates and HCI (g). This reaction, however, requires oxidising conditions to occur and might not take place in the furnace region, but further on in the flue gas path.

Clay-type minerals such as kaolin and other layered alumino silicates are commonly used as alkali-capturing fuel/bed additives. Kaolin has a large specific surface, allowing it to adsorb troublesome species in the flue gases.

Ca and P in the bed, either from the fuel or from an additive, can form CaKPO₄, thus capturing alkali and reducing the presence of alkali chlorides in the flue gases. However, a deficiency in Ca can lead to the formation of low melting alkali phosphates and a surplus of Ca can lead to capture of sulphur that would otherwise have formed alkali sulphates and in turn lead to an increase of alkali chlorides in the flue gases.

Al- and Ca-based materials, such as lime (CaO, CaCO₃) and kaolin, can serve as heavy metal sorbents in fluidised beds, capturing heavy metals by physical deposition and chemical adsorption.

Five additives were selected for further testing, sulphur, digested sewage sludge, kaolin, foundry sand and lime.

Sulphur was selected as a reference, since there is much experience from using this additive in plants. It is known to have a positive effect on superheater corrosion and there was a hope that it might also be beneficial when it comes to waterwall corrosion.

Digested sewage sludge was selected as this is a cheap additive (or actually the plant is paid for receiving it) and since it addition has been shown to reduce bed agglomeration, deposit formation, and superheater corrosion in fluidised bed boilers.

The positive effects from both kaolin and foundry sand are expected to come from clay minerals, even though the content in foundry sand is much lower than in kaolin. Kaolin was selected as it was expected to cause a substantial reduction in alkali in the deposits and flue gases in the furnace, and possible also a reduction of heavy metals. Foundry sand was selected as a possible cheaper alternative to kaolin.

The sulphur capturing properties of lime means that it probably not is a good additive for reducing waterwall corrosion. It will probably not reduce the content of alkali chlorides in the flue gases to any larger extent, possibly even increasing it. It might however adsorb heavy metals. The other additives to be used in the project, sulphur, kaolin, foundry sand and sewage sludge will all bind alkali or convert alkali chlorides to less corrosive compounds. All additives, except sulphur, are also expected to bind heavy metals to some extent. This means that lime will be the only additive tested that will only decrease heavy metals, but not decrease alkali chlorides.

Using lime in one test could lead to a better understanding of reactions/mechanisms that influence waterwall corrosion and the mechanisms for the other additives, by making it possible to separate the two suggested corrosion mechanisms, one involving alkali chlorides and the other involving heavy metals.

3 Analysis of composition of fuels and additives

The fuel and additives that were used for the laboratory tests described in section 5 (Laboratory tests), have been characterised by chemical fractionation and/or chemical analysis. The implications of these analyses on the corrosivity of the fuel and the ability of the additives to prevent corrosion are also discussed.

3.1 Chemical fractionation

Chemical fractionation is a method based on selective leaching by water, ammonium acetate and hydrochloric acid. The method was originally developed by Benson and Holm [43] for the characterisation of coal. Baxter [42] used a modified version for the characterisation of 7 biomass fuels. At Åbo Akademi University the method has been further developed for biomass characterisation [48] and has been used for characterisation of over 100 different types of fuels presented. This method can be helpful when determining how ash-forming elements are bound in the fuel and thus how they may behave during combustion. There are two ways of using the fractionation data. One is to take the soluble parts of the elements and use them as input values in the thermodynamic calculations and the other is to use the analysis results in a more empirical way in some simple calculations of certain key ratios. The ratios are explained in more detail in chapter 3.3. Normal standard analysis would not give the same results, especially not in cases where the alkali is also present as insoluble compounds in the fuel, which was actually the case with both the pellets and the sewage sludge studied in this project. However, although the fractionation is a good method to evaluate fuels it is a very tedious and relatively costly procedure and in that sense it is more of a research tool than a standard analysis method.

Figure 1 shows a simplified scheme showing that the stepwise leaching distinguishes between different types of ash-forming matter in a fuel according to their solubility in different solvents.

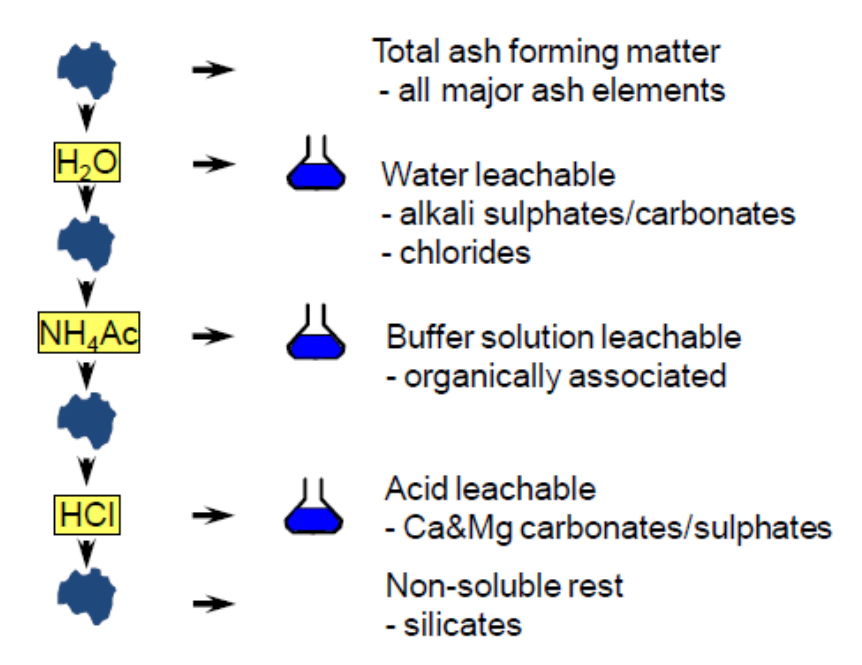


Figure 1 The principle of chemical fractionation by stepwise leaching (from e.g. Handbook of Combustion, Vol. 4, 2010).

Figur 1 Principen för kemisk fraktionering genom stegvis lakning (Handbook of Combustion, Vol. 4, 2010)

Fuel samples are usually milled to a particle size below 5 mm to facilitate handling and acceptable leaching times. Too small particles have shown to clog filters, whereas too large particles demand too long leaching times. Increasingly aggressive solvents, i.e. water (H2O), 1M ammonium acetate (NH4Ac) and 1M hydrochloric acid (HCl) leach samples into a series of four fractions (including the remaining solid residue). The untreated samples, the liquid fractions and the remaining solids were analysed by an external laboratory according to Swedish standards.

Depending on the metals analysed, the solid residues after leaching were either ashed, after which the ash was dissolved in hydrochloric acid and analysed, or dissolved in HNO3/H2O2, or molten in LiBO2 after which dissolution took place in HNO3. In most cases ICP-AES or ICP-SFMS were used as analytical techniques for the dissolved solids as well as the leachates. Typical ash-forming components, which are leached out by water include alkali sulphates, -carbonates, -phosphates and -chlorides. Elements leached out by NH4Ac are believed to be organically associated, such as Mg and Ca as well as K and Na. HCl leaches the carbonates and sulphates of alkaline earth and other metals. Silicates and other minerals remain in the insoluble residue.

3.2 Results of fuel analyses and fractionation

In this work the fuel pellets and the sewage sludge, that were used for the laboratory tests described in section 5 (Laboratory tests), were chemically

fractionated and analysed, while the kaolin and the foundry sand were analysed by SEM/EDX. All materials were provided by SP.

Below in Table 7 the ultimate analysis, ash amount and moisture are presented and in Table 8 some of the key elements concerning deposits and corrosion, are presented.

Table 7 Fuel analysis, heating value, ash amount and moisture of waste wood pellets and sewage sludge. All data given in weight-% on dry basis except for moisture and heating value.

Tabell 7. Bränsleanalys, värmevärde, askhalt och fukthalt för RT-flispellets och avloppsslam. Alla data är i vikt-% på torr bas förutom fukthalt och värmevärde.

Fuel	С	H	0	N	S	Ash, 550°C	Moisture, w-%	LHV, MJ/kg
Waste wood pellets	45.2	5.5	37.7	1.90	0.143	9.6	8.5	15.5
Sewage sludge	36.5	5.1	18.3	4.96	1.267	33.8	8.1	13.7

Table 8 Comparison between two pellet analyses and an analysis of the sewage sludge for some key elements. ÅA-sample: parenthesis for Ca indicates the amount analysed in the solutions + the solid rest (see also Table 9).

Tabell 8. Jämförelse mellan två analyser av pellets och en analys av avloppsslammet för några utvalda element. "ÅA-sample": värdet i parantes för Ca anger mängden i lösning + olöslig rest. (Se också Tabell 9)

Element (mg/kg fuel on dry basis)	Waste wood pellets, (ÅA sample, spring 2012)	Waste wood pellets (SP sample)	Sewage sludge
Ash, w-%	9.6	8.6	33.8
S	1 430	1 000	12 670
CI	1 860	2 600	740
Ca	6 450 (8 630)	7 140	22 870
K	1 590	1 630	3 540
<u>Na</u>	1 950	2 150	1 880
Р	189	232	26 660
Pb, Zn, Cu	376, 212, 1 050	361, 602, 43	11.8, 451, 254

From Table 8 we can see that there are some differences between the ÅA sample and the SP sample. Some of the differences are probably common deviations between samples and also within the analysis error (S, Ca, K, Na, P, and Pb). The chlorine amounts are quite high (compare e.g. to stem wood with about 100 mg/kg dry fuel) and also the difference between the analyses is relatively large, but since the pellets were made from waste wood including demolition wood also large differences may occur and there seems to be some other source from where the chlorine came (not plastic since all Cl was soluble in water). The origin of the fuel may also explain the differences in the Zn and Cu analyses.

Figure 2 shows the results from fractionation of the waste wood pellets and Figure 3 the results of the sewage sludge in different y-axis scales.

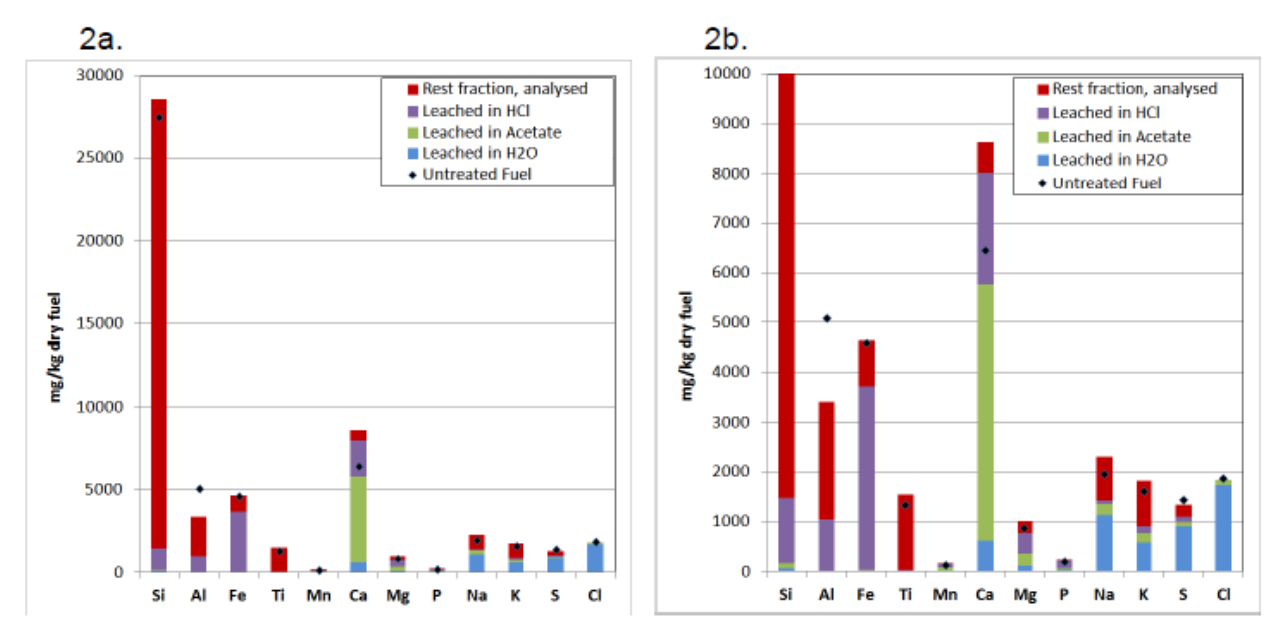


Figure 2 The fractionation results of waste wood pellets.

Figur 2 Resultaten av fraktionering för RT-flis-pellets.

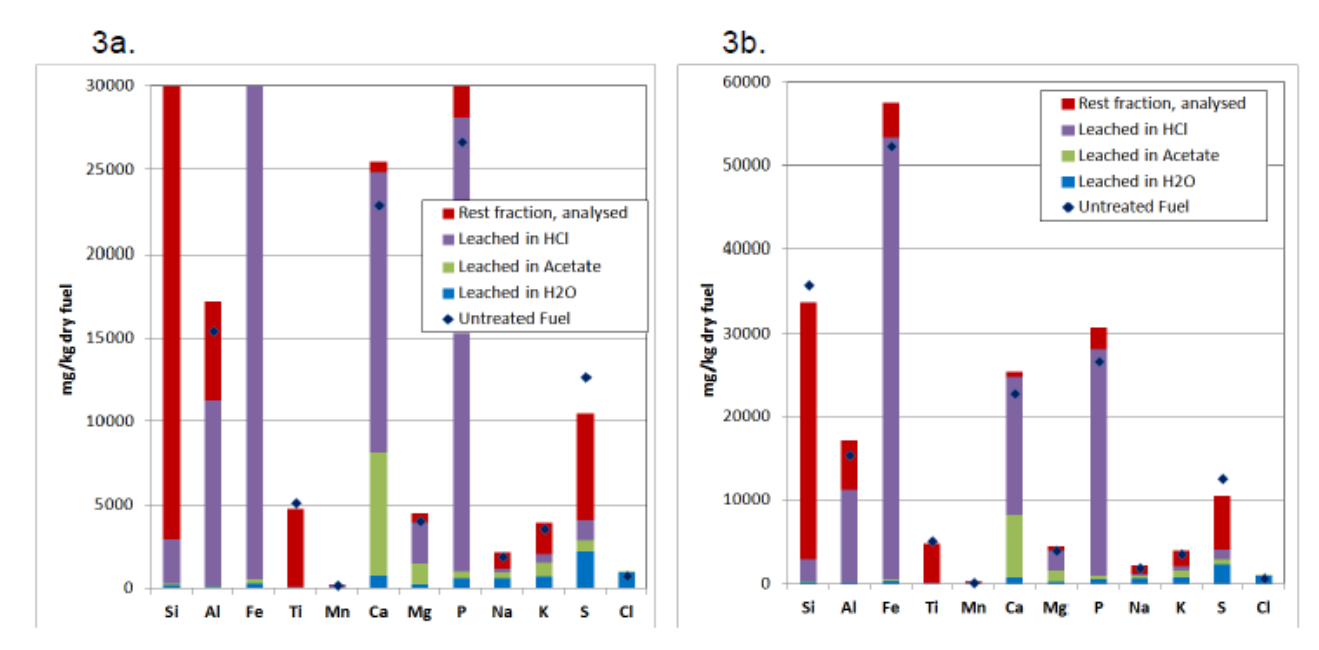


Figure 3 The fractionation results of sewage sludge.

Figur 3 Resultaten av fraktionering för avloppsslam.

Generally, one can say that the elemental balances in the fractionations were quite good. In some cases, they may be a bit off (e.g. Al and Ca for the pellet analyses). However, in the case with Ca we have also earlier noticed that it is sometimes difficult to dissolve all Ca for analyses of untreated wood. Accordingly, the higher number in the parenthesis in Table 8 is probably closer to the correct one. In the case with alumina the reason for the discrepancy is not clear, it may have been caused by sample inhomogeneity or by some analytical error. Quite clear is that there is not an error in the fractionation realisation or e.g. calculations since the error does not show in other elements. The numbers for Figure 2 and Figure 3 are shown in Table 9 and in Table 10, respectively.

Table 9 Fractionation results for waste wood pellets

Tabell 9. Resultat av fraktionering för RT-flis-pellets

Waste wood pellets, mg/kg dry fuel	Si	Al	Fe	Ti	Mn	Ca	Mg	Р	Na	K	S	CI
Untreated Fuel	27487	5075	4588	1319	125	6447	862	189	1951	1594	1430	1860
Leached in H2O	72	15	18	0	8	605	112	33	1126	584	909	1727
Leached in Acetate	89	5	6	1	68	5165	248	36	230	177	77	100
Leached in HCI	1311	1017	3685	28	67	2245	402	147	61	147	103	0
Rest fraction, analysed	27079	2366	934	1502	11	617	236	26	879	903	244	0
Total out, analysed	28550	3402	4643	1531	154	8632	998	242	2297	1810	1333	1827
Balance ratio (in/out)	0.96	1.49	0.99	0.86	0.81	0.75	0.86	0.78	0.85	0.88	1.07	1.02

Table 10 Fractionation results for sewage sludge

Tabell 10. Resultat av fraktionering för avloppsslam

Sludge, mg/kg dry fuel	Si	Al	Fe	Ti	Mn	Ca	Mg	P	Na	K	S	CI
Untreated Fuel	35855	15453	52318	5125	178	22870	4004	26663	1877	3536	12670	743
Leached in H2O	177	74	300	7	1	742	200	573	612	701	2222	953
Leached in Acetate	120	54	238	1	6	7392	1289	413	329	834	675	18
Leached in HCI	2604	11126	52726	58	178	16679	2432	27116	195	510	1173	0
Rest fraction, analysed	30830	5926	4220	4689	23	632	552	2610	1013	1850	6391	0
Total out, analysed	33731	17180	57483	4754	209	25445	4473	30712	2148	3896	10461	971
Balance ratio (in/out)	1.06	0.90	0.91	1.08	0.85	0.90	0.90	0.87	0.87	0.91	1.21	0.77

Kaolin and foundry sand were analysed by means of SEM/EDX. The results are shown below. (Figure 4 and Figure 5)

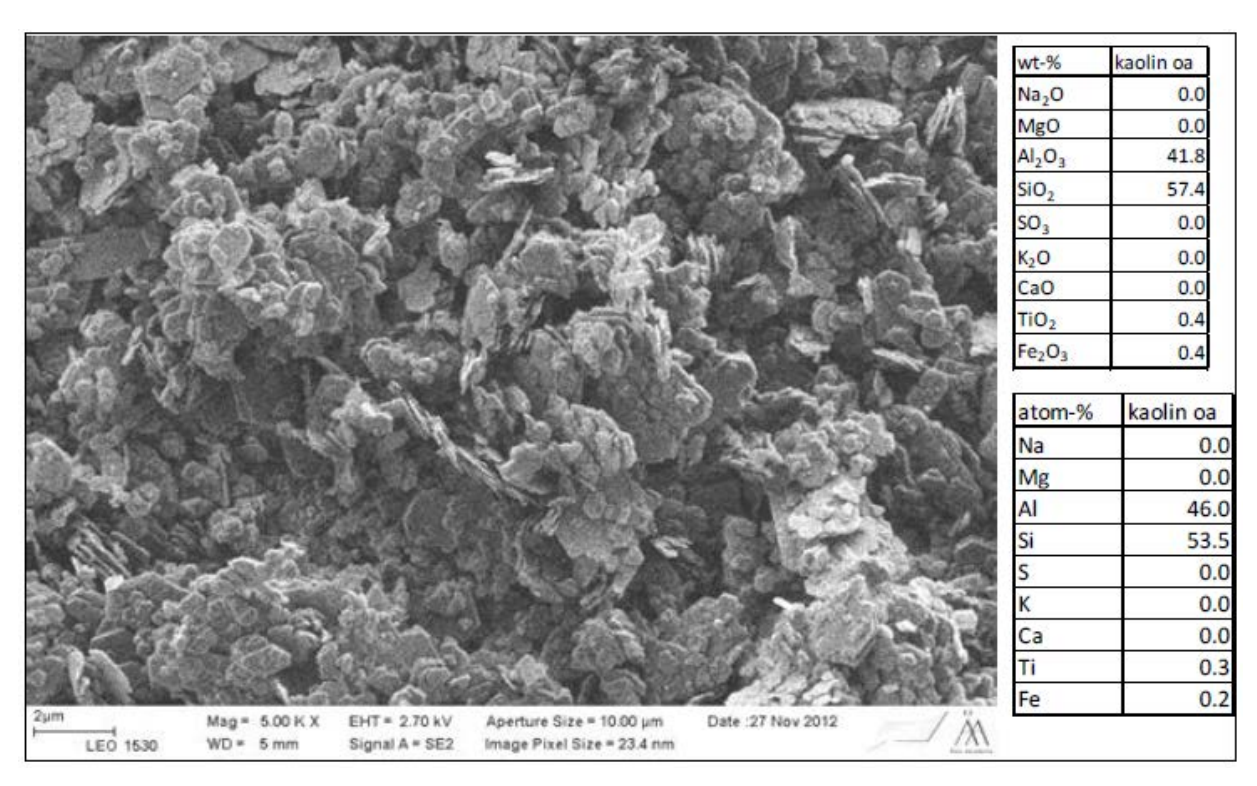


Figure 4 SEM image and EDX analyses of kaolin (Al₂Si₂O₅(OH)₄).

Figur 4 SEM-bild och EDX-analys för kaolinit (Al₂Si₂O₅(OH)₄).

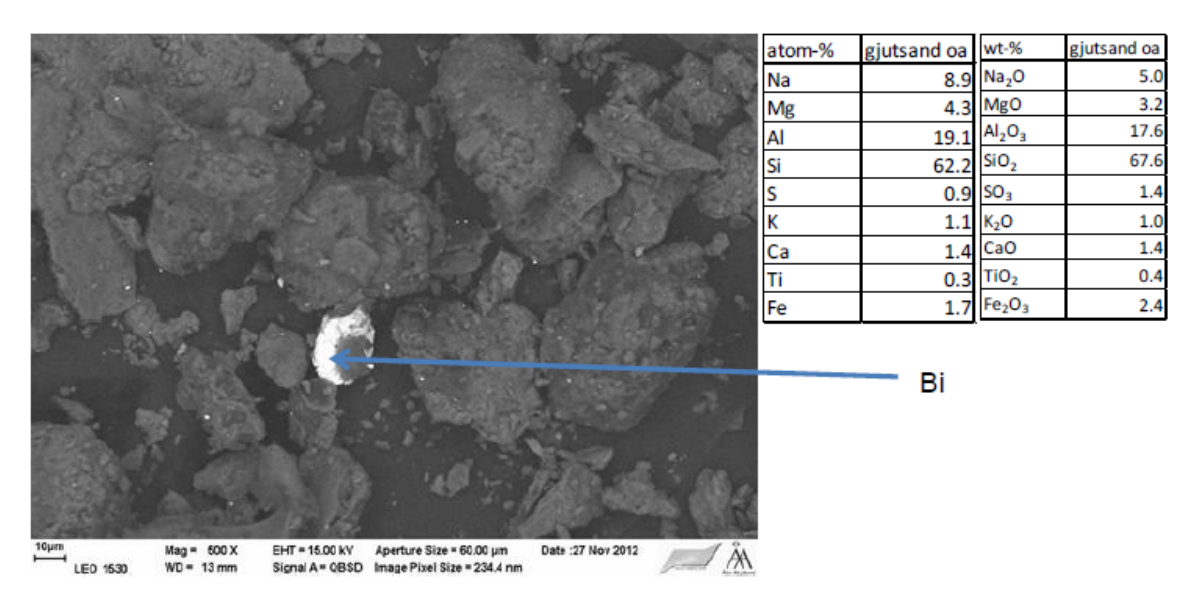


Figure 5 SEM image and EDX analyses of foundry sand.

Figur 5 SEM-bild och EDX-analys för gjuterisand.

The analyses of the kaolin showed that the kaolin is quite pure with only very small amounts of impurities and maybe with some excess SiO₂ or alternatively Si can be bonded in some other ratio than 1/1 to Al.

The foundry sand is more complex. It consists mostly of Si and AI, but also Na is present in relatively large amounts together with some K. Further, it was noticed that the foundry sand lost weight during heating (about 10 weight-%) up to 1000°C, which could indicate the presence of some organic matter (the colour of the untreated sand was black/grey and after heating it was orange). The bright spot was identified to being bismuth, which probably just was an impurity in the sample.

3.3 Discussion - Implications of the analysis results

From the chemical fractionation analysis a couple of key numbers can be determined. These numbers are not absolute but may give an indication if the fuel will be problematic in view of chlorine containing deposits. These numbers have often been produced from experiences in oxidising parts of the boiler. Thus, it can be questioned if the results are also valid for the bottom part of a boiler and the waterwalls. In the lower part of the furnace the conditions are commonly slightly reducing and thus reactions involving oxygen may not have a strong influence. However some of the reactions limiting corrosion may also in take place in the lower part of the boiler.

One commonly used number is the S/Cl molar ratio and it has been suggested that this value has to be at least four to prevent chlorine corrosion (see references e.g. in [45]). The thought behind this ratio is that any formed

alkali chloride would be sulphated by the sulphur according to Equation 1, where K can also be Na:

$$2KCI(g,s) + SO_2(g) + 1/2O_2(g) + H_2O(g) \Leftrightarrow K_2SO_4(s) + 2HCI(g)$$
 (1)

However, the S/CI ratio totally omits the amounts of alkali and calcium that participate in the sulphur capture reactions. These elements actually determine if there is any alkali left to react to alkali chlorides. Consequently, another number has been defined; S/(Na2+K2) or alternatively S/(Na2+K2+Ca) ([46], [47]). These numbers are also based on Equation 1 and in the latter ratio additionally also on Equation 2:

$$CaO(s) + SO_2(g) + 1/2O_2(g) \Leftrightarrow CaSO_4(s)$$
 (2)

The idea behind these two ratios is that a higher sulphur concentration will result in a lower the amount of free Na and/or K available for reaction with chlorine to KCI or NaCI. In the latter ratio also Ca is included since many biomass fuels contain significant amounts of Ca, usually present as calcium oxalate (CaC2O4), which will decompose during combustion and form quite small and porous CaO-particles. When using these ratios one has to know how much of the fuel's Na, K, and Ca that is actually available for reaction and not bound to combustion stable compounds like e.g. alkali silicates or calcium sulphates. To determine this we are using the results from the chemical fractionation, and often, especially in cases with woody biomasses, the water and acetate soluble alkali is easily reactive. In the case with Ca it is more tricky since calcium oxalate is not water soluble but acid soluble, and it may be a little risky to add all the soluble Ca (H2O+Ac+HCl) into one reactive phase, especially if the fuels are not woody biomass fuels. For example Yrjas et al. [46] reported that the acid soluble Ca in a bark was nearly 100% oxalate while the corresponding number for a sewage sludge was 15%.

Another way of decreasing the risk of alkali chloride formation is to use fuels or additives containing alumina silicates. The principle behind this is to capture alkali with the alumina silicates and releasing HCl to the flue gas according to Equation 3:

$$Al2O3 \cdot 2SiO2(s) + 2KCI(g) + H2O(g) = K2O \cdot Al2O3 \cdot 2SiO2(s) + 2HCI(g) (3)$$

Equation 3 is written to simply describe the reaction as an example, and it should be noted that the reaction is probably not equimolar and the actual "alkali capacity" of the alumina silicates is not clear.

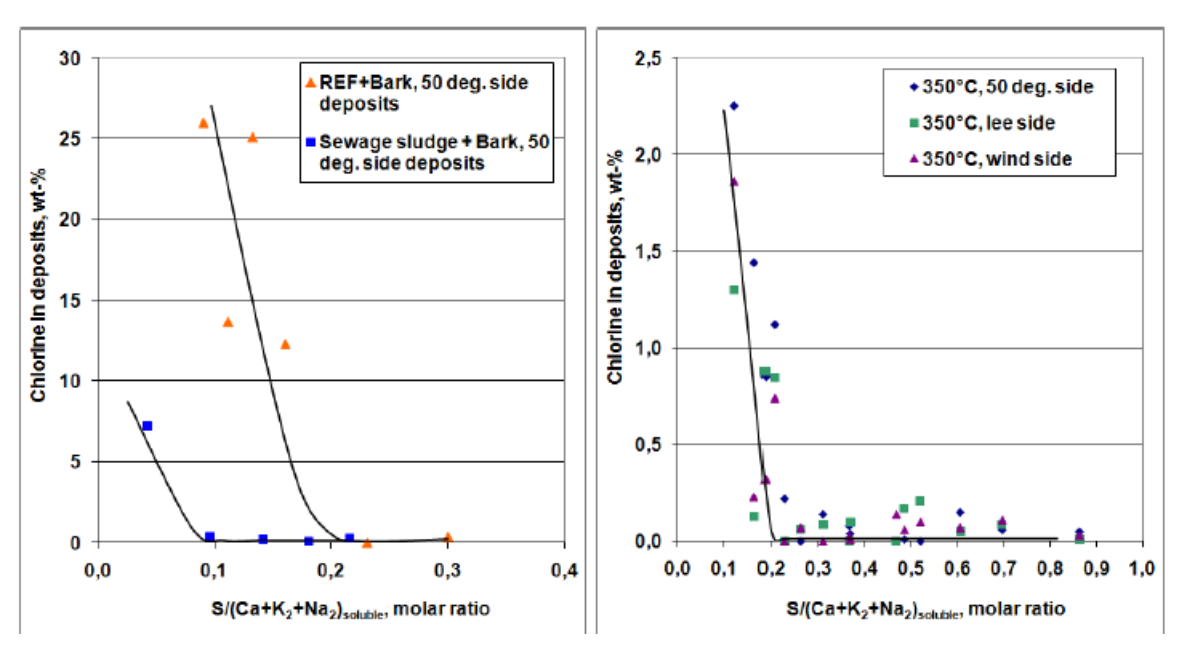


Figure 6 The chlorine amount in deposits as a function of the molar ratio S/(Ca+Na2+K2), ([46], [47]) in fluidised bed combustion. Left picture from pilot scale tests and right picture from results from a large scale plant.

Figur 6 Klormängden i avlagringar som funktion av molkvoten S/(Ca+Na2+K2), ([46], [47]) i förbränning i fluidiserad bädd. Vänster bild från test i pilotanläggning och höger från test i en fullskalig anläggning.

From Figure 6 we can see that when the S/(Ca+Na2+K2) molar ratio is lower than about 0.2 chlorine starts to appear in the deposits. In the left hand picture, the curve with the blue points describes a case where a sewage sludge containing alumina silicates was added [41] in different amounts. From Figure 6 we can see that in this case a ratio of 0.1 (2% sewage sludge) was enough to prevent chlorine deposition, while in cases without alumina silicates the ratio was about 0.2.

It should be observed that Figure 6 represents deposits sampled in the freeboard in the test facilities studied. Thus, it can be questioned if the results are also valid for the bottom part of a boiler and the waterwalls. In the lower part of the furnace the conditions are commonly slightly reducing and thus the sulphur reaction according to Equation 1 may not have a strong influence. However, Equation 3 may also in the lower part of the boiler play an important role, although the study representing Figure 6 was done for superheater deposits.

3.3.1 Sewage sludge

Table 11 lists the above mentioned ratios of the waste wood pellets mixed with different amounts of the sewage sludge analysed in this work. When Table 11 was calculated it was assumed that the Si and Al in the pellets were not present as alumina silicates and in the case with sewage sludge the alumina silicate amount present as kaolin was based on the amount of insoluble Al.

Table 11 Some key molar ratios based on fuel analysis.

Tabell 11. Några molkvoter baserade på bränsleanalys.

Sewage sludge, wt-%	S/CI	S/(Na2+K2)	S/(Ca+Na2+K2)	Alumino silicate/alkali
0	0.85	1.14	0.19	0
1	0.92	1.23	0.20	0.04
2	1.00	1.32	0.22	0.08
4*	1.15	1.50	0.25	0.16
8*	1.46	1.85	0.30	0.32
35	4.0	4.23	0.70	1.40

^{*}amounts tested by SP (section 5, Laboratory tests)

Based on Table 11 it could be expected that about 4 wt-% sewage sludge should be sufficient to hinder chlorine in the deposits, maybe even less, while about 35% would be needed if looking only at the S/CI ratio.

3.3.2 Kaolin

Based on the SEM/EDX analysis (Figure 4) there is a slight excess of Si if we assume that all alumina silicate is present as kaolinite (Al2Si2O5(OH)4). Observe also that the analysis does not include crystallised water. Table 12, showing the molar ratio of kaolin to water and acetate soluble alkali in the pellets, was calculated by including water in the kaolin and simultaneously assuming that the Si and Al in the pellets are not present as active alumina silicates and that the excess Si in the kaolin material is present as inert SiO2.

Table 12 Molar ratio of kaolin to easily soluble alkali in dry waste wood pellets at different addition amounts of the kaolin material.

Tabell 12. Molkvot för kaolin mot lättlösligt alkali i torr RT-flispellets vid olika mängder tillsatt kaolin.

Kaolinite material, weight-%	Kaolinite/Alkali, molar ratio
0	0
1	0.44
2	0.89
3*	1.36
4	1.83

^{*}amount tested by SP

Combining Table 11, Table 12 and Figure 6 it can be assumed that the amount used in the laboratory tests performed by SP (section 5, Laboratory tests) should be enough with a clear margin. Even a lower amount of the kaolin material may give quite similar results.

3.3.3 Foundry sand

Even if assuming that all aluminium as analysed by the SEM/EDX represents the content of kaolin type material in the foundry sand, the content is quite low. Also, by taking into account the observation that the foundry sand contains about 10% of organic material, lowers the amount further. Table 13 shows the molar ratio of the alumina silicates (as kaolin) to water and acetate soluble alkali in the pellets. It was assumed that the Si and Al in the pellets are not present as active alumina silicates and that the excess Si in the foundry sand is present as inert SiO2.

Table 13 Molar ratio of kaolin type material to easily soluble alkali in dry waste wood pellets at different addition amounts of the foundry sand.

Tabell 13. Molkvot för kaolinlika föreningar mot lättlösligt alkali i torr RT-flispellets vid olika mängder tillsatt gjuterisand.

Foundry sand, weight-%	Kaolinite/Alkali, molar ratio
0	0
1	0.19
2	0.39
3*	0.60
4	0.80

^{*}amount tested by SP

If the aluminium amount describes the amount of kaolin type material it could be expected that the amount used in the laboratory tests performed by SP (section 5, Laboratory tests) would clearly show a positive effect. However, the foundry sand also contains other elements (K, S, and Ca) which may have an effect, depending on the compounds. Especially, the alkali content may cause hesitation to any boiler operator.

3.3.4 Sulphur

In the test with sulphur addition performed by SP (section 5, Laboratory tests), the addition was 10 g sulphur/kg fuel resulting in a S/(Ca+K2+Na2) molar ratio of about 1.5, which should be clearly enough to hinder chlorine to deposit. Even lower amounts may be sufficient.

3.3.5 Limestone

In the test with limestone addition performed by SP (section 5, Laboratory tests), the addition was 30 g limestone/kg fuel resulting in a S/(Ca+K2+Na2) molar ratio of about 0.08, if it is assumed that the limestone is 100% CaCO3 (no analyses available). This is far too low and there is a clear risk for chlorine deposition according to Figure 6. It should, however, be noted that the reactivity of different types of limestone can differ significantly from each other and thus the above mentioned ratio is only a very rough estimation.

3.3.6 Final remarks

Five different additives have been considered – sewage sludge, kaolin, foundry sand, sulphur and limestone – to decrease the risks (deposits, fouling, and corrosion) in the combustion chamber in a boiler. The bright spot was identified to being bismuth, which probably just was an impurity in the sample. Sewage sludge is clearly one of the best since it is a material that needs to be disposed of and in combustion it brings both sulphur and alumina silicates to the process which clearly decreases the risk for chlorine deposition and corrosion. Kaolin and sulphur are also both effective. Limestone increases the risk for chlorine deposition and corrosion, while foundry sand also contains other elements e.g. potassium, which may be risky. However, the effect of foundry sand based on only SEM/EDX analyses remained somewhat unclear.

4 Thermodynamic equilibrium calculations

Thermodynamic equilibrium calculations have been performed, using the chemical composition of the fuel and additives used in the laboratory tests performed by SP (section 5 Laboratory tests) in order to check ability of the software to predict/simulate the system from the chemical point of view. The composition was analysed by Åbo Akademi and the analysis is presented in section 3, Analysis of composition of fuels and additives.

Two different calculation tools have been used and compared. Åbo Akademi has used FactSage and Vattenfall has used HSC Chemistry.

4.1 Calculations performed by Abo Akademi using FactSage

4.1.1 Method

Thermodynamic equilibrium calculations were made to predict the speciation of the ash-forming elements as a function of temperature and a function of the amount of additives at both oxidising (λ =1.2) and reducing (λ =0.8) conditions. The advanced thermodynamic modelling was performed using the software package FactSage, version 6.3 [50]. A tailor-made thermodynamic database was used for the calculations. The data for the gas phase and the stoichiometric solid phases of the elements C – H – O – N – S – Cl – Na – K – Zn – Pb – Ca – Mg – Fe – Al – Si – P – Ti – Cu – Mn were taken from the FACT53 database in the FactSage software. It was assumed that N₂ was the only stable nitrogen compound as the formation of NO_x compounds in biomass combustion is strongly dependent on kinetics and N-speciation in the fuel.

The thermodynamic data for the multicomponent liquid phase Na⁺, K⁺, Ca²⁺, Mg²⁺, Zn²⁺, Pb²⁺//SO₄²⁻, CO₃²⁻, Cl⁻, S²⁻, O²⁻ has been developed recently and more detailed descriptions of the liquid phase can be found in the papers by Lindberg et al. [51] to [55] and Robelin & Chartrand [56]. A review of the present status of thermodynamic databases for ash components in biomass and waste combustion is given by Lindberg et al. [57]. Certain solid solution and subsystems of the liquid phase also appear in the FTSalt and FTPulp databases in the FactSage software.

Thermodynamic calculations can be done by considering all the ash-forming elements as well as the C-H-O components in the fuel to predict the ash chemistry and associated gas-phase chemistry for oxidising and reducing conditions. However, this method may often predict chemical interactions that may not occur in a real furnace due to kinetic constraints. These kinetic are known for some gas-solid phase reactions, such as for sulphation of CaO and oxidation of SO_2 to SO_3 at low temperatures. Other constraints are the reactions of silicates, which in general are much slower than the reactions of

salt-like phases. For example, the availability of K to react with other components is much different for example for $KAISi_3O_8$ and KCI.

One approach is to utilise results from chemical fractionation as more detailed input for the calculations. To simplify the modelling and to see clearer effects of realistic chemistry, the water-leached and ammonium acetate-leached fractions are used as input. Al, Si, and Fe which often form different oxides are often considered to be inert. However, this may be different from case to case. A schematic of the procedure is shown below (Figure 7).

Ash Behavior Predictions for Fuel Mixes

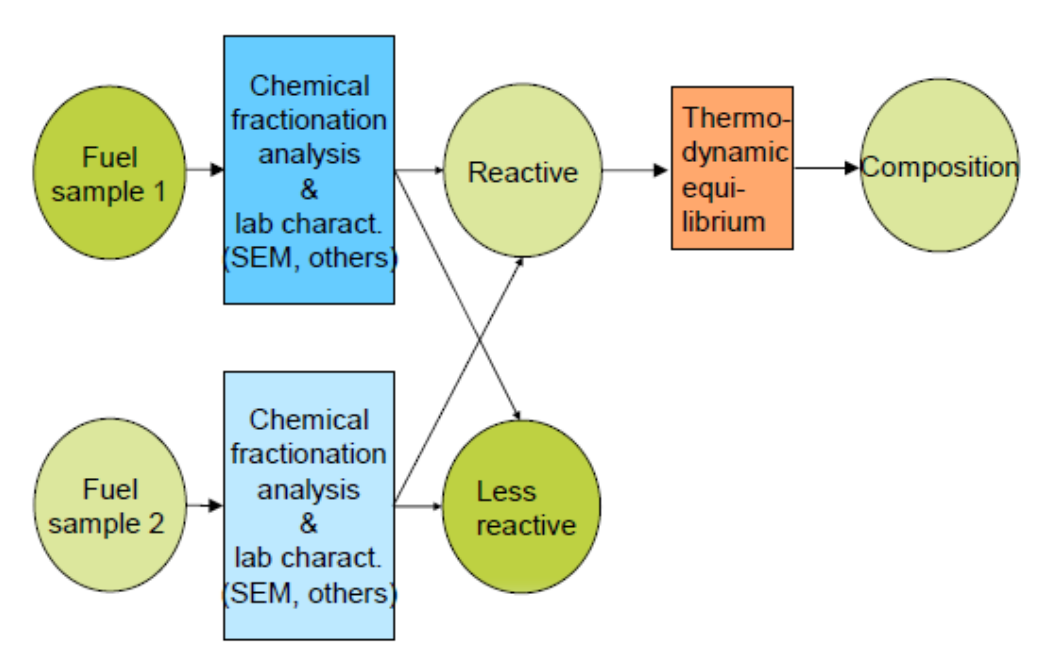


Figure 7 Ash behaviour prediction model for fuel mixes

Figur 7 Modell för prediktion av askbeteende för bränsleblandningar.

The various input compositions and parameters for the calculations are given in Table 14 below. The composition of the ash-forming elements is taken from the chemical fractionation analysis presented in section 3, Analysis of composition of fuels and additives.

Table 14 Input compositions and parameters used for the calculationsTabell 14. Sammansättnignar och andra indata använda för beräkningarna

Calculation	Fuel input	Additive	Temperature	٨
1	All elements	-	300-1300	1.2*
2	Fractionation results	Sulphur	850	1.2
3	Fractionation results	Sulphur	850	0.7**
4	Fractionation results	CaO	800	1.2
5	Fractionation results	CaO	800	0.7
6	-	Sewage sludge – all elements	300-1300	1.2
7	-	Sewage sludge - fractionation	300-1300	1.2
8	Fractionation results	Sewage sludge	800	1.2
9	Fractionation results	Sewage sludge	800	0.7
10	Fractionation results	Kaolin	800	1.2

^{*}λ= 1.2 corresponds to an O₂ partial pressure of ~0.03 bar

4.1.2 Results

Ash chemistry of waste wood pellets

The predicted phases and species at oxidising conditions if all ash-forming elements are included are shown in Figure 8 and Figure 9 for the waste wood pellets. The stable phases are mainly SiO2 and different Ca-Na-K-alumino silicates. Chlorine is mainly stable as HCl in the gas phase and sulphur is mainly stable as CaSO4 and SO2. However, it is very unlikely that all the ash-forming elements will interact with each other and reach equilibrium during combustion of the fuel in a real boiler setting. Therefore, to investigate the effect of the additives on ash chemistry, only the easily leached fractions (water + ammonium acetate) from the fractionations were used as input for the following elements K, Na, Ca, Mg, and P. All S, Cl, Zn, Pb, and Cu were included in the calculations. No Fe, Al, Si, Mn or Ti was included in the calculations, except for the cases with sewage sludge.

^{**} λ = 0.7 corresponds to an O₂ partial pressure of ~10⁻¹⁸ bar

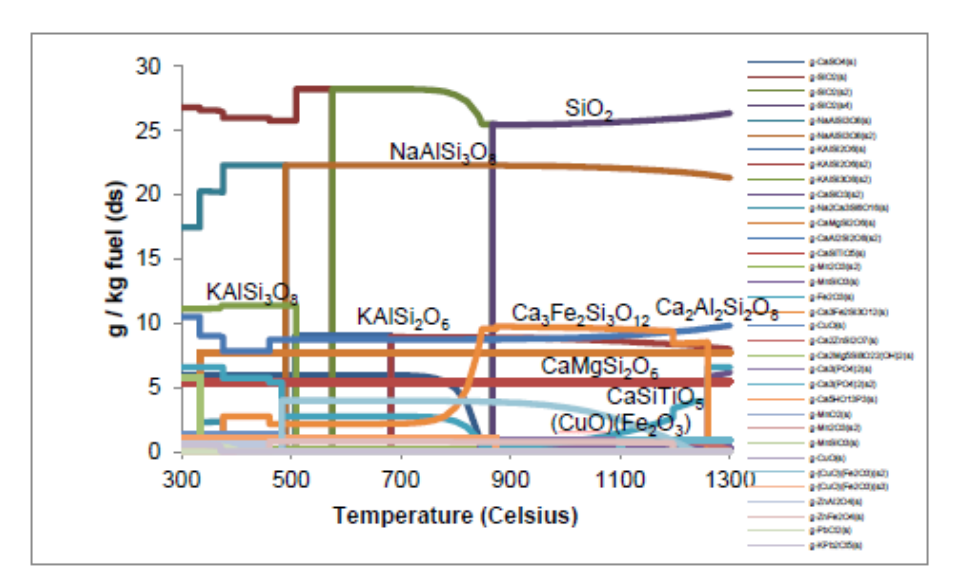


Figure 8 Condensed phases for waste wood pellets as a function of temperature at oxidising conditions, assuming all elements interact

Figur 8 Kondenserade faser för RT-flis-pellets som funktion av temperaturen vid oxiderande förhållanden, under förutsättning att alla ämnen reagerar med varandra.

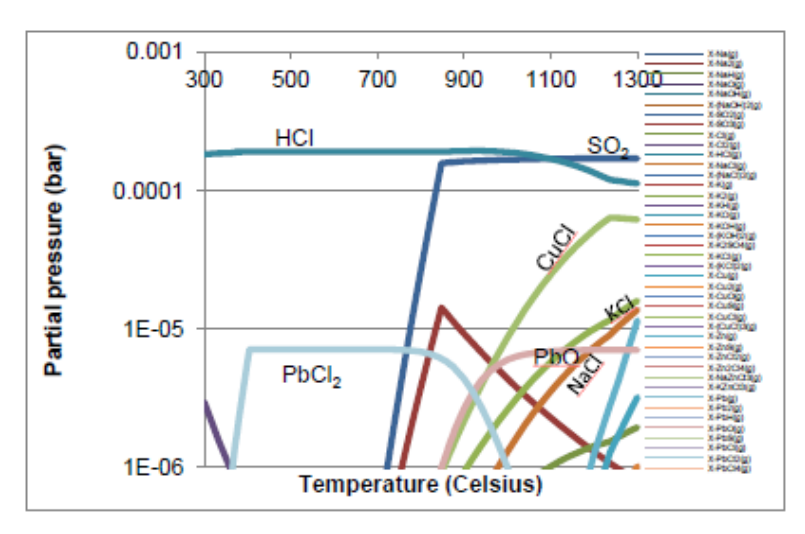


Figure 9 Gas components for waste wood pellets as a function of temperature at oxidising conditions, assuming all elements interact

Figur 9 Gaskomponenter för RT-flis-pellets som funktion av temperaturen vid oxiderande förhållanden, under förutsättning att alla ämnen reagerar med varandra.

Sulphur additive

The effect of sulphur additions on the gas phase chemistry and total ash chemistry at oxidising conditions at 850°C is shown in Figure 10. It can be seen that the addition of sulphur will mainly lead to capture of sulphur by CaO and formation of CaSO4 until a total of around 7 g S/kg dry fuel. At higher additions, the alkali chlorides will almost fully convert to alkali sulphates and chlorine will mainly form HCI (maximum of around 200 ppm) (Figure 11). The additional sulphur will convert to SO2. Lead and zinc are mainly in the oxide form at low additions of sulphur and will convert to PbSO4 and ZnSO4 as considerable amounts of SO2 in the gas phase is formed. It should be noted that at around 7 g S/kg dry fuel, there is a peak of both PbCl₂(g) and ZnCl₂(g) connected to the formation of HCI in the gas phase (Figure 12). The increase in HCl is connected to the sulphation of alkali chlorides. When enough sulphur is added for complete sulphation of alkali chloride, the released HCl can react with Pb and Zn to form PbCl₂ and ZnCl₂, leading to a calculated sharp increase in PbCl₂ and ZnCl₂ in the gas phase. However, at higher sulphur additions, PbCl₂ and ZnCl₂ are also sulphated. Thus, additive additions leading to an increased level of HCl but no or insignificant increase in SO2 may increase the formation of PbCl₂ and ZnCl₂.

Sulphur additions under reducing conditions do not have a significant effect on the chlorine chemistry. The amount of alkali chlorides will not change dramatically with the addition of sulphur. Additions of sulphur lead to the formation of metal sulphides and H_2S in the gas phase (Figure 13 to Figure 15). However, the sulphide formation does not affect the amount of chloride in the gas phase.

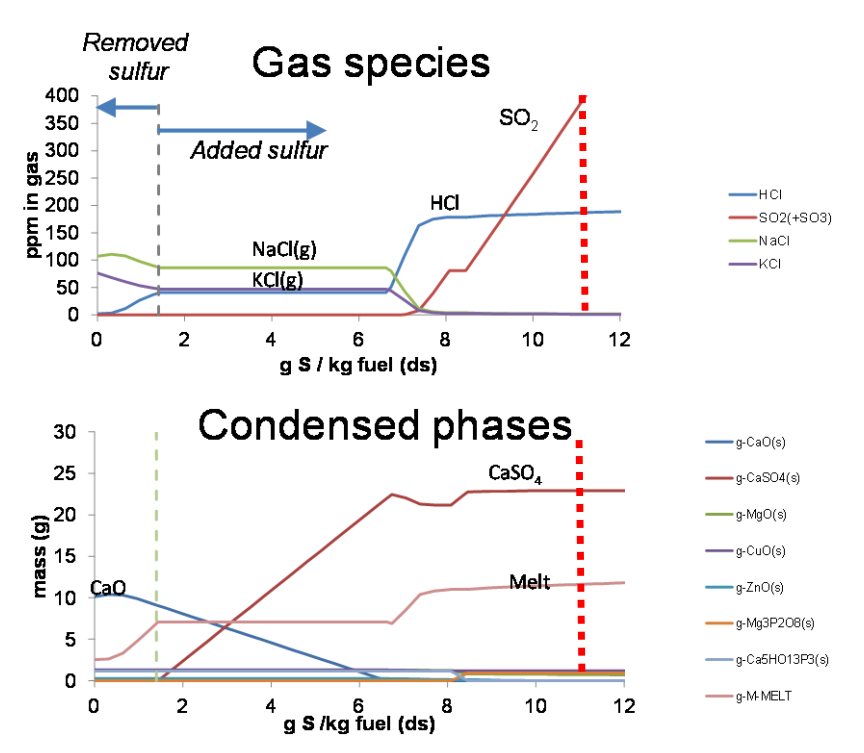
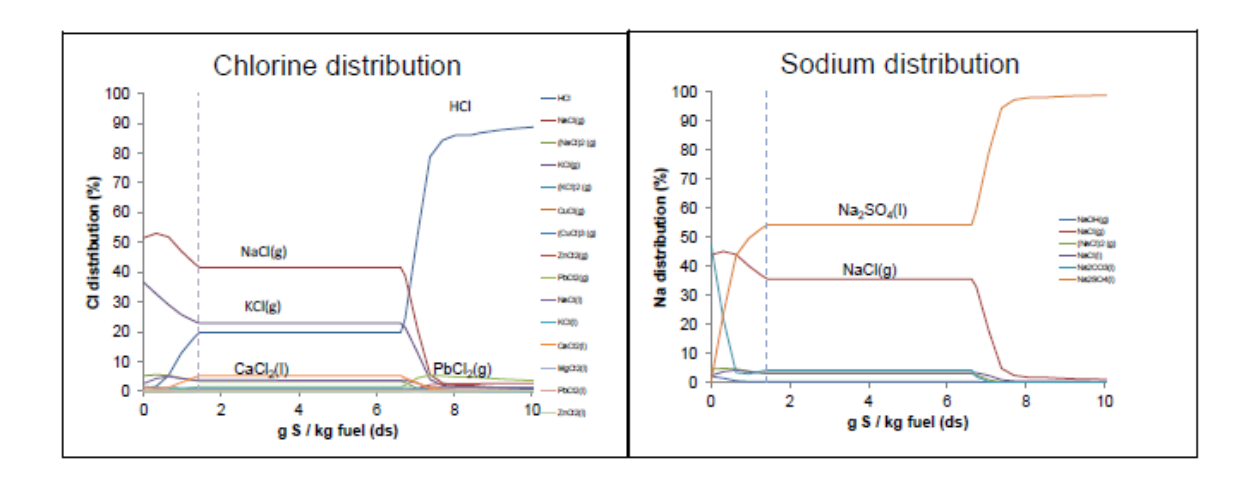


Figure 10 Gaseous species and condensed phases for sulphur addition at 850°C and oxidising conditions. The dotted grey line shows the sulphur composition of the fuel and the dotted red line shows the total sulphur composition during the experiments (Sulphur in fuel + 10 g added sulphur / kg dry fuel).

Figur 10 Gasformiga komponenter och kondenserade faser vid tillsats av svavel vid 850°C och oxiderande förhållanden. .Den streckade grå linjen visar svavelinnehållet i bränslet och den röda streckade linjen visar det totala svavelinnehållet under testet (svavel bränslet + 10 g tillsatt svavel / kg torrt bränsle)



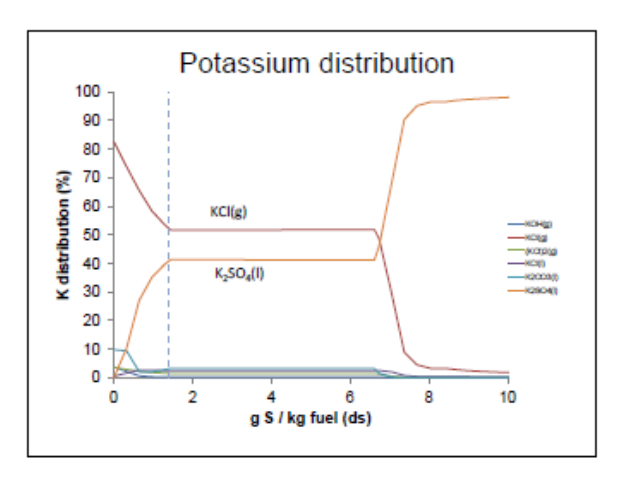


Figure 11 CI, Na, and K distribution for sulphur addition at 850°C and oxidising conditions

Figur 11 Fördelningen av CI, Na och K vid tillsats av svavel vid 850°C och oxiderande förhållanden.

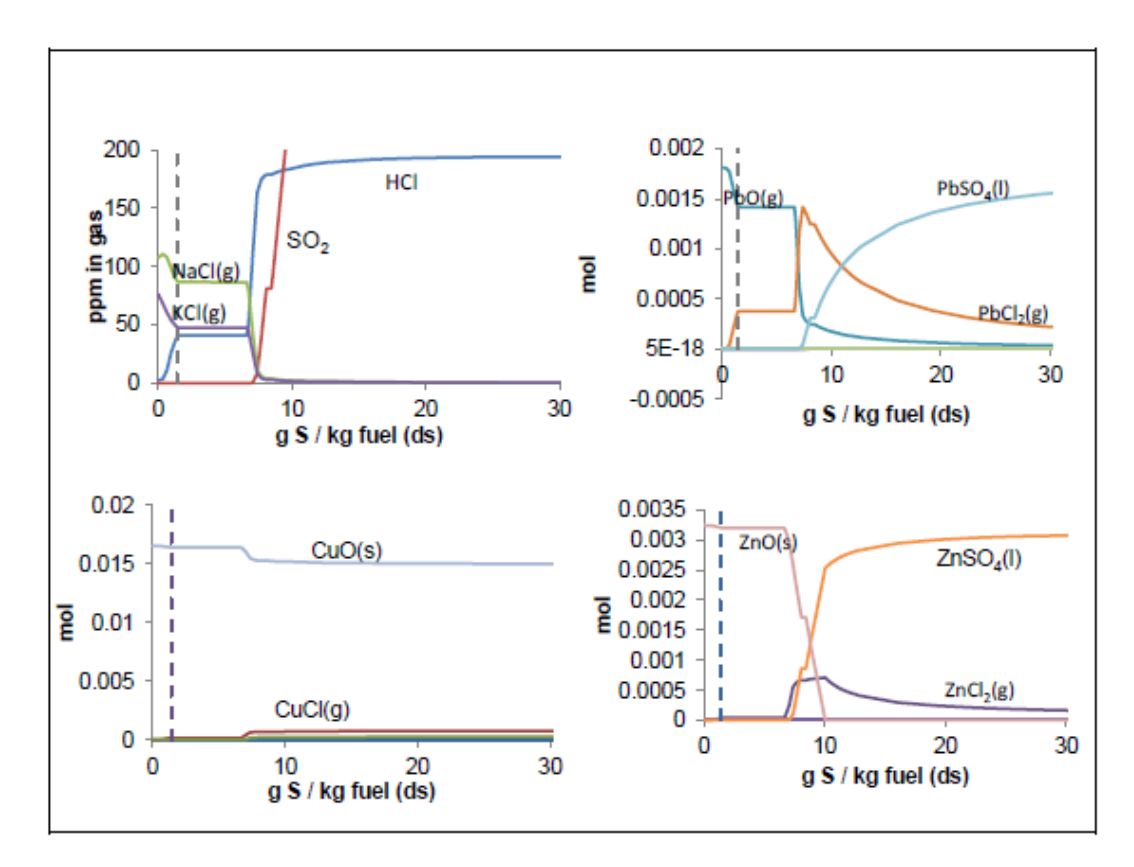


Figure 12 Pb, Cu, Zn distribution for sulphur addition at 850°C and oxidising conditions.

Figur 12 Fördelningen av Pb, Cu och Zn vid tillsats av svavel vid 850°C och oxiderande förhållanden.

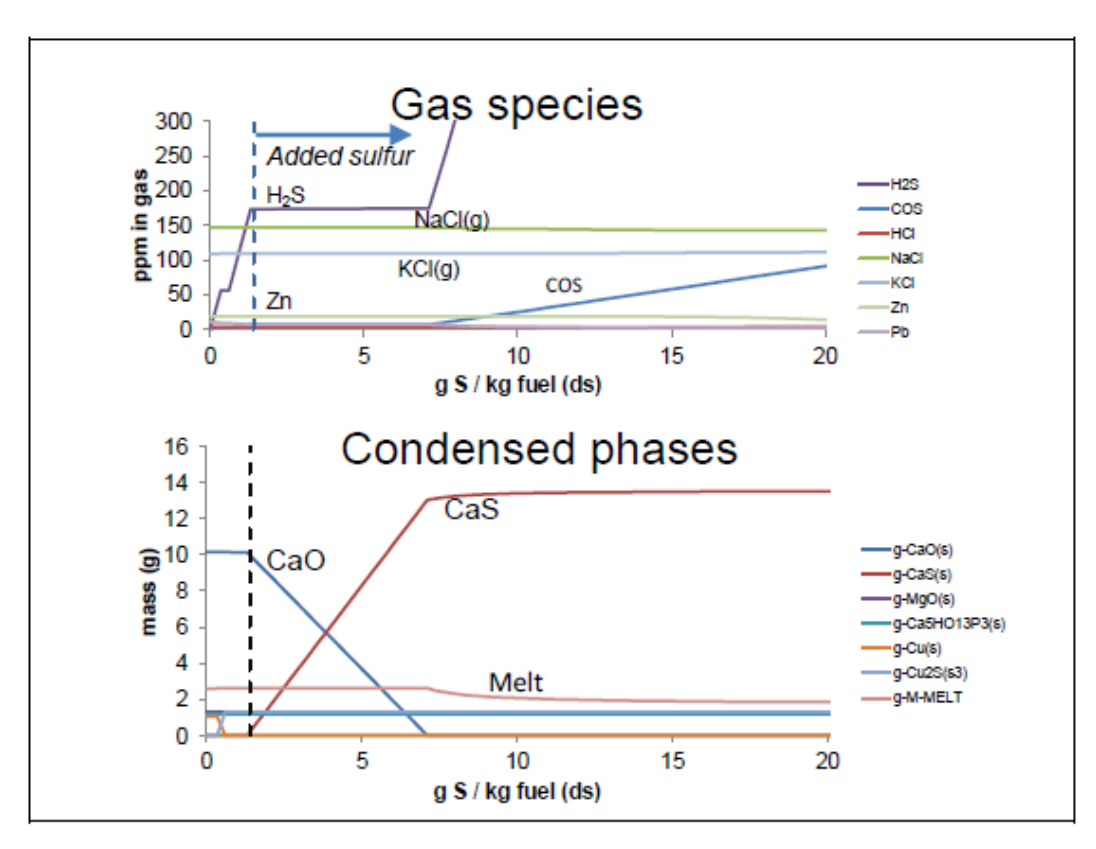
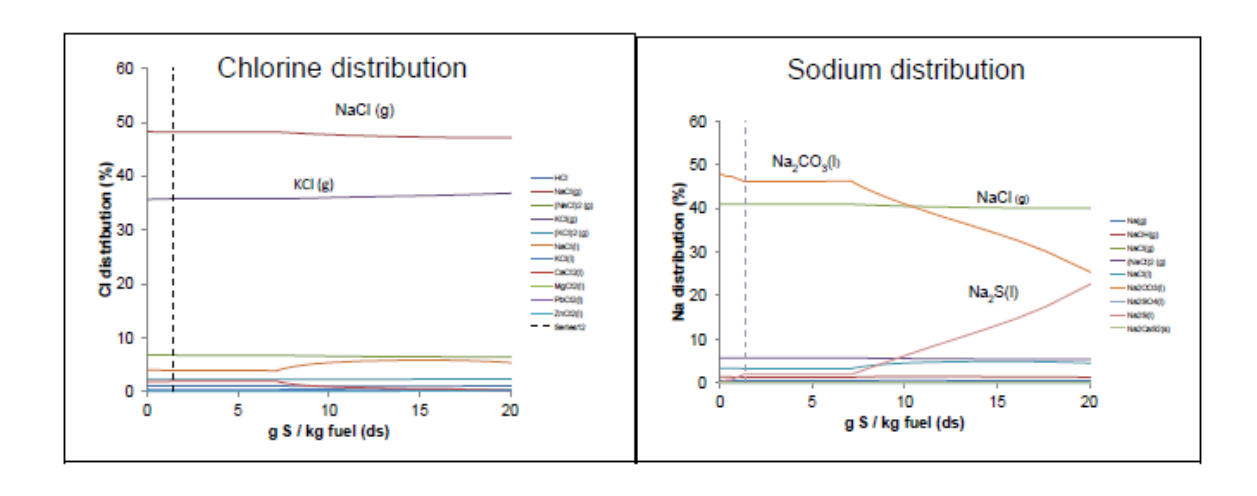


Figure 13 Gaseous species and condensed phases for sulphur addition at 850°C and reducing conditions.

Figur 13 Gasformiga komponenter och kondenserade faser vid tillsats av svavel vid 850°C och reducerande förhållanden



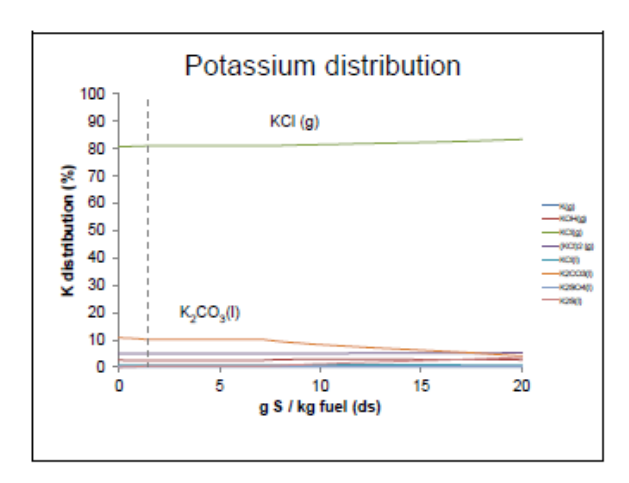


Figure 14 CI, Na, and K distribution for sulphur addition at 850°C and reducing conditions

Figur 14 Fördelningen av CI, Na och K vid tillsats av svavel vid 850°C och reducerande förhållanden.

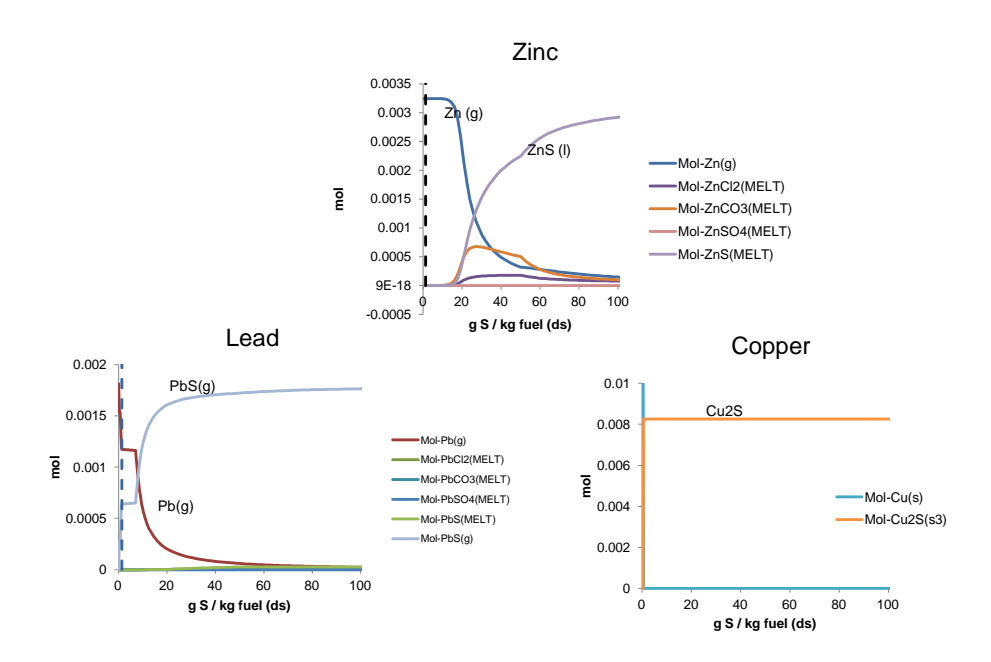


Figure 15 Pb, Cu, Zn distribution for sulphur addition at 850°C and reducing conditions.

Figur 15 Fördelningen av Pb, Cu och Zn vid tillsats av svavel vid 850°C och reducerande förhållanden.

Lime additive

The effect of CaO additions on the gas phase chemistry and total ash chemistry at oxidising conditions at 800°C is shown in Figure 16. It can be seen that the addition of lime will have no effect on the ash chemistry or gas chemistry if the total CaO in the mixture is around 2 g CaO/1 kg dry fuel waste wood pellets or higher. The waste wood pellets contain calcium equivalent to around 12 g CaO/1 kg dry fuel, meaning additions of lime should not affect the chemistry of flue gas or ash.

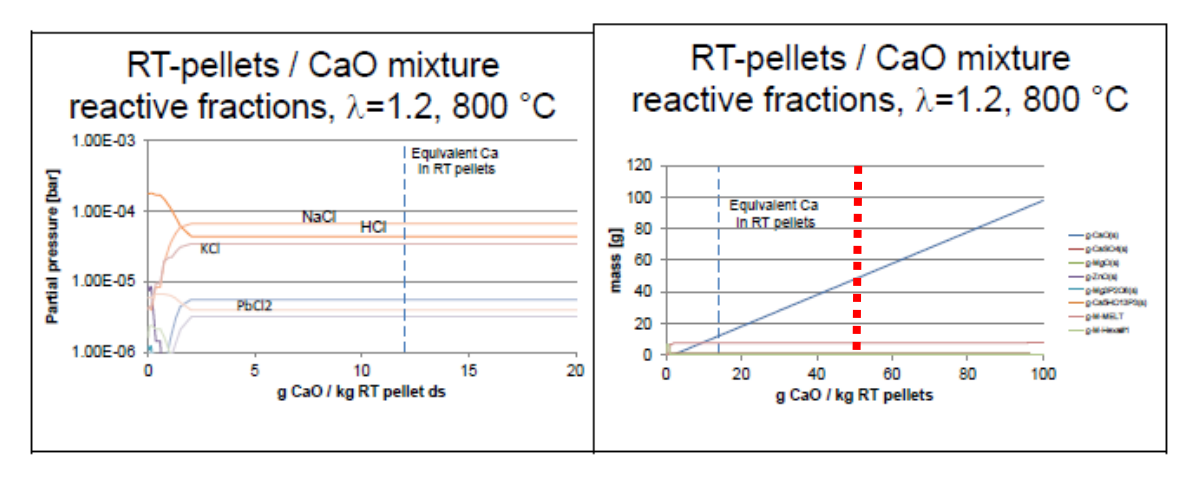


Figure 16 Gaseous species and condensed phases for CaO addition at 800°C and oxidising conditions. The dotted blue line shows the equivalent amount of CaO in the fuel. Values to the left indicate situations where CaO is removed or considered unreactive. The red line on the right-hand figure shows the total amount of CaO in experiments (Calcium from fuel + 30 g added CaO).

Figur 16 Gasformiga komponenter och kondenserade faser vid tillsats av CaO vid 800°C och oxiderande förhållanden. Den streckade blå linjen visar det ekvivalenta innehållet av CaO i bränslet och den röda streckade linjen visar det totala innehållet av CaO under testet (kalcium från bränslet + 30 g tillsatt CaO / kg torrt bränsle).

The same trends can be seen for reducing conditions (Figure 17) except that zinc is volatilised as Zn(g) and lead occurs as Pb and PbS instead of PbCl₂. The level of KCl and NaCl is also higher in the reducing case as HCl is not predicted to form to any large extent compared to the oxidising case.

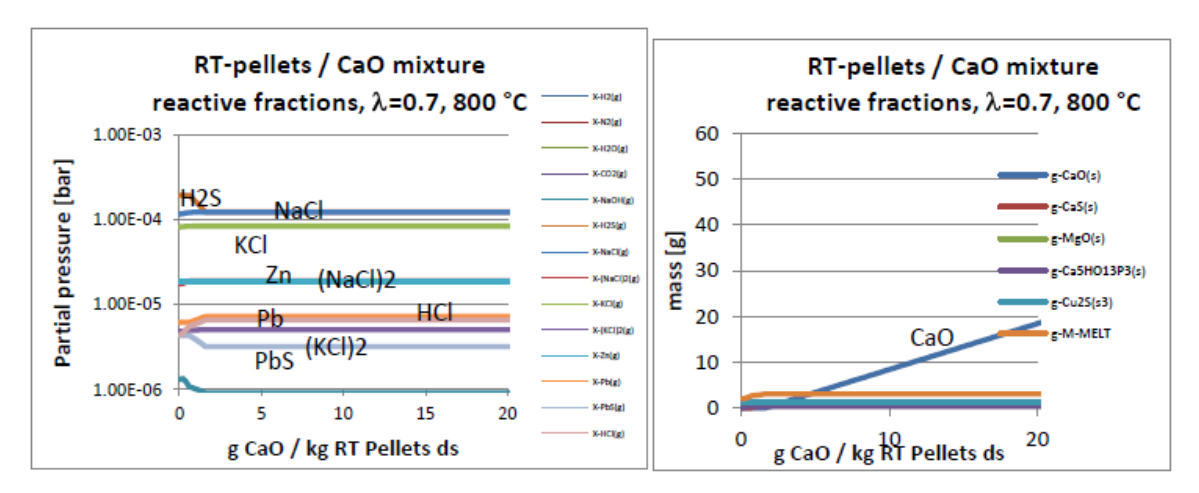


Figure 17 Gaseous species and condensed phases for CaO addition at 800°C and reducing conditions

Figur 17 Gasformiga komponenter och kondenserade faser vid tillsats av CaO vid 800°C och reducerande förhållanden.

Sewage sludge

The ash chemistry of sewage sludge (only, not with fuel) at oxidising conditions was calculated, both for the case were all ash-forming elements were included in the calculation, and for the case were the leached fractions were included in the calculation. Silicon was not included in the calculations were the leached fractions were included in the calculation.

The predicted stable condensed phases are oxides (mainly SiO₂, Fe₂O₃, NaAlSi₃O₈, and KAlSi₃O₈), phosphates (AlPO₄, Fe₂PO₄, Mg₃(PO₄)₂, Ca₃(PO₄)₂, Zn₃(PO₄)₂), and sulphates (Na₂Ca(SO₄)₂, K₂Ca₂(SO₄)₃, and CaSO₄) (Figure 18 to Figure 19)

Chlorine is mainly as HCl in the gas phase for both cases. For the case using the leached fractions as input, HCl is partly transformed to gaseous KCl at temperatures above 900°C. At temperatures 700°C and higher, considerable amounts of SO₂ (+SO₃) are predicted to be stable due to the decomposition of the sulphates.

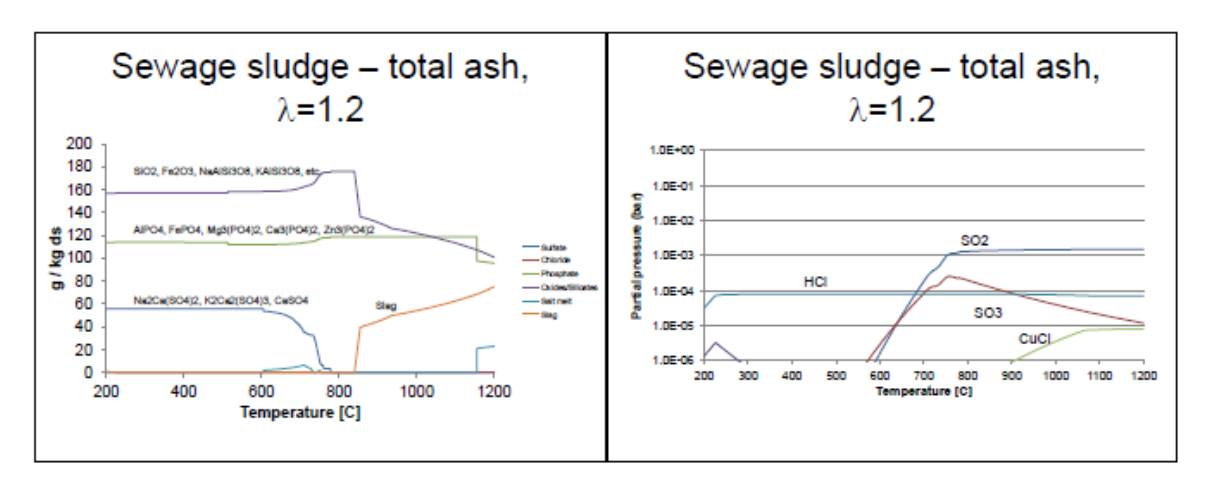


Figure 18 Gaseous species and condensed phases for sewage sludge as a function of temperature at oxidising conditions. Total elemental analysis was used as input

Figur 18 Gasformiga komponenter och kondenserade faser vid tillsats av avloppsslam som funktion av temperaturen och oxiderande förhållanden. De totala halterna av de olika elementen i bränslet användes som indata.

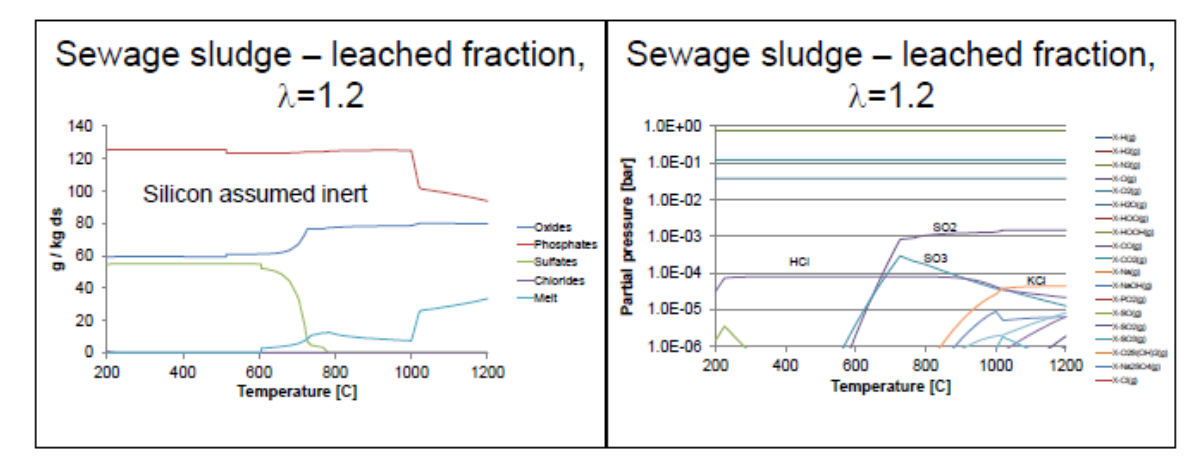


Figure 19 Gaseous species and condensed phases for sewage sludge as a function of temperature at oxidising conditions. Results from chemical fractionation analysis was used as input.

Figur 19 Gasformiga komponenter och kondenserade faser vid tillsats av avloppsslam som funktion av temperaturen och oxiderande förhållanden. Resultaten från den kemiska fraktioneringen användes som indata.

For the calculations of waste wood pellets/sewage sludge mixtures, the conditions were set at $\lambda=1.2$ and 800°C . Only the leached fractions were included in the calculations. No silicon was included in the calculation. The results for the gas phase chemistry are shown in Figure 20. The results show that around 0.1 kg of sewage sludge/kg waste wood pellets on a dry fuel

basis is needed to get a significant decrease of NaCl and KCl in the gas phases. At higher additions of sewage sludge, also SO2 and SO3 increase considerably. Levels of PbCl2 do not change considerably as a function of sewage sludge additions.

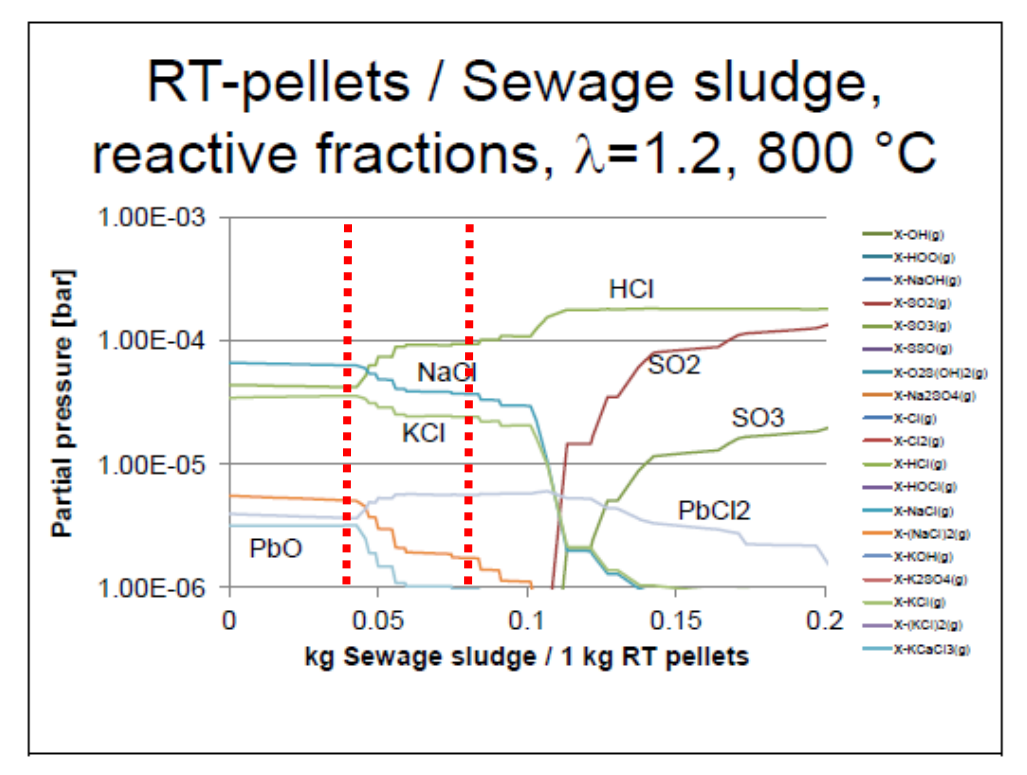


Figure 20 Gaseous species for sewage sludge addition at 800°C and oxidising conditions. The red dotted lines indicate the two levels of added sewage sludge in the tests (40 g and 80 g sewage sludge per kg dry fuel).

Figur 20 Gasformiga komponenter och kondenserade faser vid tillsats av avloppsslam vid 800°C och oxiderande förhållanden. De två röda streckade linjerna visar de två nivåerna av tillsatt slam under testerna (40 g och 80 g torrt avloppsslam / kg torrt bränsle).

For reducing conditions of waste wood pellets/sewage sludge mixtures, the conditions were set at λ =0.7 and 800°C. Only the leached fractions were included in the calculations. No silicon was included in the calculation. The results for the gas phase chemistry are shown in Figure 21. The results show that around 0.1-0.3 kg of sewage sludge/kg RT pellets on a dry fuel basis is needed to get a significant decrease of NaCl and KCl in the gas phases. However, the reduction of KCl and NaCl in the gas phases is not as extensive as for the oxidising conditions. Gaseous lead is mainly as Pb(g) and PbS(g) and zinc as Zn(g), with no significant effect of the addition of sewage sludge.

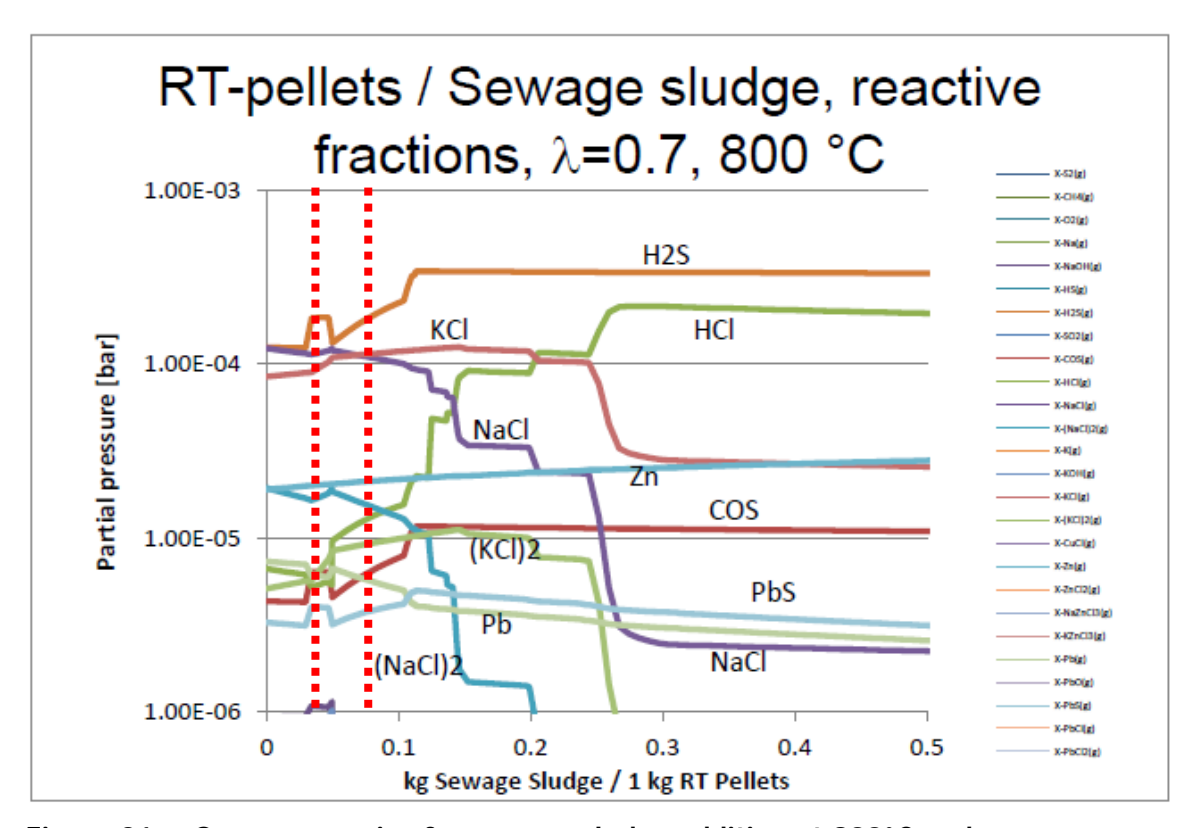


Figure 21 Gaseous species for sewage sludge addition at 800°C and reducing conditions. The red dotted lines indicate the two levels of added sewage sludge in the tests (40 g and 80 sewage sludge per kg dry fuel).

Figur 21 Gasformiga komponenter och kondenserade faser vid tillsats av avloppsslam vid 800°C och reducerande förhållanden. De två röda streckade linjerna visar de två nivåerna av tillsatt slam under testerna (40 g och 80 g torrt avloppsslam / kg torrt bränsle).

Kaolin

Due to the complex nature of KCl capture by kaolin, two cases were made in the modelling. In the first case, it is assumed that kaolin may only react with alkalis to form various Na-and K- silicates or alumina silicates. In the second case, the reaction mechanisms are not considered, only the fraction of Na and K that is captured is considered; thus, the detailed capture mechanism is not included. In the first case, it is calculated that around 10 g kaolin/kg dry fuel is needed to capture all alkalis (Figure 22). In the second case it can be seen around 50% capture of Na and K or higher is needed to get a decrease in the KCl and NaCl in the gas phase. (Figure 23)

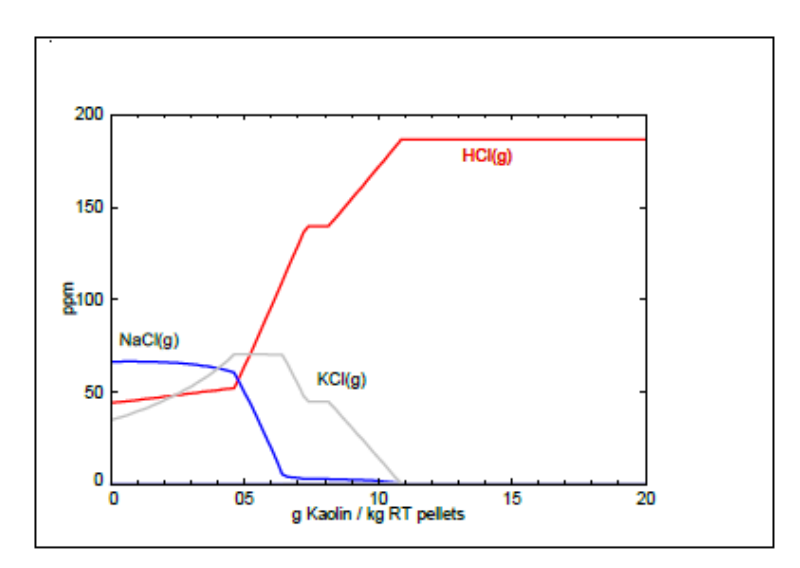


Figure 22 Predicted gaseous NaCl, KCl and HCl for kaolin addition at 800°C and oxidising conditions. Kaolin addition in tests are at 30 g kaolin / kg dry fuel.

Figur 22 Gasformigt NaCl, KCl och HCl vid tillsats av kaolin vid 800°C och oxiderande förhållanden. Tillsatsen av kaolin är 30 g kaolin / kg torrt bränsle.

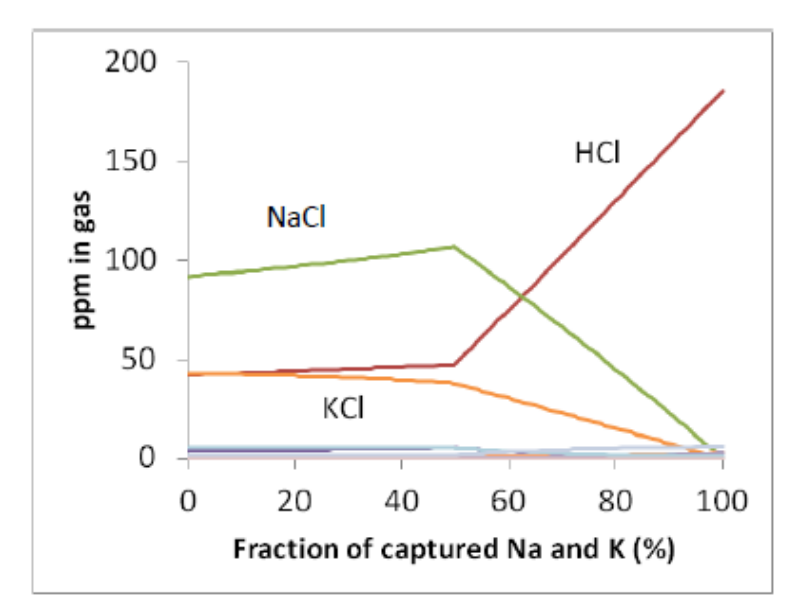


Figure 23 Gaseous NaCl, KCl and HCl as a function of captured Na and K at 800°C and oxidising conditions.

Figur 23 Gasformigt NaCl, KCl och HCl som funktion av fångat Na och K vid 800°C och oxiderande förhållanden.

4.1.3 Summary

Sulphur: At oxidising conditions, the sulphation KCl and NaCl is predicted when all CaO has been sulphated to CaSO4. The levels of PbCl2 and ZnCl2 have a peak as alkali chlorides are sulphated, but when the sulphur level is further increased, Zn and Pb are sulphated as well. At reducing conditions, concentrations of KCl and NaCl are not affected by sulphur additions.

Lime (CaO): No effects on ash or flue gas chemistry can be seen for lime additions.

Sewage sludge: At oxidising conditions, KCl and NaCl are sulphated, however, much higher additions of sewage sludge than what was used in the laboratory tests (and also much higher than what would be realistic in a real boiler) is needed to get a significant reduction of KCl and NaCl. At these additions, also SO₂ and SO₃ increase considerably.

At reducing conditions KCI and NaCI are not affected that much, and the concentrations of NaCI and KCI in the gas phase are higher at reducing conditions.

Levels of Pb compunds do not change considerably as a function of sewage sludge additions.

Kaolin: The reduction of NaCl and KCl by kaolin additions has been modelled, but thermodynamic modelling may not be fully suitable to predict the interactions of alkali chlorides with kaolin.

4.2 Calculations performed by Vattenfall using HSC Chemistry

4.2.1 Method

The objective was to simulate the wood pellets based system with addition of sludge in order to compare the simulation results with the experimentally collected data and to test the effectiveness of sludge as a means to reduce furnace wall corrosion during combustion. The response of the system to the sludge addition as well as different sulphur and chlorine concentrations was investigated.

HSC Chemistry software has been used to perform the calculations. The software calculates the defined state at equilibrium for gas/liquid/solid compounds.

As a first step in order to collect experience with the software and fine tune the system response, the simulation results for different conditions were compared with the results by Åbo Akademi done with FactSage software.

An overview of all simulated cases is presented in Table 15.

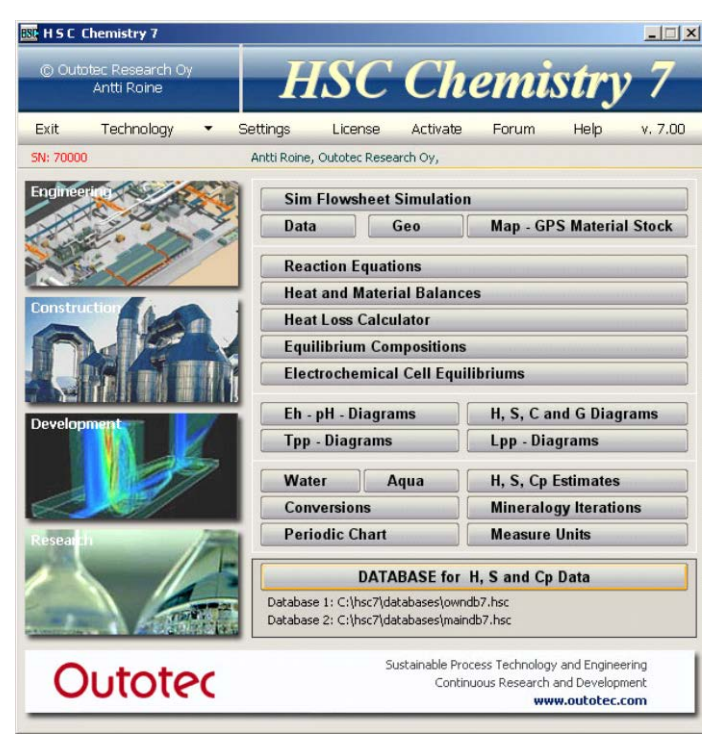


Figure 24 HSC Chemistry 7
Figur 24 HSC Chemistry 7

Table 15. Overview of all simulated cases

Tabell 15. Översikt över alla simulerade fall

	Simulated case	Lambda	Purpose
1	AA-Pellets with Al, Si, Fe	1.2	Fine tuning HSC
2	AA-Pellets without Al, Si, Fe	1.2	Fine tuning HSC
3*	Sulphur added in steps - no saturation reached	1.2	Fine tuning HSC
4*	Sulphur added in steps - saturation reached	1.2	Fine tuning HSC
5	40 g of sludge / kg of fuel	1.2	Sludge as additive
6	80 g of sludge / kg of fuel	1.2	Sludge as additive
7	Clx2	1.2	Varying chlorine content
8	Clx4	1.2	Varying chlorine content
9	Clx0.1	1.2	Varying chlorine content
10	80 g of sludge / kg of fuel + Clx4	1.2	High chlorine + sludge

^{*} For results, see Appendix B

The equilibrium system has been calculated with the fuel composition provided by Åbo Akademi (Table 16). The main focus was on the AA-Pellets sample (the red circle) and this composition has been used for all calculations. Additionally, the sewage sludge composition was used (the grey circle).

Table 16. Fuel and additive composition used in calculations

Tabell 16. Sammansättning använd i beräkningar för bränsle och additiv

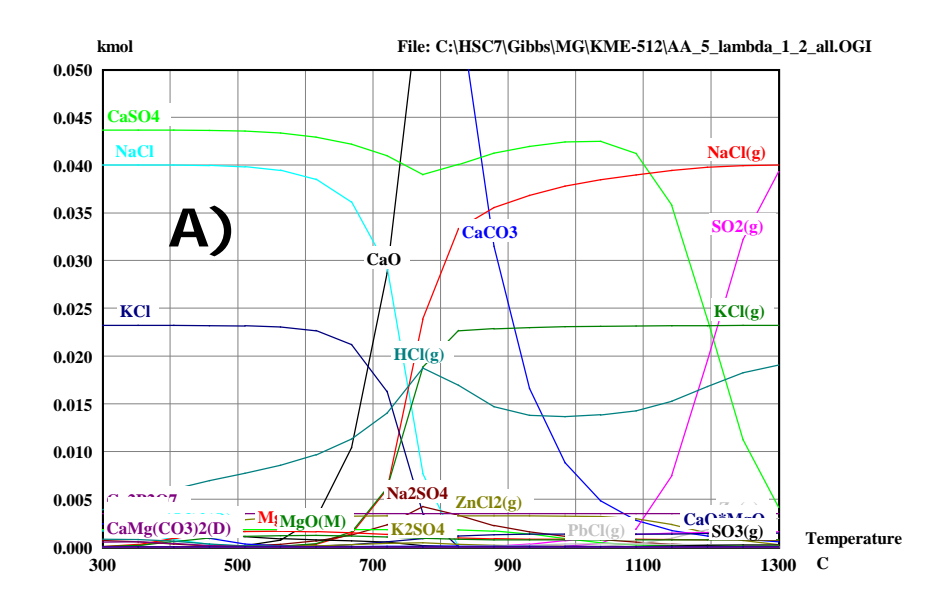
Element (mg/kg fuel on dry basis)	Pellets, ÅA-sample (Spring 2012)	SP Test Pellets (data from SP presentation 2013-02-21)	Sewage sludge
Ash, w-%	9.6	8.6	33.8
S	1 430	1 000	12 670
Cl	1 860	2 600	740
Ca	6 450 (8 630)	7 140	22 870
K	1 590	1 630	3 540
<u>Na</u>	1 950	2 150	1 880
Р	189	232	26 660
Pb, Zn, Cu	376, 212, 1 050	361, 602, 43	11.8, 451, 254

4.2.2 Results

The results are presented in more detail in Appendix B.

If all elements from the fuel analysis are included in the calculations, the system is dominated by Al and Si and the equilibrium composition is shifted towards formation of alkali alumina silicates (M-Al-Si). Different forms of K, Na, Ca based alumina silicates dominate over the whole temperature range. However, the system where Al and Si dominate the system completely is far from reality. In reality not all reactions with alumina silicates take place. Therefore, Al, Si and Fe have been excluded from the calculations.

In Figure 25 (A and B) the results without AI, Si and Fe are presented. In this figure formation of CaO and $CaCO_3$ together with decomposition of solid NaCl and KCl into the gaseous forms is visible. The simulation of the system without AI, Si and Fe allows checking the response of the system to these elements and allows better tracking of the fate of alkali chlorides. The results comply with the results from Åbo Akademi done with the help of FactSage software (see Figure 9).



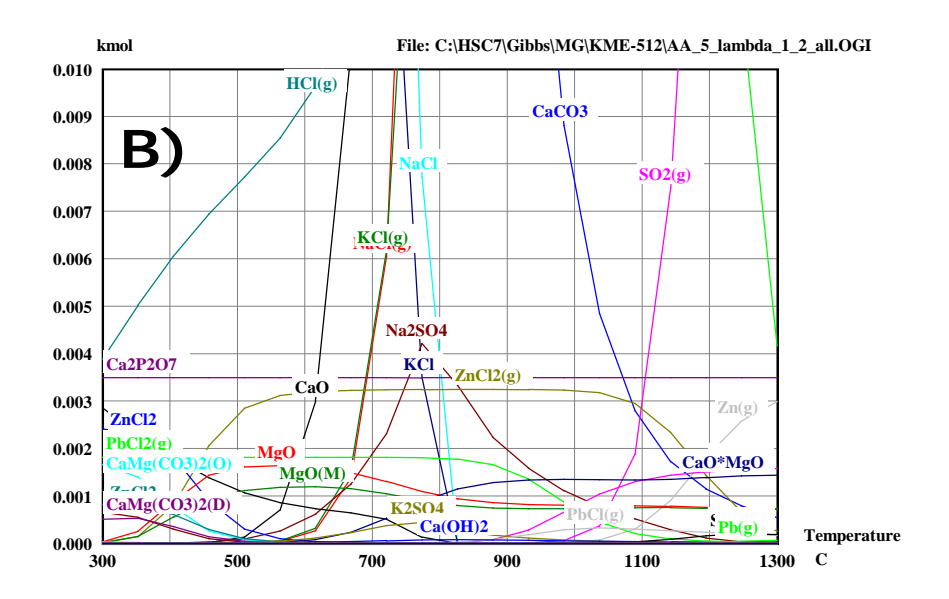


Figure 25 Base equilibrium system for the fuel AA-pellets, AI, Si, Fe have been excluded from the system. A) scale bis 0.05 kmol, B) scale bis 0.01 kmol – compounds with lower concentrations visible

Figur 25 Jämviktssystem för basfallet, ÅA-pellet. Al, Si och Fe har exkluderats från systemet. A) skala till 0,05 kmol, B) skala till 0,01 kmol – där syns även föreningar med lägre koncentrationer.

Adding sludge to the system

The composition of the sludge presented in Table 16 has been used. It can be seen that the sludge has much higher content of sulphur, calcium and phosphorus than the AA-pellets. Especially sulphur is expected to act as sulphating agent for corrosive alkali metals based compounds when sludge is added as additive to the combustion process. In order to test this approach and see if there is influence of sulphur on the whole system together with side effect of Ca and P, addition of sludge has been simulated with the HSC chemistry software. Two different amounts of sludge have been added to the system, 40 g of sludge/kg of fuel and 80 g of sludge /kg of fuel. The whole temperature range between 300°C and 1300°C has been shown in order to show and track the changes between components predicted by the chemical equilibrium. In Figure 26 one can observe that at 300°C the alkali metals are at equilibrium in solid form. It has to be stressed that the system presented at the underlying figures does not always represent the reality in the boiler but indicate the chemically stable compounds at the certain temperature range. The actual release of alkali metals may follow other paths and depends on heating rates, combustion technology and is discussed in section 4.3.2.

40 g of sludge / kg of fuel

It can be seen (Figure 26) that sludge addition causes some shifts in the global equilibrium of the system comparing to the base case scenario (Figure 25), especially in Ca and P chemistry. One can observe that calcium and phosphorus are much more present (Figure 26– red circle). From other side there is little effect on alkali system and related sulphating type of reactions.

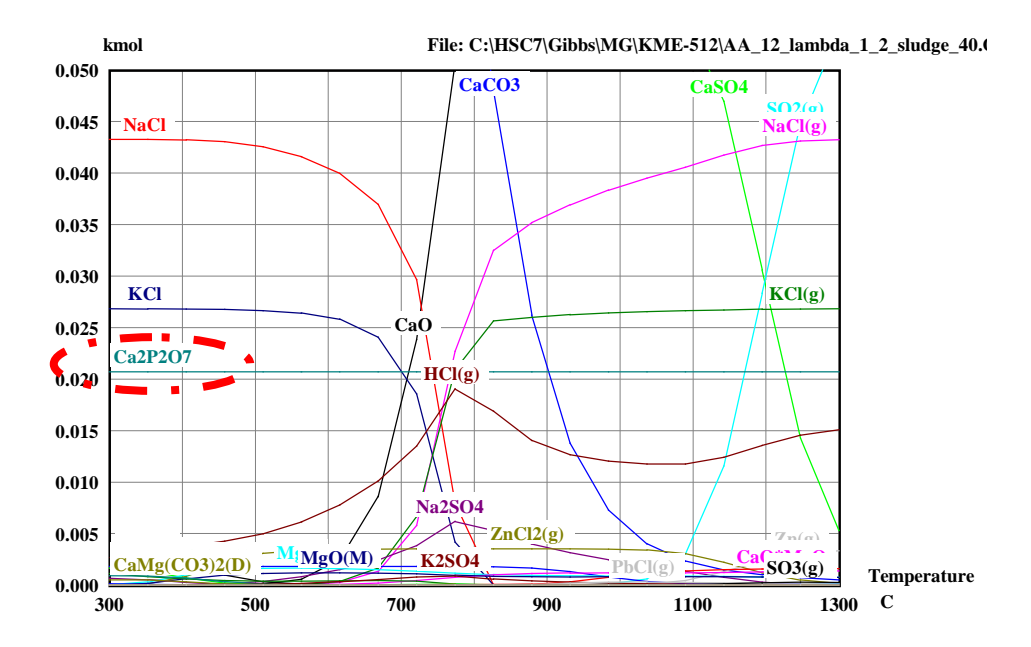


Figure 26 The equilibrium system for the fuel AA-pellets. 40 g of sludge / kg of fuel added to the system, some shift towards formation of Ca/P compounds visible (red circle)

Figur 26 Jämviktssystem för ÅA-pellets vid tillsats av 40 g slam/kg bränsle. En förskjutning mot bildanden av Ca/P-föreningar kan ses (röd cirkel).

80 g of sludge / kg of fuel

As the next step the double amount of sludge has been used, namely 80 g of sludge per kg of fuel has been added. It means even more Ca, P and S present in the system. It can be seen (Figure 27) that sludge addition causes some shifts in the global equilibrium of the system especially in Ca and P chemistry comparing to the base case scenario (Figure 25) and the shift is stronger than in the 40 g/kg case. Twice as much of $Ca_2P_2O_7$ is present in the system according to the equilibrium software. There is little effect on alkali system and related sulphating type of reactions.

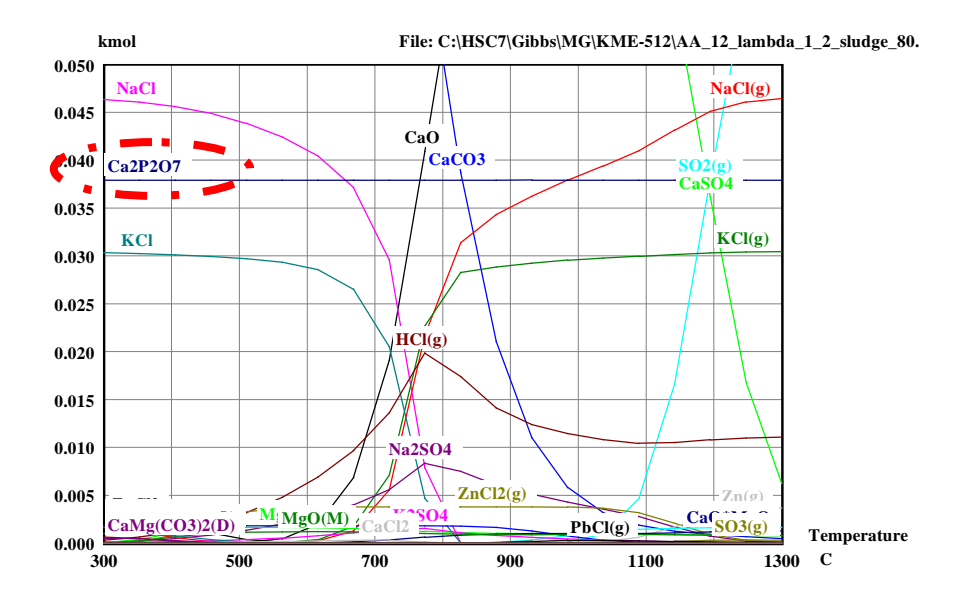


Figure 27 The equilibrium system for the fuel AA-pellets. 80 g of sludge / kg of fuel added to the system, some shift towards formation of Ca/P compounds visible (red circle)

Figur 27 Jämviktssystem för ÅA-pellets vid tillsats av 80 g slam/kg bränsle. En förskjutning mot bildanden av Ca/P-föreningar kan ses (röd cirkel).

Varying the chlorine content of the system

In order to test the system sensitivity to the chlorine content the chlorine content in the fuel has been changed (calculated S/Cl ratio – see Table 17). The equilibrium conditions have been calculated for:

- chlorine content x 2
- chlorine content x 4
- chlorine content x 0.1

Additionally to that for the case where 4 times more of chlorine was present in the system also 80 g of sludge composition has been added and calculated.

Table 17 The sulphur to chlorine ratio for the simulated cases

Tabell 17. Svavel/klor-kvoten för de simulerade fallen

Case	Ratio (2S/CI)
base case	3.01
Clx2	1.51
Clx4	0.75
Clx0.1	30.11

Chlorine content x 2

It can be seen (Figure 28) that the increased chlorine content causes an increased HCl presence comparing to the base system presented in Figure 25. The amount of KCl is at the same level comparing to the base case (Figure 25). It means that no more potassium is available or the reaction to form HCl is preferable.

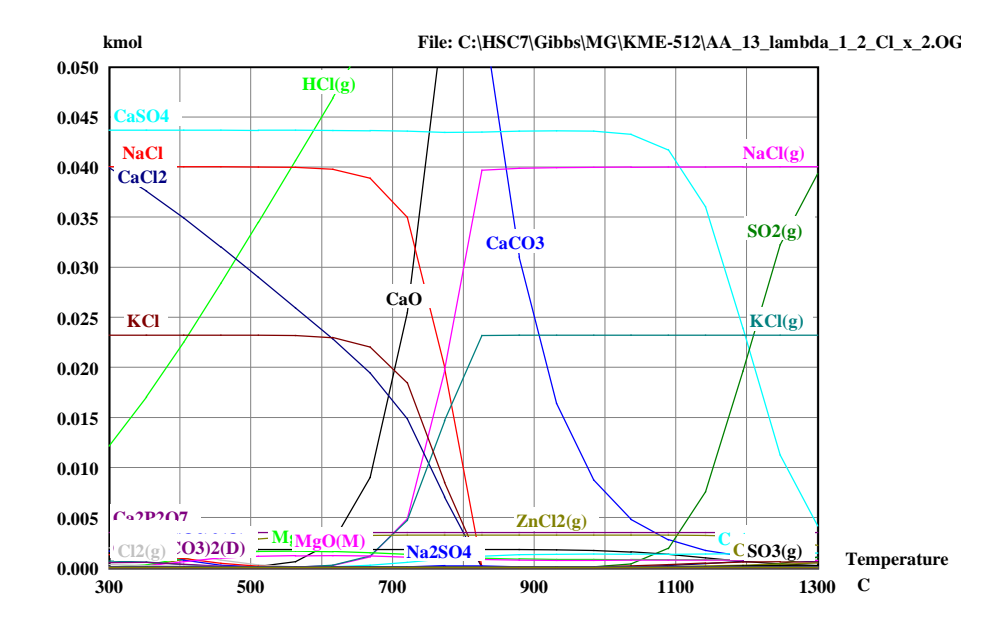


Figure 28 AA-pellets with chlorine content x 2

Chlorine content x 4

In Figure 29 it can be seen that the increase chlorine content caused even more radical increased of HCl presence comparing to the base case system presented in Figure 25.

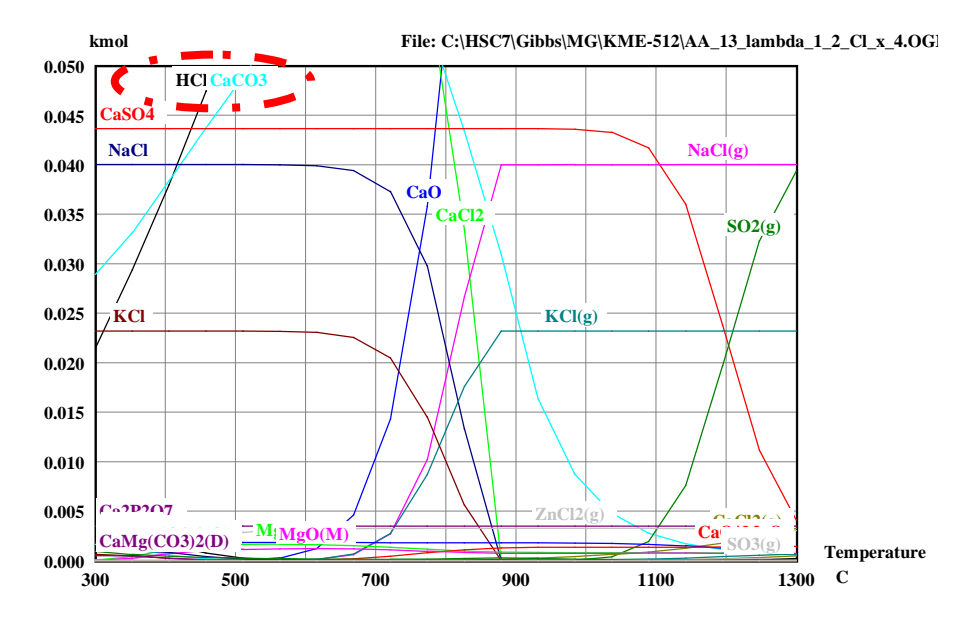


Figure 29 AA-pellets with chlorine content x 4
Figur 29 ÅA-pellets med fyrdubblad klorhalt

The HSC software predicts that at equilibrium the additional chlorine added to the system is being released as HCl. Also $CaCl_2$ is present on much higher concentrations than for the case chlorine x 2 (Figure 28). Other compounds seem to be not much influenced. The KCl concentrations are at the same level as for the case with double chlorine amount (Figure 10) and at the same level comparing to the base case Figure 25. The formation of KCl is limited by the K availability. Calcium carbonate is predicted to be the most stable Ca based compound.

Chlorine content x 0.1

It is visible that ten times lower chlorine content (Figure 30) causes very significant changes in the system comparing to the base case Figure 25 scenario. The amount of NaCl and KCl is much lower than in other scenarios. Also the HCl(g) is not visible in the gas phase. All available chlorine is being present as alkali chlorides. Calcium carbonate is predicted to be the most stable Ca based compound.

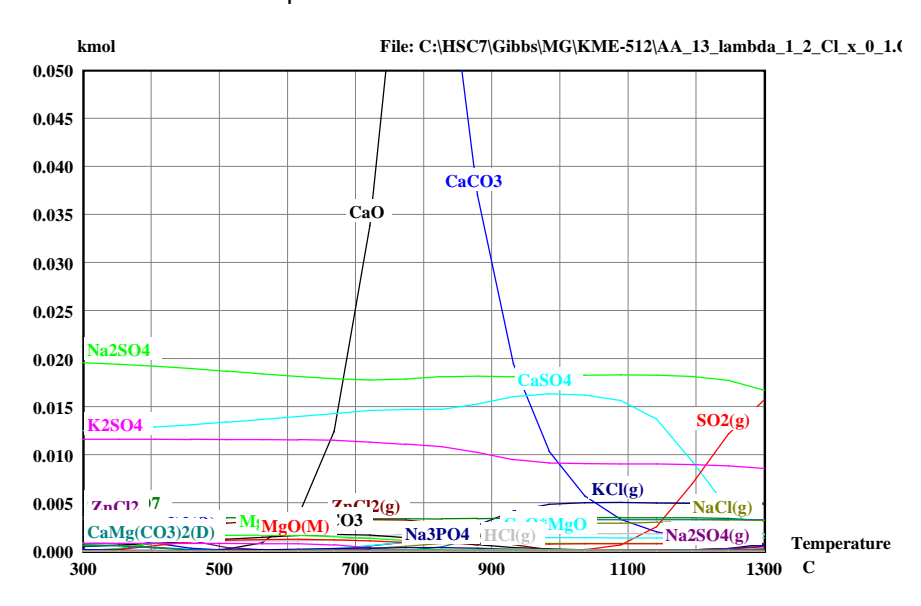


Figure 30 AA-pellets with chlorine content x 0.1

Figur 30 AA-pellets med klorhalt x 0,1

Chlorine content x 4 + sludge 80 g sludge / kg fuel

In order to check the interactions of increased chlorine content in combination with increased sulphur amount originating from sludge, a case with increased chlorine content and sludge addition has been simulated.

The results reveal that there is little difference on the chlorine/sulphur chemistry comparing the case chlorine content x 4 (Figure 29) with the case chlorine + sludge case (Figure 31, mind scale difference comparing with Figure 29). With sludge some potassium and sodium has been added to the system and as a result the concentration of alkali chlorides increased. There is much more influence on the Ca/P system as observed previously with the sludge only simulations.

According to the HSC software this amount of sludge was not able to lower the gaseous KCl and NaCl content with help of more present sulphur in the gas phase but even increased the amount of KCl and NaCl slightly due to more K and Na present in the system originating from the sludge.

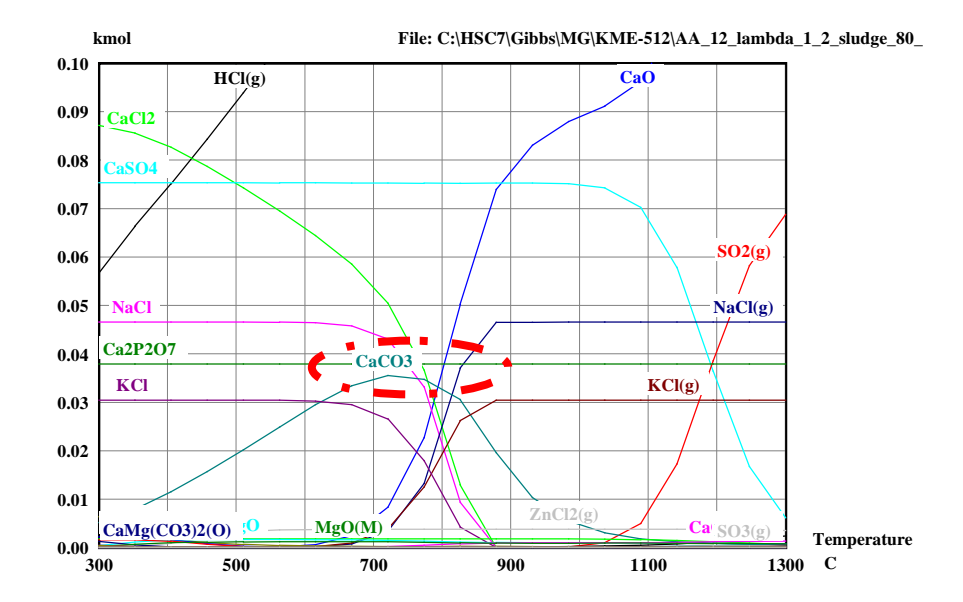


Figure 31 AA-pellets with chlorine content x 4 and sludge added (80 g of sludge/kg of fuel)

Figur 31 ÅA-pellets med fyrdubblad klorhalt samt tillsats av slam (80 g slam / kg bränsle)

4.2.3 Summary

Increasing the CI content of the system led to an increase in HCI emissions and a slight increase in KCI and NaCI.

Adding sludge to the system caused substantial shift in Ca toward compounds with P, due to the high Ca and P content. The use of sludge as additive in a case with increased Cl content (the last simulated case) did not modify the corrosive alkali-chlorine system in a substantial way.

4.3 Discussion

4.3.1 Comparing thermodynamic equilibrium calculations with experimental findings

In order to relate the results of simulations with the experimental findings delivered within the project by SP, a comparison is made between the outcome of the calculations and the results of the laboratory tests performed by SP. The operational conditions for the SP tests have been summarised in Table 18 and the results of the thermodynamic equilibrium calculations and the laboratory tests are summarised in Table 19 below.

Table 18 Operational parameters for the SP tests

Tabell 18. Driftparametrar för testen på SP

	Ref 1	SWS1	s	Kao	FS	Lime	Ref 2	SWS2	PbO	PbO +SWS
O ₂ [%, d.g.]	4,90	5,07	5,22	5,14	5,09	5,26	5,26	5,18	5,30	5,34
CO [ppm,d.g.]	37	19	34	36	15	16	15	30	13	10
NO [ppm, w.g.]	267	287	280	339	289	272	266	300	270	312
SO ₂ [ppm, w.g.]	11	20	<u>284</u>	24	19	8	4	43	5	33
HCI [ppm, w.g.]	213	244	<u>348</u>	248	230	<u>117</u>	231	227	266	281
H ₂ O [%, w.g.]	12,4	12,6	13,0	13,0	13,1	12,8	12,7	12,3	13,0	13,0
CO ₂ [%, w.g.]	13,9	14,5	14,6	14,7	14,5	14,2	14,4	14,3	14,5	14,1
T _{bed} [°C]	799	799	800	800	800	800	800	800	800	800
T_1 [°C]	907	911	903	878	875	879	873	871	875	870
T_2 [°C]	924	936	935	924	934	930	940	919	937	919
T_3 [°C]	779	779	785	784	785	786	784	782	778	780

 $SWS-Sewage\ sludge,\ S-elemental\ Sulphur,\ FS-Foundry\ Sand,\ w.g.-wet\ gas,\ d.g.-dry\ gas.$

Table 19 Comparison between laboratory test results, FactSage and HSC results

Tabell 19. Jämförelse mellan resultat för laboratorietester, FactSage och HSC

	FactSage (Åbo Akademi)	HSC (Vattenfall)	Lab tests (SP)
Waste wood	To avoid unrealistic results, Al, Si, Fe, Mn and Ti from the fuel were omitted in the calculations. Only the easily leached fractions from the fractionations were used as input for the following elements K, Na, Ca, Mg, and P. All S, Cl, Zn, Pb, and Cu were included in the calculations.	To avoid unrealistic results, AI, Si and Fe from the fuel were omitted in the calculations.	
Sulphur, oxidising	At oxidising conditions, sulphation of KCl and NaCl is predicted when all CaO has been sulphated to CaSO ₄ . If sulphur is added in larger amounts than needed for sulphation of KCl, NaCl and CaO, HCl will reach a maximum concentration in the gas phase and SO ₂ will increase as a function of sulphur addition. The level of PbCl ₂ and ZnCl ₂ has a peak as alkali chlorides are sulphated. PbCl ₂ and ZnCl ₂ are predicted to be sulphated with higher sulphur additions.	Additional sulphur addition led to the formation of calcium sulphate and with further addition of sulphur, the surplus of S is being released as SO ₂ .	CI was nearly eliminated, whereas S increased on the SH probe. Nearly all CI was present as HCI, which was increased as compared to the reference case. High increase of SO ₂ in flue gases. Pb increased slightly on SH probe and in fly ash.
Sulphur, reducing	At reducing conditions, concentrations of KCI and NaCI are not affected by sulphur additions.		CI was slightly decreased and S increase in the deposits on the BW probe. Pb increased slightly in fly ash and was slightly reduced on BW probe and walls.
Lime, oxidising	No effects on the chemistry for lime additions.		Decreased content of HCl in the flue gases, instead binding the Cl to the ashes (and deposits). Strongly increased amount of fly ash. Increased amounts of Cl in the fly ash and on SH probe. A small part of the Pb has been bound to the bottom ash by lime, but the main part still remains in the fly ash. Zn, on the other hand does not seem to have been influenced by addition of lime.

Lime, reducing	No effects on the chemistry for lime additions.		Increased amounts of CI and slightly increased amount of S in the fly ash and BW probe. Strongly increased amount of fly ash. A small part of the Pb has been bound to the bottom ash by lime, but the main part still remains in the fly ash. Zn, on the other hand does not seem to have been influenced by addition of lime.
Sewage sludge, oxidising	At oxidising conditions, KCI and NaCI are sulphated.	Adding sludge to the system caused substantial shift in Ca toward compounds with P, due to the high Ca and P content.	SO ₂ in the flue gases increases. The amount of CI is significantly decreased on both probes. Zn is decreased on both probes. P is increased in all solid fractions.
Sewage sludge, reducing	KCI and NaCl are not affected that much. At high sewage sludge additions, part of the alkali metals are transformed into alkali phosphates.		The amount of CI is significantly decreased on both probes. Zn is decreased on both probes. P is increased in all solid fractions.
Kaolin	The reduction of NaCl and KCl by kaolin additions has been modelled but thermodynamic modelling may not be fully suitable to predict the interactions of alkali chlorides with kaolin due to complex reaction mechanisms between the kaolin and the alkali chlorides.		The amounts of deposits on the BW probe, fly ash and bottom ash are strongly reduced. The amount of loose deposits on the SH probe increases and the amount of hard deposits decreases. The amount of Cl is reduced in fly ash, in bottom ash and on the BW probe. Kaolin substantially reduces both BW and SH corrosion.

The influence of sulphur on the chemistry is well predicted by the calculations, whereas the predicted influence on the chemistry of the other additives did not clearly match the experimental observations. The reason why the predictions for sulphur additions were similar to the experimental observations may be related to the rather simple chemistry of the sulphur additive, and possibly also related to the formation of reactive gaseous sulphur species, such as SO_2 , SO_3 , and H_2S , which can react easily with the ash-forming elements in the primary fuel. Reactions between sulphur species and volatile chlorides may occur directly in the gas phase. On the other hand, the other additives are either complex mixtures (sewage sludge) or may require complex surface reactions involving solid phases, which are more complex and generally slower than gas phase reactions. This may be a reason why the calculations for these additives do not predict the chemical reactions as well as for the sulphur case, as chemical equilibrium will not be attained to the same degree.

A comparison has also been made between the outcome of the thermodynamic equilibrium calculations and the composition of the deposits collected during the tests at SP. Figure 32 presents the fly ash composition as collected and analysed by SP and Figure 33 presents SH deposits and their composition as collected and analysed by SP. It is assumed that the temperature in the SP reactor varied depending on the location and was between 770 - 930°C.

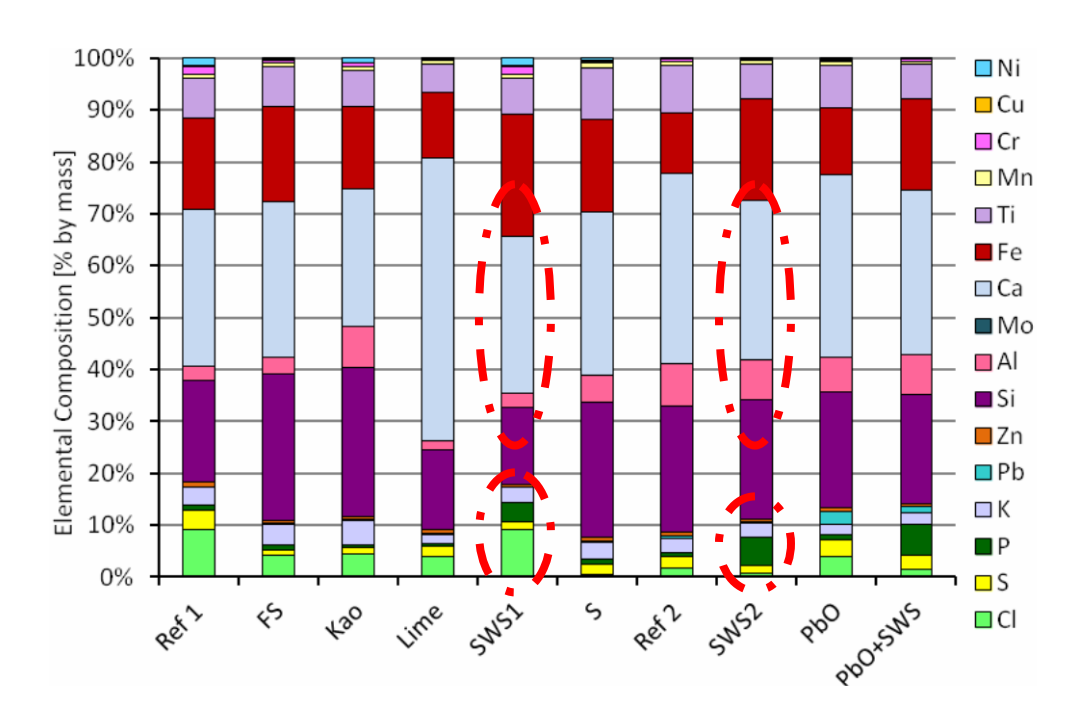


Figure 32 Fly ash composition – SP tests

Figur 32 Flygaskans sammansättning vid SPs test

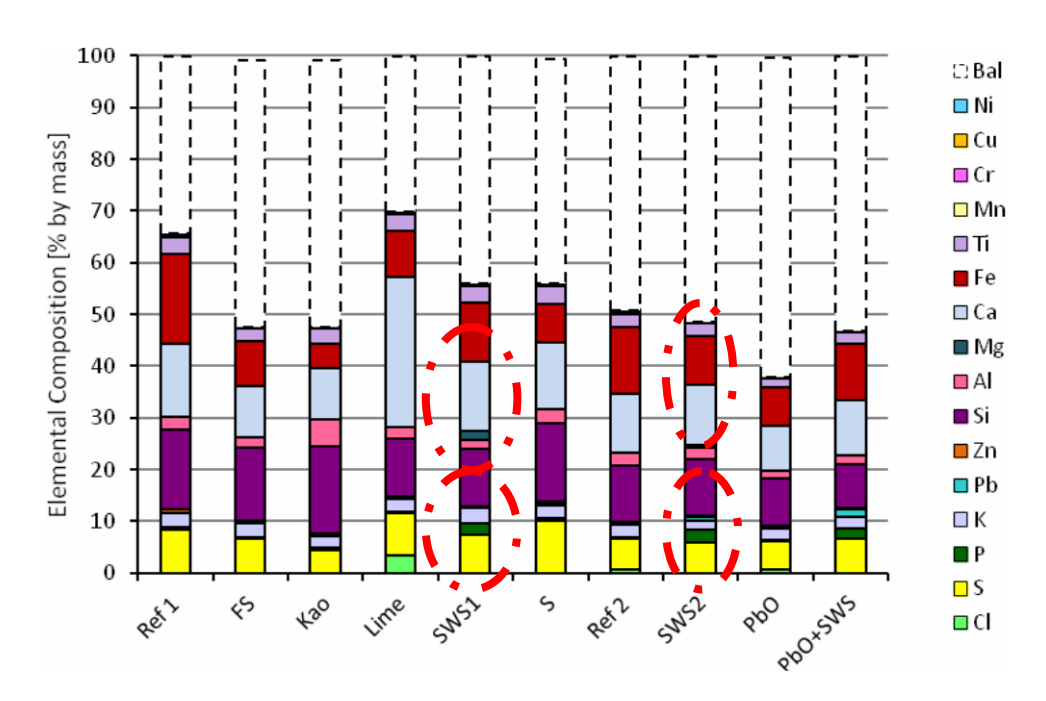


Figure 33 SP tests, SH deposits composition

Figur 33 Test på SP, sammansättning för avlagringar på överhettarna

It is visible that the fly ash composition has been influenced by the sludge composition (SWS1) added to the system as one of the additives. One can observe that P content for sludge (SWS) in the fly ash and SH deposits are clearly higher than for all other cases. The Ca content remains constant (Figure 32 + Figure 33) but there is no increase as in the case of lime addition. The sludge added to the system adds also these two elements. This was predicted with HSC equilibrium software where the formation of Ca and P based compounds was clearly visible after the sludge addition. Looking at the fly ash composition one can observe that also the chlorine content remains quite high after the sludge addition. For the SH ash it is not the case any more. Also for the double amount of sludge case (SWS2) the chlorine content both in the fly ash and in the superheater deposits was lower.

One has to be aware of different mechanisms which may take place. It is still open which mechanism is responsible for the corrosion reduction observed by SP in case of sludge addition. It can be related to the sulphur present and sulphating reactions taking place primary or secondary in deposits, reducing the chlorine attack. It can also be related to the alumina-silicates present in sludge. The reaction between alkalis and alumina-silicates with release of chlorine are thermodynamically favourable and may be result of the sludge addition.

Analysing the Ca-P based HSC response and comparing it with the experimental findings from SP one has to be careful when modelling a system with phosphates being present. The thermodynamic data for solid and liquid phosphates in the commercial databases as HSC are usually very scarce [71]. Many of the K-Ca-phosphates even lack experimental determination of the thermodynamic properties. It means that the HSC response to phosphates present in the sludge may not always be correct.

One can observe that the SH deposits show a similar trend. Only for the lime addition, the Ca content in fly ash and SH deposits were higher in Ca, but this is due to lime added to the system. In case of SH deposits there was no Cl found which could indicate deposits sulphation. This type of reaction is very difficult to predict with HSC due to the programme limitations to the gas phase mostly.

4.3.2 Chemical equilibrium calculations – applicability and limitations Chemical equilibrium analysis is a useful tool in the study of a variety of processes, and it has been widely used to evaluate many environmental, geochemical, and technical processes. Moreover, equilibrium studies have proven valuable in verifying and understanding the chemistry of heavy metals in combustion systems.

Chemical equilibrium calculations can be a useful tool for R&D and operational engineers when dealing with new (biomass) fuel types and mixtures and helping with operational issues like corrosion or deposits formation. They can predict general trends in ash chemistry, such as elemental distribution and chemical speciation at varying conditions (T, lambda, amount of additive). They can also be used to calculate local chemical equilibria, for example melting of deposits. Of course the method will not provide all answers but may indicate problem areas.

The equilibrium calculation itself takes into account only the chemistry of the system and based on the mathematical calculations tries to minimise the Gibbs free energy of the system to check at which composition the system is at equilibrium. The equilibrium calculation process assumes infinite amount of time available for the chemical reactions to happen in contrary to the situation in real boilers. In reality some reactions will happen faster and some slower, all of them controlled by kinetics. One has to be careful when analysing the results. One example can be alkali release and the secondary sulphation reactions of alkali metals which happen in two steps and one step is kinetically slow (Figure 34).

Another limitation is that variations in reactivity of ash-forming matter cannot be accounted for without additional information about the fuel.

During the first stages of decomposition fuel particles dry and devolatilise. In this process, hydrocarbons, CO, CO $_2$ and H $_2$ O are released from the fuel particle. It has been suggested that the alkali release in case of biomass may already start during the devolatilisation of the biomass fuel at relatively low temperatures (around 400°C). Further increase in the temperature causes an increased amount of alkalis detected. It is believed that there are two different types of alkalis, namely the pyrolysis alkalis, organically bound in the structure of the fuel and the ash alkalis emitted in the higher temperature range. Moreover Davidsson [69] observed that small particles release more alkali per unit initial particles mass than large ones.

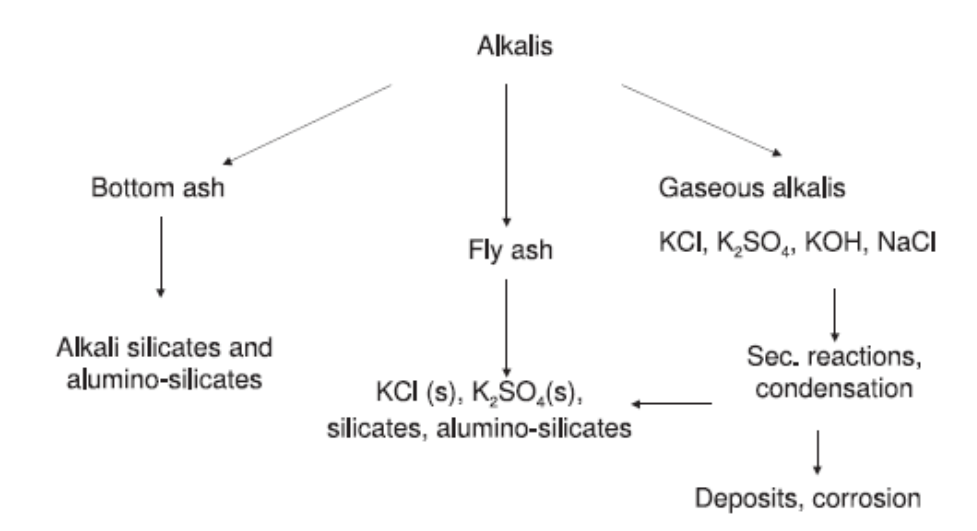


Figure 34 Fate and release of the alkali metal in a typical combustion system [49]

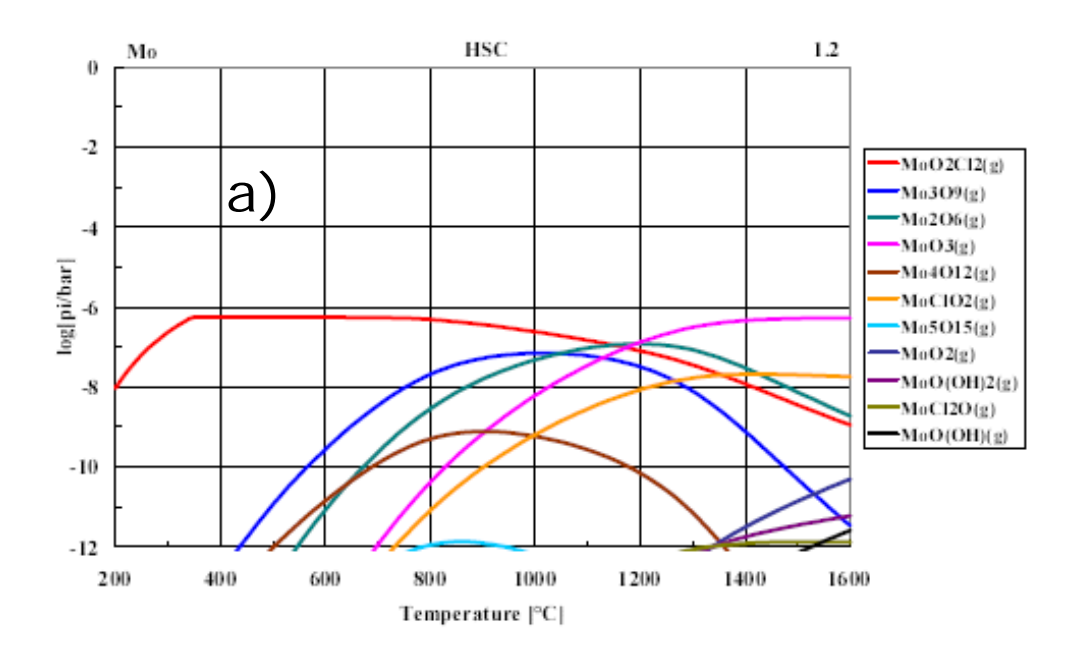
Figur 34 Beteende hos alkalimetaller i ett typiskt förbränningssystem. [49]

According to literature, if the temperature is high enough several inorganic transformations take place. Especially the alkali metals will experience surface migration, vaporisation to the gas phase or coalescence with incorporation into the fuel silicate structures or for coal into alumina silicate structures [70]. Not all alkalis from high alkali biomass are released to the gas phase. Cl acts as a shuttle in transporting potassium from the fuel structure to the outside. Depending on the conditions in a reactor (reducing, oxidising environment) the alkalis can be released in the form of chlorides, hydroxides or sulphates or transferred to sulphates in secondary reactions. The form, composition and place of deposits depend also on the flow conditions and the temperature field in the boiler. The chemical equilibrium method does not take into account anything related to the flow conditions in the boiler and boiler geometry which may influence the deposits formation and composition.

Equilibrium predictions are highly sensitive to the input data. All relevant species of the system must be taken into account, and the numerical values of the constants must be correct and consistent. If some important species are omitted from the calculations or the data is not correct, the results can be very misleading. In practice, investigators often attribute the discrepancies between the experimental data and the results of calculations to the absence of chemical equilibrium in the system or to incorrect parameters in the model used, while the actual reason may be errors in the thermodynamic data. Even in cases where equilibrium is not actually reached, equilibrium analysis might

still be the best approximation possible since kinetic data are not always available for the chemical systems that occur in combustion systems [68].

There appear to be significant differences in the thermodynamic values of compounds in different databases. Figure 35 shows all the gaseous molybdenum compounds that are formed under oxidising conditions according to the HSC (a) and FACT (b) databases. It can be clearly seen that there are far more gaseous compounds formed according to HSC than according to FACT. While most of the compounds are also present in the FACT database, their thermodynamic values are so different that they do not become stable.



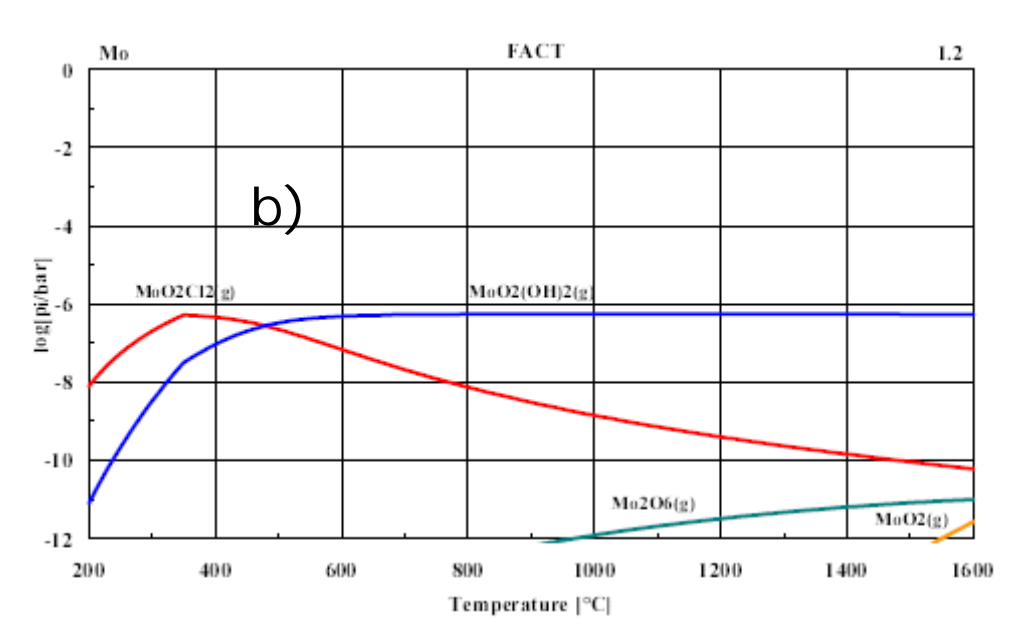


Figure 35 Comparison between a) HSC and b) FactSage and their ability to predict the equilibrium for Mo compounds. The figure illustrates the significant differences between the results.

Figur 35 Jämförelse mellan a) HSC och b) FactSage och deras förmåga att beräkna jämvikter för Mo-föreningar. Figuren visar på betydande skillnader mellan resultaten.

Summarising, thermodynamic equilibrium calculations are a useful tool for some initial analysis of a new fuel and its influence on the boiler. It can also be used to help analyse operational problems experienced at the site. Process optimisation like optimal fuel mix for a certain specific type of boiler is also a possible application. Nevertheless one has to be careful and always an expert knowledge needs to be applied when analysing the results. The results often need to be supported by experimental findings and sound thermodynamic databases.

4.3.3 Comparing the two calculation programmes

A comparison between the Åbo Akademi calculations (FactSage) and Vattenfall calculations (HSC) reveals that the oxidising conditions cases were characterised in a similar way by the both calculation tools. (Table 19)

The main conclusions (lessons learned) from the comparison between the two software can be summarised:

- IT is difficult to compare the cost for the two software, since the setup of licenses is different for HSC and FactSage. However, in general it seems that HSC is cheaper than FactSage.
- FactSage can include multicomponent liquid phases, such as slags and molten salts. Molten slags were not well represented by the HSC software used by Vattenfall. HSC software has in general limited ability to predict molten slags due to database limitations. For this area FactSage shows better performance.
- The Thermodynamic databases of FactSage are often evaluated, leading to more reliable thermodynamic data.
- HSC contains thermodynamic data for more compounds, but the quality not necessarily checked.
- K₂Si₄O₉ (s,I) are K2Si4O5 (s,I) are not present in the HSC database. These compounds might be present during biomass combustion and form sticky deposits.
- The equilibrium system is heavily influenced by Si and Al presence. Addition of Si and Al based on the AA pellet composition moved the whole equilibrium system heavily into alumina silicates formation. Although the effect of silica-alumina binding is positive in general such a strong influence will not occur in reality. Therefore in order to test the influence of other elements (like sulphur and chlorine) Al, Si and Fe have been excluded in the HSC calculations. During 100% biomass combustion no (or little) stable (alkali) alumina silicates are formed because the Si and Al in biomass are in a different, form than the alumina silicates in coal (or kaolin). Investigation of the saturated kaolin by means of XRD reveals that it contains primarily nephelite and carnegieite which are sodium alumina silicates polymorphs with the chemical formula Na20. Al203. 2SiO2. These compounds are stable and have high melting temperatures. In pure biomass combustion is it less probable they will be formed. That is the reason AA removed the Si + Al from the system. The Vattenfall investigation using HSC

- showed similar system results meaning the HSC software was responding in a similar way as FactSage
- Sulphur addition to the system has been tested. In general all sulphur added formed CaSO₄ until there has been free Ca present in the system. When the level of Ca (CaSO₄) stabilised the concentration of SO₂ increased. These results from HSC response are also in agreement with the results from FactSage.

4.4 Conclusions

The calculated results show that FactSage and HSC chemistry can be effectively used to predict the reactions in the gas phase from the fuel or/and (new) fuel mixtures. The tools can be used to check potential influence of a fuel blend and the dominant chemical reactions in the system.

Additional sulphur addition led to the formation of calcium sulphate and with further addition of sulphur, the surplus of S is being released as SO_2 . In case of Cl addition one could observe an increase in HCl emissions and a slight increase in KCl and NaCl.

Adding sludge to the system caused substantial shift in Ca toward compounds with P, due to the high Ca and P content. The use of sludge as additive in a case with increased Cl content (the last simulated case) did not modify the corrosive alkali-chlorine system in a substantial way.

According to the HSC software the sludge was not able to lower the gaseous KCI and NaCI content with help of more present sulphur in the gas phase but even increased the amount of KCI and NaCI slightly due to more K and Na present in the system originating from the sludge. The measurements performed by SP revealed that sludge was effective in reducing chlorine induced corrosion and the amount of chlorine observed in deposits collected experimentally was lower. It can be related to the alumina-silicates present in sludge. The reaction between alkalis and alumina-silicates with release of chlorine are thermodynamically favourable and may be result of the sludge addition. This can be related to secondary sulphation reactions which are not being represented properly by HSC chemistry.

HSC software could a useful tool for some initial analysis of a new fuel and its influence on the boiler. It can be also use to help analyse the operational problems experience at the site. Nevertheless caution and proper analysis is required.

In general, the Factsage software offers similar capabilities as HSC, with the main difference being that the formation of complex molten ash phases can be predicted in Factsage, but not with HSC. The thermodynamic databases are also different in HSC and Factsage, which also gives rise to differences in results when comparing the two programs. Differences between predicted ash chemistry and experimental observations may partly be explained by differences in thermodynamic data, but the main uncertainty and source for error in both the predictions by HSC and Factsage is the proper choice of

input from the fuel analysis as well as assessing the attainment of chemical equilibrium when chemically complex additives and ash interact.

Thermodynamic equilibrium calculations may be more useful in studying trends when adding different elements or additives then trying to fit detailed experimental observations with predicted ash chemistry.

5 Laboratory tests

The laboratory tests were performed in a fluidised bed reactor fired with demolition wood mixed with different additives. The additives tested were kaolin, sewage sludge, lime, foundry sand and sulphur. Since it is believed that lead (Pb) can aggravate waterwall corrosion, addition of lead in the form of PbO to the fuel was also tested. Corrosion probes were inserted in two positions. One probe was located in the primary combustion zone with gas conditions similar to boiler wall conditions in the lower part of the furnace in a large-scale unit. The other probe was located close to the exit of the reactor, and exposed at conditions similar to a superheater. The material temperatures of the two probes were 400°C and 550°C, respectively. The corrosion probes were exposed for 8 hours per test, and each probe carried three metal ring samples parallel mounted, of three different steels: 16Mo3, 253 MA and Kanthal A1.

The deposits formed on the exposed sample rings were weighed and chemically analysed by handheld XRF. After removal of the deposits, the extent of the corrosion attacks on the sample rings were studied by optical microscopy. Selected rings were also analysed by SEM-EDX. Furthermore, analyses were also made on bottom ashes, fly ashes, wall deposits and the gas concentrations of NO_x , SO_2 , HCl and CO_2 were monitored by conventional gas analysers and FTIR-instrument.

5.1 Test plan

In total ten tests have been performed in the laboratory reactor, divided in two sets. In the first set, five different additives were investigated and compared to a reference run with no additive. Based on the results from the first set of tests, sewage sludge was selected for further testing in the second set of tests and tests with addition of lead (Pb) in the form of PbO to the fuel were also performed.

The amounts of additives to be used in the tests were decided based estimates of the effectiveness of the different additives in reducing waterwall corrosion. What amount that could realistically be used in a boiler was also considered. This is further described in Appendix A. The amount of sulphur, however, is higher than what is used in a real boiler.

The composition of the fuel pellets, including the additives used is presented in Table 21.

Table 20 Test matrix, showing additives added to the fuel, waste wood.

Tabell 20. Testmatris som visar vilka additiv som tillsatts till bränslet, returträ

Case	Additive	Conc.	Materials investigated	Temp. SH	Temp. Wall	Temp. bed	Air ratio (SH)
		[g/kg]		[°C]	[°C]	[°C]	
Ref 1	None (Reference)	0	KanthalA1/253MA/16Mo3	550	400	800	1,3
S	Sulphur	10	KanthalA1/253MA/16Mo3	550	400	800	1,3
SWS1	SWS*	40	KanthalA1/253MA/16Mo3	550	400	800	1,3
Kao	Kaolin	30	KanthalA1/253MA/16Mo3	550	400	800	1,3
Lime	Limestone	30	KanthalA1/253MA/16Mo3	550	400	800	1,3
FS	Foundry sand	30	KanthalA1/253MA/16Mo3	550	400	800	1,3
Ref 2	None (Reference)	0	16Mo3/253MA/16Mo3	550	400	800	1,3
SWS 2	SWS*	80	16Mo3/253MA/16Mo3	550	400	800	1,3
PbO	PbO	1 + 0	16Mo3/253MA/16Mo3	550	400	800	1,3
PbO+ SWS	PbO + SWS*	1 + 80	16Mo3/253MA/16Mo3	550	400	800	1,3

^{*} Digested sewage sludge

Table 21 Composition of fuel pellets and fuel pellets with additives as analysed by handheld XRF (%, by mass a.r.).

Tabell 21. Sammansättning för bränslepellets och pellets med bränsle och additiv analyserat med handhållen XRF (vikt-%)

	Ref 1	FS	Kao	Lime	SWS1	s	Ref 2	SWS2	PbO	PbO + SWS
Pb	0,036	0,046	0,044	0,055	0,041	0,034	0,039	0,041	0,168	0,130
Zn	0,06	0,03	0,03	0,03	0,04	0,03	0,03	0,05	0,04	0,03
Cu	0,006	0,006	0,006	0,006	0,007	0,009	0,007	0,010	0,006	0,010
Fe	0,56	0,61	0,45	0,50	0,95	0,45	0,47	1,13	0,57	1,00
Cr	0,01	0,01	0,01	0,01	0,01	0,01	0,01	0,01	0,01	0,01
Ti	0,20	0,24	0,22	0,23	0,27	0,19	0,23	0,26	0,28	0,26
Ca	1,4	1,4	1,2	3,0	1,4	1,1	1,6	1,6	1,7	1,7
K	0,19	0,20	0,12	0,17	0,15	0,13	0,17	0,17	0,17	0,18
Al	0,10	0,16	0,33	0,12	0,13	0,11	0,12	0,15	0,15	0,19
Р	0,03	0,04	0,03	0,01	0,22	0,03	0,03	0,32	0,05	0,40
Si	1,2	1,9	1,6	1,0	0,9	0,8	1,2	1,0	1,4	1,3
CI	0,30	0,26	0,27	0,29	0,30	0,29	0,36	0,38	0,40	0,29
S	0,34	0,36	0,29	0,33	0,43	3,27	0,40	0,53	0,49	0,68

5.2 Methods

5.2.1 Laboratory reactor

The outline of the laboratory reactor that was used for the combustion experiments is shown in Figure 36. All tests were performed under as stationary conditions as possible, with an operating set-point listed in Table 22.

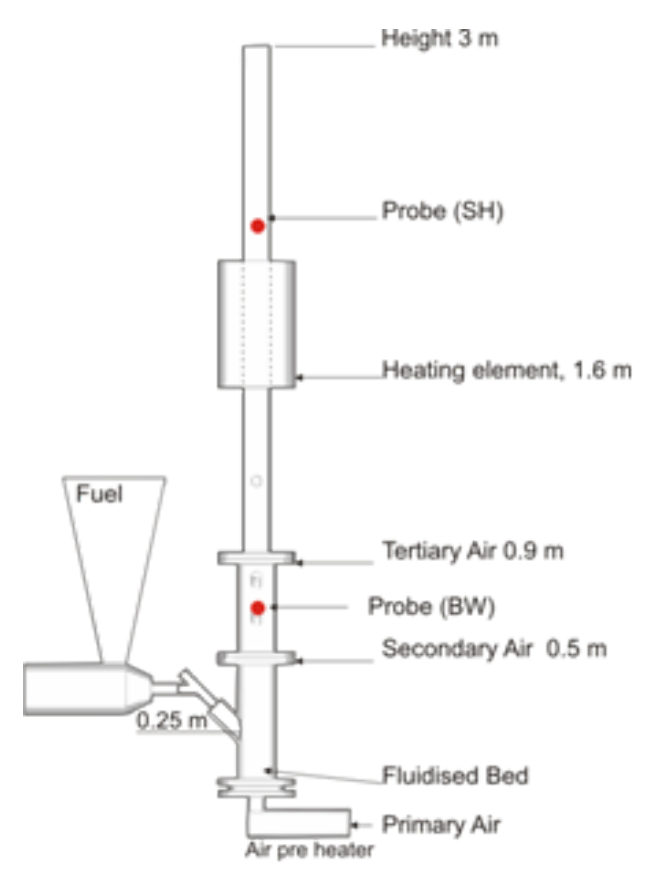


Figure 36 Outline of the laboratory reactor.

Figur 36 Skiss av lab-reaktorn.

Table 22 Operational conditions for tests.

Tabell 22. Driftparametrar vid testerna.

Parameter	Value
Duration time	8 h (for probes) + start up
Amount of bed sand	500 ml of B35
Average O ₂ at outlet	5 % (d.g.)
Primary air flow	50 Nlpm
Sec. air flow	22 Nlpm
Tert. Air flow	58 Nlpm
Bed temperature	800°C
Air ratio at SH-probe	1.3
Air ratio at BW-probe	0.72

d.g. - dry gas

Nlpm - normal liters per minute

The reactor has an inner diameter of 0.10 m. The bed temperature is automatically controlled by an electrical air preheater of the primary air, which is, if needed, complemented by a manually controlled water cooled tube coil in the bed. No arrangement for flue gas recirculation exists at present. The steel tube walls are refractory lined at the inside up to a height of 0.9 meters from the air distributor. The reactor is insulated outside the steel tube along the whole reactor. An external electrical heating element surrounds the reactor at about 1.6 meter, in order to keep a sufficiently high flue gas temperature at the sampling ports on top of the reactor. The fuel is fed into the reactor by a manually controlled screw feeder at 0.25 meter above the bottom of the reactor.

An outlet oxygen concentration of 5.0 %, dry gas corresponds to an air factor of 1.3 in the reactor above the inlet of the tertiary air. At the port for the boiler wall probe, between secondary and tertiary air, the corresponding air factor is about 0.72, calculated from the ratio between the total added air and the air factor at the reactor outlet. Additional measurements of oxygen at the position of the boiler wall probe showed no oxygen above the detection limit of about 0.1 %, by volume, verifying that the gas conditions are indeed reducing at the boiler wall probe. There may be intermittent spikes of short duration of oxygen passing the position due to the "turbulent" nature of a fluidised bed, but if so, that could not be detected by the conventional gas analyser used.

5.2.2 Fuels and additives

Waste wood to be used for the laboratory tests was taken from Vattenfall's CHP plant Idbäcken in Nyköping in April 2012. The waste wood was imported from Great Britain. The fuel was taken after the fuel preparation process in Idbäcken, which means that the fuel has been sieved and that much of the magnetic metal in the fuel has been removed before the fuel for the laboratory tests was taken. This fuel is representative of the waste wood used in the boiler in Idbäcken. Vattenfall sent 4 m³ waste wood to SP in May 2012.

Results from a standard analysis of the fuel to be used in the laboratory tests are shown in Appendix C. The analysis shows that the fuel is representative for the fuel that Vattenfall imports from Great Britain for use in the Idbäcken plant.

The fuel was milled and pressed to pellets at SP. Larger pieces of scrap metals and stones were manually removed prior to milling. The fuel has been analysed several times within the project;

- 1. a standard analysis fuel (Appendix C)
- 2. a chemical analysis of a sample of pelletised fuel
- advanced fuel analysis of pellets by Åbo Akademi. See section 3
 (Analysis of composition of fuels and additives) for results of these
 analyses.

The pellets (6 mm diameter) were pressed from waste wood for reference case as well as waste wood with different additives as shown in Table 20. All additives were mixed with the milled waste wood prior to being pelletised.

The additives used in the tests were sulphur, digested sewage sludge, kaolin, lime stone and foundry sand. The compositions of sewage sludge, kaolin and foundry sand has been analysed by Åbo Akademi and the result is presented in section 3. Analyses of the additives used can be found in appendix C.

5.2.3 Test materials used in the laboratory tests

Two temperature controlled cylindrical probes with material samples were inserted to the reactor during the test runs at the positions marked by red dots in Figure 36. One probe was located between the inlets of secondary and tertiary air, with a material temperature of 400°C simulating boiler wall (BW) conditions. The other probe was located further downstream, simulating conditions of a super heater (SH) with a material temperature of 550°C. Each probe carried three rings of different materials (16Mo3, 253 MA and Kanthal A1). The outer diameter of the rings was 25 mm. The material samples were exposed during 8 hours.

Kanthal A1

Kanthal A1 is a ferritic iron-chromium-aluminium (FeCrAI) alloy. It is mainly used for electrical heating and is characterised by high resistivity and its high oxidation resistance at high temperatures. The material was chosen for this project to study how an alumina former would perform at lower temperatures in these specific environments. The alloy can be used for overlay welding, but for construction other FeCrAIs would be more suitable. For nominal composition, see Table 23.

Table 23 Nominal composition of Kanthal A1 [73]

Tabell 23. Sammansättning enligt specifikation för Kanthal A1 [73]

	C %	Si %	Mn %	Cr %	Al %	Fe %
Nominal composition					5.8	Bal
Min	-	-	-	20.5	-	
Max	0.08	0.7	0.4	23.5	-	

253 MA

253MA is a heat resistant, Cr-Ni austenitic stainless steel that has additions of N, Si and Rare Earth Metals (REM) which include Ce. The steel shows a relatively good performance at 850-1100°C, particularly for conditions involving erosion-corrosion in oxidising and neutral environments, as well as sulphur attack. The interest in this material was to study how the corrosion resistance would perform at lower temperatures in these environments involving both reducing and oxidising conditions in corrosive media. [10]

Its specific characteristics are:

- Good resistance to embrittlement
- High mechanical strength at high temperatures
- Excellent weldability

Table 23 Nominal composition of 253 MA [10]

Tabell 23 Sammansättning enligt specifikation för 253 MA [10]

	C %	Cr %	Ni %	Si %	N %	Ce %
Nominal composition	0.05-0.10	20.0-22.0	10.0-12.0	1.4-2.0	0.14-0.20	0.03-0.08

16Mo3, reference material

16Mo3 (previously 15Mo3, the name was changed in 1993 but the properties are virtually the same) is a Mo containing steel with a ferritic/perlitic structure, specially developed for pressurised vessels with elevated service temperature. Due to the acceptable corrosion resistance and its relatively low cost the steel is widely used in boilers in the power production industry. The corrosion resistance in combustion environments is considered to be comparable with steels alloyed with lower amounts of Cr, contributing to its wide usage.

Table 24 Nominal composition of 16Mo3

Tabell 24. Sammansättning enligt specifikation för 16Mo3.

	C max	Mn	N	Cu	Si	Р	Cr	Ni	Мо
Nominal composition	0.12- 0.2	0.40- 0.90	0.012	0.30	0.35	0.025	0.30	0.30	0.25- 0.35

5.2.4 Test procedure

Prior to each test run, the reactor was cleaned and filled with 500 ml unused sand (Baskarp B35, an analysis can be found in Appendix C) and a weighed amount of fuel was filled into the fuel hopper. The first step when heating the reactor is by letting the air preheater heating the primary air flow. Then, a gas burner is ignited and fired on top of the bed to further increase the temperature. After one hour of gas heating, the screw feeder for the solid fuel is started. The solid fuel flow was running for two hours, in order to let the reactor to reach stationary conditions, before the probes, holding the material samples, were inserted at both BW and SH positions. About four hours after insertion of the probes, a fly ash sampling probe was inserted at the outlet of the reactor for a sampling period of one hour. The probes holding the material samples were removed after 8 hours, after which the solid fuel screw feeder was stopped and the reactor cooled down.

During the steady state operation of the reactor, the inlet air flows were fixed by mass flow controllers while the fuel screw feeder rate had to be manually adjusted to get an oxygen concentration of about 5 % in the flue gas. The bed temperature was controlled by the electric air preheater. From the ash content in the fuel, the amount of bed material gradually increased during the tests. To counteract this, some bed material was tapped off through a chute a few times during operation.

After each test, when the reactor had cooled down, the bed material in the reactor was collected in a plastic container. The reactor walls were swept and the removed dust was collected in a separate container. The fuel remaining in the hopper was weighed to enable calculation of the fuel consumption.

5.2.5 Measurement methods

Fly ash

Fly ash was sampled at the outlet of the reactor during one hour per test case. The sampling was started after at least 4 hours of continuous operation of the furnace, in order to sample under as representative conditions as possible.

Flue gas was sampled by a probe with a tip facing downwards, meeting the flow, see Figure 37. To get a representative particle distribution, the suction rate through the probe was adjusted to reach isokinetic conditions at the probe tip (meaning that the gas velocity into the probe tip is the same as the gas velocity in the reactor). After the bent probe tip, there is a heated horizontal section reaching out of the reactor. The inner diameter of this horizontal section is wider than the probe tip, implying that the gas velocity in the horizontal section of the probe is reduced compared to the probe tip. Since the flue gas velocity in the lab reactor is lower than in a normal flue gas duct for which the probe is designed, the flue gas velocity in the probe was lower than the design value. This resulted in more solid deposits in the horizontal part of the probe than usual. Most likely, these deposits consist predominantly of relative large particles that settled in the tube due to the relatively low gas velocity.

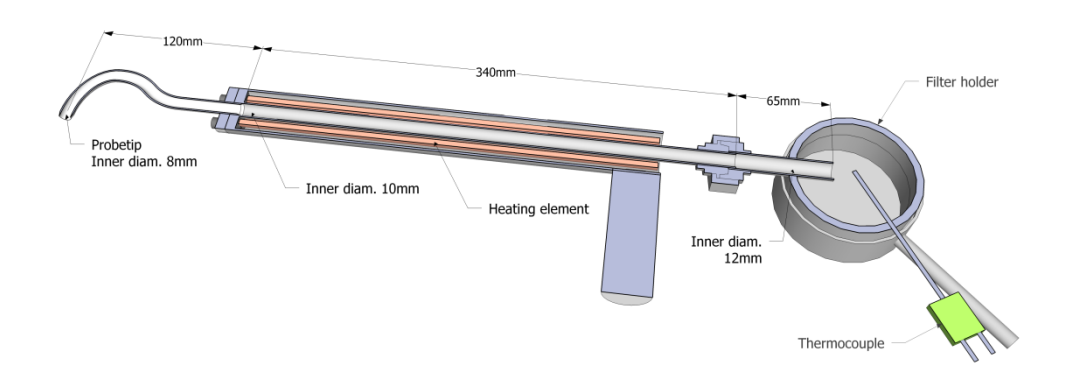


Figure 37 Sketch of the fly-ash sampling probe.

Figur 37 Skiss av sonden för insamling av flygaska.

After the horizontal section of the probe, the particle laden flue gas passes two parallel Teflon filters of 90 mm in diameter, where the remaining particles are collected. After the filters, the gas passes a silica gel dryer, a gas meter and a suction pump, which controls the sample gas flow.

After each test, the probe was rinsed with acetone to flush out the fly ash deposited. Then the acetone in the fly ash/acetone mixture was vaporised in an oven. Afterwards, the ash from the probe was weighed and analysed by handheld XRF. The filters were analysed by conventional methods, as described later in this section.

Bottom ash

The bed material, containing a mixture of bed sand and bottom ash, was collected after each test run.

Deposit probe sampling

During the test runs, two temperature controlled cylindrical probes with steel samples were inserted into the reactor at the positions marked by red dots in Figure 36. One probe was located between the inlets of secondary and tertiary air, with a material temperature of 400°C simulating boiler wall (BW) conditions. The local air factor at the position of the BW-probe is estimated to about 0.72 based on the flow rates of air and fuel. That is, the condition is clearly sub-stoichiometric, implying reducing conditions. The other probe was placed further downstream (at an air factor of 1.3), simulating conditions of a super heater (SH) with a material temperature of 550°C. Each probe carried three rings of different materials: 16Mo3, 253 MA and Kanthal A1 (which was replaced by another 16Mo3 ring in the last four test runs, because only negligible corrosion was found on Kanthal A1). The diameter of the rings was 25 mm. The material samples were exposed during 8 hours.

The deposit probes are heated by the flue gas and are temperature controlled by cooling air at the inside of the deposit rings. The material temperature is measured by thermocouple in an adjacent ring with same diameter. The air distributor of the cooling air was adjusted during pre-tests to accomplish a uniform temperature on the three parallel test rings, resulting in a final temperature difference less than 10°C. During these pre-tests, each ring had an individual thermocouple wielded into the material.

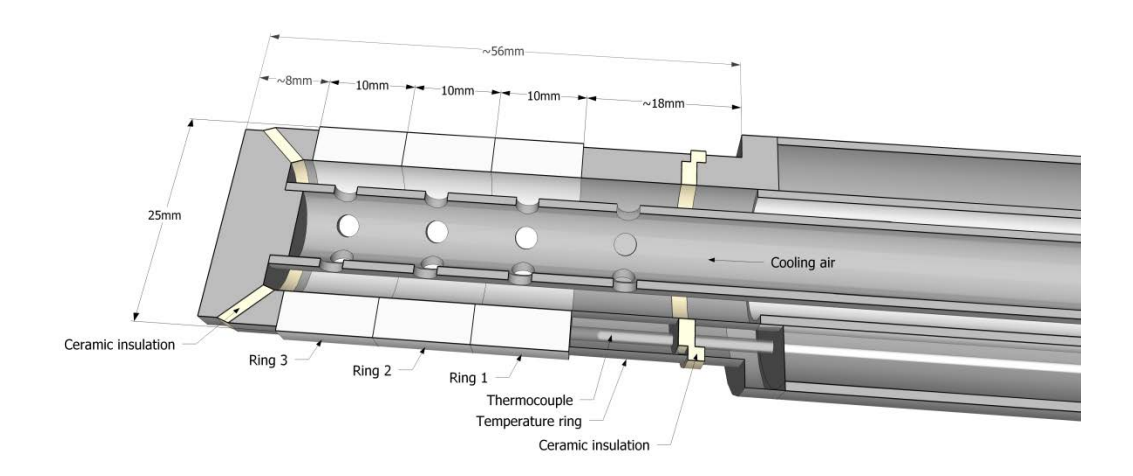


Figure 38 Cross section sketch of the deposit probe. The light-coloured parts are the deposit rings.

Figur 38 Avlagringssonden i genomskärning. De ljusa delarna är avlagringsringarna.

The procedure for the handling of deposit/corrosion samples are as follows: The sample rings are cleaned in an ultrasonic bath in isopropanol. The samples are dried and placed in a desiccator.

- 1. The sample rings are individually weighed together with a labelled plastic container prior to exposure in the furnace.
- 2. The rings are mounted on the probes, three materials on each of two probes.
- 3. The rings are exposed in the furnace. At first the probe is inserted with a shielding cover to be heated without being exposed directly to the flue gas. At the start of the 8-hours sampling, the shield is removed.
- 4. After exposure, the probe is cooled in a tin containing silica gel. The rings are later dismounted from the probe. Loose deposits falling off during the procedure are collected in separate plastic containers for each probe.
- 5. The rings are stored in individual plastic containers, which subsequently are placed in a desiccator.
- 6. To remove loose deposits, a ring is threaded on a fall tube where it is being held by a pin, see Figure 39. The fall tube is vertically fixed in a laboratory tripod. When the pin is removed, the ring falls 100 mm before hitting the expanded end of the fall tube. The shock of impact removes the loose deposits which are being collected in a container under the fall tube.
- 7. The loose dust and the ring with the hard deposits are individually weighed, before being stored in a desiccator for later chemical analyses.

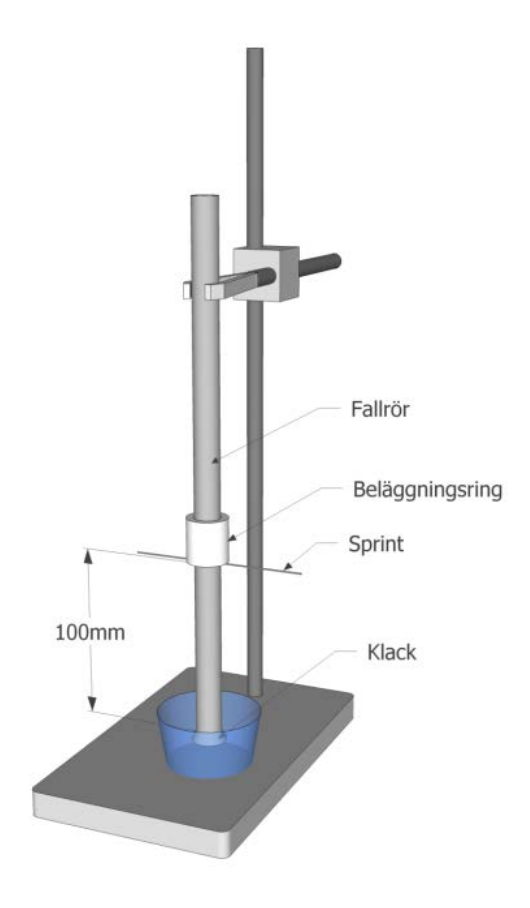


Figure 39 The set up for separating loosely attached deposits from the steel ring.

Figur 39 Anordningen för att avlägsna löst sittande avlagringar från provringen.

Handheld XRF analysis of deposits and ashes

Handheld XRFs have been on the market for almost 20 years, during which technical development has improved the measurement accuracy, especially of lighter elements. At present, elements down to Mg (element no. 12) can be analysed by handheld XRF devices, without the use of helium or vacuum in the sample holder. The detection limits, however, is higher and the precision is lower for lighter elements compared to heavier elements. A Thermo Scientific Niton XL3t handheld X-Ray Fluorescence (XRF) analyser has been used within this project.

For many sample matrices, such as typical mining samples, it is necessary to measure both lighter elements that emit lower energy x-rays (that are easily absorbed) as well as heavier elements that emit much higher energy x-rays (that penetrate comparatively long distances through the sample). In these multi-element samples, it is possible that one or more of the elements present act as critical absorbers. The effects of absorption, enhancement, and secondary fluorescence vary widely depending on the chemistry of the sample

matrix; but in a sample with many elements in substantial concentrations, such effects are typically present.

Modern XRF-analysers automatically adjusts for such effects, as well as various geometric effects, to determine the chemical constitutions of samples of widely different composition, without any requirement for instrument users to input empirical sample-specific calibrations. Occasionally, there are samples that require sample-specific calibrations to give accurate results. The case of the ashes and deposits analysed within present project fall in this category where sample-specific calibrations are beneficial. A calibration has been implemented by SP Chemistry department by comparison of handheld XRF results of a number of ashes and fuels analysed with various conventional methods of analysis. Although this calibration has improved the accuracy of the XRF instrument, the accuracy cannot be guaranteed for all elements in all the different kind of samples obtained within this project. Therefore, the concentrations obtained by the XRF within this report should be regarded as qualitative, but to be used mainly for comparison between test cases. Nevertheless, even if the concentrations measured by XRF should be inaccurate for some elements, the values remain essentially proportional to actual concentrations.

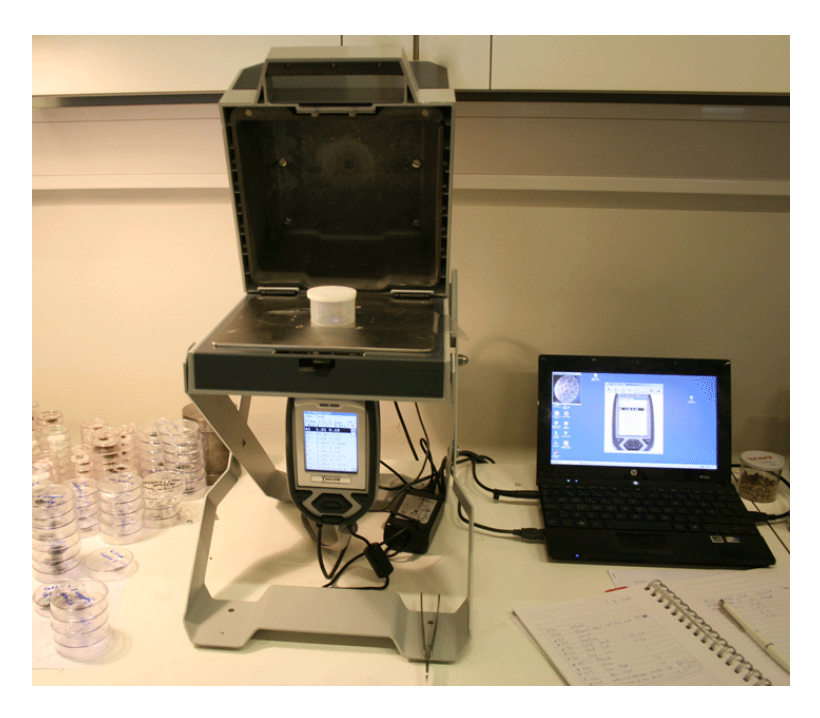


Figure 40 The shielded test stand provides a safe platform for the handheld XRF analyser attached underneath the table.

Figur 40 Det avskärmade provstället ger en säker plats för den handhållna XRF-instrumentet som sitter fast under bordet.

It is important to note that the handheld XRF does not measure C, N, O and Na. To measure such light elements with the XRF technique, the sample should be placed in vacuum or in helium atmosphere to avoid fluorescence or absorption of gas molecules in the pathway of the photons in x-rays and

fluorescence. The handheld XRF enables fast analysis of a large number of samples that would be very costly to do with ordinary wet chemical methods.

The ash samples were analysed in a plastic cup with a 6 μ m PE-foil at the bottom standing on the test stand. The deposit rings were suspended in a sample holder on the test stand while analysed, see Figure 41.

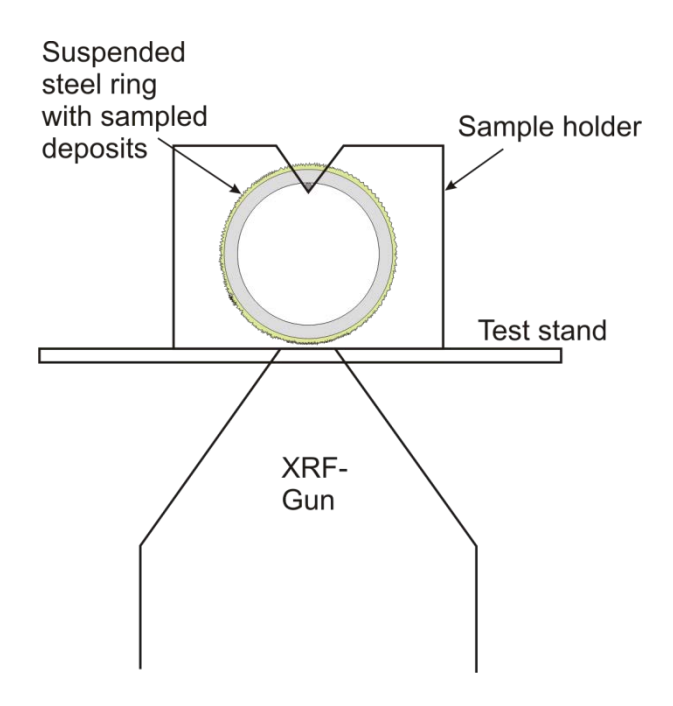


Figure 41 Sketch of set-up when analysing sample deposits by handheld XRF.

Figur 41 skiss över uppställning för analys av avlagringar med det handhållna XRF-instrumentet.

Chemical Analysis of fly ash on filters

The filters from the fly-ash sampling were leached in water (80°C in 24 h) where after the amount of leached chlorine was determined by ion chromatography with a conductivity detector. The liquid was sequentially evaporated and the rest were leached in an acid mixture of nitric acid, hydrochloric acid and hydrofluoric acid (80°C in 4 h). Leached amounts of Al, Ba, Ca, Cd, Cu, Fe, K, Mg, Mn, Na, Ni, P, Pb, S, Si, Ti and Zn were determined by inductively coupled plasma optical emission spectrometry (ICP-OES). There could be a loss of silicon during the leaching in the acid mixture, implying that the given Si-concentrations may be an underestimation of the real value.

Corrosion analysis

After the exposure in the furnace, and subsequent analysis of the deposits, the sample rings were cleaned by isopropanol and lightly brushed with a cloth in order to see the alloy surface. A more extensive abrasive cleaning could have removed corrosion products formed, in addition to the deposits. However, doing so would also have required much more effort.

Macroscopic photos were taken at the inclination angle of the flue gas stream (wind side, 0°). The corrosion attacks were mostly limited to the windward side.

The first set of tests performed is the first six cases listed in Table 20: Ref 1, FS, Kaolin, Lime, SWS1 and Sulphur. The corrosion of the test rings was not analysed in detail for this first set of tests. Instead, the overall corrosion was studied in optical microscope, which was sufficient to provide a tentative ranking of additives tested.

In the second set of tests micrographs were taken by optical microscopy. The cross-sections had been ground with emery paper and polished with diamond paste. The images were taken under polarised light, colourising different areas, with a slight side-view to emboss the relief structure. In order to strengthen the colour difference, some cross-sections were etched with water. The magnification is between 200x and 350x.

Some of the samples from test set two were also analysed by SEM (Scanning Electron Microscope) and EDX (Energy Dispersive X-Ray). The BSE-option (Backscatter Electrons) was used when the aim was to identify heavier elements, e.g. Pb. The samples were mounted in resin, ground with emery paper and polished with 1.5 μm diamond paste. The analyses were made at several positions round the circumference of the sample ring.

5.3 Results

5.3.1 Gas concentrations and temperatures

Gas concentrations and reactor temperatures, as average for the 8 hours of deposit/corrosion probe exposure, are summarised in Table 25 (without correction for occasional disturbances).

Table 25 Average values of operational parameters during deposit/corrosion probe exposure.

Tabell 25. Medelvärden för driftparametrar under exponeringen av avlagrings/korrosionssonder.

	Ref 1	SWS1	S	Kao	FS	Lime	Ref 2	SWS2	PbO	PbO +SWS
O ₂ [%, d.g.]	4,90	5,07	5,22	5,14	5,09	5,26	5,26	5,18	5,30	5,34
CO [ppm,d.g.]	37	19	34	36	15	16	15	30	13	10
NO [ppm, w.g.]	267	287	280	339	289	272	266	300	270	312
SO ₂ [ppm, w.g.]	11	20	<u>284</u>	24	19	8	4	43	5	33
HCI [ppm, w.g.]	213	244	<u>348</u>	248	230	<u>117</u>	231	227	266	281
H ₂ O [%, w.g.]	12,4	12,6	13,0	13,0	13,1	12,8	12,7	12,3	13,0	13,0
CO ₂ [%, w.g.]	13,9	14,5	14,6	14,7	14,5	14,2	14,4	14,3	14,5	14,1
T _{bed} [°C]	799	799	800	800	800	800	800	800	800	800
T_1 [°C]	907	911	903	878	875	879	873	871	875	870
T_2 [°C]	924	936	935	924	934	930	940	919	937	919
T_3 [°C]	779	779	785	784	785	786	784	782	778	780

SWS – Sewage sludge, S – elemental Sulphur, FS – Foundry Sand, w.g. – wet gas, d.g. – dry gas

In Table 25, temperature T_{-1} refers to the zone with the wall probe (presented as an average of two thermocouples), T_{-2} is the temperature above tertiary air and T_{-3} is the measured gas temperature close to the SH probe. All these temperatures are measured with bare thermocouples (type K) inserted into the reactor.

5.3.2 Fly ash

For each test run, fly ash was collected during a one-hour sampling at the outlet of the reactor, where the gas temperature was about 400°C. The method is described in section 5.2.5. A summary of the concentrations of collected fly ashes is given in Figure 42 below.

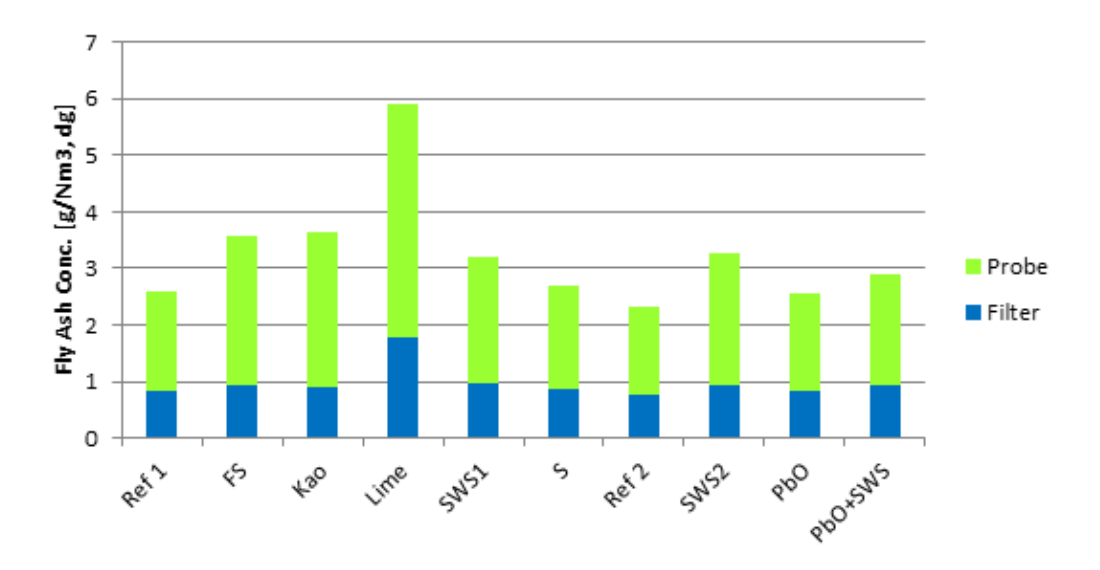


Figure 42 Measured concentrations of fly ash. The green parts of the bars represent the fly ash deposited inside the probe and the blue parts are fly ash collected on the filters.

Figur 42 Uppmätta koncentrationer av flygaska. De gröna delarna på staplarna motsvarar flygaskan inuti sonden och de blå delarna motsvarar de delar av flygaskan som samlats upp på filtren.

The elemental compositions of the fly ash sampled on filters, analysed by conventional wet chemical methods, are shown in Figure 43. The top fields of the bars "Bal" (dashed boundaries with white filling) contain undetermined elements to make up for the total collected mass. A large part of this is probably oxygen. A table of concentrations of selected elements, especially those in too low concentrations to be visible in the bar plot, is given in Table 26. Solids removed from the probe after each sampling period were analysed by XRF, providing the elemental distributions presented in Figure 44 and in Table 27.

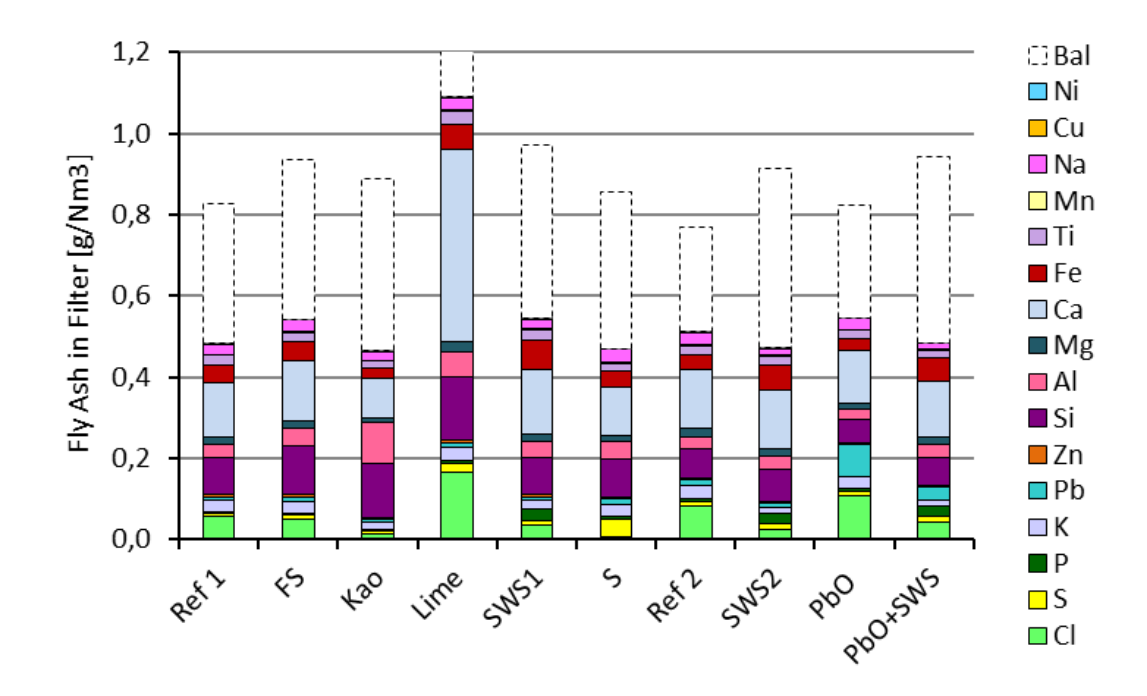


Figure 43 Elemental composition of fly ash on filters, as analysed by conventional wet chemical methods.

Figur 43 Kemisk sammansättning av flygaska från filter, analyserad med konventionella våtkemiska analysmetoder.

Table 26 Elemental concentrations in fly ash on filters, based on the same data as in Figure 43

Tabell 26. Kemisk sammansättning av flygaska från filter, baserat på samma data som Figur 43.

Element	Test Ca	Test Case											
%, by mass	Ref 1	FS	Kao	Lime	SWS1	S	Ref 2	SWS2	PbO	PbO+ SWS			
CI	6,7	5,3	<u>1,5</u>	9,3	<u>3,5</u>	0,65	9,6	2,8	12,7	5,1			
S	0,93	0,92	0,70	1,1	1,0	5,2	1,1	1,5	1,1	1,6			
Р	0,67	0,62	0,41	0,44	3,0	0,56	0,73	<u>3,1</u>	0,60	3,0			
Na	3,0	3,2	2,5	1,6	2,4	3,7	3,4	1,9	3,1	1,7			
K	3,1	2,8	2,0	1,9	2,3	3,4	3,8	1,8	3,5	1,6			
Pb	1,1	1,4	0,8	0,7	0,9	1,7	1,7	1,1	9,1	3,9			
Zn	0,87	0,53	0,45	0,29	0,50	0,56	0,46	0,45	0,42	0,38			

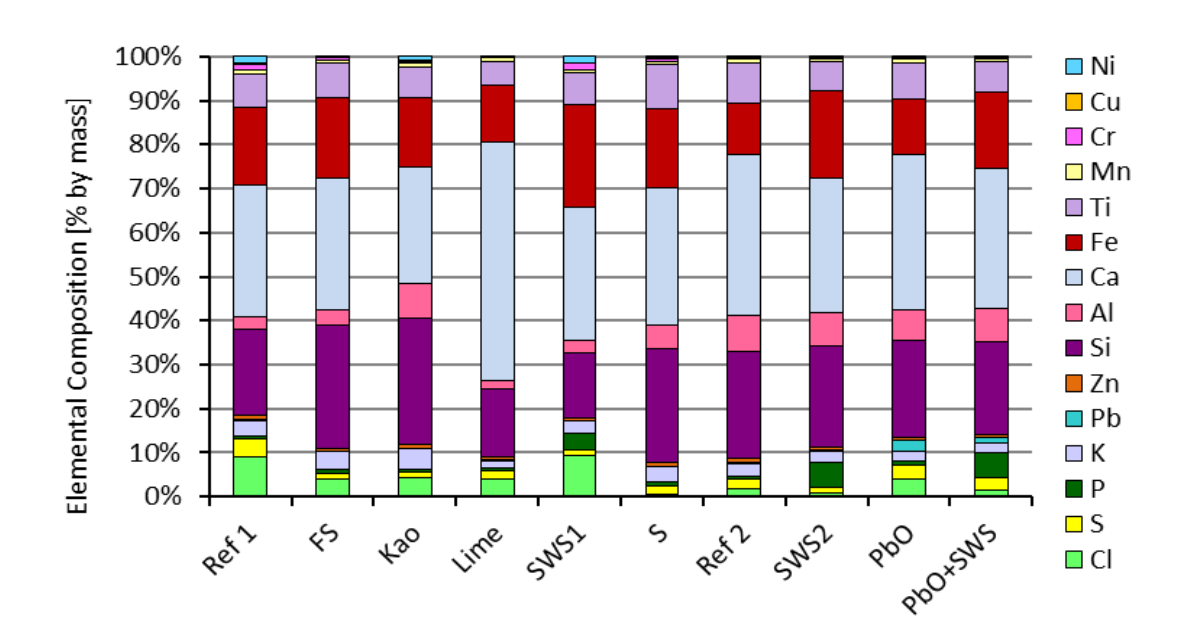


Figure 44 Elemental composition of dust deposited in probe during fly ash sampling, as analysed by XRF.

Figur 44 Kemisk sammansättning av stoft som samlats upp i sonden vid insamling av flygaska, analyserad med XRF.

Table 27 Elemental concentrations in fly ash, deposited in probe, same data as in Figure 44.

Tabell 27. Kemisk sammansättning av flygaska från filter, baserat på samma data som Figur 44.

Element	Test Case									
%, by mass	Ref 1	FS	Kao	Lime	SWS1	S	Ref 2	SWS2	PbO	PbO + SWS
CI	6,4	2,3	2,1	1,9	6,0	0,31	1,5	0,59	2,8	1,2
S	2,7	0,60	0,55	0,88	1,0	0,98	1,7	1,1	2,4	2,0
Р	0,60	0,52	0,35	0,31	2,4	0,60	0,76	4,2	0,59	4,3
K	2,4	2,3	2,2	0,80	1,9	1,8	2,3	2,0	1,6	1,6
Pb	0,08	0,09	0,09	0,10	0,07	0,10	0,38	0,31	1,8	0,97
Zn	0,70	0,39	0,35	0,36	0,33	0,44	0,62	0,39	0,48	0,33

5.3.3 Bottom ash and wall deposits

The bed material was weighed before and after the test runs, both the bed material remaining inside the reactor and the bed material tapped off during operation are considered here. The difference is roughly considered to represent the amount of bottom ash. The deposits on the wall that fell down during "chimney sweep" after each test run were also collected and weighed. A summary of the amounts of bottom ash is given in Figure 45, on a scale of the vertical axis as the fraction of the mass of the fuel (including additives) added during the test run. The elemental distributions of the bed material after the tests (bottom ash+ sand) are given in Figure 46, with additional details in Table 28. The elemental composition of the dust removed from the reactor walls during sweeping is given in Figure 47 and Table 29. The compositions of the wall deposits are strikingly consistent for the different test cases, even if the Lime additive gives higher concentrations of Ca, Cl and S. Other, more or less expected, observations are that the cases involving sewage sludge provide more phosphorous to the wall deposits and that the sulphur additive increases the sulphur content in the wall deposits.

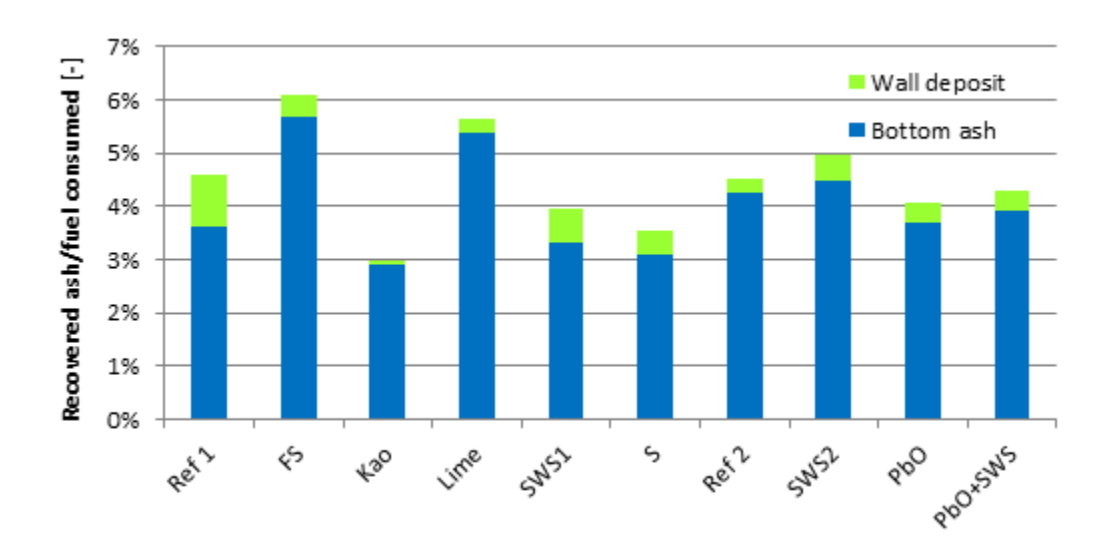


Figure 45 Fraction of fuel recovered as bottom ash.

Figur 45 Andel av bränslet i bottenaskan.

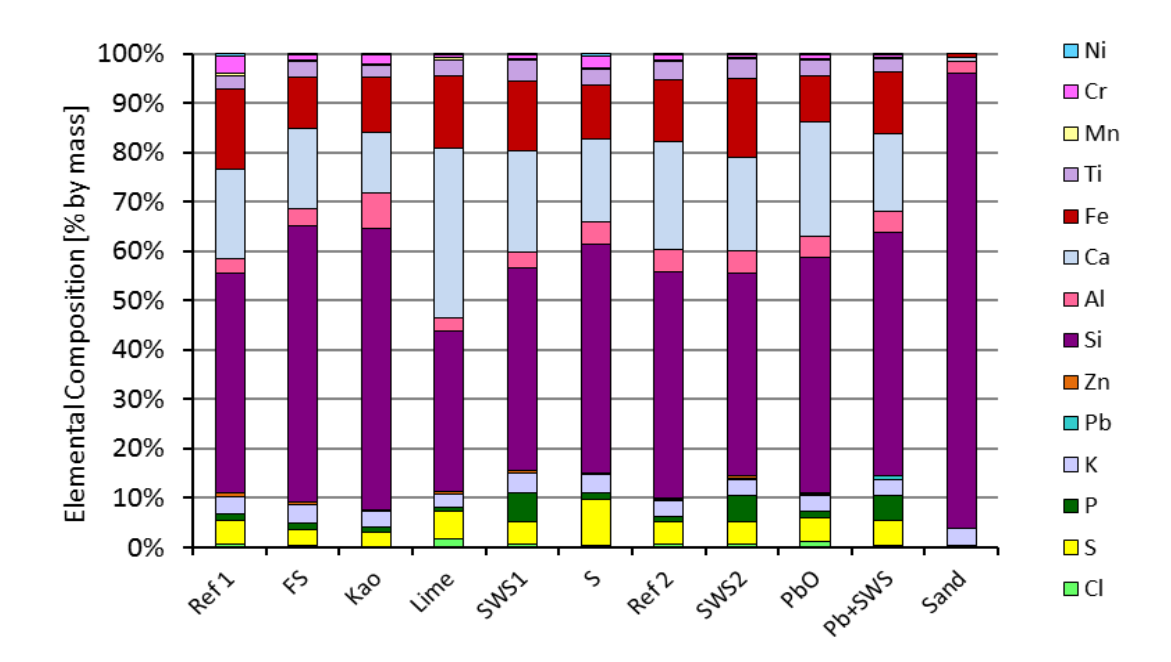


Figure 46 Elemental composition of bed material after test runs, as analysed by XRF. An analysis of virgin sand used as bed material included as reference to the right.

Figur 46 Kemisksammansättning av bäddmaterial efter testerna analyserad med XRF. En analys av ren sand är infogad som referens till höger.

Table 28 Concentrations of elements in bed material, same analysis as illustrated in Figure 46.

Tabell 28. Kemisk sammansättning av flygaska från filter, baserat på samma data som Figur 46.

Element	Test C	ase									
[%, mass]	Ref 1	FS	Kao	Lime	SWS1	S	Ref 2	SWS2	PbO	PbO+ SWS	Sand
CI	0,24	0,12	0,03	0,65	0,22	0,10	0,21	0,22	0,33	0,18	0,00
S	1,4	1,0	1,0	1,9	1,4	<u>2,9</u>	1,5	1,7	1,5	1,7	0,01
Р	0,41	0,35	0,28	0,34	<u>1,8</u>	0,37	0,37	2,0	0,43	1,8	0,12
K	1,0	1,2	1,1	0,92	1,2	1,2	1,0	1,2	0,98	1,2	1,2
Pb	0,005	0,010	0,009	0,017	0,013	0,008	0,04	0,09	0,11	0,21	0,000
Zn	0,25	0,15	0,06	0,13	0,16	0,14	0,12	0,12	0,12	0,09	0,00

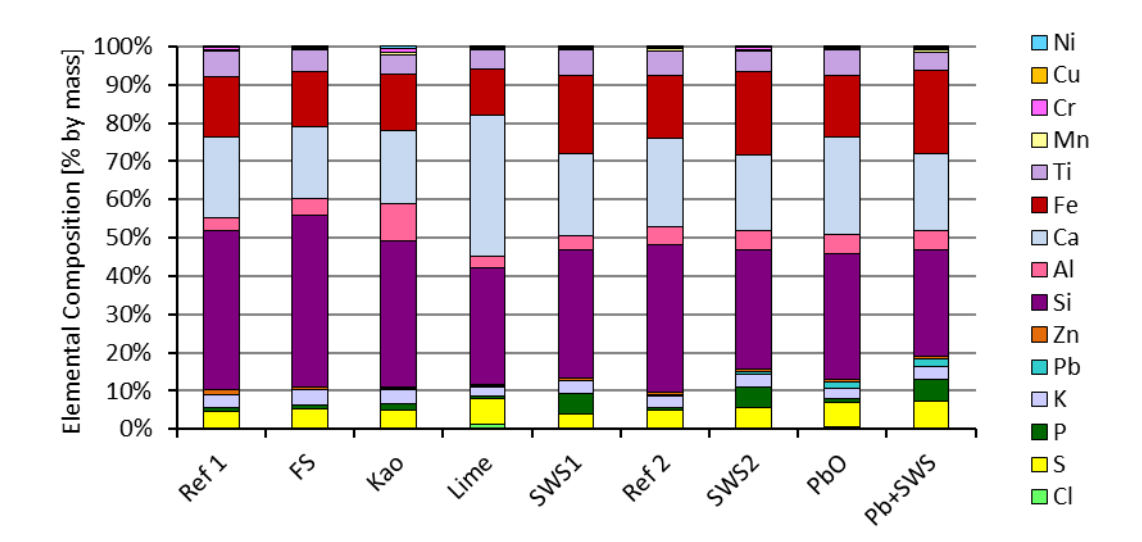


Figure 47 Elemental composition of solids removed from the vertical walls after each test, as analysed by XRF. The sample from the "sulphur case" is omitted because the sample handling failed.

Figur 47 Kemisk sammansättning av fast material från väggarna för varje test, analyserad med XRF. Provet från "svavelfallet" har inte tagits med eftersom det förstördes i provhanteringen.

Table 29 Concentrations of some elements, same data as illustrated in Figure 47

Tabell 29. Koncentration av några ämnen, samma data som illustreras i Figur 47.

	Ref 1	FS	Kao	Lime	SWS1	Ref 2	SWS2	PbO	PbO+ SWS
CI	0,09	0,11	0,08	0,57	0,13	0,14	0,10	0,25	0,14
S	1,7	1,9	1,9	2,8	1,5	1,9	2,4	2,7	3,2
Р	0,43	0,37	0,65	0,33	<u>2,1</u>	0,35	2,6	0,37	<u>2,7</u>
K	1,3	1,5	1,5	1,1	1,3	1,2	1,5	1,1	1,5
Pb	0,044	0,040	0,047	0,044	0,046	0,22	0,26	0,82	0,93
Zn	0,46	0,20	0,24	0,26	0,23	0,22	0,22	0,27	0,28

5.3.4 Deposits

Some of the deposits on the rings fell off during handling and another part was intentionally removed by a controlled mechanical "knock" on each ring, see Figure 39. The collected loose deposits could not be referred back to individual rings and were consequently handled as lump samples for the three rings on each probe. In some cases, the masses of the "loose" deposits were

significantly higher than the corresponding masses of the "hard" deposits. The masses of the "loose" deposits are generally fairly unreliable because some of the loose dust may have fallen off inside the reactor during the withdrawal of the probe. However, the "loose" deposits are of secondary interest here as they probably would have been easily removed by ordinary soot blowing methods in commercial boilers.

Deposits collected on boiler wall (BW) probes

The deposition rates measured on the BW-probes are shown in Figure 48, where the blue part of the bars represent the amount of deposits that stuck to the sample rings even after a mechanical knock, and the red part represents the recovered loose dust that fell off during handing and knocking. For the case of kaolin, it was observed that build-ups were formed on the walls during operation. These build-ups appeared to be of a "fluffy" structure, and occasionally, when grown large in size, they detached from the walls and fell down towards the bed. Such falling wall deposits may have removed some of the loose deposits from the BW-probe, implying that the red fraction of the bar for the kaolin case (in Figure 48) probably is unrepresentatively low. The amounts of "hard" deposits on the individual rings are compared in Figure 50. Please note that part of the mass gain can be caused by corrosion products, especially for the 16Mo3 samples. The elemental composition of the loose material (as analysed by XRF) is shown in Figure 49 and Table 29.

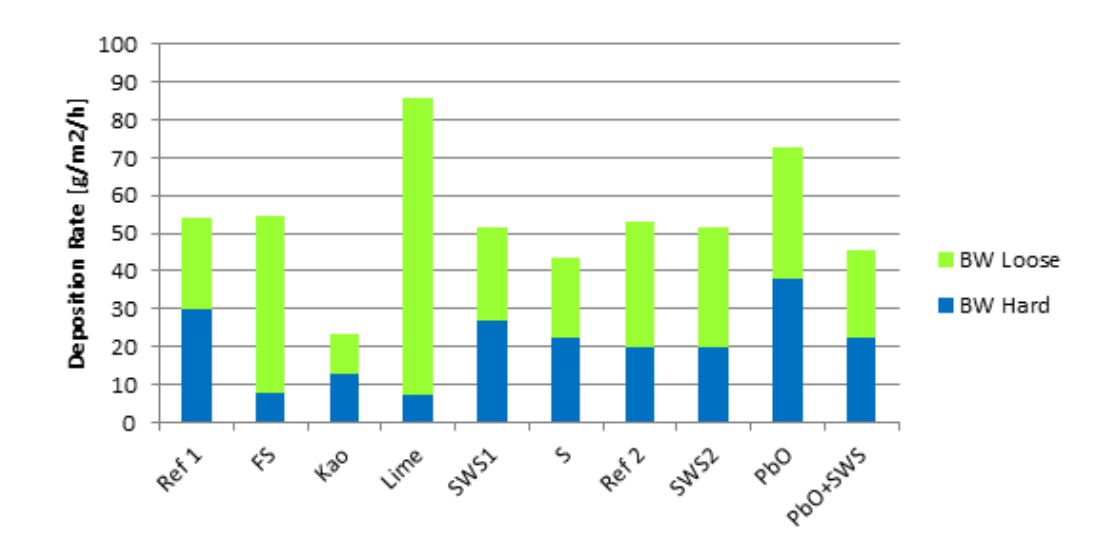


Figure 48 Deposition rate on rings at boiler wall (BW) position, as average of three rings.

Figur 48 Deponeringshastighet för avlagringar på eldstadssondsprover, medelvärde för tre ringar.

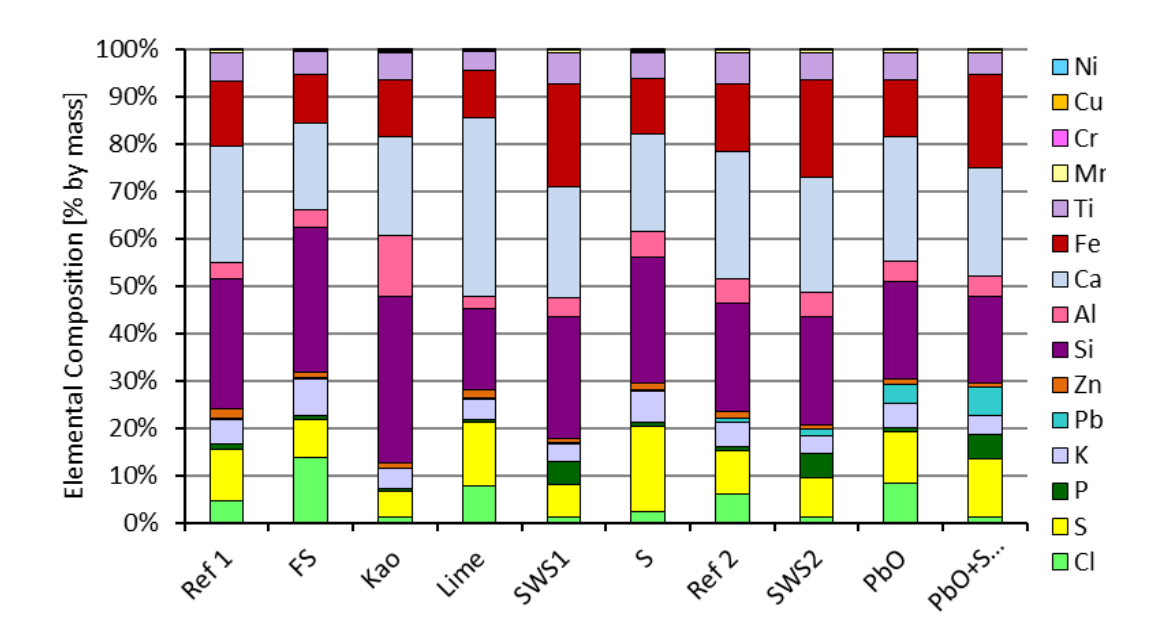


Figure 49 Elemental composition of "loose" deposits on BW probes, analysed by XRF

Figur 49 Kemisk sammansättning för löst sittande avlagringar på eldstadssonden, analyserade med XRF

Table 30 Concentrations of some selected elements in loose deposits on BW probe, same data as illustrated in Figure 49

Tabell 30. Koncentration av några utvalda ämnen i löst sittande avlagringar på eldstadssonden, samma data som illustreras i Figur 49.

% mass	Ref 1	FS	Kao	Lime	SWS1	s	Ref 2	SWS2	PbO	PbO+ SWS
CI	2,5	6,4	1,0	4,2	0,71	1,1	3,0	0,68	4,1	0,67
S	5,6	3,6	3,9	7,1	3,7	9,2	4,7	4,2	5,1	6,3
Р	0,57	0,38	0,60	0,38	2,6	0,50	0,42	2,7	0,40	2,7
K	2,7	3,6	3,0	2,3	2,0	3,2	2,6	1,9	2,5	2,1
Pb	0,079	0,087	0,13	0,16	0,11	0,17	0,42	0,68	1,78	3,05
Zn	1,1	0,52	0,70	0,83	0,51	0,78	0,74	0,51	0,66	0,50

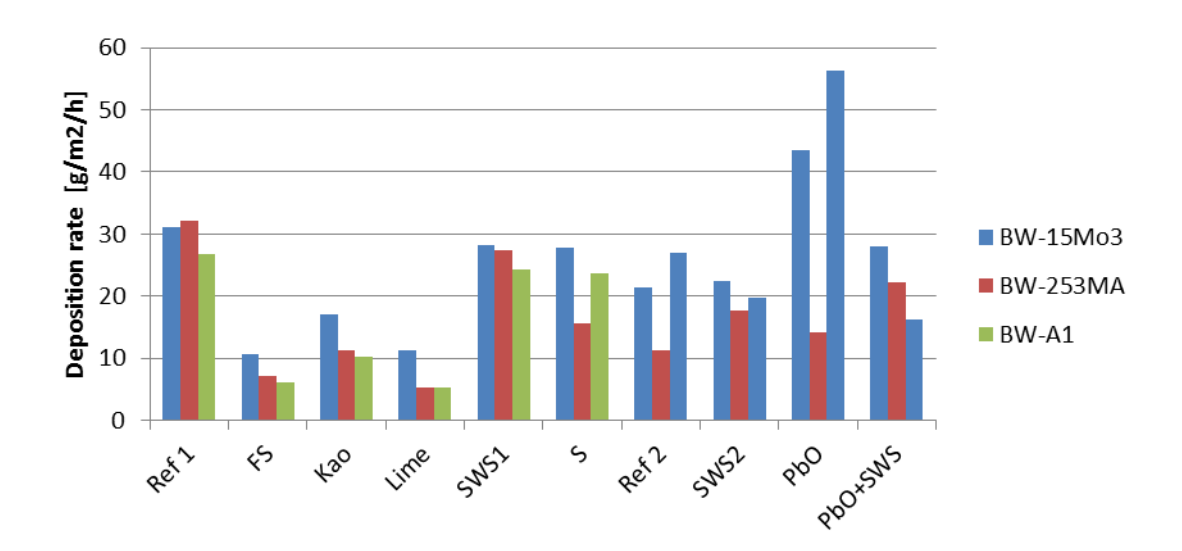


Figure 50 Deposition rate of "hard" deposits on individual rings.

Figur 50 Deponeringshastighet för hårt sittande avlagringar på eldstadssondsprover för de enskilda ringarna

Table 31 Average concentrations of some selected elements in hard deposits on BW probe

Tabell 31. Medelvärden för koncentrationen av några utvalda ämnen i hårt sittande avlagringar på eldstadssonden.

% mass	Ref 1	FS	Kao	Lime	SWS1	S	Ref 2	SWS2	PbO	PbO+ SWS
CI	7,6	<u>18,0</u>	2,6	<u>17,3</u>	3,0	9,4	12,6	<u>4,1</u>	9,9	<u>1,8</u>
s	5,7	<u>18,5</u>	2,0	<u>25,3</u>	3,8	<u>16,7</u>	11,9	<u>3,5</u>	13,1	8,4
Р	1,6	1,4	1,1	1,6	<u>7,0</u>	1,1	1,3	<u>5,6</u>	1,3	<u>5,7</u>
K	4,9	10,7	5,6	5,5	3,0	9,7	8,5	4,2	5,6	3,8
Pb	1,4	2,6	1,3	3,2	1,7	1,0	6,4	6,9	15,5	7,6
Zn	9,2	5,5	5,7	<u>2,5</u>	7,1	<u>3,6</u>	3,7	3,5	2,1	3,4

Observations from the analysis of elements in the hard deposits are listed below:

- **Lime** reduced concentrations of Zn and increased concentrations of Pb in the BW deposit, compared to the reference case. Lime increased the concentrations of both Cl and S in the BW deposits.
- Foundry sand was found to reduce the concentrations of Zn and increase the concentrations of Pb in the BW deposits. The foundry sand increased concentrations of K and Cl on the windward side of the BW

- deposits. It increased the S concentrations in the deposits at the BW position.
- Kaolin gave reductions of Zn, Cl, and S in the deposits at the BW position.
- **Sulphur** reduced Zn in the BW position. The sulphur additive increased S-concentrations in the deposits. The concentration of K increased in BW position.
- Sewage sludge reduced the concentrations of CI in the deposits. The sewage sludge also reduced the concentration of K in the BW deposits. On the other hand, sewage sludge showed the least improvement of the additives tested regarding Zn in the BW deposits. It may also be noted that the addition of sewage sludge increased concentrations of P in all deposits.
- Spiking the fuel with PbO resulted in increased concentrations of Pb in the deposits and it also reduced the concentration of Zn in the BW deposits.

The influence of the additives on elemental concentrations found in the hard deposits are summarised in Table 32. In this table, the symbols represent the ratios calculated from the average concentrations in deposits from a test case (3 rings) relative to the average concentrations in the deposits from the reference case as:

- ++ Concentration is more than 200% of the reference case
- + Concentration is between 125 and 200% of reference case Concentration is between 75% and 125% of reference case (insignificant)
- Concentration is between 50% and 75% of reference case
- -- Concentration is less than 50% of reference case

Table 32 Summary of concentration deviation from reference case BW.

Tabell 32. Sammanställning över skillnader i koncentrationer jämfört med referensfallet för eldstadssonden.

BW	FS	Kao	Lime	SWS1	S	SWS2	PbO	PbO+SWS
CI	++		++					
S	++		++	-	++			-
Р		-		++	-	++		++
K	++			-	+		-	
Pb	+		++		-		++	
Zn	-	-					-	
Ca	-		-					

Deposits on super heater (SH) probes

The average deposition rates found on the SH-probes are shown in Figure 51, where the blue part of the bars represent the amount of deposits that stuck to the sample rings after a mechanical knock, and the red part represents the loose dust that fell off during handing and knocking. The distribution of "hard" deposits between the individual rings is shown in Figure 53 and the elemental compositions of the loose material (as analysed by XRF) are shown in Figure 52.

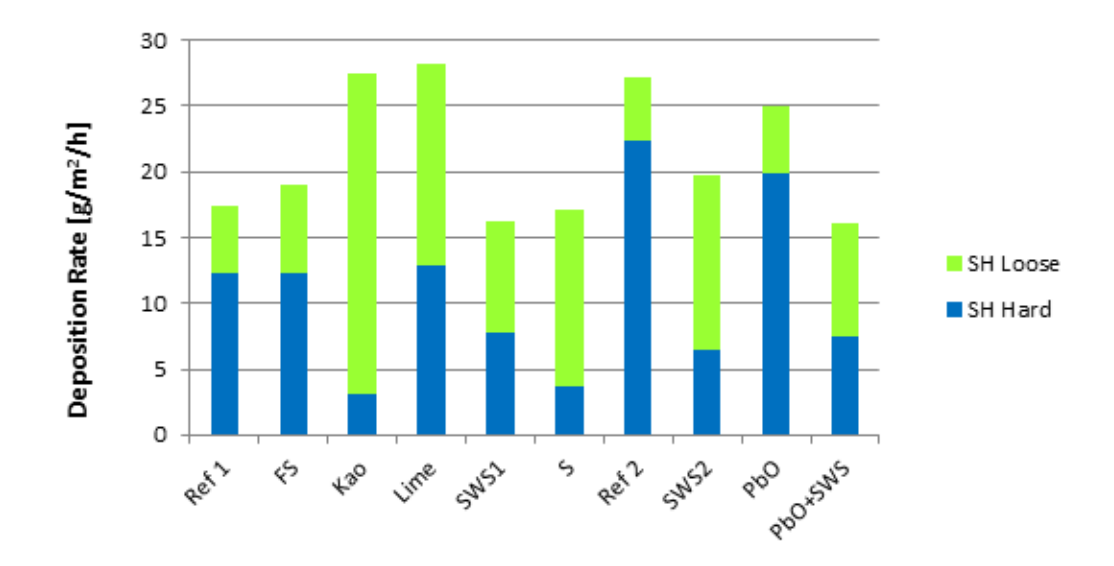


Figure 51 Deposition rate on rings at superheater position, as average of three (3) rings.

Figur 51 Deponeringshastighet för avlagringar på överhettarsondsprover, medelvärde för tre ringar.

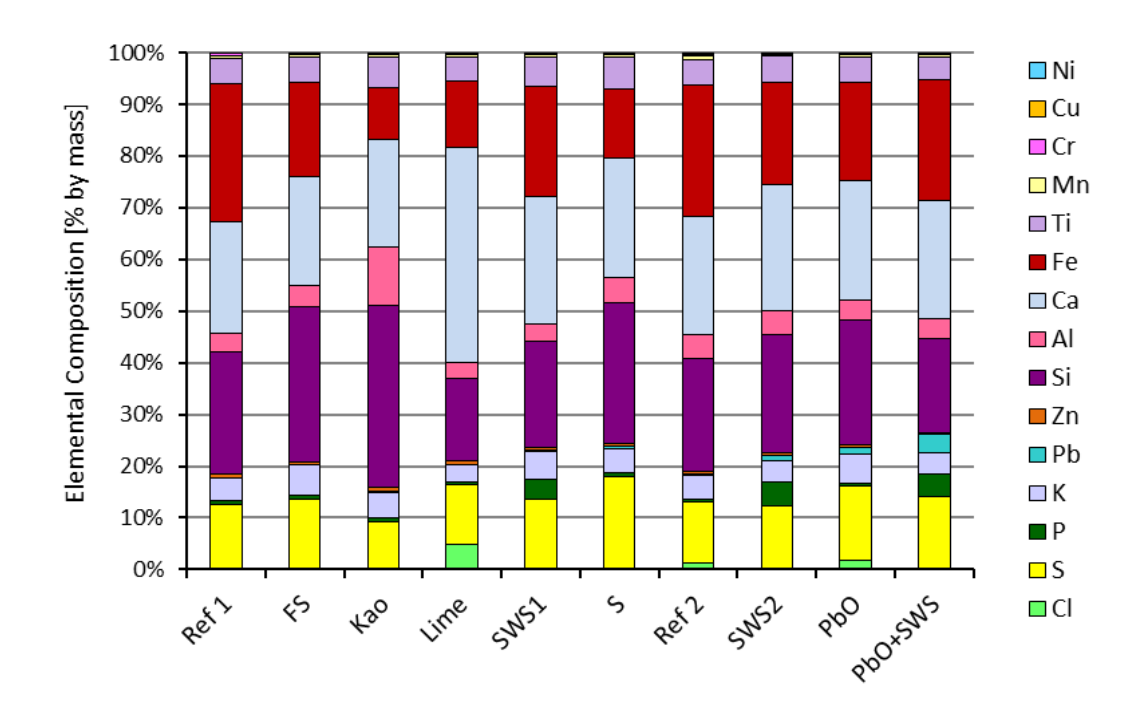


Figure 52 Elemental composition of "loose" deposits on superheater probes Figur 52 Kemisk sammansättning för löst sittande avlagringar på prover

Table 33 Loose SH deposits, selected elements of low concentrations in Figure 52

från överhettarsonden.

Tabell 33. Löst sittande avlagringar på ÖH-sonden, koncentration av några utvalda ämnen, samma data som illustreras i Figur 52.

%, mass	Ref 1	FS	Kao	Lime	SWS1	S	Ref 2	SWS2	PbO	PbO+ SWS
CI	0,22	0,15	0,022	3,3	0,16	0,034	0,61	0,08	0,62	0,09
S	7,9	6,3	4,8	8,1	7,2	10,3	6,0	5,8	5,4	6,5
Р	0,53	0,42	0,44	0,43	2,15	0,45	0,31	2,3	0,23	2,0
K	2,8	2,7	2,5	2,3	2,9	2,7	2,4	2,0	2,2	2,0
Pb	0,054	0,067	0,15	0,060	0,11	0,24	0,14	0,54	0,47	1,6
Zn	0,54	0,25	0,35	0,44	0,30	0,26	0,26	0,22	0,19	0,23

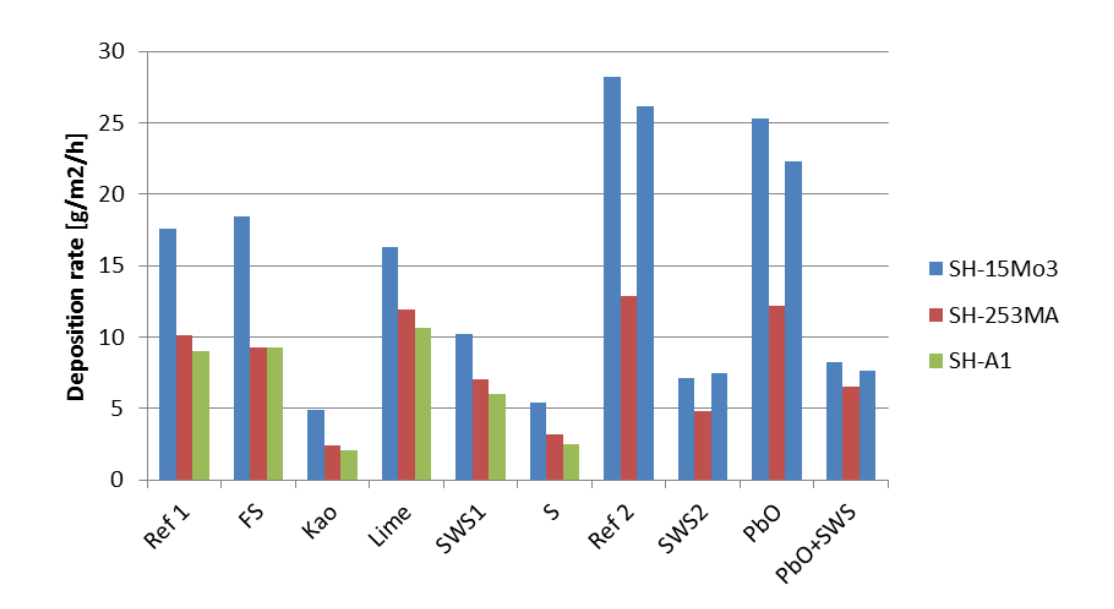


Figure 53 Deposition rate of "hard" deposits on individual rings at SH.

Figur 53 Deponeringshastighet för hårt sittande avlagringar på överhettarsondsprover, på enskilda ringar.

Table 34 Hard SH deposits, average concentrations of selected elements.

Tabell 34. Hårt sittande avlagringar på ÖH-sonden, medelvärden för koncentration av några utvalda ämnen.

%, mass	Ref 1	FS	Kao	Lime	SWS1	S	Ref 2	SWS2	PbO	PbO+ SWS
CI	3,8	1,4	0,1	19,3	0,5	0,2	8,1	0,2	10,8	0,4
S	34,2	31,9	20,8	13,8	32,4	48,1	19,3	30,5	22,4	33,3
Р	0,9	1,0	0,9	0,8	4,4	1,0	1,0	4,0	0,9	4,1
K	19,2	16,9	6,8	12,5	17,6	10,7	14,2	12,9	14,8	11,6
Pb	0,1	0,1	0,4	0,1	0,2	1,2	0,8	1,3	2,4	6,0
Zn	1,1	0,6	0,5	0,5	0,7	0,7	0,8	0,5	0,7	0,5

Observations from the analysis of elements in the hard deposits are listed below:

• Lime did, to some degree, reduce the concentrations of Zn in the SH position, while the Pb concentrations remained almost unaffected. In the deposits at the SH position, the lime additive showed severely increased concentrations of Cl while the concentrations of S were reduced. Lime reduced concentrations of K and increased concentrations of Ca in the SH deposits.

- **Foundry sand** increased the S concentrations in the deposits both at the SH position. Overall, this additive was found to have little effect on the SH deposits, even if the analyses show a tendency of slightly lowered concentrations of CI.
- For **kaolin**, some measurements of the concentrations of elements in the SH deposits failed, but the few analyses obtained indicate reduced concentrations of Zn, Cl, and S at the SH-position.
- **Sulphur** reduced Zn in the SH position but increased concentrations of Pb in the SH position. The sulphur additive increased S-concentrations in the deposits and reduced the concentration of Cl at the SH position. The concentration of K decreased in SH deposits.
- **Sewage sludge** reduced the concentrations of CI in the deposits. On the other hand, it increased concentrations of Pb in the deposits at the SH position. It may also be noted that the addition of sewage sludge increased concentrations of P in all deposits.
- Spiking the fuel with **PbO** resulted in increased concentrations of Pb in the deposits.

The influence of the additives on elemental concentrations found in the deposits are summarised in Table 35. In this table, the symbols represent the ratios calculated from the average concentrations in deposits from a test case (3 rings) relative to the average concentrations in the deposits from the reference case as:

- ++ Concentration is more than 200 % of the reference case
- + Concentration is between 125 and 200% of reference case Concentration is between 75% and 125 % of reference case (insignificant)
- Concentration is between 50 % and 75 % of reference case
- -- Concentration is less than 50 % of reference case

Table 35 Summary of concentration deviation from reference case at SH
 Tabell 35. Sammanställning av avvikelse i koncentration jämfört med referensfallet för överhettarproverna.

SH	FS	Kao	Lime	SWS1	s	SWS2	PbO	PbO+SWS
CI			++					
S		-			+	+		+
Р				++		++		++
K			-		-			
Pb		++		++	++	+	++	++
Zn	-			-	-	-		-
Ca			++					

5.3.5 XRD analyses

Several deposit samples from the BW-probes were analysed by XRD (X-Ray Diffraction) at Vattenfall's laboratory. The relatively small amounts of deposits made the measurements difficult, and only five samples were successfully analysed. They were:

- 1. Loose deposits from BW-probe, Case Ref 2
- 2. Loose deposits from BW-probe, Case SWS 2
- 3. Loose deposits from BW-probe, Case PbO
- 4. Loose deposits from BW-probe, Case PbO+SWS
- 5. Hard deposits from BW-probe, Case PbO+SWS

The large number of chemical compounds present in the samples made identifications difficult for the compounds present in low concentrations. For instance, Pb_2O , PbO, ZnS, FeS and FeS_2 shows overlapping peaks with each other as well as with NaCl and KCl, which prevented positive identification of these compounds.

A semi-qualitative estimation of the distribution of identified compounds in the samples is given below in Table 36.

Table 36 A semi-qualitative estimation of the distribution of identified compounds in the samples by XRD

Tabell 36. Semikvalitativ uppskattning av fördelningen av identifierade föreningar i proverna genom analys med XRD.

Compound	Loose Deposit Ref1	Loose Deposit SWS2	Loose Deposit PbO	Loose Deposit PbO+SWS	Hard Deposit PbO
SiO ₂	S	S	S	S	W
NaCl	М		М		S
CaSO4	М	М	М	М	W
KCI	W		М		М
TiO2	W	W	W	W	
Fe2O3	W		W	М	М
CaAl2Si2O8	W	W	W	W	
Fe3O4*		М		W	

^{*)} Fe3O4 may be difficult to distinguish from Fe₂O₃ by this method

From Table 36, it is notable that the XRD failed to detect neither NaCl nor KCl for the two cases when sewage sludge was added to the fuel (SWS2 and PbO+SWS). In the reference case, the fraction of alkali chlorides was estimated to 21 %, which was increased to 28 % when PbO was added to the fuel. The loose deposits did contain a high fraction of SiO_2 and a substantial amount of $CaSO_4$. When sewage sludge was added to the fuel, the iron was

detected as Fe₃O₄ instead of Fe₂O₃, but this is uncertain because it is hard to differentiate between these two compounds with this measurement technique.

In the hard deposit, closer to the tube surface, the fraction of alkali chlorides increases, as indicated by the last column of Table 36. This is from the PbO case, which was the worst case regarding the corrosion rate and the XRD analysis indicates an alkali fraction over 80%! Even though the estimations come from a basically qualitative method it gives an idea of the situation.

The XRD results show that for most cases, the fraction of NaCl is higher than the fraction of KCl; it is four times more NaCl than KCl in the loose deposits in the Ref 2 case and almost three times more in the hard deposits of the PbO. On the other hand, the fractions of NaCl and KCl are quite evenly matched in the loose deposit of the PbO case. The comparison between NaCl and KCl is of interest here because the XRF analyser used detects the concentrations of K but not Na. Since the fuel contains roughly the same quantities of these alkali metals, it could have been assumed that they would show up at roughly equal concentrations in the deposits as well. However, these XRD analyses show that such an assumption may be incorrect.

5.3.6 Distribution of selected elements in ashes, deposits and gas The distribution of some elements between different ashes, deposits and in gas phase (for Cl and S) are calculated from measured amounts of ash and the concentrations of elements. There are of course uncertainties in these numbers; for example the fly ashes were sampled for 60 minutes and it has to be assumed that the fly ash concentrations were constant for the 8 hours of a testing period. It is possible that wall build-ups occasionally disconnected from the walls and caused irregular fly ash concentrations. Nevertheless, the balances shown below may indicate trends of different additives. The studied elements are Cl, S, Zn, Pb and K.

For the test case of the Sulphur additive, the wall deposits could not be properly analysed due to a sample handling mistake. Instead an average concentration from the other test cases has used in the figures below as it is probably closer to the truth than disregarding it completely. Anyway, the wall deposits constitute only a minor fraction of the distribution for most elements.

Distribution of CI

The distribution of chlorine between bottom ashes, fly ashes, HCl in gas phase, and the deposits on the probes are shown in Figure 54. Most of the Cl is apparently leaving the furnace in the gas phase as HCl, except when using the lime additive. For the lime additive, a substantially increased fraction of Cl was found in the ashes, fly ash as well as the bottom ash. The additives minimising the Cl in ashes are sulphur and kaolin followed by sewage sludge (SWS2). For these cases, the fraction of Cl as HCl increased instead. The additives of kaolin and sewage sludge reduce the fraction of Cl in deposits, both at BW and SH. The sulphur additive reduces the Cl fraction at SH but not so at BW.

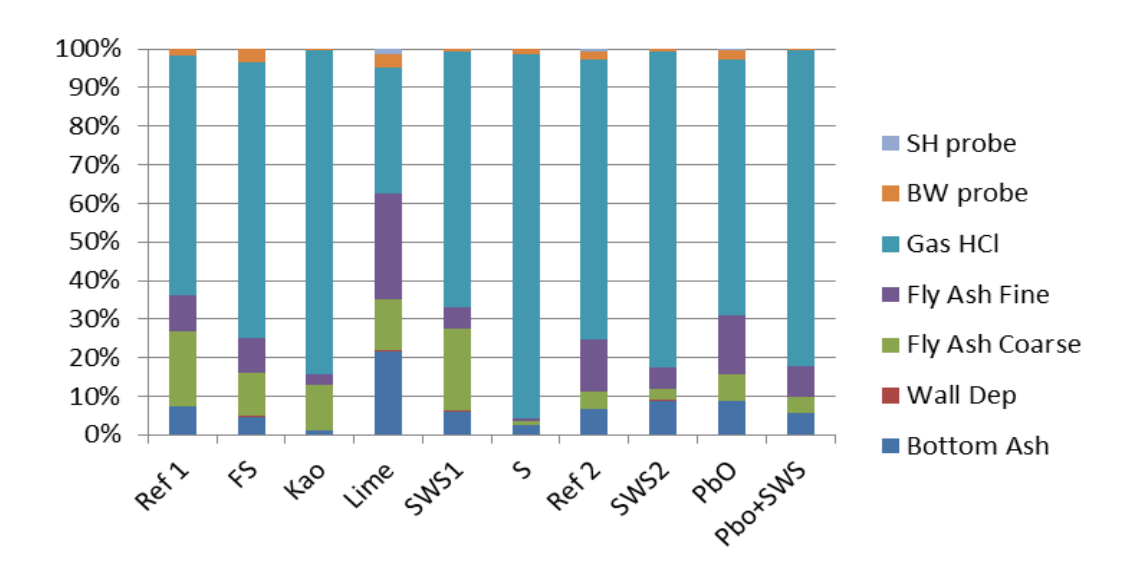


Figure 54 The distribution of CI recovered in ashes, flue gas and deposits.

Figur 54 Fördelningen av CI mellan askor, rökgaser och avlagringar.

Distribution of S

Most of the S supplied by the fuel is recovered in the bottom ash, except when S is used as an additive which causes a high fraction of S leaving the reactor in the flue gas as SO_2 . The additive Lime increases the fractions of S in the bottom bed, fine fly ash, and in the deposits at the BW. The additives reducing the fraction of S in the BW deposits are kaolin, sulphur and sewage sludge.

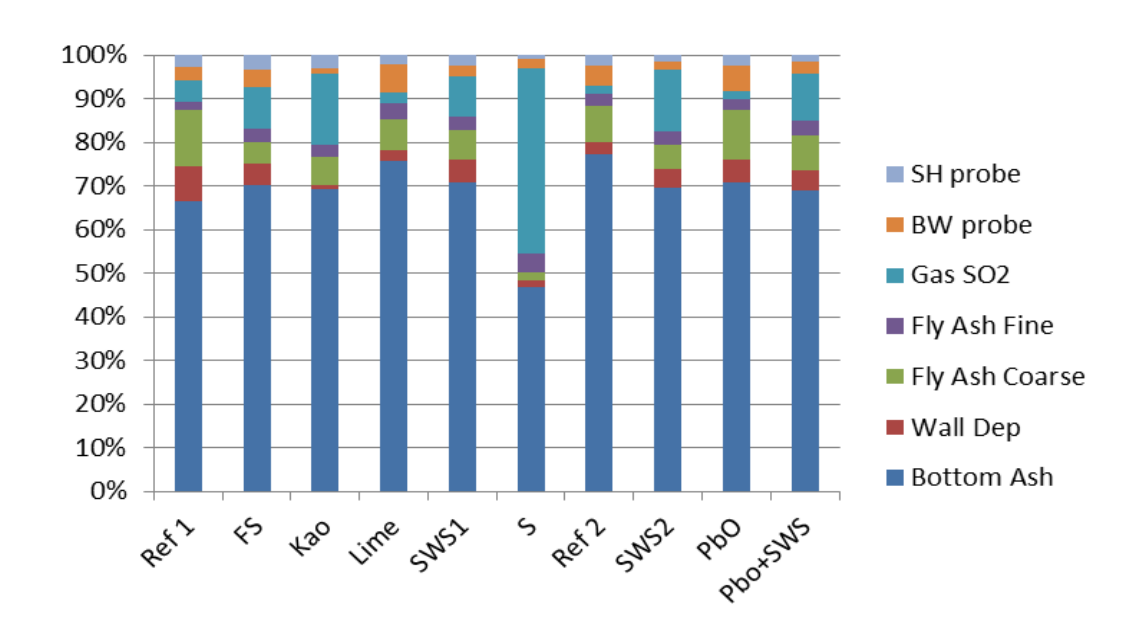


Figure 55 The distribution of S recovered in ashes, flue gas and deposits.

Figur 55 Fördelningen av S mellan askor, rökgaser och avlagringar.

Distribution of Zn

For Zn, shown in Figure 56, between 50 and 60 % is found in the bottom ash, except for the case of kaolin additive, which instead shows increased amounts of Zn in the fly ashes. The two additives with the least fractions of Zn in the BW deposits were foundry sand and lime. These two additives were, however, the two least efficient with respect to reducing the corrosion on the 16Mo3 samples in the furnace. It is not obvious in Figure 56 that lime captures Zn, but it does increase the fraction of the Zn recovered in the coarse fly ash, maybe as a consequence of that the amount of fly ash was increased by the lime.

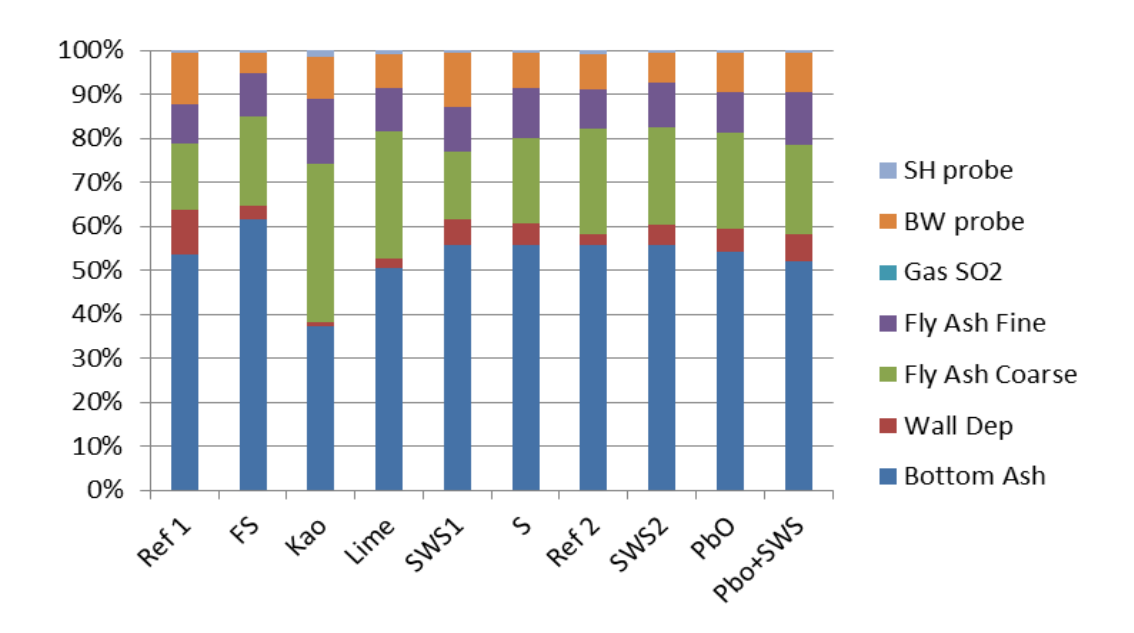


Figure 56 The distribution of recovered Zn in ashes, flue gas and deposits.

Figur 56 Fördelningen av Zn mellan askor, rökgaser och avlagringar.

Distribution of Pb

The distribution of Pb in Figure 57 is quite different from Zn (in Figure 56), with relatively low fractions of the Pb in the bottom ash, but instead rather high in the fine fraction of the fly ash. Here, it seems that lime and also sewage sludge capture some of the Pb in the bottom ash and in the coarse fraction of the fly ash. Consequently, these additives reduce the fraction of Pb found in the fine fly ash. Adding kaolin increased the amount of Pb in the coarse fraction and reduced it in the fine fraction of the fly ash. On the other hand, sulphur, gives increased fraction of Pb in the fine fly ash and reduced fraction in the coarse fly ash.

The two cases of clearly visible fractions of Pb (in Figure 57) in SH deposits are kaolin and sulphur, which coincidentally were the two additives showing the least corrosion on the SH samples (see next section). This may be explained by the Pb here being present in another form than the highly corrosive PbCl₂. At the BW, the additives reducing the fraction of Pb were foundry sand, sulphur and kaolin.

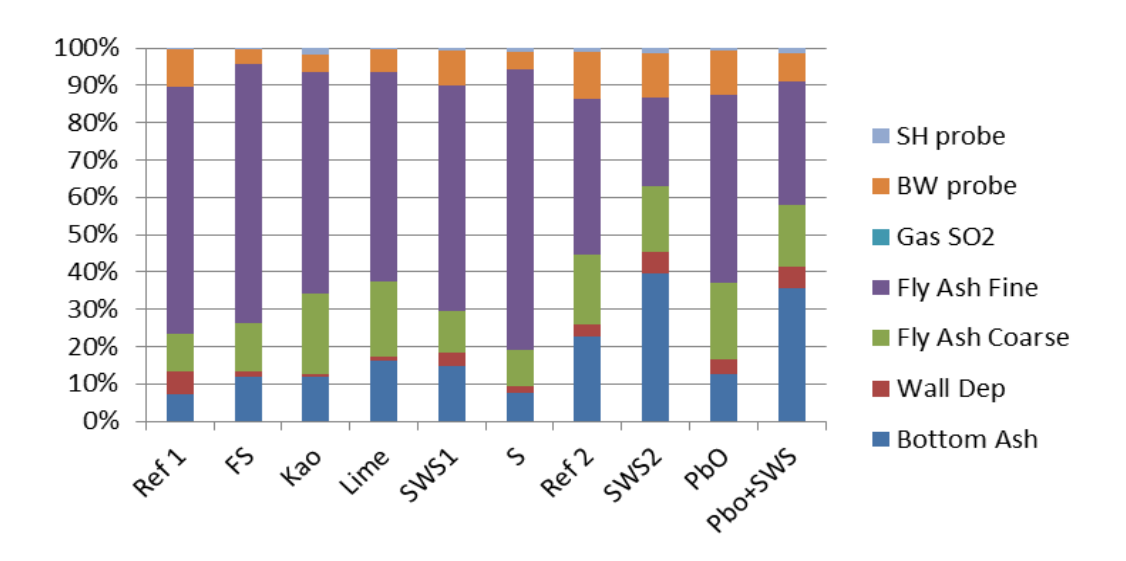


Figure 57 The distribution of recovered Pb in ashes, flue gas and deposits.

Figur 57 Fördelningen av Pb mellan askor, rökgaser och avlagringar

Distribution of K

As can be seen in Figure 58, most of the K found was in the bottom ash. It should be noted, however, that most of this K was contained already in the fresh sand used as bed material. Nevertheless, the sewage sludge tends to increase the fraction of K in the bottom ash, while the fraction is reduced somewhat by kaolin.

The fractions of the K recovered in the fine fly ashes were reduced by kaolin, foundry sand and sewage sludge, while it was increased by the additives lime and sulphur.

Another observation is that the additives of sewage sludge and kaolin minimises the fractions of K in the deposits on the probes (both SH and BW). Sulphur reduces the fraction of K captured at SH but increases the fraction at BW. Lime increases the fractions of the K in both BW and SH.

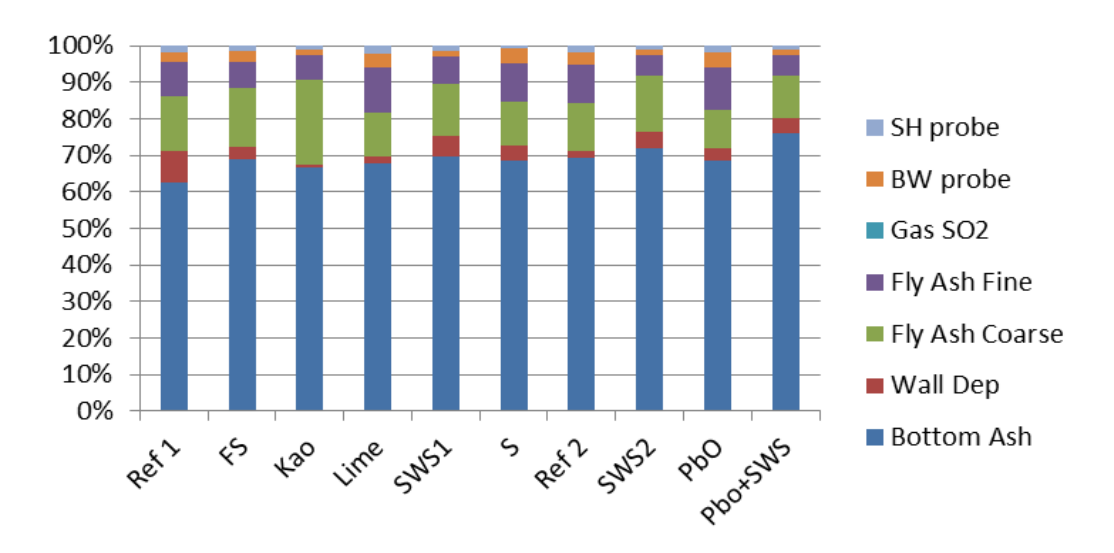


Figure 58 The distribution of recovered K in ashes, flue gas and deposits.

Figur 58 Fördelningen av K mellan askor, rökgaser och avlagringar.

5.3.7 Corrosion analysis

Material probes were inserted into the flue gas stream in positions representing the boiler walls and the superheaters and exposed for 8 hours. The material samples on the probes were cooled to 400°C (waterwall) and 550°C (superheaters) respectively. In the first set of tests, three materials were tested on each probe, 16Mo3, 253 MA and Kanthal A1. In the second set of tests, two rings of 16Mo3 and one ring of 253 MA were used on each probe.

In the first set of tests a comparison was made between five different additives and a reference case with no additive. The additives were foundry sand, kaolin, digested sewage sludge, lime and sulphur.

In the second set of tests a deeper investigation of the effects of sewage sludge and Pb on corrosion was performed. Addition of a larger amount of sewage sludge was tested and two tests were also performed where the fuel had been spiked with PbO, to investigate the influence of Pb on the corrosion and the ability of sewage sludge to mitigate that type of corrosion. A reference run with no additions to the waste wood fuel was also performed.

The corrosion of the samples was evaluated from the appearance of the test ring after removal of the deposits. Macroscopic photos showing the corrosion damages have been taken at the inclination angle of the gas flow (wind side). The corrosion attack was in general limited to the wind side.

The most pronounced corrosion attack was seen on the 16Mo3 samples, whereas little corrosion was observed on the other samples. Therefore, only the results for the 16Mo3 samples are presented in detail here, a detailed report of the corrosion of all samples can be found in Appendix C. The Kanthal A1 material performed best, slightly better than 253 MA, which was far better than 16Mo3.

The corrosion of the samples from the firsts set of tests was only macroscopically investigated. This was sufficient to provide a ranking of the additives tested since the outcome was very distinct. The scales formed, which consist of the outer "hard" deposit, the mediate corrosion scale and the inner oxide layer, whichever are still attached to the rings, are also analysed by XRF.

The samples from the second test set were thoroughly investigated, by optical microscopy as well as by SEM-EDX, in addition to the methods used for the samples in the first test set. Optical microscopy was used to investigate the thickness of the oxide layer and SEM-EDX was used to investigate the nature of the corrosion attack. In the SEM images, the thickness and quality of the oxide layer can be studied, as well as the occurrence of internal corrosion. The EDX analysis provides information on what elements have been involved in the corrosion attack and gives an opportunity investigate if an additive has reduced the amounts of corrosive species in the different parts of the sample, such as corrosion front, bulk oxide and (if present) deposit.

5.3.8 BW comparison of additives (first set of tests)

The first set of tests performed is the first six cases listed in Table 20: Ref 1, FS, Kaolin, Lime, SWS1 and Sulphur. The corrosion of the test rings was not analysed in detail for this first set of tests. Instead, the overall corrosion was evaluated by optical evaluation by means of optical microscope, which was sufficient to provide a tentative ranking of additives tested.

Macroscopic photos, taken in optical microscope, of the 16Mo3 rings after exposure, in the boiler wall (BW) position of the furnace and subsequent removal of deposits are shown in Figure 59. These photos of corrosion attacks on the surface of the sample rings can be compared to the XRF analyses of selected elements in the deposits, prior to its removal, in Figure 60.

The two rings in Figure 59 that obviously are least attacked by corrosion are from the Kaolin and SWS1 cases (C) and (E) on which the grinding marks from the sample preparation are still visible.

- In the case of Ref 1 (A), corrosion products have scaled off between -100° to +100°.
- The ring from the case of **foundry sand** (B) has corroded spots between -90° and +90°. This attached scale has higher concentrations of S, Cl and K than the reference case, at least on the windward side.
- For the **kaolin** case (C), the ring is somewhat discoloured after the exposure, whereas the XRF analysis shows that the scale contains less S and Cl than the remaining scale from the reference case (A and C). The K concentration, however, is less affected by the additive.
- The ring from the **lime** case (D) is visibly corroded. The XRF analysis of the scale shows that the S and CI concentrations increase, while the K concentration is slightly reduced (perhaps replaced by Ca).
- The 16Mo3 ring from the **sewage sludge** case (E) shows only minor spots of onset of corrosion. The XRF analysis reveals that the concentration of CI is reduced compared to Ref 1, while the S concentration has increased on the leeward side. The K concentration is lower on the windward side but higher on the leeward side. The P content in the scale increase by the sewage sludge additive.
- The ring from the **sulphur** case (F) is corroded between -40° and +40°. This scale contains more S and K than reference, while the Cl content is only marginally affected by the sulphur additive.

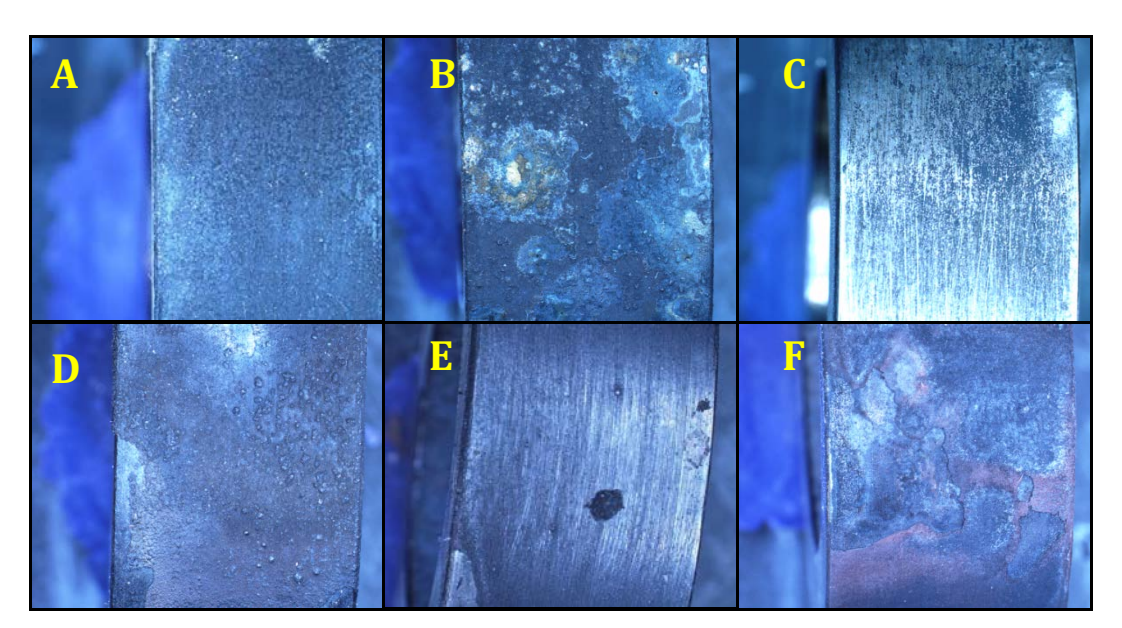


Figure 59 16Mo3 rings from BW position, after cleaning. A) Ref 1, B) FS, C) Kaolin, D) Lime, E) SWS1 F) Sulphur.

Figur 59 16Mo3-prover från eldstadssonden efter rengöring. A) Ref 1, B) FS, C) Kaolin, D) Lime, E) SWS1 F) Svavel.

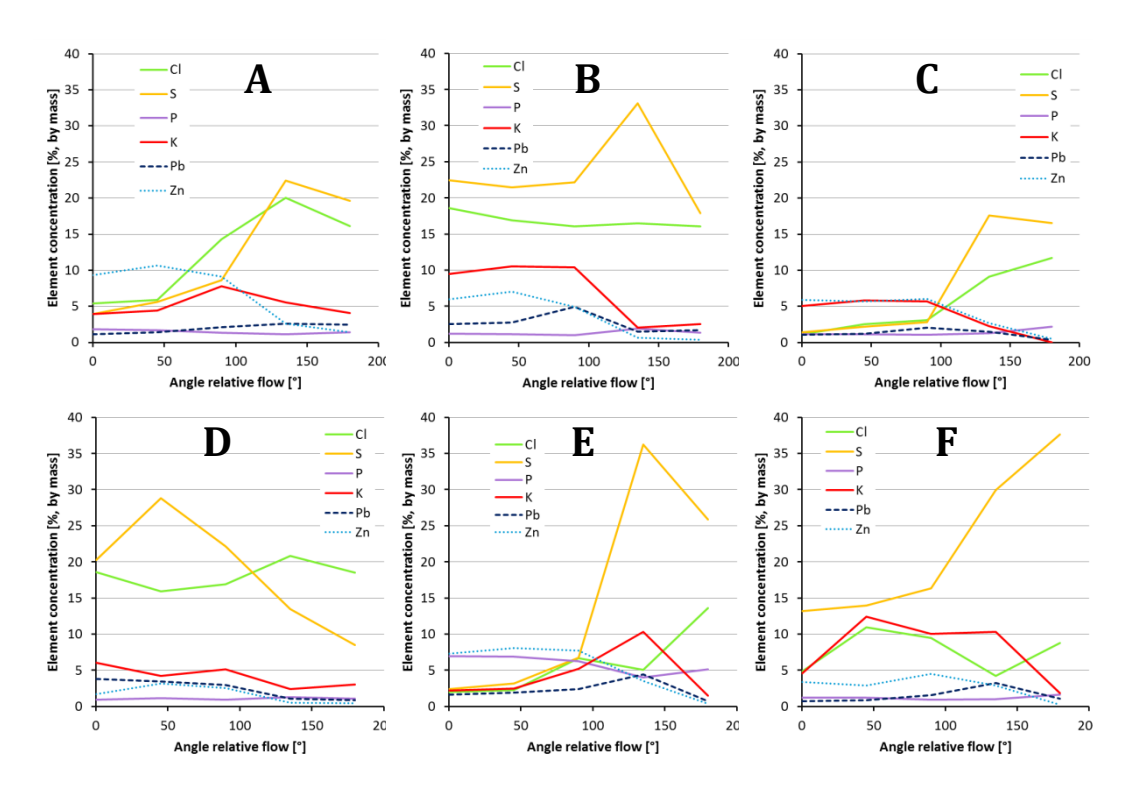


Figure 60 Elemental concentrations in deposits on the BW 16Mo3 rings, measured by XRF on the surface at varied angles relative to the windward side. A) Ref 1, B) FS, C) Kaolin, D) Lime, E) SWS1, F) Sulphur.

Figur 60 Koncentrationer av utvalda ämnen på 16Mo3-ringarna från eldstadssonden, uppmätt med XRF på ytan med olika vinklar i förhållande till vindsidan. A) Ref 1, B) FS, C) Kaolin, D) Lime, E) SWS1, F) Svavel.

5.3.9 BW comparison between reference case and sewage sludge addition (second set of tests)

The exposed test rings from a case of sewage sludge additive (SWS2) are compared to the second reference case (Ref 2) in order to highlight observed effects of the additive on the deposits and signs of initial corrosion.

Figure 61 shows the windward ring surfaces after removal of the deposit. For the ring from case Ref 2 (left), the corrosion product spalled off during the cleaning process revealing a severely corroded surface. The surface of the ring from case SWS2 is also corroded, but the metallic lustre and grinding grooves remain visible (right).

The graphs in Figure 62 show the concentrations of selected key elements (measured by XRF). The major alloying elements of the test rings, i.e. Fe, Cr and Ni are normally detected but are not accounted for in the shown concentrations. The left hand graphs show the results from Ref 2 and the right hand graphs from SWS2.

Figure 62 shows that the CI-and S-concentrations in the scale are reduced when sewage sludge is added to the fuel. The maximum value of the CI concentration found at 90° is reduced from about 17 mass-% to about 13 mass-%, and the CI reduction is even higher elsewhere around the ring. The average S concentration is also significantly reduced, even though the thin scale towards the leeward sides show high concentrations. The Zn concentrations are similar between the cases. The K and Pb concentrations are found to be in similar ranges for the two test cases. The P concentration increases when sewage sludge is added.



Figure 61 Photos of the windward sides of the 16Mo3 rings after deposit removal (BW position). Left) Ref 2, Right) SWS2.

Figur 61 Foton på vindsidorna på 16Mo3-ringarna efter att avlagringen tagits bort (eldstadssond). Vänster) Ref 2, Höger) SWS2

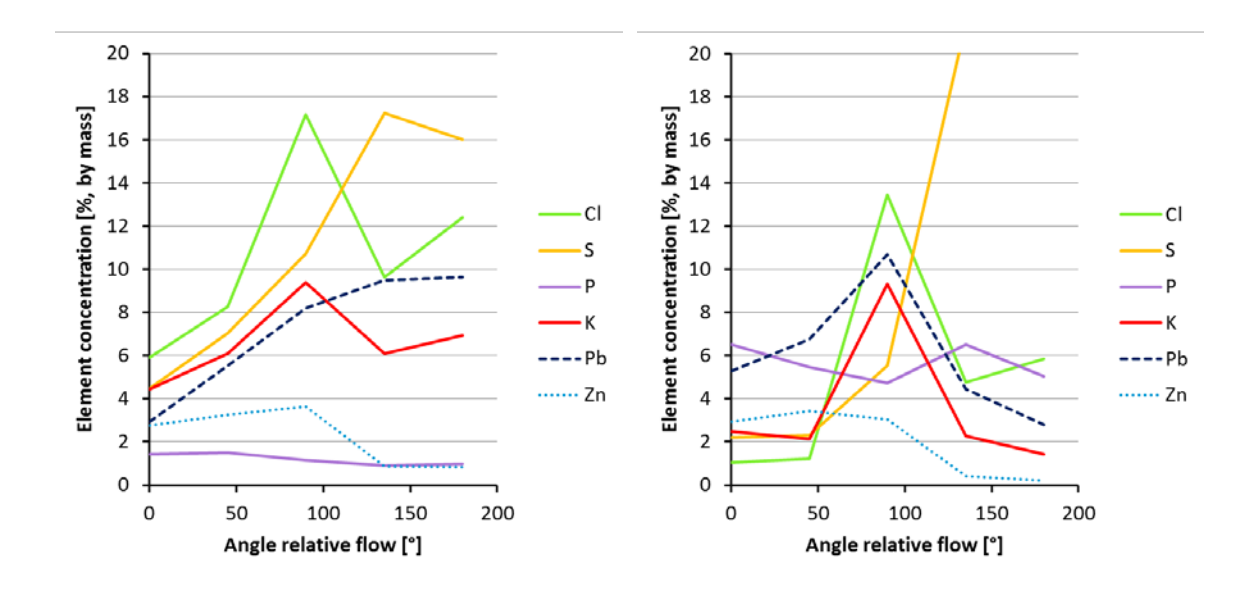


Figure 62 Elemental concentrations in BW deposits on 16Mo3 rings by XRF analyses. Left) Ref 2. Right) SWS2.

Figur 62 Avlagringarnas sammansättning på eldstadssondens ringar av 16Mo3, bestämd med XRF. Vänster) Ref 2, Höger) SWS2.

Optical microscopy analysis

The micrographs in this section are taken by optical microscopy. The upper dark areas in the micrographs are the mount resin material.

Figure 63 shows cross sections of 16Mo3 rings exposed in the BW-position from the test cases of Ref 2 (top figure) and SWS2 (bottom figure). The top image (case Ref 2) shows the yellow/grey steel with a 40-50 μ m thick corrosion layer. A thicker dark greyish layer is observed between the corrosion layer and the resin. The cross-section of the ring from case SWS2 (Figure 63 , bottom) shows a reddish steel substrate with a 20-30 μ m thick corrosion layer outside. An outer dark layer can also be seen between the corrosion layer and the resin. The samples have been etched with water

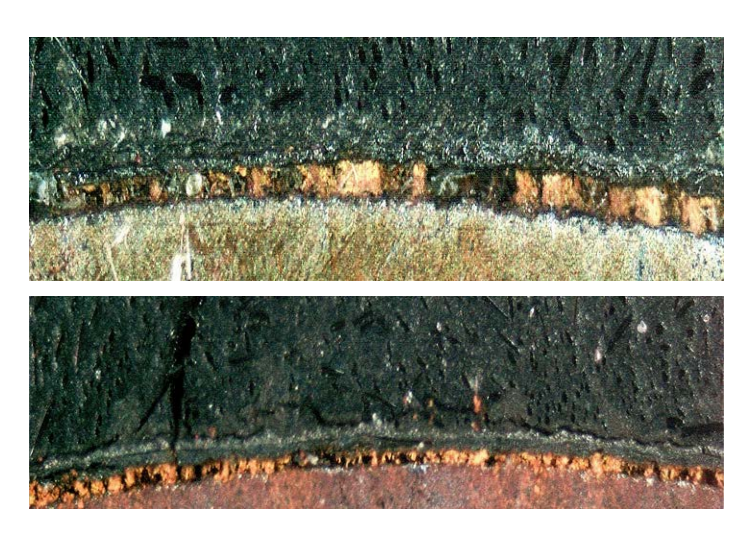


Figure 63 Micrographs cross-sections of windward sides of 16Mo3 rings exposed in the BW-position. Top) Ref 2. Below) SWS2.

Figur 63 Tvärsnitt av vindsidan på 16Mo3-ringar från eldstadssonden. Ovan) Ref 2. Nedan) SWS2

Figure 64 shows the cross-sections of the leeward sides of the 16Mo3 rings. A very thin brown-reddish layer can be seen between the ring substrate and the resin but some of the scale might have fallen off during sample preparation. The leeward side of the 16Mo3 ring from case SWS2 is shown to the right in Figure 64. No layer between the test ring and the resin is found. (The scratches on the substrates may originate from the sample preparation when some corrosion scales came loose and the particles caused grooves in the steel.)





Figure 64 Micrographs cross-sections of leeward sides of 16Mo3 rings exposed in the BW-position. Left) Ref 2. Right) SWS2.

Figur 64 Tvärsnitt av läsidan på 16Mo3-ringar från eldstadssonden. Vänster) Ref 2.Höger) SWS2.

SEM/EDX-analysis Windward side – Ref 2

The figures in this section show cross-sections analysed by means of SEM (Scanning Electron Microscope) and EDX (Energy Dispersive X-Ray). The BSE mode (Backscatter Electrons) was used when the aim was to identify heavier elements, e.g. Pb. The BSE mode shows heavier elements as brighter than lighter elements. This means that positions on the sample with high concentrations of Pb can be seen as bright spots or areas.

The top image in Figure 65 is taken by means of BSE-SEM-imaging on the windward side of the 16Mo3 ring from case Ref 2. The steel substrate is seen at the lower and left part of the image. A layered 75 – 80 μm thick scale, appears dark grey, adjacent to the steel substrate. At the rightmost upper part, the black resin with bright areas is seen. At the outermost part of the scale Pb is present, represented by the bright areas. Some Pb is also dispersed within the scale.

The element EDX-mappings shown in the matrix of smaller images, show the lateral distribution of selected elements over the area shown in the BSE-SEM image. Chlorine is present in the corrosion front at locally high concentrations. On the other hand, S is not detected at the corrosion front. Instead, the highest S-concentrations are found further out in the scale. The alkali metals are found at the outer part of the scale. Pb is mainly present at the outer part of the scale but some Pb can also be found dispersed in the scale. Zn is also

present in higher concentrations at the outer part of the scale. Ca is mainly present in the resin. O can be found throughout the whole scale.

The chemical analysis of the point in the outer part of the corrosion layer denoted "Spectrum 1" in the top SEM-image in Figure 65 is displayed in Table 37. The S and Pb concentrations are relatively high, 22 and 17 atomic-%, respectively. The Cl concentration is close to zero. O and Fe are also present. The corrosion product may consist of Fe–O–Pb compounds, with a different composition compared to the point in Figure 66 which is closer to the corrosion front.

Table 37 Elemental composition of the point labelled "Spectrum 1" in Figure 65

Tabell 37. Elementsammansättning i punkten märkt "Spectrum 1" i Figur 65.

Element	Weight%	Atomic-%
0	12.71	46.17
Si	0.15	0.31
S	12.32	22.33
CI	0.22	0.37
Ca	0.16	0.23
Fe	12.17	12.66
Zn	0.35	0.31
Pb	61.69	17.30

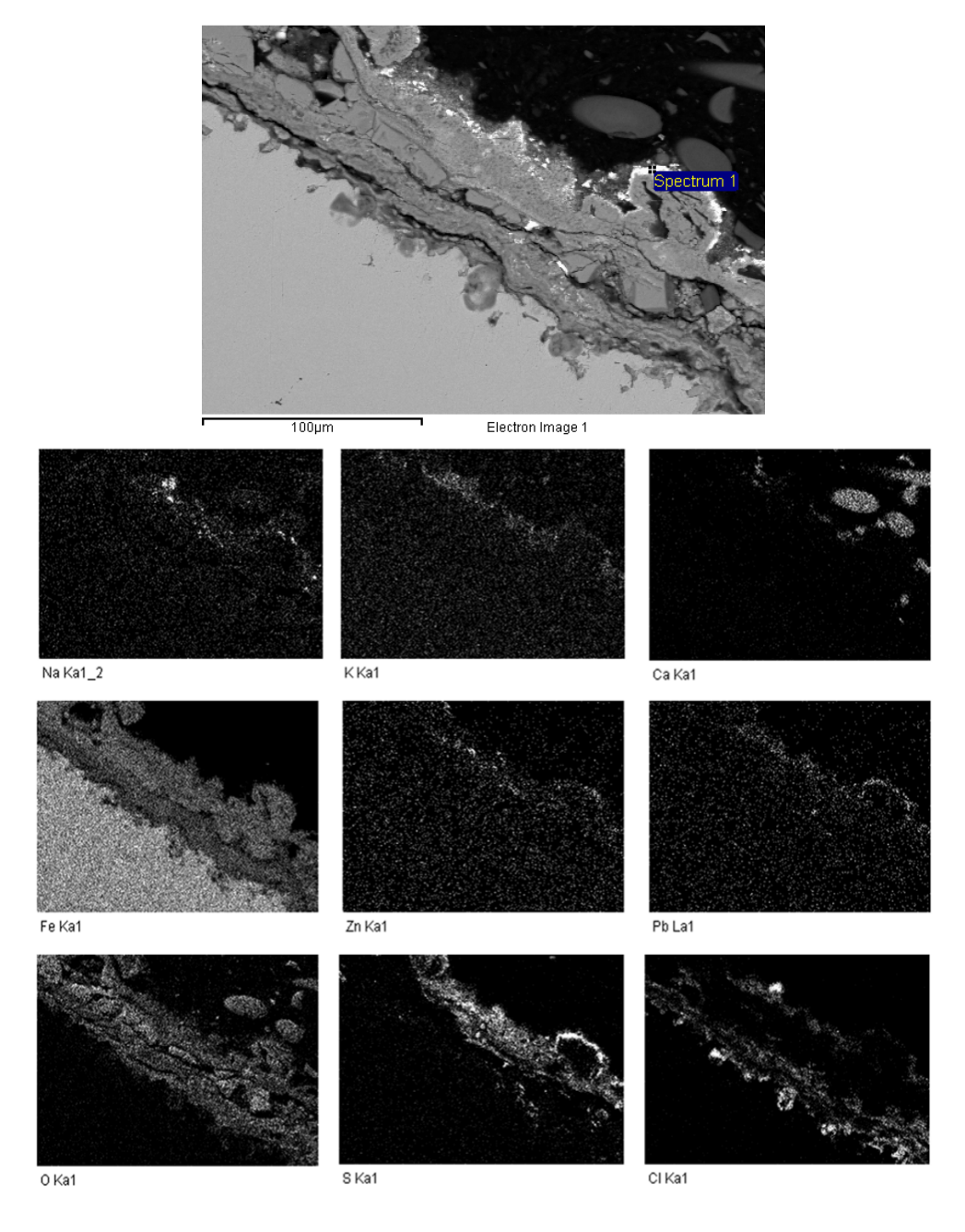


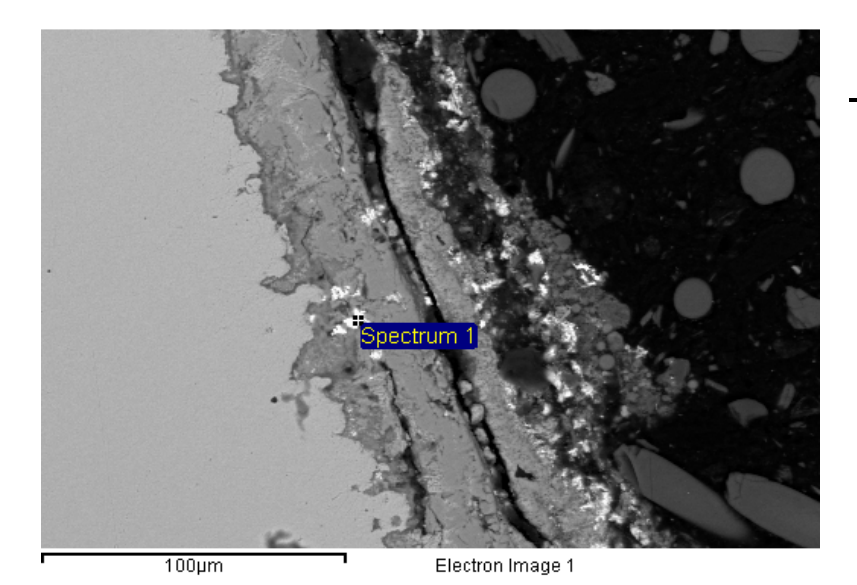
Figure 65 BSE-SEM image of the scale formed at the windward of a 16Mo3 ring from case Ref 2. Below images of element mappings.

Elemental composition of point "Spectrum 1" is given in Table 37

Figur 65 SEM-bild på beläggnings/korrosionsprodukten på vindsidan av en 16Mo3-ring från fallet Ref2. Översta bilden tagen i BSE-SEM-mode och nedanför visas fördelningen av olika ämnen.

Sammansättning i punkten "Spectrum 1" ges i Tabell 37.

Figure 66 is also taken at the windward side, from the same ring as in Figure 65, showing the presence of Pb as bright spots. The chemical analysis made in the bright spot, relatively close to but not at the corrosion front, denoted "Spectrum 1" is also shown. About 14 atomic-% of Pb was found, Cl is present at 10 atomic-%. Na, K and Zn are also present at relatively low concentrations, below 1 atomic-%. It is worth to notice that no S was detected. Fe and O are also present. It can be speculated if the corrosion product includes Pb — O — Cl compounds.



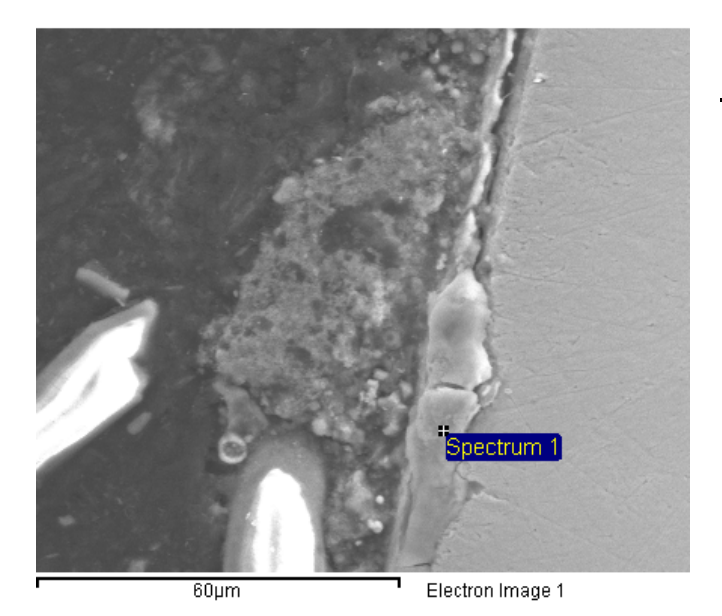
Element	Weight%	Atomic%
0	20.80	63.48
Na	0.48	1.01
S	0.00	0.00
CI	7.20	9.92
K	0.20	0.24
Fe	11.64	10.17
Zn	0.58	0.44
Pb	58.47	13.78

Figure 66 SEM image of the formed layers at the windward of a 16Mo3 ring from case Ref 2.The bright areas consist of Pb, O and S. Elemental composition of point "Spectrum 1" is given.

Figur 66 SEM-bild av korrosions/beläggningsprodukterna som bildats på vindsidan av en 16Mo3-ring från fallet Ref2. De ljusa fälten består av Pb, O och S. Sammansättning i punkten "Spectrum 1" visas.

Leeward side - Ref 2

The SEM-image in Figure 67 is taken at the leeward side of the same ring as above (16Mo3, BW-position, case Ref 2). The thicknesses of the formed scale vary in the range between 5 and 15 μ m. The chemical composition in "Spectrum 1" is shown. The CI concentration is relatively high, 12.7 atomic-%. Only minor amounts of Pb, K, Ca, Mn and Na are detected, less than 0.5 atomic %. No S is detected. Fe and O are present. N is present at relatively high concentration; 12.2 atomic %. It is not clear if this concentration is an artefact or if N actually is present.



Element	Weight%	Atomic%
N	5.68	12.17
0	24.07	45.13
Na	0.33	0.43
Si	0.14	0.15
CI	15.04	12.73
K	0.49	0.37
Ca	0.13	0.09
Mn	0.37	0.20
Fe	53.38	28.68
Pb	0.38	0.05
	₹	

Figure 67 SEM image of the formed layers at the leeward side of a 16Mo3 ring from case Ref 2. Elemental composition of point "Spectrum 1" is given.

Figur 67 SEM-bild av den bildade beläggnings/korrosionsprodukten på läsidan av en 16Mo3-ring från fallet Ref2. Sammansättning i punkten "Spectrum 1" visas.

Windward side - SWS2

Figure 68 below is taken at the windward side of a 16Mo3 sample ring exposed during test case SWS2. The metal substrate is at the top of this image and the oxide layer thickness is about $70-80~\mu m$ and adjacent a deposit layer can also be seen in the image. The correlating element maps show that CI is present in the corrosion front but also elsewhere in scale in correlating with certain layer structures.

Some S is present a relatively low concentration in the oxide layer but S is present at higher concentrations elsewhere in the scale. No alkali metals are detected in the corrosion front, but can be found in low concentrations in the outer part of the scale. Pb is detected in the outer parts of the scale but some is also dispersed in the scale. However, no Pb is detected in the corrosion

front. P (originating from the sewage sludge) is found in the outer part of the scale (in the deposit).

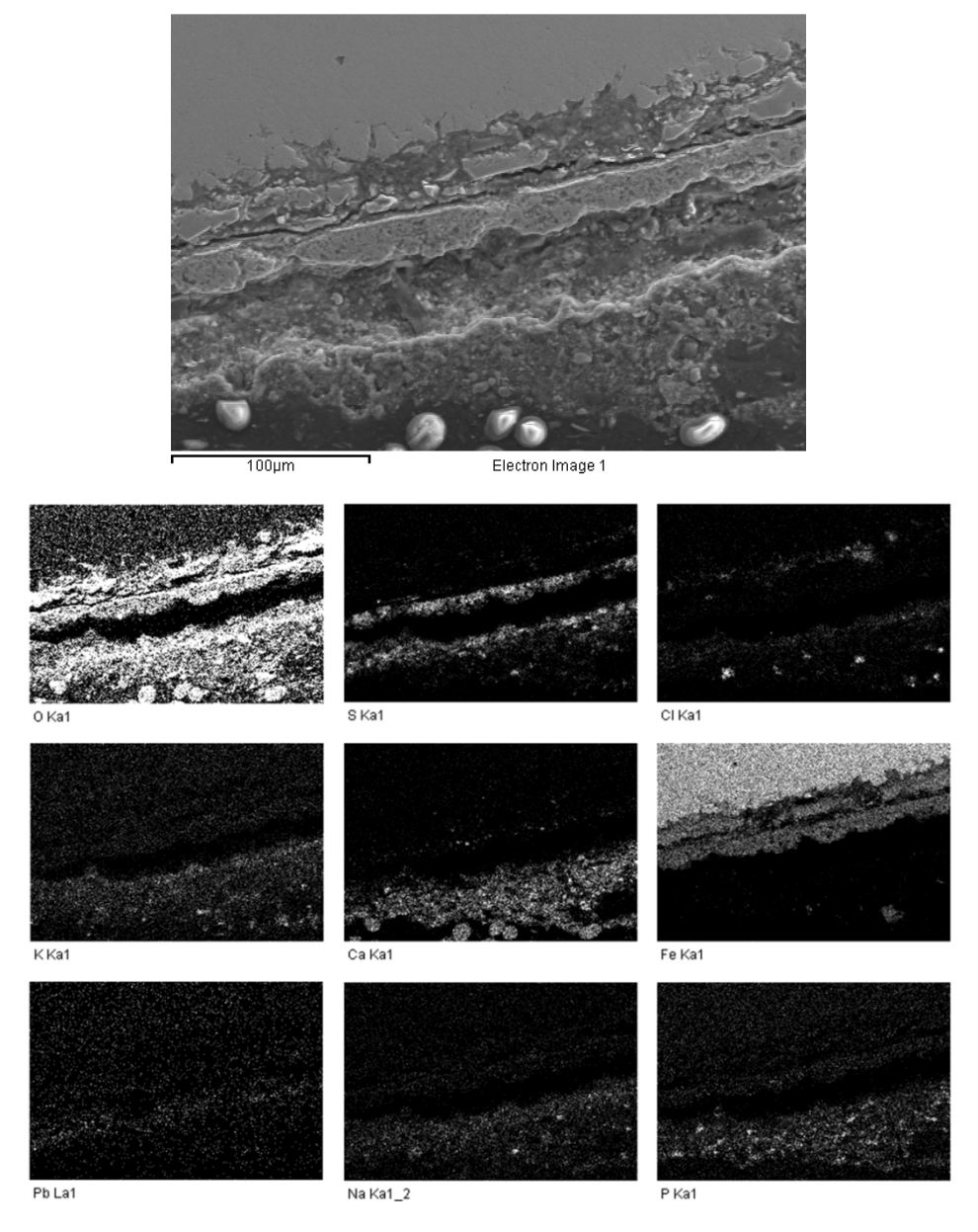


Figure 68 SEM/EDX image of the corrosion/deposit layer at the windward of a 16Mo3 ring from case SWS2. Top photo by BSE-SEM, below images of element mappings.

Figur 68 SEM-bild av korrosionsprodukt/påslagprodukt på vindsidan av en 16Mo3-ring från fallet SWS2. Översta bilden tagen i BSE-SEM-mode, nedanför visas spridning av vissa ämnen över analysytan.

SEM/EDX-analysis of leeward side - SWS2

Figure 69 below is taken at the leeward side of the same sample ring as above. The oxide thickness is thin, only some μm thick. The chemical analysis at the point denoted "Spectrum 3" consists mainly of Fe and O. Several other elements are present at low concentrations.

- 60μm	Spectrum 3	Element	Weight%	Atomic%
		0	33.53	60.67
		Na	1.54	1.94
		Mg	1.55	1.85
		Al	0.96	1.03
		Si	1.47	1.52
		Р	0.50	0.47
		S	0.41	0.37
		CI	2.21	1.81
		K	0.48	0.35
		Ca	2.12	1.53
		Cr	0.24	0.13
		Mn	0.35	0.19
		Fe	54.21	28.10
		Pb	0.43	0.06

Figure 69 SEM image of the thin corrosion layer at the leeward of a 16Mo3 ring from case SWS2. Elemental composition in "Spectrum 3" is given.

Figur 69 SEM-bild av en tunn korrosionsprodukt på läsidan av en 16Mo3ring från fallet SWS2. Den kemiska sammansättningen i analyspunkten "Spectrum 3" visas.

5.3.10 Comparison between PbO spiked fuel with and without sewage sludge addition at the BW position (second set of tests)

This section gives a comparison between the two test cases of waste wood spiked with PbO (1g Pb per kg dry fuel) and PbO + SWS (1 g Pb + 80 g sewage sludge per kg dry fuel). The purpose of the additional PbO is to study the influence of Pb on waterwall corrosion and the comparison here is to see if the corrosive attacks of Pb can be mitigated by sewage sludge.

Figure 70 shows the wind side of the ring surface. The corrosion product on the ring from the PbO-case spalled off repeatedly during the cleaning process, finally revealing a severely corroded surface. The surface of the ring from case PbO+SWS is also corroded, but spalled off only on limited areas. The difference between the rings is, unfortunately not really made clear by the photos in Figure 70.

Figure 71 shows the concentrations of selected key elements in the attached scale as a function of the circumference (0° and 180° corresponds to the windward side and leeward side, respectively). The left hand graphs show the results from case PbO and the right hand graphs show case PbO+SWS.

The concentrations of CI and Pb are reduced when sewage sludge is added to the fuel. The S concentration appears to be insignificantly affected by the additive. The Zn concentration is slightly increased by the sewage sludge additive while K may be somewhat reduced. The P concentration is increased when sewage sludge is added.





Figure 70 Photos of the windward sides of the 16Mo3 rings after deposit removal, BW position.

Left) PbO. The corrosion products have spalled off repeatedly. Right) PbO+SWS. The corrosion layer has spalled off at some areas.

Figur 70 Vindsidan på 16Mo3-ringar från eldstadssonder efter att avlagringarna tagits bort.
Vänster) PbO, korrosionsprodukterna har lossnat flera gånger.
Höger) PbO+SWS, korrosionsprodukter har lossnat från några ytor.

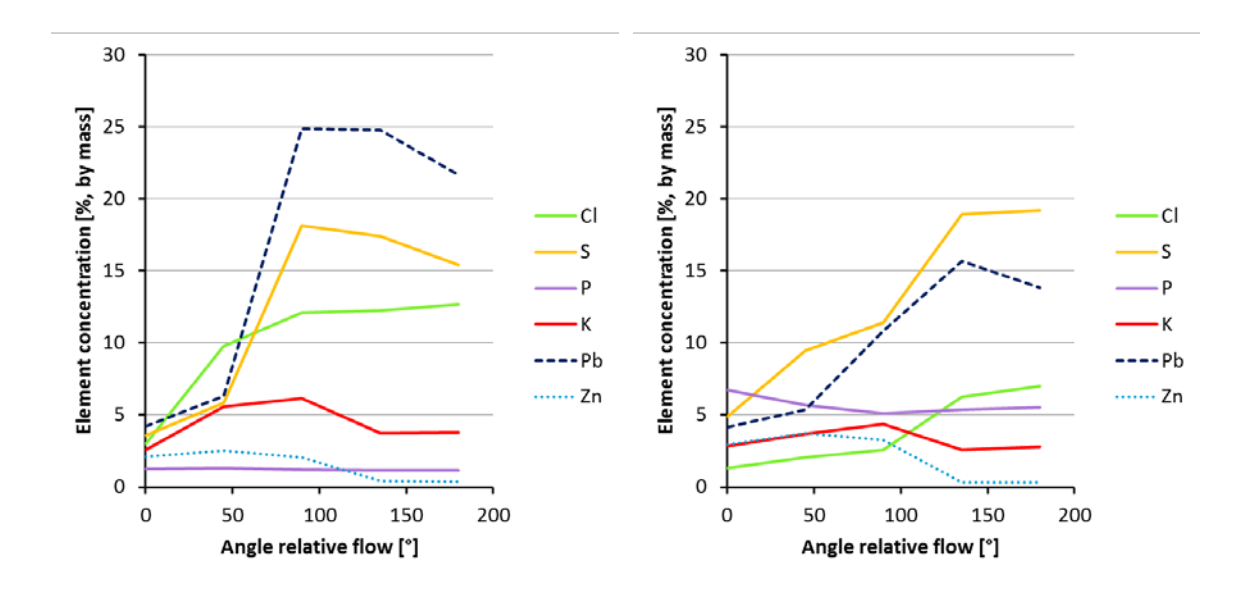


Figure 71 Elemental concentrations in the scales on 16Mo3 rings from BW position. Left) PbO. Right) PbO+SWS.

Figur 71 Kemisk sammansättning för påslag på eldstadssondens ringar av 16Mo3, analyserad med XRF. Vänster) PbO, Höger) PbO+SWS2.

Optical microscope images

The micrographs in Figure 72 are taken by optical microscopy on the wind side of the sample rings of 16Mo3. The upper dark areas in the micrographs are the mount resin material and the red areas at the bottom are the steel substrates. The top photo in Figure 72 shows a reddish 16Mo3 steel substrate with a 1 mm thick corrosion layer outside, from case PbO. The figure below, from case PbO+SWS, shows a reddish steel substrate with a 300-500 µm corrosion layer on the outside. The samples have been etched with water.

Corresponding images from the leeward side of the sample rings are presented in Figure 73. At this side of the rings, the corrosion layers are much thinner, about 100 µm for case PbO and considerably less for case PbO+SWS.

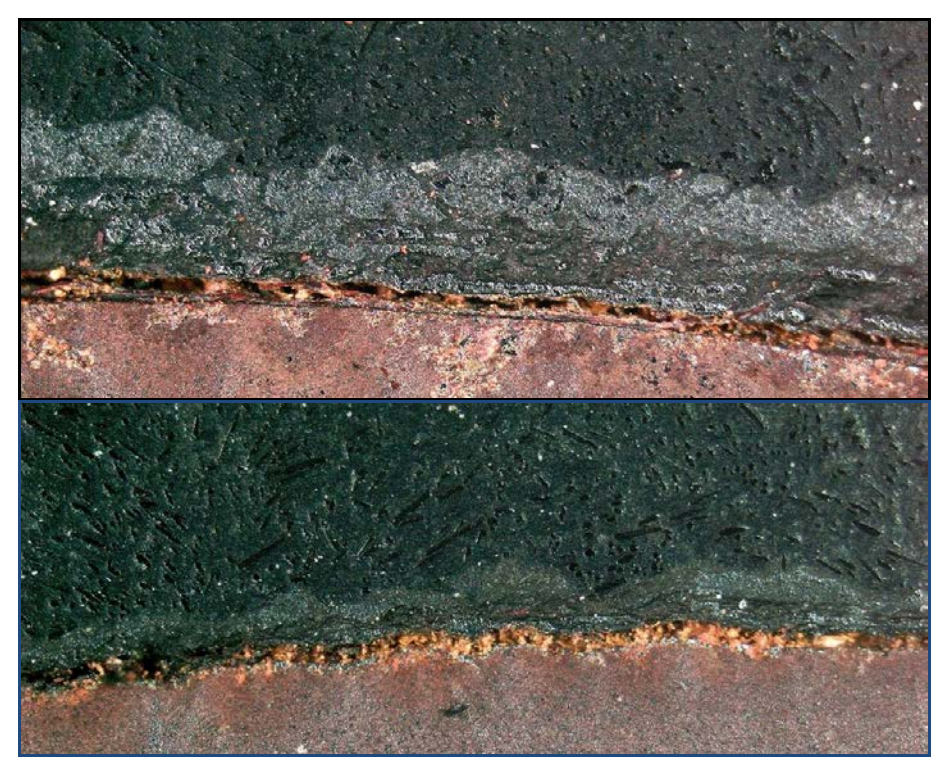


Figure 72 Micrographs over cross-sections of windward sides of 16Mo3 rings exposed in the BW-position. Top) PbO. Scale thickness is about 1mm. "Water etched". Bottom) PbO+SWS. Corrosion layer: 300-500µm. Water etched. Different magnification.

Figur 72 Tvärsnitt av vindsidan på 16Mo3-ringar från eldstadssonden.
Ovan) PbO. Oxidtjocklek 1 mm. Nedan) PbO+SWS.
Korrosionslager 300-500µm. Etsat med vatten.Olika förstoring.

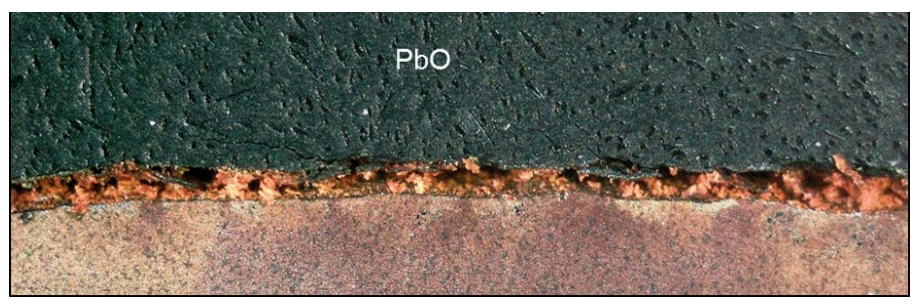




Figure 73 Micrographs cross-sections of leeward sides of 16Mo3 rings exposed in the BW-position. Top) PbO. Corrosion layer about 100 µm. "Water etched". Bottom) PbO+SWS..

Figur 73 Tvärsnintt av läsidan på 16Mo3-ringar från eldstadssonden. Ovan) PbO. Korrosionsprodukten är c:a 100 µm, Nedan) PbO+SWS.

SEM/EDX-analysis Windward side - PbO

A SEM/EDX image of the cross section of the 16Mo3 sample exposed in the BW position during case PbO is shown in Figure 74, with the steel substrate is to the left. The corrosion product is thicker than 500 µm. The correlating element maps in Figure 74 show that CI is concentrated in the corrosion front but also elsewhere in the structures of the layer. There is no visual evidence of S being present anywhere in the corrosion layer. No alkali metals are present directly in the corrosion front, but they can be found dispersed in the other parts of the scale. The maps for Pb and Zn show many small dots that may be noise.

The corrosion front was scanned further in search of for Pb, using the SEM, because it was unexpected that no clear Pb mapping appeared in Figure 74, considering that the fuel had been spiked with PbO and high concentrations of Pb were detected by XRF in Figure 71. An EDX analysis of an area where Pb was found is also given, with the corresponding SEM image in Figure 75. Only lower Pb concentrations were found elsewhere.

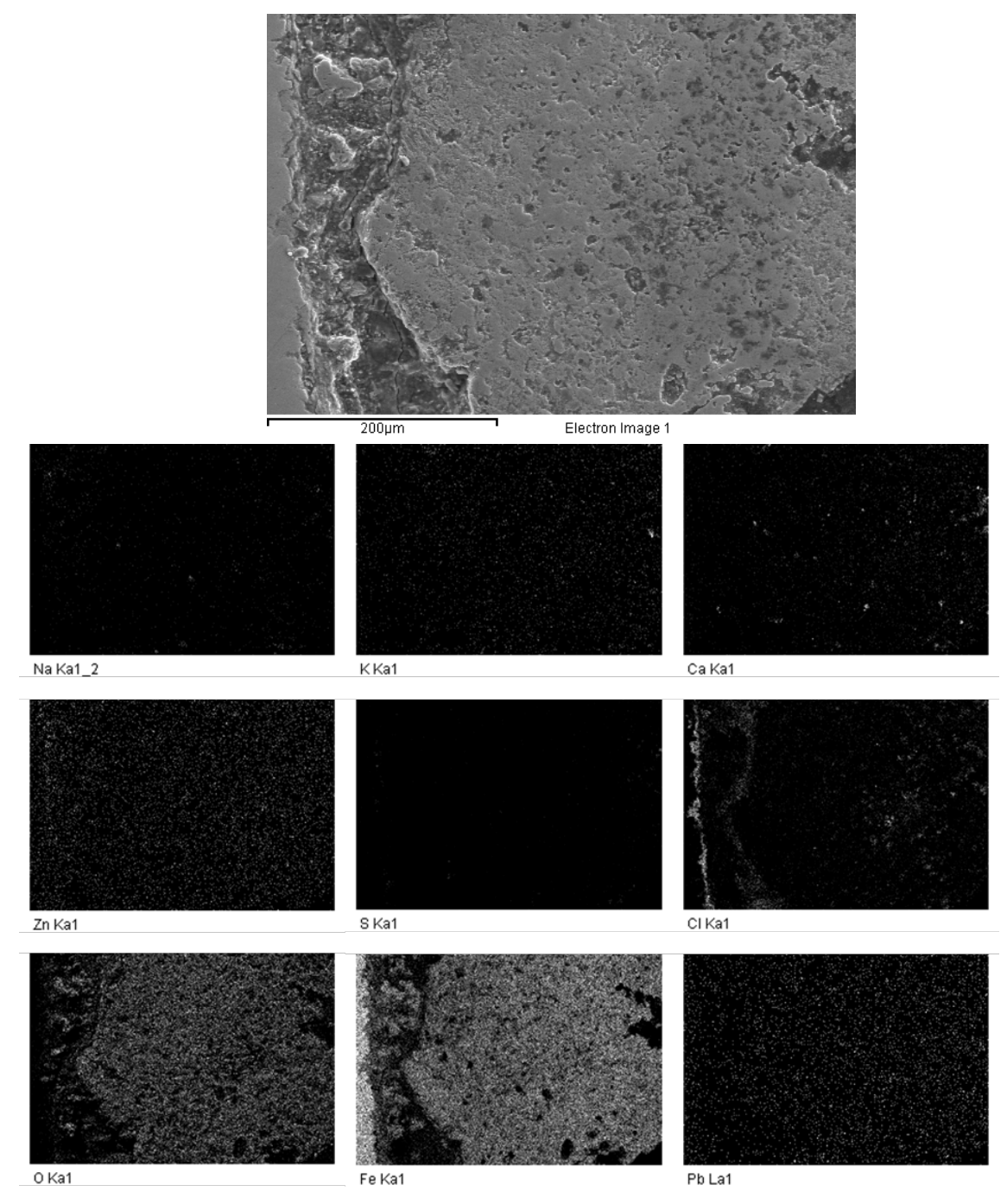


Figure 74 SEM/EDX image of the scale at the windward side of a 16Mo3 ring from case PbO. Top photo by BSE-SEM, below a matrix of element mapping.

Figur 74 SEM-bild av beläggnings/korrosionsprodukt på vindsidan av en 16Mo3-ring från fallet PbO. Översta bilden i med BSE-SEM-mode, nedanför visas utbredningen av vissa ämnen.

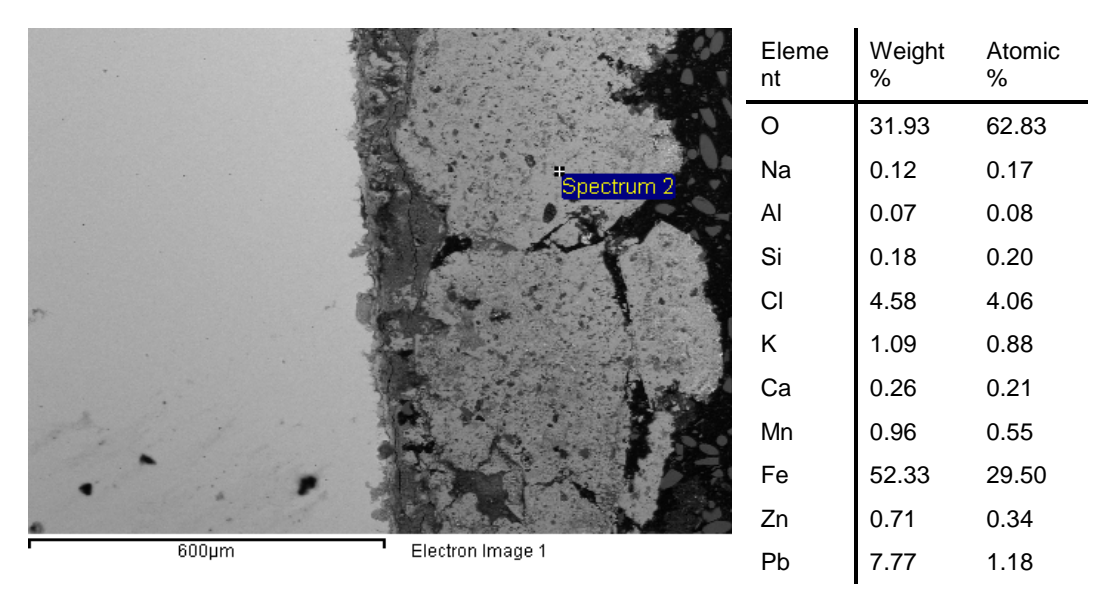


Figure 75 SEM image from cross-section of a 16Mo3 ring exposed in the BW position during case PbO. Elemental composition in point "Spectrum 2" given.

Figur 75 SEM-bild av beläggning/korrosionsprodukten på vindsidan av en 16Mo3-ring från fallet PbO. Sammansättning i punkten "Spectrum 2" visas.

Windward side - PbO+SWS

A SEM/EDX image of the cross section of the 16Mo3 sample exposed in the BW position during case PbO+SWS is shown in Figure 76, in which the steel substrate is to the upper right. The thickness of the formed scale is about 150 μ m. The correlating element maps in Figure 76 show that CI is concentrated mainly to the corrosion front but is also present in an outer layer interface. S is present in boundaries at the outer corrosion layer. Some alkali metals are detected in the outer part of the scale but not at the corrosion front. Also P detected is in the outer scale. The maps for Pb and Zn are a bit prickled by noise, but there is a faint line of Pb at the outer corrosion layer.

An example of SEM/EDX analysis of a spot in the inner corrosion layer is given in Figure 77, composed mainly of O, Fe and CI, with small amounts of alkali metals, Zn and a little Pb.

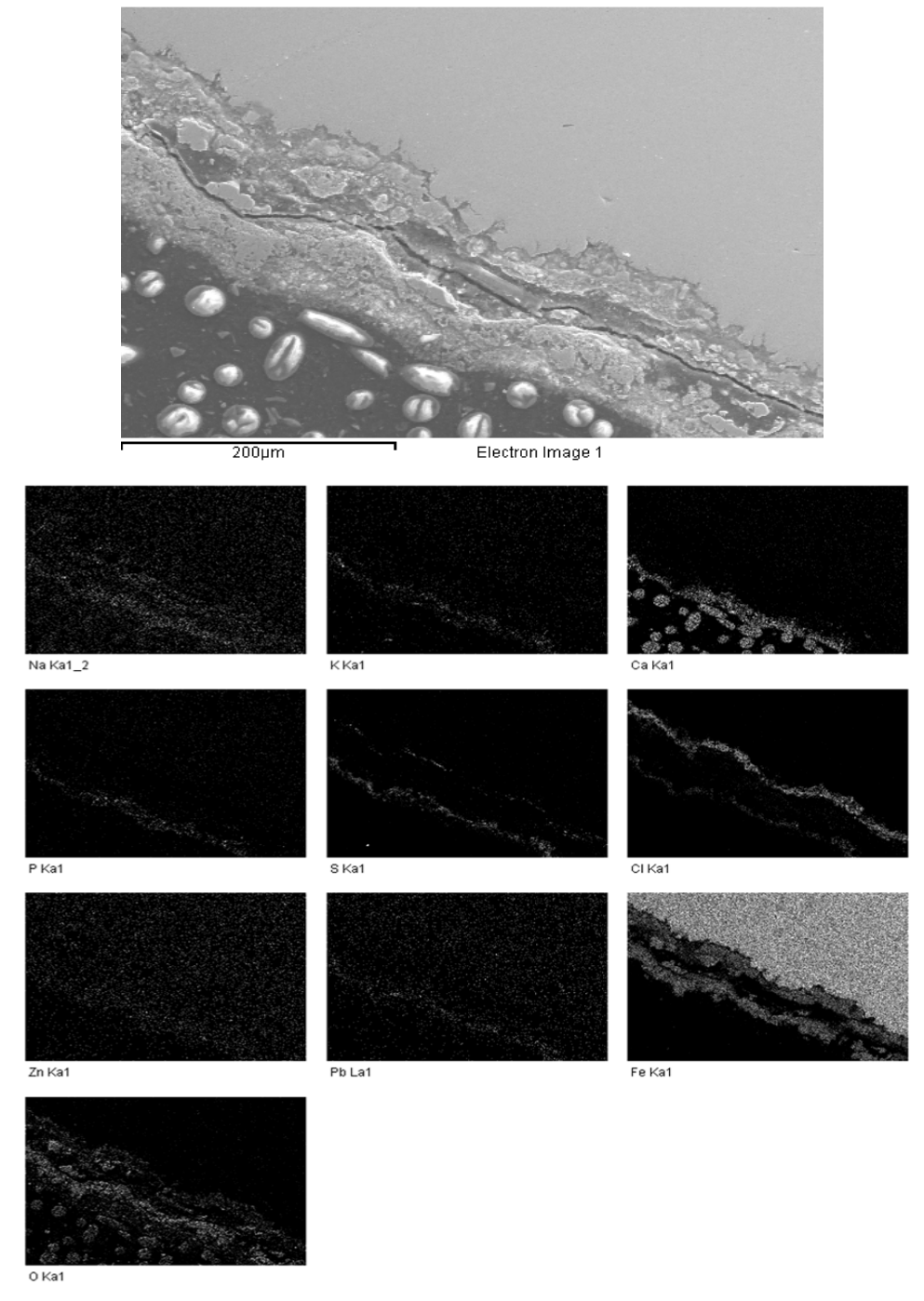


Figure 76 SEM/EDX image of the corrosion layer at the windward side of a 16Mo3 ring from case PbO+SWS. Top image taken in BSE-SEM-mode, below a images of element mappings.

Figur 76 SEM-bild av korrosionslagret på vindsidan av en 16Mo3-ring från fallet PbO+SWS. Översta bilden tagen i BSE-SEM-mode, nedanför bilder som visar fördelningen av vissa ämnen över analysytan.

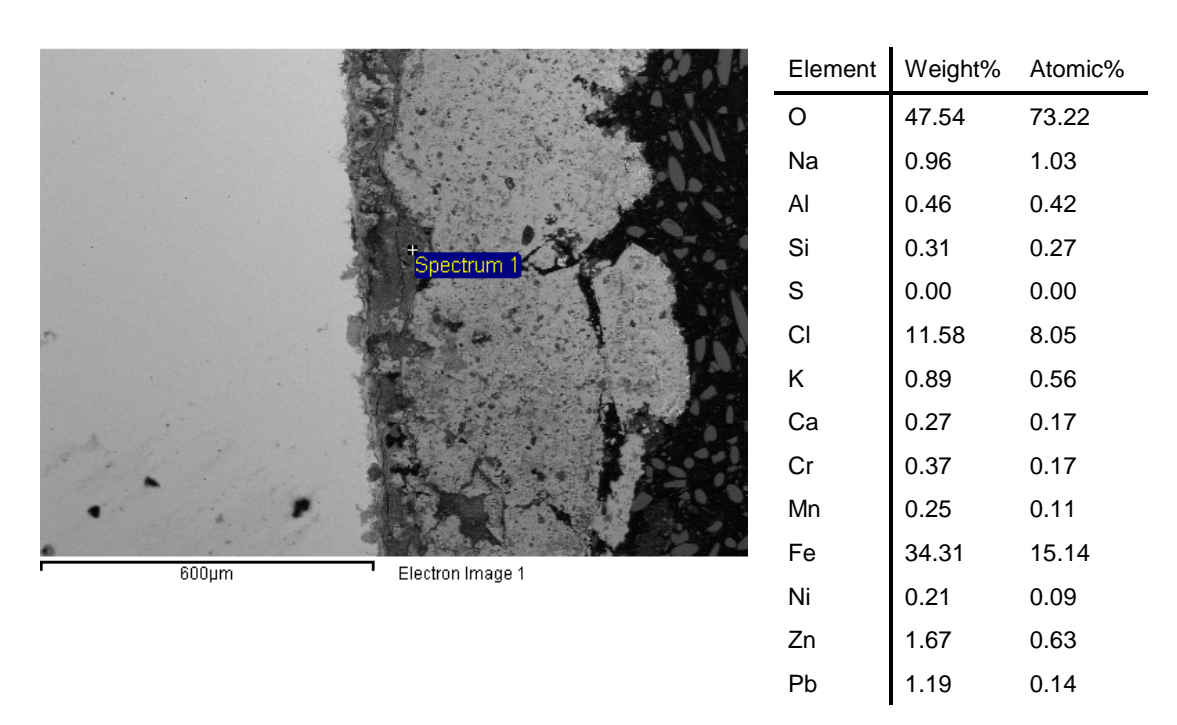


Figure 77 SEM image from windward cross-section of a 16Mo3 ring exposed in the BW position during case PbO+SWS. The elemental composition in point "Spectrum 1" given.

Figur 77 SEM-bild av korrosions/beläggningsprodukten på vindsidan av en 16Mo3-ring från fallet PbO+SWS. Kemisk sammansättning i punkten "Spectrum 1" visas.

Leeward side - PbO+SWS

The SEM image from the leeward side of the 16Mo3 sample from case PbO+SWS in Figure 78 displays a corrosion layer of about 20 μ m. The EDX analysis of the spot marked in the figure is also given.

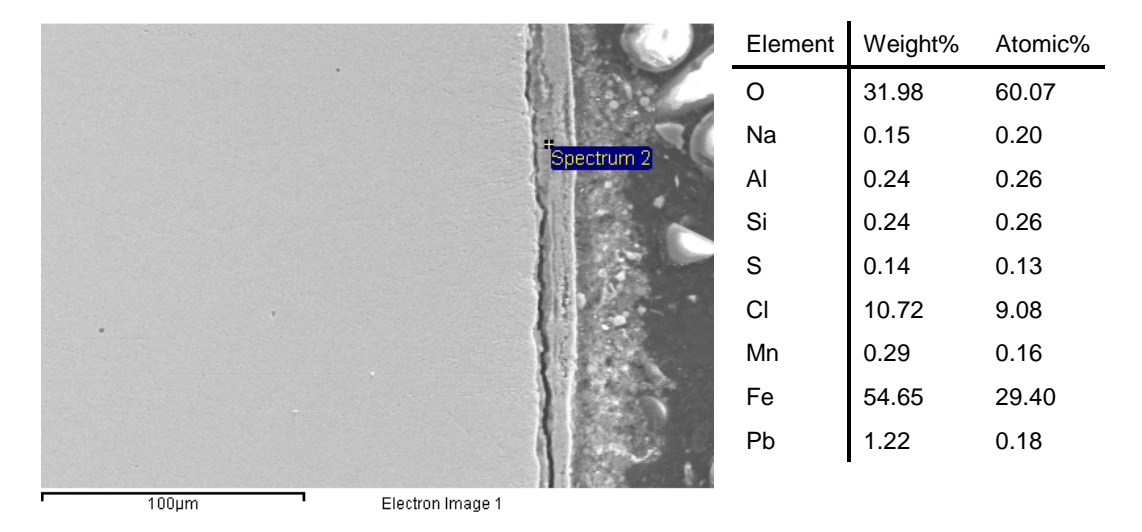


Figure 78 SEM image from leeward cross-section of a 16Mo3 ring exposed in the BW position during case PbO+SWS. Elemental composition in point "Spectrum 2" is given. The corrosion scale is about 20 µm thick.

Figur 78 SEM-bild av korrosions/beläggningsprodukten på läsidan av en 16Mo3-ring från fallet PbO+SWS. Sammansättning i punkten "Spectrum 2" visas.

5.3.11 Comparison of additives at the SH position (first set of tests)

Macroscopic photos of the 16Mo3 rings after exposure in the superheater (SH) position of the furnace and subsequent removal of deposits are shown in Figure 79. These photos of corrosion attacks on the substrate can be compared to the XRF analyses of selected elements in the deposits, prior to its removal, in Figure 80.

- The SH positioned 16Mo3 ring from the case of **Ref 1** (A in Figure 79) have scaled in the region between -90° and 90°. The corresponding XRF analysis of its scale (in A) shows that it contains fairly high concentrations of S and K and up to 10 % CI.
- The ring from the case of **foundry sand** (B in Figure 79) is corroded in the region between -20° and 20°, and discoloured elsewhere. That is, it suffered somewhat less from corrosion than the ring from the reference case. The analysis of its scale (in Figure 80B) reveals that the CI content is reduced from the reference case, while the S and K concentrations are less affected by the additive.
- The grinding marks from the preparation of the 16Mo3 ring remained intact for the **kaolin** case (C in Figure 79), indicating that the corrosion is not severe in this case, although traces of light corrosion could be found all around the ring. Unfortunately, the XRF analysis of this deposit failed.
- The ring from the **lime case** (D in Figure 79) fare a lot worse and is corroded between -20° and 20°. The analysis of the scale (in Figure 80 D) shows significantly higher Cl and lower S concentrations than the reference case.
- The additive of **sewage sludge** (SWS1, Figure 79E) results in corroded spots all around the ring. The corresponding analysis of the scale reveals relative low chlorine content, but both S and K are higher than in the reference case. The P from the additive is rather evenly distributed around the ring.
- The 16Mo3 ring from the case of **sulphur** additive (Figure 79F) is only lightly corroded in the region between -90° and 90°. The analysis of the scale on this ring shows Cl and K at significantly lower levels than in the reference case. On the other hand, the content of S is higher.

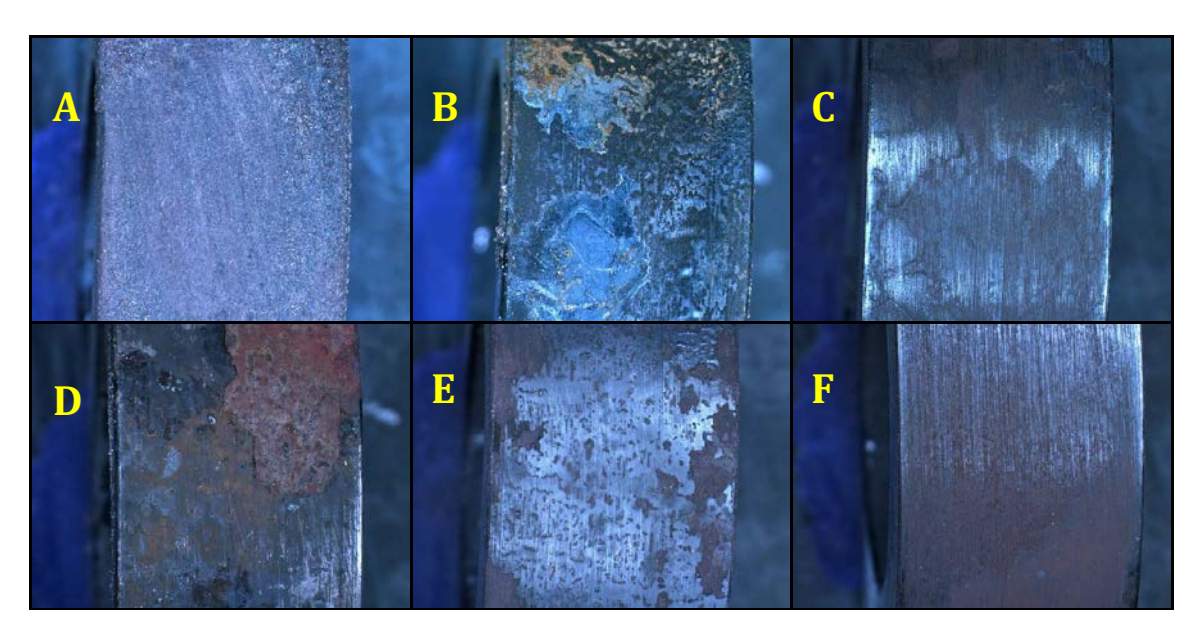


Figure 79 16Mo3 rings from SH position, after cleaning. A) Ref 1, B) FS, C) Kaolin, D) Lime, E) SWS1, F) Sulphur.

Figur 79 16Mo3-ringar från överhettarpositionen, efter rengöring. A) Ref 1, B) FS, C) Kaolin, D) Lime, E) SWS1, F) Svavel.

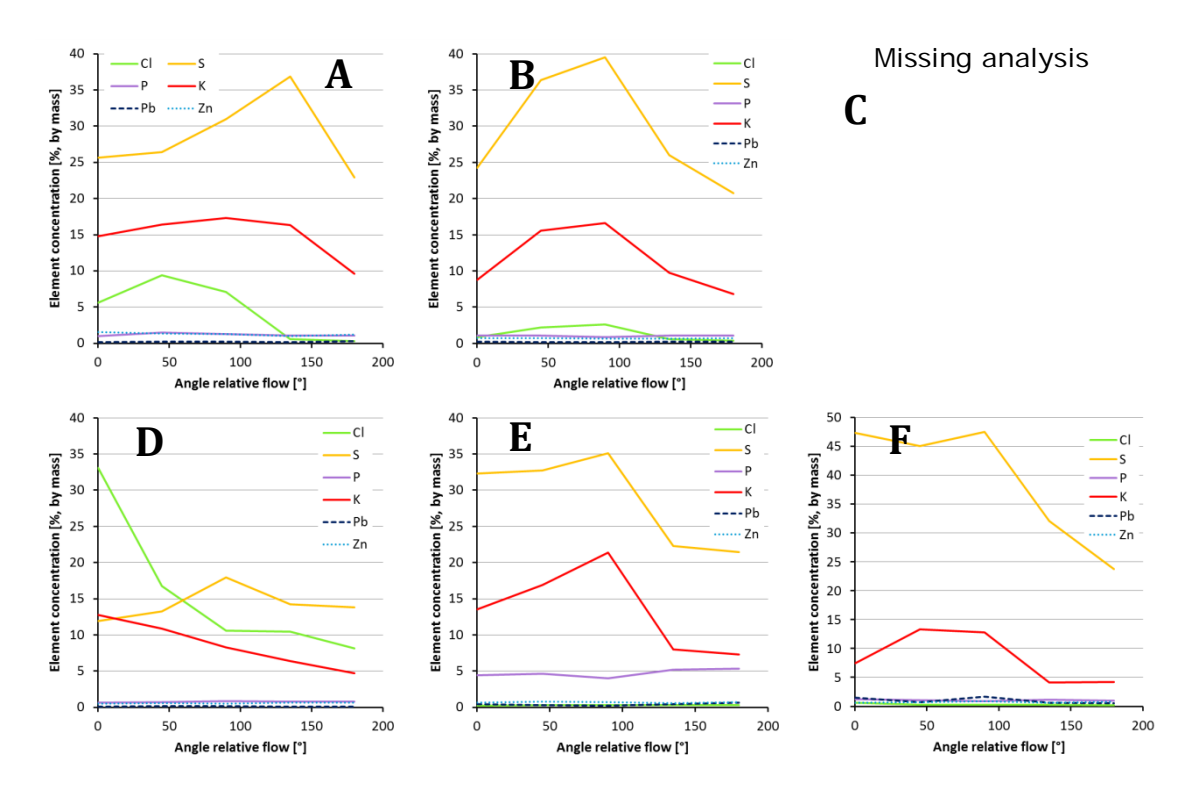


Figure 80 Elemental concentrations in scales on the SH 16Mo3 rings, measured by XRF on the surface at varied angles relative to the windward side. A) Ref 1, B) FS, C) Kaolin, D) Lime, E) SWS1, F) Sulphur.

Figur 80 Elementsammansättning för avlagringar på ringar av 16Mo3 från överhettarpositionen, uppmätt med XRF vid olika vinklar på ringen relativt vindsidan A) Ref 1, B) FS, C) Kaolin, D) Lime, E) SWS1, F) Svavel.

5.3.12 Comparison between reference case and sewage sludge addition in the SH position (second set of tests)

The metal surfaces of the wind sides of the 16Mo3 rings from the SH position, after removal of the deposits, are shown in Figure 81. The surface is severely corroded for case Ref 2 and much less corroded in the case of SWS2, where still some grinding marks remain. On the leeward sides of these rings, less signs of corrosion are found.

The XRF analyses of these rings scales are shown in Figure 82, revealing that that the additive of sewage sludge reduces the CI content in the deposits while increasing the concentrations of S and P. The content of Pb is also increased by the sewage sludge, whereas concentrations of K and Zn are less affected.





Figure 81 Photos of the windward sides of the 16Mo3 rings after deposit removal, from the SH position. Left) Ref 2, severely corroded surface. Right) SWS2, brownish surface but no obvious corrosion products.

Figur 81 Vindsidan på 16Mo3-ringarna efter att avlagringarna tagits bort, från överhettarpositionen. Vänster) Ref2, kraftigt korroderad yta. Höger SWS) brunaktig yta, men inga uppenbara korrosionsprodukter.

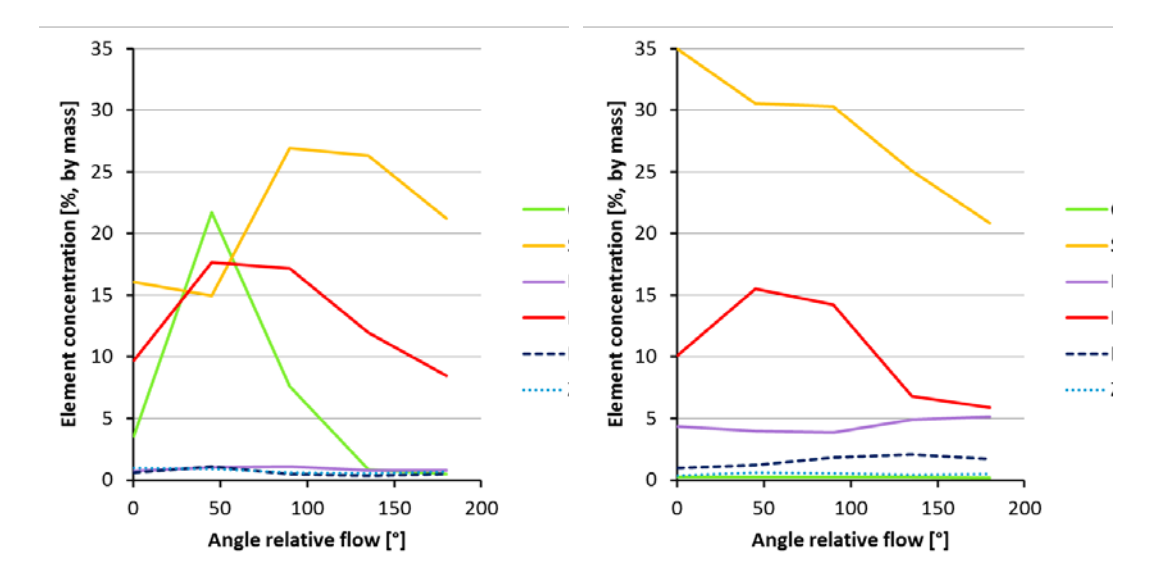


Figure 82 Elemental concentrations in SH scales on 16Mo3-steel. Left) Ref 2. Right) SWS2.

Figur 82 Elementsammansättning för påslagen på 16Mo3-ringarna i överhettarpositionen. Vänster) Ref 2, Höger) SWS2.

5.3.13 Comparison between PbO spiked fuel with and without sewage sludge addition at SH position (second set of tests)

After removal of the loosely attached scales, it was obvious that the 16Mo3 steel was severely corroded on the windward side of the ring from case PbO (Figure 83) while the leeward side fared better with only partial corrosion. For case PbO+SWS, the surfaces were less corroded than for the PbO case, but corrosion products still have spalled.

The elemental analyses of the scales, in Figure 84, show that the sewage sludge in the case of PbO+SWS drastically reduces the chlorine content in the deposits. On the other hand, the contents of S, P and Pb are increased by the addition of sewage sludge to the fuel. The content of K is somewhat reduced by the sewage sludge.





Figure 83 Photos of 16Mo3-steel rings from the SH position, windward side after scale removal Left) PbO. Severely corroded surface. The corrosion products have spalled. Right) PbO+ SWS. The scale has spalled.

Figur 83 16Mo3-ringar från överhettarpositionen, vindsidan efter borttagning av avlagringar. Vänster) PbO, kraftigt korroderad, korrosionsprodukter har fallit av. Höger) PbO+SWS. korrosionsprodukter har fallit av.

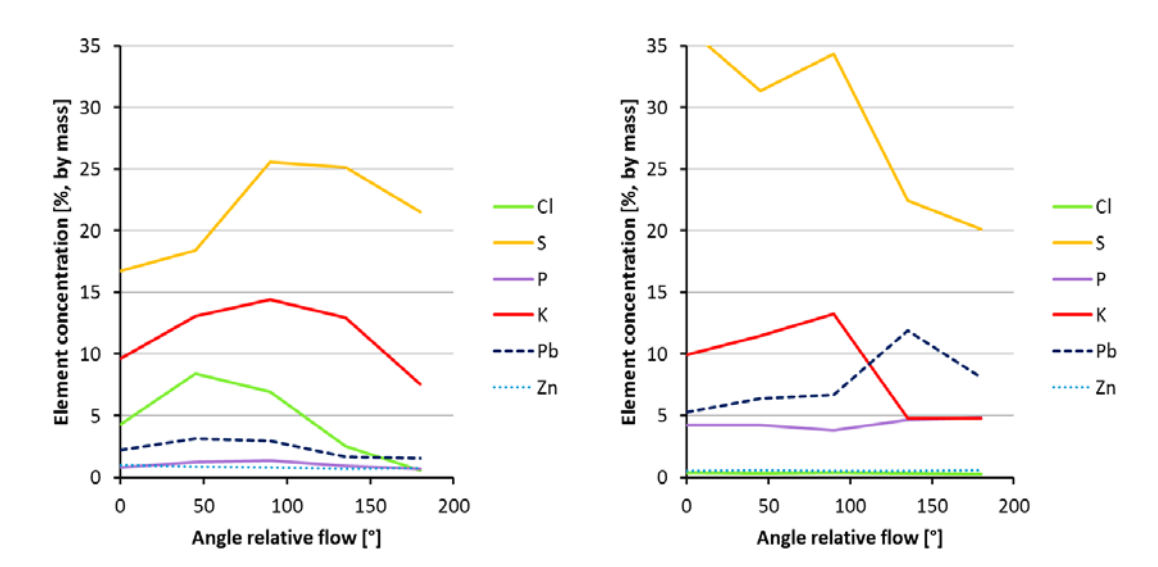


Figure 84 Elemental concentrations in SH deposits on 16Mo3 rings, by XRF analysis. Left) PbO. Right) PbO+SWS..

Figur 84 Kemisksammansättning för avlagringarna på 16Mo3-ringarna i överhettarpositionen. Vänster) PbO, Höger) PbO+SWS.

5.3.14 Summary of corrosion analysis

In the BW samples, kaolin and sewage sludge are the additives that have the highest impact in decreasing the corrosion rate. 16Mo3 did not show any corrosion when these additives were used during the first set of tests but did corrode somewhat during the second set of tests. No corrosion attack could be observed on Kanthal A1 for any additive. The only case when corrosion attack could be observed on 253 MA was when the lime additive was tested. It should be noted that lime seems to enhance the corrosion rate compared to the reference case.

All 16Mo3 SH samples showed signs of corrosion. The best results were coming from the use of kaolin and sulphur. Neither Kanthal A1 nor 253 MA corroded. In general all additives reduced the corrosion compared to the reference (lime/253 MA as an exception). Kaolin, sulphur and perhaps sewage sludge showed the highest reduction of the corrosion rates.

Ref 2-SWS2

Optical microscopy on the windward sides of 16Mo3 samples exposed at the boiler wall position (BW) showed a reduction of corrosion scale from about 50 μm for test case Ref 2 to about 30 μm for test case SWS2. The additive of sewage sludge reduced concentrations of Cl and S but increased concentrations of Pb and P in the deposits on the 16Mo3 samples. The 253 MA rings were less affected by corrosion and the analyses of their deposits showed that the sewage sludge reduced concentrations of Cl, S and K but increased concentrations of P.

SEM/EDX analyses of the corrosion layers on the 16Mo3 samples reveal that the compositions are different near the corrosion front compared to the outer corrosion layers. In general, there are higher concentrations of CI at the corrosion front than anywhere else in the layers, while S and P are present elsewhere than in the corrosion front or mostly in outer part of the scales. There are also tendencies that K, Na and Pb are mostly present in outer part of the scales and at least not in the corrosion front. The division of elements throughout the corrosion layer may be explained by the gradual movement of the corrosion front, eating its way into the substrate steel, in this case about 75 µm. On the other hand, in the case of 253 MA steel, under the same test conditions, the corrosion layer was only about 15 µm, implying a less pronounced elemental separation. A spot analysis in this corrosion layer revealed a composition of 8% CI, 5% S, 8% alkali, 2.4% Zn and 2.5%Pb. That is, the most critical elements are mixed. This composition is probably a closer representation of the scales conditions under the initial corrosion attacks on the boiler steel tubes.

At the superheater (SH) position, the additive of sewage sludge did visually reduce the corrosion on both the 16Mo3 and 253 MA steels. Most corrosion occurred on the windward side. The additive reduced the CI concentrations on the windward side (it was low on the leeward side for both test cases), meanwhile concentrations of S increased on the windward side and P concentrations increased all around the ring.

PbO-PbO+SWS

Optical microscopy on the windward side of the 16Mo3 samples from the boiler wall position (BW) showed a scale thickness of almost 1 mm for the test case PbO, which can be compared to 50 μ m for the reference case. Thus, the addition of PbO to the fuel significantly increases the corrosiveness of the deposits. When also sewage sludge was added to the fuel (case PbO+SWS) the resulting scale on the windward side was found to be about 400 μ m. That is a clear reduction compared to the PbO case, but still far worse than the reference case.

A comparison of the XRF analyses of the BW scales between the test cases of PbO and PbO+SWS shows that the additive of sewage sludge reduces concentrations of Pb and Cl as well as increases concentrations of P and Zn. There is also a weak tendency of reduced concentrations of S and K on the 253 MA test rings.

The SEM/EDX analyses reveal the same separation of elements in the corrosion scales as described above for the 16Mo3 steel in the reference case. However, even though the deposits contained a large amount of Pb according to the XRF analysis, it was difficult to find any areas of high Pb concentrations by the SEM/EDX instrument. Instead, it is possible that the Pb is dispersed throughout the corrosion layers, which were thick in this case.

It is visually obvious that the corrosion on the rings exposed at the superheater position is somewhat reduced by the sewage sludge. The XRF

analyses of the scale reveal that the sewage sludge reduces the concentration of CI significantly, meanwhile concentrations of S, Pb and P increase.

5.3.15 Ranking of additives

Tentative rankings of additives and materials tested are presented below in figures. The rankings are based on the 8 hours of exposure. However, any estimates of long-term corrosion rates from such a short exposure are purely speculations.

The test cases are colour coded: reference: cyan, kaolin: green, sewage sludge: grey, sulphur: yellow, foundry sand: red, lime: orange for the first set of trials. For the second set of trials: reference: cyan, sewage sludge: violet, PbO: magenta, sewage sludge + PbO: green.

Since the two set of tests were performed at different occasions the results are presented in different graphs. The reason is that the waste wood fuel is heterogenetic and the chemical compositions of the fuel may vary significantly.

The graphs are vertically divided by the three different test materials, when applicable. The wind side of each test ring was compared to the other test rings by comparing the optical appearance, the cross-sections and the chemical analyses, each method contributing with different impact of the overall results.

The corrosion rates for the rings to the right of the "Start of Corrosion" label shows signs of corrosion. If a sample is located to the far right in the figure the corrosion has been severe. No or only minor corrosion attacks were observed for the test samples located to the left in the figures. This indicates that the corrosion rate may be acceptable for use in boiler. Samples with corrosion products formed are located on the right in the figures and it is an indication that the corrosion rate is too high for use in boiler.

Ranking of samples at boiler wall (BW) conditions

Figure 85 below shows a ranking of all additives and materials tested in the furnace (i.e. boiler wall position, BW) during the first set of tests. A similar ranking for the second set of tests are presented in Figure 86. For the samples exposed to BW conditions, generally, the Kanthal A-1 material performs slightly better than 253 MA, which in turn is far better than 16Mo3. The stainless steels do not show clear evidence of corrosion with the exception of 253 MA from the lime case. The 16Mo3 steel did not show any corrosion when kaolin or sewage sludge were used as additives in test set 1 but in test set 2, but did corrode during the exposures with sulphur-, limeand foundry sand- additives in addition to the reference. In general, kaolin and sewage sludge showed the highest reduction of the corrosion rate. Kanthal A-1 does not show any corrosion attacks for any the additives.

It should be noted that lime seems to enhance the corrosion rate compared to the reference case. A conclusion from the comparison may be that the results originating from the 16Mo3 steels may be more significant for the ranking of the additives than the results from the high alloyed steels, since generally no real corrosion have started.

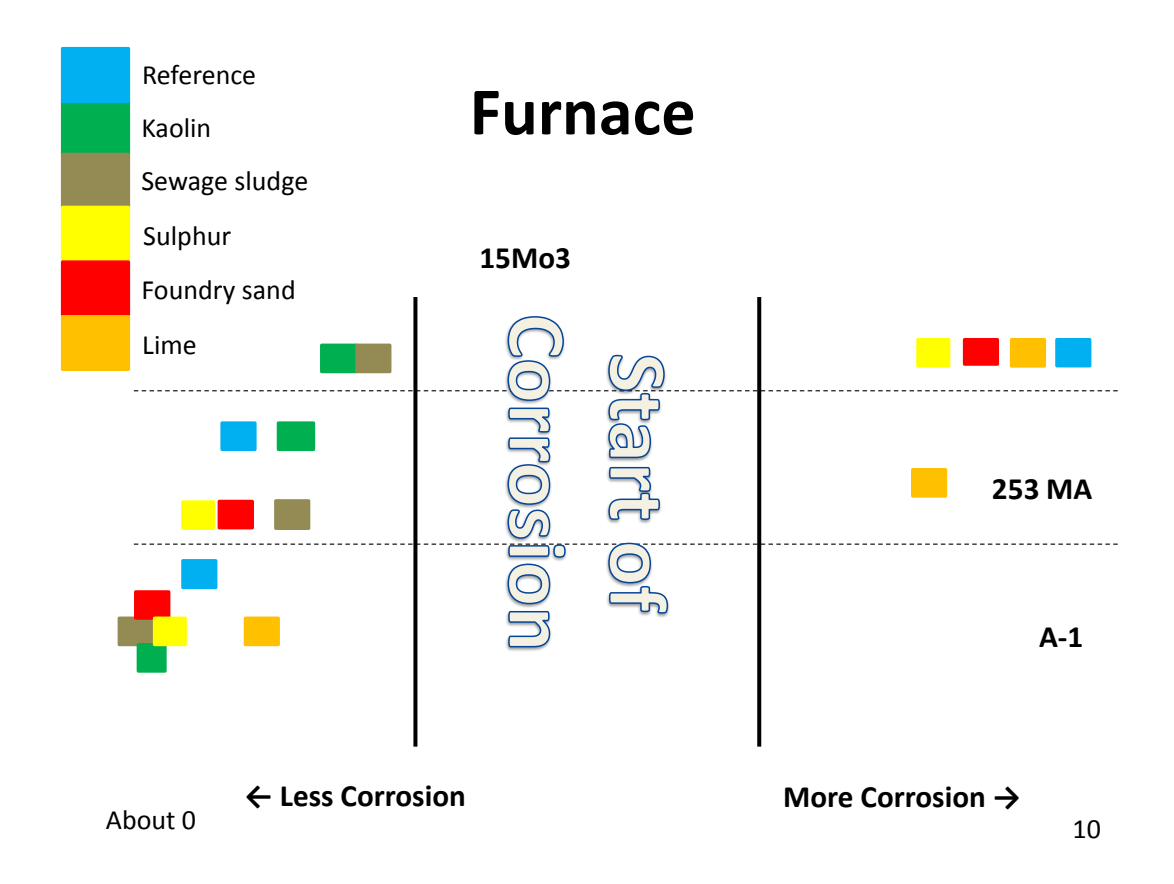


Figure 85 Ranking of additives and materials located in the furnace (BW) in 1st set of tests.

Figur 85 Rankning av additiv och material i eldstadspositionen från den första testomgången.

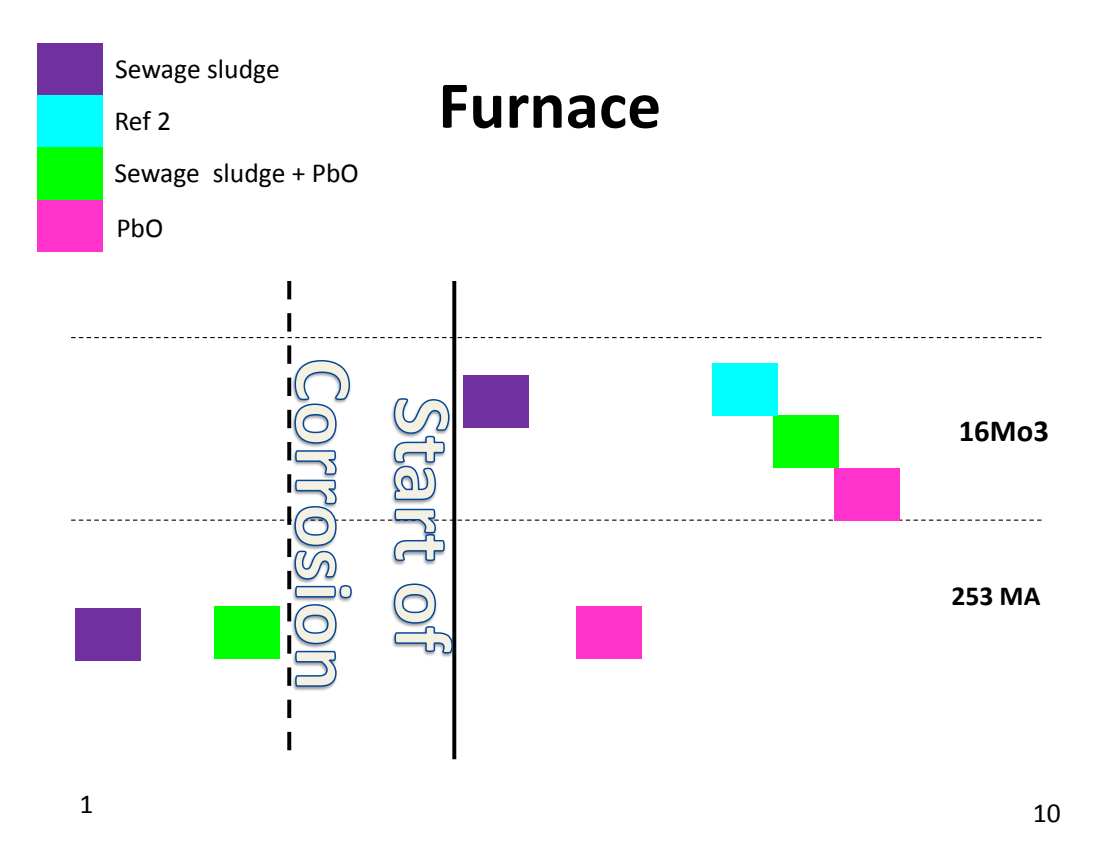


Figure 86 Ranking of additives and materials located in the furnace (BW) in 2nd set of tests.

Figur 86 Rankning av additiv och material i eldstadspositionen från den andra testomgången.

Ranking of samples at superheater (SH) conditions

Figure 87 is showing the corresponding ranking of the rings from the 1^{st} set of tests at superheater conditions. The same ranking of the tests in the 2^{nd} set of tests are given in Figure 88.

The ranking of the material is the same as for the furnace; Kanthal A-1 is slightly better than 253 MA, which in turn is far better than 16Mo3.

The 16Mo3 steel corroded no matter which additive that was tested. The best results were coming from the additives of kaolin and sulphur. The test cases of sewage sludge, lime, and foundry sand, and also the reference case clearly showed higher corrosion. Neither the Kanthal A-1- nor the 253 MA steel did corrode. In general all additives did reduce the corrosion compared to the reference with the exception of the 253MA steel when lime was tested. Kaolin, sulphur, and perhaps sewage sludge did show the highest reduction of the corrosion rates. The addition of PbO increased the corrosion.

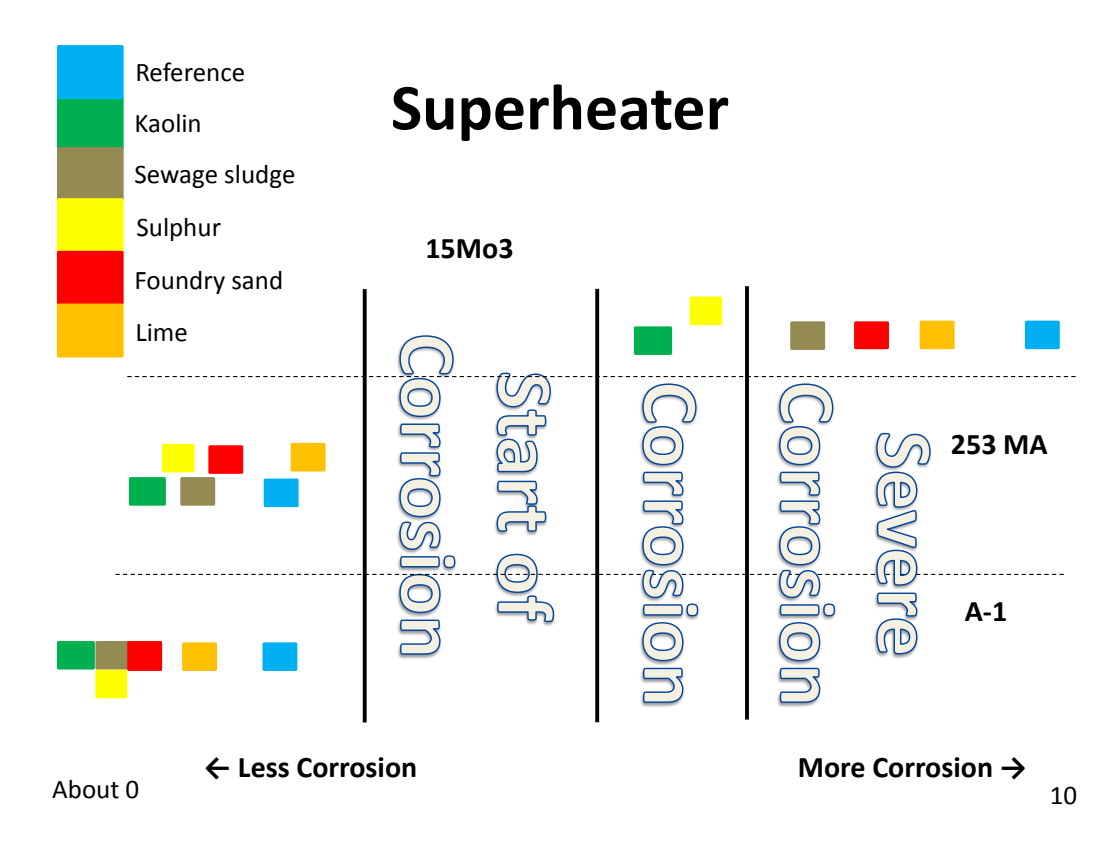


Figure 87 Ranking of additives and materials at SH from comparison study of 1st set of tests.

Figur 87 Rankning av additiv och material i överhettarpositionen från den första testomgången.

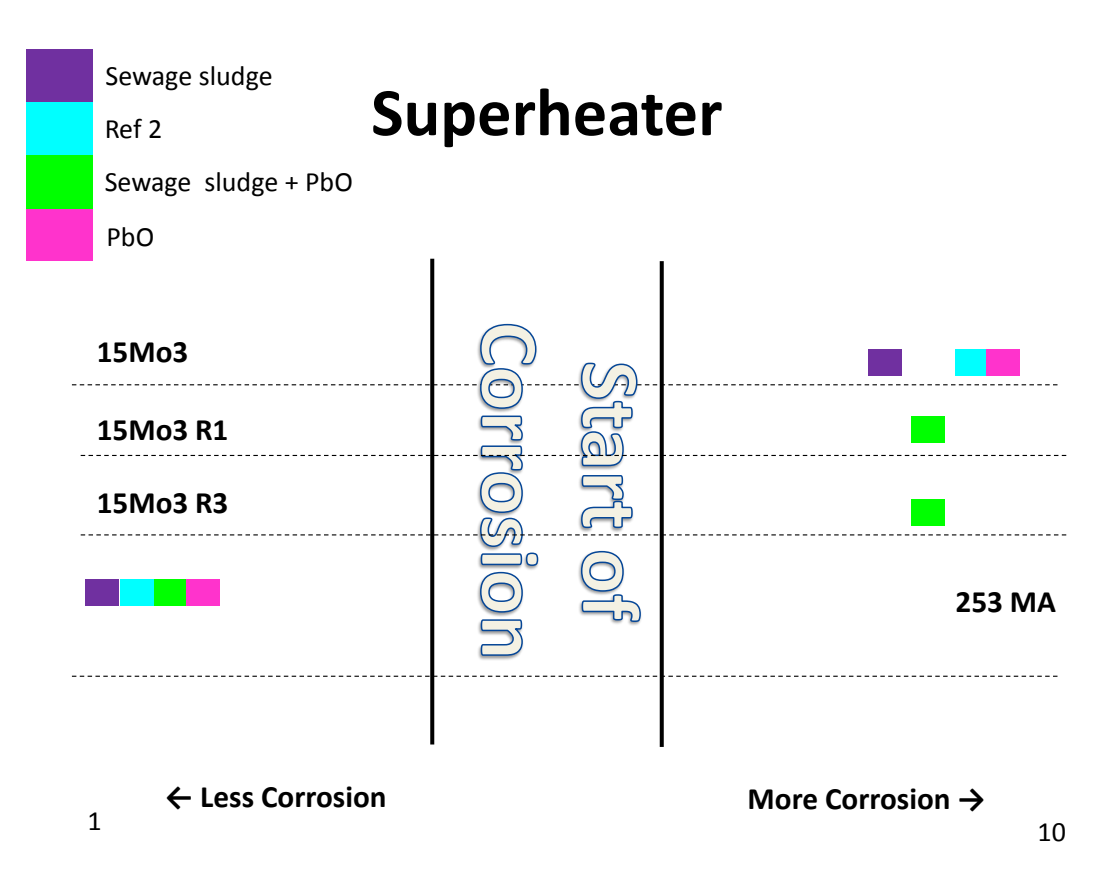


Figure 88 Ranking of additives and materials at SH from comparison study of 2nd set of tests.

Figur 88 Rankning av additiv och material i överhettarpositionen från den andra testomgången.

6 Impacts and cost estimates of additives

Estimated costs for the selected additives are shown in Table 38.

Table 38. Estimated costs for suggested additives

Tabell 38. Uppskattad kostnad för föreslagna additiv

Additive	Price	Assumed consumption		Cost
	(SEK/ton)	(kg/ton fuel)	(kg/MWh fuel)	(SEK/MWh)
Elemental sulphur (granular)	5 200	10	1,9	10
Digested sewage sludge	-100 (75% moisture)	50 (dry)	9,6 (dry)	- 0,96
Kaolin	2 000	30	5,8	11,5
Foundry (casting) sand	0	30	5,8	0
Lime	~400**	30	5,8	2,3*

^{*} Using a heating value of 5.2 MWh/ton dry fuel

In addition to the cost for the additive in itself and transport of the additive to the plant, there could be additional costs such as increased deposition fees due to increased amounts of fly ash and bottom ash and increased emission fees. The personnel costs for handling the additive and costs for dosing equipment should be fairly similar for most additives, except for sludges, which would need different type of equipment. If there is limited space at the site for storing the additive this could induce extra costs.

In order to make a total cost estimate for the additives including additive price, investments and costs/benefits of impacts of the additives, a detailed cost-benefit analysis would have to be made for each plant.

The impacts on the boiler and an estimation of the costs connected to the use of the additives elemental sulphur, kaolin and sewage sludge are presented below. Since foundry sand and lime were found to have no positive effect on waterwall corrosion, these additives are not included here.

^{**} including transportation

6.1 Sulphur

Impact on the classification of the fuel mix: Sulphur is not classified as a waste material, and thus will have no impact on the classification of the fuel mix.

Impact on the flue gas path after the furnace: Addition of elemental sulphur to the bed is expected to reduce superheater corrosion. Sulphur in the fuel or in additives is regarded as beneficial during combustion of fuels rich in alkali and chlorine. With a S/Cl ratio >4 in the fuel mix, the superheater corrosion risk may be regarded as low, while a ratio <2 indicates a high corrosion risk. However, increasing the sulphur content in the flue gases might also increase the risk for low temperature corrosion.

Cost and potential supplier: Sulphur is sold in big bags containing ~1 000 kg by Jakokem AB. Their price per bag is 5 200 SEK (not including transport). Buying smaller quantities can increase the cost/kg considerably.

Investments (changes in the boiler, components for feeding the additive): Sulphur dust is explosive, which has to be considered when choosing dosing equipment and storage.

Changes in boiler operation: None expected, except possible consequences of reduced superheater corrosion or increased low temperature corrosion.

Impact on ash quality: None expected.

Impact on emission levels (need for more chemicals for flue gas cleaning and/or investment in flue gas cleaning equipment): Addition of elemental sulphur may increase the need for sulphur reduction in the flue gas cleaning to avoid exceeding SO_2 emission limits.

6.2 Sewage sludge

Impact on the classification of the fuel mix: Sewage sludge is classified as a waste material (in Sweden and Finland) so the plant will need a permit for co-incineration with waste materials. It is not entitled to green certificates.

Impact on the flue gas path after the furnace: The use of sewage sludge is expected to reduce superheater corrosion. It also reduces the risk for bed sintering and reduces the amount of deposits on superheaters and economiser. The high ash content of sewage sludge will result in an increase in the amount of ashes.

Cost and potential supplier: Wastewater treatment plants will pay receivers of (wet) sewage sludge. There are large variations in paid price depending on quality of the sludge, transportation costs and demand. However, a lowest paid price of 0 SEK/ton can be assumed.

Investments (changes in the boiler, components for feeding the additive): If the sludge hasn't been thermally dried (only mechanically dewatered), special equipment will be needed for feeding it into the boiler. It will also be needed to store the sludge in a closed compartment since there is a bad smell from wet sewage sludge.

At Idbäcksverket tests have been performed using fuel that has been premixed with sewage sludge. This means that no extra equipment was needed for feeding the additive into the boiler, however some extra work was needed to mix the "sludge fuel" with "normal fuel" in the right proportions. Possibilities to store the fuel mix, sheltered from downfall and wind, are also needed. There were also some problems when storing the fuel mix for a longer period of time with decomposition of the fuel mix leading to a bad smell and heat build-up.

Sewage sludge can also be thermally dried before delivery to the plant. In this case no extra equipment for feeding the sludge into the boiler is needed, however, there will probably be less pay for receiving the sludge.

Changes in boiler operation: The use of wet sludge will require changes in the operation of the boiler. When testing the use of sewage sludge in Händelö P14 it was experienced that the flue gas recirculation had to be reduced when the sludge was fed into the boiler, due to the high water content of the sludge (~75-80%). Otherwise, the flue gas fan was overloaded and/or the boiler bed got too cold (which both cause the load to go down). The moisture to the NID-reactor, the flue gas cleaning, also had to be reduced, because of the moisture of the sludge.

Impact on ash quality: The high ash content of sewage sludge can lead to dilution of detrimental substances in the ashes and hence an improvement of the ash quality. The phosphorus content of the ashes will be increased. Some sludges also contain unwanted metals that influence the quality of the ashes negatively.

Increasing the amount of ashes will increase the costs for ash deposition, however, dilution of the ashes could also lead to that the ashes are not classified as hazardous waste. This would reduce the costs for ash deposition, from approximately 1200 SEK/ton to approximately 300 SEK/ton.

Impact on emission levels (need for more chemicals for flue gas cleaning and/or investment in flue gas cleaning equipment): Addition of sewage sludge may increase the need for sulphur reduction in the flue gas cleaning to avoid exceeding SO2 emission limits. The amounts of sulphur and phosphorus can vary significantly between different sources. It is possible that selection of a high phosphorus, low sulphur sludge can be an option in plants where a high sulphur content of the sludge causes problems.

The use of sewage sludge can also result in an increase of NOx emissions. This will increase the consumption of NOx reducing chemicals, such as ammonia (NH3), which can lead to increased ammonia slip.

In the future there might be increased restrictions of content of phosphorus in the ashes and demands to separate the phosphorus from the ashes when using sewage sludge.

The increased amount of ashes will put higher demands on dust removal.

6.3 Kaolin

Impact on the classification of the fuel mix: Kaolin is not classified as a waste material, and its use will have no impact on the classification of the fuel mix.

Impact on the flue gas path after the furnace: The use of kaolin is expected to reduce superheater corrosion. It may also reduce the risk for bed sintering and reduce the amount of deposits on superheaters and economiser.

Cost and potential supplier: Kaolin is sold by ACM AB. Their price for low grade kaolin (too low grade for use in the paper industry) is ~1,8-2,0 SEK/kg.

Investments (changes in the boiler, components for feeding the additive): Kaolin will form lumps if not stored dry and can be difficult to feed into the boiler, especially designed feeding equipment has to be used.

Changes in boiler operation: None expected, except possible consequences of reduced superheater corrosion.

Impact on ash quality: None expected.

Impact on emission levels (need for more chemicals for flue gas cleaning and/or investment in flue gas cleaning equipment): None expected.

7 Analysis of the results

Below is a summary of the results of all the tested additives and the conclusions drawn from the results.

7.1 Foundry sand

Expected effect/result

- FS was expected to bind alkali, Pb and Zn
- These elements should be enriched in the fractions containing FS, especially bottom ash and reduced in other fractions, such as deposits on the probes
- If alkali from alkali chlorides or heavy metals from heavy metal chlorides are bound by foundry sand, HCl should be released to the flue gases.

Result, chemical analysis

- The main components of foundry sand are Si and Al. Fairly high content of alkali, especially Na (8.9 atomic %)
- The Al content of FS (19 at-%) is lower than for kaolin (46 at-%)

Result, lab tests

- The amount of bottom ash increased.
- The amount of loose ashes increased and the amount of hard deposits decreased on the BW probe
- The content of CI increased in both loose and hard deposits on the BW probe.
- Pb increased on BW probe
- Foundry sand did not seem to have a strong influence on either BW or SH corrosion.

Conclusions, comments

• Even though no negative effect on corrosion could be observed from the tests, the increased CI content on the BW probe and the high alkali content of foundry sand give reason to doubt the suitability of foundry sand as an additive in boilers.

7.2 Kaolin

Expected effect/result

- · Kaolin was expected to bind alkali, Pb and Zn
- These elements should be enriched in the fractions containing kaolin, especially bottom ash and reduced in other fractions, such as deposits on the probes. As kaolin has a high content of AI, fractions containing kaolin should also have a high content of AI
- If alkali from alkali chlorides or heavy metals from heavy metal chlorides are bound by kaolin, HCl should be released to the flue gases.

Result, chemical analysis

 The kaolin used in the project is clean, with a slight surplus of Si compared to Al.

Thermodynamic equilibrium calculations

• The reduction of NaCl and KCl by kaolin additions has been modelled but thermodynamic modelling may not be fully suitable to predict the interactions of alkali chlorides with kaolin.

Result, lab tests

- The amounts of deposits on the BW probe, fly ash and bottom ash were strongly reduced.
- The amount of loose deposits on the SH probe increased and the amount of hard deposits decreased.
- The amount of CI was reduced in fly ash, in bottom ash and on the BW probe.
- Kaolin substantially reduced both BW and SH corrosion

Other effects

 The use of kaolin is expected to reduce superheater corrosion. It may also reduce the risk for bed sintering and reduce the amount of deposits on superheaters and economiser

Conclusions, comments

 Kaolin seems to be well fitted for use for reduction of waterwall corrosion and seems to have several other positive effects on the boiler as well.

7.3 Lime

Expected effect/result

- Lime was expected to bind Zn and Pb.
- These elements should be enriched in the fractions containing lime, especially bottom ash and reduced in other fractions, such as deposits on the probes. Fractions containing lime should also have a high content of Ca
- Ca in the lime was also expected to bind S. This should lead to an increase in S in combination with Ca and a reduced sulphation of other elements, such as alkali, which in turn should lead to an increase in the amounts of alkali chlorides.

Thermodynamic equilibrium calculations

• The Ca content of the fuel is so high that further additions will not influence the composition of condensed or gas phases.

Result, lab tests

- Decreased content of HCl in the flue gases.
- Strongly increased amount of fly ash.
- Increased amounts of CI in the fly ash, on SH probe and BW probe.
- Slightly increased amount of S in bottom ash and on BW probe.
- A small part of the Pb has been bound to the bottom ash by lime, but the main part still remained in the fly ash. Zn, on the other hand did not seem to have been influenced by addition of lime.
- Lime had a negative effect on BW corrosion, at least for higher alloyed materials.
- Lime did not seem to have a strong influence on SH corrosion

Conclusions, comments

- Lime was included in the tests to aid in the interpretation of the results from the other additives and it was not expected to have a positive effect on corrosion.
- As expected, addition of lime lead to reaction of Ca with sulphur and thereby an increased release of chlorine, thereby increasing the chlorine content on BW and SH probes.
- Lime does not seem to bind heavy metals to any large extent.

7.4 Sulphur

Expected effect/result

- Sulphur was expected to convert alkali chlorides to alkali sulphates in oxidising conditions, it was hoped that this should also happen in the furnace.
- If so, the amounts of CI should decrease on BW and SH probe, while S is increased.
- As sulphates are less sticky than chlorides, less K and Na should be found on the probes and more in the bottom and fly ashes.
- This reaction also leads to the formation of HCI, which should increase in the flue gases.

Thermodynamic equilibrium calculations

- At oxidising conditions addition of S primarily leads to transformation of CaO to CaSO₄.
- Depending on the amount of calcium available in the system and the amount of added sulphur, alkali chlorides from the fuel will be sulphated, leading to a strong increase of HCl in the flue gases and, at further additions, also to an increase of SO₂.
- At the release of HCl, PbCl₂ and ZnCl₂ are formed.
- At reducing conditions, the CI chemistry is not influenced to a high degree. CaO forms CaS, Na₂CO₃ forms Na₂S and Pb, Zn and Cu also forms sulphides. In gas phase H₂S is formed.

Result, lab tests

- Cl was slightly decreased in the deposits on the BW probe
- CI was nearly eliminated on the SH probe.
- S increased on both probes.
- Nearly all CI was present as HCI, which was increased as compared to the reference case.
- High increase of SO₂ in flue gases.
- Pb increased slightly on SH probe and in fly ash and was slightly reduced on BW probe and walls.
- Sulphur reduced SH corrosion, but only had a minor effect on BW corrosion.

Other effects

- Addition of elemental sulphur to the bed is expected to reduce superheater corrosion. However, increasing the sulphur content in the flue gases might also increase the risk for low temperature corrosion.
- Addition of elemental sulphur may increase the need for sulphur reduction in the flue gas cleaning to avoid exceeding SO_2 emission limits.

Conclusions, comments

- The thermodynamic calculations predict a fourfold increase of HCl in the flue gases when all alkali chloride has been converted to sulphates. The flue gas analyses show an increase of HCl of 60%.
- Sulphur is not recommended as an additive for reduction of waterwall corrosion.

7.5 Sewage sludge

Expected effect/result

- Alkali chlorides were expected to be converted to sulphates and phospates.
- Heavy metals were expected to be bound by minerals, such as zeolites.
- The amounts of CI should decrease on BW and SH probe, while S and P are increased.
- As sulphates and phosphates are less sticky than chlorides, less K and Na should be found on the probes and more in the bottom and fly ashes.
- These reactions also lead to the formation of HCI, which should increase in the flue gases.
- Heavy metals should be enriched in the fractions containing sewage sludge ash, especially bottom ash and reduced in other fractions, such as deposits on the probes.

Thermodynamic equilibrium calculations

- Additions of sewage sludge does not have a large impact on the gas composition at additions below 4% and a reduction of NaCl and KCl in the flue gases can only be seen at additions above 10% (based on S)
- At additions above 10% the amounts of SO_2 and SO_3 starts to increase.
- KCI and NaCI are not affected that much. Part of Na and K may be sulphidised at reducing conditions.
- At reducing conditions H₂S is formed but no SO₂ or SO₃.
- 2 to 3 times more sewage sludge than with ox cond. is needed to get an effect in reducing cond.

Result, lab tests

- SO₂ in the flue gases increases
- The amount of CI is significantly decreased on both probes.
- Zn is decreased on both probes.
- P is increased in all solid fractions.
- Sewage sludge substantially reduced BW corrosion and also reduced SH corrosion, even though to a lesser degree.

Other effects

- The use of sewage sludge is expected to reduce superheater corrosion.
 It also reduces the risk for bed sintering and reduces the amount of deposits on superheaters and economiser. The high ash content of sewage sludge will result in an increase in the amount of ashes.
- The use of wet sludge will require changes in the operation of the boiler.
- Addition of sewage sludge may increase the need for sulphur reduction in the flue gas cleaning to avoid exceeding SO₂ emission limits.

Conclusions, comments

 According to the thermodynamic equilibrium calculations 4% of sewage sludge is the lower limit when an effect can be seen on alkali and chlorine, based on reactions with sulphur. The major effect at this level is sulphation of CaO. However, a reduction of Cl and a slight increase of S can be seen on the probes as well as an increase of P. This could indicate sulphation and phosphation of alkali chlorides.

- The S in the sewage sludge used corresponds to ~1 g S/kg dry fuel.
 The S added as elemental sulphur was 10 g S/kg dry fuel. This implicates that the principal effect of sludge probably is not due to its S content. This could be explained by reactions including alumina silicates in the sludge.
- The quality of sewage sludge can vary and the quality must be locally assessed before use.
- The sewage sludge used in the tests in this project was high in sulphur compared to much of the available sewage sludges.
- Sewage sludge seems to be well fitted for use for reduction of waterwall corrosion and seems to have several other positive effects on the boiler as well, if the increase in SO₂ can be handled.

8 Conclusions

It was possible to give a tentative ranking between test cases based on visual inspection of the corrosion attacks on the sample rings. It was found that the additives kaolin and sewage sludge were among the most effective additives counteracting the corrosion both at the boiler wall and superheater conditions. The lime additive showed poor corrosion limiting abilities.

The results from this project supports the results from KME 508, indicating that for low alloyed steels, which are mostly used for furnace walls, chlorine is the main component in the deposits causing corrosion. For higher alloyed materials (austenitics and nickel based alloys) alkali and lead also seems to take part in the process. It is not known for either process yet in what form the corrosive species are deposited on the furnace walls.

Since waterwall corrosion is thought to be caused by chlorine, alkali chlorides, heavy metals or a combination of these, the aim should be to find an additive that can reduce these components in the deposits on the walls and/or the flue gases in the furnace, either by chemical reactions or adsorption.

Clay-type minerals such as kaolin and other layered alumino silicates seem to be the best type of additives for this purpose.

Five different additives have been considered – sewage sludge, kaolin, foundry sand, sulphur and limestone – to decrease the risks (deposits, fouling, and corrosion) in the combustion chamber in a boiler. Two of these additives are clearly the most favourable – sewage sludge and kaolin. Sewage sludge is clearly one of the best since it is a material that needs to be disposed of and in combustion it brings both sulphur and alumina silicates to the process which clearly decreases the risk for chlorine deposition and corrosion. Kaolin is also effective, whereas sulphur mainly reduces superheater corrosion. Limestone increases the risk for chlorine deposition and corrosion, while foundry sand also contains other elements e.g. potassium, which may be risky.

The above results are well supported by the laboratory tests. Kaolin was found to be the best one followed by sewage sludge, but the differences between these were relatively small. It should also be noted that the amount of added kaolin was significantly higher than the amount of sewage sludge when comparing the alumina silicate/alkali molar ratios (Table 11 and Table 12). Further, in the laboratory tests, kaolin and sewage sludge were followed by sulphur, which could indicate that some sulphation actually takes place in the lower part but not as effectively as in the freeboard. Both limestone and foundry sand were found to increase the risk of corrosion.

Addition of PbO to the fuel increased the corrosion attack immensely. However, on the 16Mo3 samples, no Pb can be found in the corrosion front, so the corrosion mechanism is not known. The amount of Pb added to the fuel

is much higher than what can be found in a real fuel. This means that there might have been a different corrosion mechanism involved than what would occur in a real boiler. The conclusion from the results is that Pb probably has a large influence on corrosion but that it needs to be further investigated.

The results from the thermodynamic equilibrium calculations show that FactSage and HSC chemistry can be used to predict the reactions in the gas phase from the fuel or/and (new) fuel mixtures. The tools can be used to check potential influence of a fuel blend and the dominant chemical reactions in the system. Nevertheless one has to be careful and always an expert knowledge needs to be applied when analysing the results. The results often need to be supported by experimental findings and sound thermodynamic databases.

9 Goal fulfilment

The project goals have been fulfilled by the following achievements:

Goal: The project will identify and then evaluate the use of additives and fuel blends to reduce furnace wall, and possibly also superheater, corrosion for wide biomass fuel mixes including waste wood.

Achievement: The project has identified four different types of additives that might reduce furnace corrosion. Five additives, representing these types were then selected and tested in a fluidised bed combustion test rig. As a result of these tests, two additives, digested sewage sludge and kaolin, were found to have a positive effect, reducing waterwall corrosion as well as superheater corrosion when burning waste wood.

Goal: The expected effect of the additives on the rest of the boiler (uncooled components in the furnace, heat exchangers in the flue gas pass, flue gas cleaning equipment, emissions) will also be investigated.

Achievement: The effects on other parts of the boiler by the tested additives have been described. The high ash content of sewage sludge will result in an increase in the amount of ashes. Addition of sewage sludge may increase the need for sulphur reduction in the flue gas cleaning to avoid exceeding SO₂ emission limits.

Goal: The project will give a recommendation if the identified additives are a viable way to reduce wall (and superheater) corrosion and, in that case, recommend some promising additive candidates for further evaluation.

Achievement: Two additives have been found to be promising for reducing waterwall corrosion, sewage sludge and kaolin. These additives are also expected to reduce superheater corrosion, reduce the risk for bed sintering and reduce the amount of deposits on superheaters and economiser. The project recommends that sewage sludge and kaolin (or some other aluminium silicate) should be further investigated for reduction of waterwall corrosion.

Goal: The project will evaluate the use of thermodynamic equilibrium calculations for predicting the chemical composition of the deposits formed at different temperatures, with different additives and under different combustion conditions.

Achievement: Thermodynamic equilibration calculations have been found to be a useful tool for predicting the effects of additives and variations in operation parameters in a boiler. However, this is a tool that must be used with some care and expert knowledge is needed for the interpretation.

10 Proposals for further research work

It is suggested that kaolin and sewage sludge should be further investigated for use as additives to reduce waterwall corrosion. Other substances containing alumino silicates are also of interest for investigation.

Investigate in industrial scale how much sludge should be added.

The roles of S, P, and ash as active components in the sewage sludge for reduced furnace wall and superheater corrosion should be investigated. How important are their effects relative to each other? What demands should be set on the composition of the sewage sludge? How do the Ca contents of fuel and sludge affect the effect of the additive? In which forms do alumina silicates exist in different sludges, and how does this affect the effect on corrosion?

It is possible that the Pb and Zn chloride release peak (according to the thermodynamic equilibrium calculations performed by Åbo, see section 3.2 and Figure 12) has a detrimental effect when adding sewage sludge. More information on if and when this happens should be sought.

The influence of Pb on corrosion and the mechanism behind this should be further investigated.

If continued tests are to be done, it is suggested to use only one material, and vary other parameters.

The performed tests indicate that it is possible to obtain results also with an 8 hour test in a small test rig. According to the KME 508 tests, temperature has a large influence on the corrosion. The temperature of the SH probe was however quite high (550°C). Also, 400°C as was used for the BW probe is a little too high for boilers burning waste wood. Lower temperatures and also temperature gradients could be tested.

Different air ratios could also be tested, but this is not prioritised compared to composition and temperature.

11 References

- [1] Henderson, P., "Furnace wall corrosion in biomass-fired boilers at higher steam temperatures and pressures", KME-508 project proposal, Vattenfall Research and Development AB, revised version to Elforsk 2011-01-04.
- [2] Henderson, P., Alipour, Y., Mattsson, M., Stålenheim, A., Ejenstam, J., Szakalos, P., Glazer, M., Hjörnhede, A., Talus, A., Norling, R., Davis, C., Jonasson, A., Enestam, S., Cho, P., "Furnace wall corrosion in biomass-fired boilers at higher steam temperatures and pressures KME 508/515", KME 508
- [3] Storesund, J., et al., "Countermeasures to furnace corrosion on boiler tubes", M06-601, Värmeforsk report 1023, December 2007.
- [4] Storesund, J., Elger, R., Nordling, M., Viklund, P., "Countermeasures to corrosion on waterwalls Part 2", M08-806, Värmeforsk draft report, 2010.
- [5] HTC project 1a, "Critical corrosion phenomena for combustion of biomass and waste", project leader Jan-Erik Svensson, assisting project leader Jesper Pettersson.
- [6] KME-601, "More Effective Power Production from Renewable Fuels Reference Power Plant (RPP) Project", Proposal (Updated 101105), dated 2010-11-05.
- [7] Stålenheim, A., Henderson, P., "Materials for higher steam temperatures (up to 600°C) in biomass and waste fired plant. A review of present knowledge", Värmeforsk report 1174, 2011.
- [8] Herstad Svärd, S., et al. "Measures for simultaneous reduction of alkali related operational problems", Phase 3, Värmeforsk report 1167, January 2011.
- [9] Pettersson, J., et al., 2009, "Evaluation of different fuel additives' ability to master corrosion and deposition on steam superheaters in a waste fired CFB-boiler", KME-411.
- [10] Personal communication with Fredrik Olsson, Outokumpu
- [11] Larsson E, Jonsson T, Svensson J-E, Liske J, Literature survey on water wall corrosion in biomass and waste fired boilers, Working document in Chalmers HTC project "Critical corrosion phenomena in biomass and waste fired boilers", Chalmers 2012
- [12] Herstad Svärd S, Åmand L-E, Bowalli J, Öhlin J, Steenari B-M, Pettersson J, Svensson J-E, Karlsson S, Larsson E, Johansson L-G, Davidsson K, Bäfver L, Almark M, Ramprogramme Åtgärder för samtidig minimering av alkalirelaterade driftproblem, Etapp 3, Värmeforsk report no 1167, January 2011
- [13] Backman R, Khalil R A, Todorovic D, Skreiberg Ø, Becidan M, Goile F, Skreiberg A, Sørum L, The effect of peat ash addition to demolition wood on the formation of alkali, lead and zinc compounds at staged combustion conditions, Fuel Process. Technol. (2011)

- [14] Stålenheim A, Henderson P, Materials for higher steam temperatures (up to 600°C) in biomass and waste fired plant A review of present knowledge, Värmeforsk report no 1174, February 2011
- [15] Barth E, Heinz H, Primary measures to reduce corrosion and fouling through regular addition of flue gas additives at the AVA GmbH in Augsburg, VGB PowerTech, 11/98, pp 50-52
- [16] http://www.ica-chemie.at
- [17] Henriksen N, Busse O, Bøgild Johnsen J, Forebyggelse af korrosion og belægningsdannelse i flisfyede kedler, Report PSO-projekt nr. 3142, Elsam A/S, October 2003
- [18] Elled A-L, Åmand L-E, Eskilsson D, Fate of zinc during combustion of demolition wood in a fluidised bed boiler, Energy & Fuels, vol 22 no 3, pp 1519–1526, 2008
- [19] Engvall K, Asksintringsproblem i konvektionspaketet tester med additiv i stor skala, Värmeforsk report no 742, August 2001
- [20] Hiltunen M, Barisic V, Zabetta C, Combustion of different types of biomasses in CFB boilers, Presented at 16th European biomass conference, Valencia, Spain, June 2-6, 2008
- [21] Tobiasen L, Skytte R, Storm Pedersen L, Thaaning Pedersen S, Lindber M A, Deposit characteristic after injection of additives to a Danish strawfired suspension boiler, Fuel Processing Technology 88, pp 1108-1117, 2007
- [22] Tran K-Q, Iisa K, Steenari B-M, Lindqvist O, A kinetic study of gaseous alkali capture by kaolin in the fixed bed reactor equipped with an alkali detector, Fuel 84, pp 169-175, 2005
- [23] Davidsson K, Eskilsson D, Gyllenhammar M, Herstad Svärd S, Kassman H, Steenari B-M, Åman L-E, Measures for simultaneous minimzation of alkali related operating problems, Report 997, Värmeforsk Service AB, Stockholm, Sweden, 2006
- [24] Gyllenhammar M, Herstad Svärd S, Davidsson K, Åmand L-E, Steenari B-M, Folkesson N, Pettersson J, Svensson J-E, Boss A, Johansson L, Kassman H, Measures for simultaneous minimization of alkali related operating problems, Phase 2, Report 1037, Värmeforsk Service AB, Stockholm, Sweden, 2007
- [25] Personal communication with Anna Jonasson, Händelöverket, E.ON Värme, Sweden
- [26] Pettersson J, Svensson J-E, Skog E, Johansson L-G, Folkeson N, Froitzheim J, Karlsson S, Larsson E, Israelsson, N, Enestam S, Tuiremo J, Jonasson A, Arnesson B, Andersson B-Å, Heikne B, Evaluation of different fuel additives ability to master corrosion and deposition on steam superheaters in a waste fired CFB-boiler, KME 411, Konsortiet Materialteknik för termiska Energiprocesser, 2010
- [27] Enestam S, Corrosivity of hot flue gases in the fluidised bed combustion of recovered waste wood, Academic dissertation, Report 11-04, Åbo Akademi, Process Chemistry Centre, Laboratory of Inorganic Chemistry, 2011
- [28] De Geyter S, Eriksson M, Öhman M, Nordin A, Boström D, Berg M, Skillnader i bäddagglomereringstendens mellan alternativa bäddmaterial

- och olika mineraler i natursand, Report 920, Värmeforsk Service AB, Stockholm Sweden, 2005
- [29] Wang L, Hustad J E, Skreiberg Ø, Skjevrak G, Grønli M, A critical review on additives to reduce ash related operation problems in biomass combustion applications, Energy Procedia, 2012
- [30] Öhman M., Eriksson G., Hedman H., Lidman M., and Boström D., Förbränningskarakterisering av osläckt tunnelugnsslagg för nyttjande som bränsleadditiv till mer problematiska pulverbränslen (åker/restbränslen) pilotstudie, 2008.
- [31] Henriksen N, Busse O, Bogild Johnsen J, Forebyggelse af corrosion og belaeggningsdannelse i flisfyrede kedler, report PSO-projekt nr. 3142, Eltra dok nr 181187, sag 3142, Elsam A/S, October 2003
- [32] Storesund J, Sund G, Pettersson R, Nordling M, Högberg J, Åtgärder mot eldstadskorrosion på panntuber, Report 1023, Värmeforsk Service AB, Stockholm Sweden, 2007
- [33] Storesund J, Elger R, Nordling M, Viklund P, Åtgärder mot eldstadskorrosion på panntuber - Etapp 2, Report 1168, Värmeforsk Service AB, Stockholm Sweden, 2011
- [34] Henderson P, Ifwer K, Stålenheim A, Montgomery M, Högberg J och Hjörnhede A, Kunskapsläget beträffande högtemperaturkorrosion i ångpannor för biobränsle och avfall ,Report 992, Värmeforsk Service AB, Stockholm Sweden, 2006
- [35] Kuo J-H, Lin C-L, Wey M-Y, Effect of particle agglomeration on heavy metals adsorption by AI- and Ca-based sorbents during fluidized bed incineration, Fuel Processing Technology 92, pp 2089–2098, 2011
- [36] Chen J-C, Wey M-Y, Lin Y-C, The Adsorption of Heavy Metals by Different Sorbents Under Various Incineration Conditions, Chemosphere, Vol. 37, No. 13, pp. 2617-2625, 1998
- [37] www.nordkalk.se
- [38] Kassman H, Bäfver L, Åmand L-E, The Importance of SO2 and SO3 for Sulphation of Gaseous KCI An Experimental Investigation in a Biomass Fired CFB Boiler, European Combustion Meeting (ECM 2009), 2009
- [39] Aho M, Silvennoinen J, Preventing chlorine deposition on heat transfer surfaces with aluminium-silicon rich biomass residue and additive, Fuel 83, pp 1299–1305, 2004
- [40] Fossenstrand I, Stabilisering och solidifiering av muddermassor i Gävle hamn, Examensarbete LTU, 2009:168 CIV
- [41] Aho M., Vainikka P., Taipale R., and Yrjas P., Effective new chemicals to prevent corrosion due to chlorine in power plant superheaters. Fuel 87, 647-654, 2008.
- [42] Baxter, L.L, Ash deposition during biomass and coal combustion: a mechanistic approach. Biomass and Bioenergy, 4 (2), 85-102, 1993.
- [43] Benson, S.A. and Holm, P.L., Comparison of inorganic constituents in three low rank coals. Industrial & Engineering Chemistry Product Research and Development, 24, 145- 149, 1985.

- [44] Handbook of Combustion, Vol. 4: Solid fuels, Chapter 14: Ash forming matter and related problems, 493-531, Wiley-VCH, Editors: Lackner M, Winter F., and Agarwal A.K., ISBN: 978-3-527-32449-1, 2010.
- [45] Salmenoja, K., Field and laboratory studies on chlorine-induced superheater corrosion on boilers fired wirth biofuels, Academic dissertation, Åbo Akademi University, Turku, Finland, ISBN: 952-12-0619-5, 2000.
- [46] Yrjas, P., Aho, M., Zevenhoven, M., Taipale, R., Silvennoinen, J., and Hupa, M., Co-firing of sewage sludge with bark in a bench-scale bubbling fluidized bed a study of deposits and emissions. Proceedings of 20th International Conference on Fluidized Bed Combustion, Xian, China, 2009.
- [47] Yrjas, P., Skrifvars, B.-J., Hupa, M., Roppo, J., Nylund, M., Vainikka, P., Chlorine in deposits during co-firing of biomass, peat, and coal in a full-scale CFBC boiler, Proceedings of 18th International Conference on Fluidized Bed Combustion, Toronto, Canada, 2005.
- [48] Zevenhoven, M., Ash-forming matter in biomass fuels. Academic dissertation, Åbo akademi University, Turku, Finland, ISBN: 952-12-0813-9, 2001.
- [49] Glazer, M., Alkali metals in combustion of biomass with coal, Academic dissertation, 2007
- [50] Bale, C.W., et al., FactSage thermochemical software and databases -- recent developments. Calphad, 2009. 33(2): p. 295-311.
- [51] Lindberg, D., R. Backman, and P. Chartrand, Thermodynamic evaluation and optimization of the (Na2SO4+K2SO4+Na2S2O7+K2S2O7) system. Journal of Chemical Thermodynamics, 2006. 38(12): p. 1568-1583.
- [52] Lindberg, D., R. Backman, and P. Chartrand, Thermodynamic evaluation and optimization of the (Na2CO3+Na2SO4+Na2S+K2CO3+K2SO4+K2S) system. Journal of Chemical Thermodynamics, 2007. 39(6): p. 942-960.
- [53] Lindberg, D., R. Backman, and P. Chartrand, Thermodynamic evaluation and optimization of the (NaCl+Na2SO4+Na2CO3+KCl+K2SO4+K2CO3) system. Journal of Chemical Thermodynamics, 2007. 39(7): p. 1001-1021.
- [54] Lindberg, D., et al., Thermodynamic evaluation and optimization of the (Na+K+S) system. Journal of Chemical Thermodynamics, 2006. 38(7): p. 900-915.
- [55] Lindberg, D. and P. Chartrand, Thermodynamic evaluation and optimization of the (Ca + C + O + S) system. Journal of Chemical Thermodynamics, 2009. 41(10): p. 1111-1124.
- [56] Robelin, C. and P. Chartrand, Thermodynamic evaluation and optimization of the (NaCl + KCl + MgCl2 + CaCl2 + ZnCl2) system. Journal of Chemical Thermodynamics, 2011. 43(3): p. 377-391.
- [57] Lindberg, D., et al., Towards a comprehensive thermodynamic database for ash-forming elements in biomass and waste combustion Current situation and future developments. Fuel Processing Technology, 2013. 105(0): p. 129-141.
- [58] Project meeting knowledge exchange Abo Akademi Vattenfall April 2013

- [59] J. Helble, The behaviour of coal minerals under combustion conditions. Atlanta Coal Cnference, 1991
- [60] M. Aho, "Reduction of superheater corrosion by co-firing risky biomass with sewage sludge" Fuel 89 (2010)
- [61] Pettersson, "Leaching of ashes from co-combustion of sewage sludge and wood", halmers, 2008
- [62] L. Wang, "A critical review on additives to reduce ash related operation problems in biomass combustion applications" Energy Procedia 20 (2012)
- [63] H. Wee "The effect of combustion conditions on mineral matter transformation and ash deposition in a utility boiler fired with a sub-bituminous coal", Proceedings of the Combustion Institute 30 (2005) 2981–2989
- [64] H. Yao "Using sorbents to control heavy metals and particulate matter emission during solid fuel combustion" Particulogy 7 (2009) 477–482
- [65] X. Wei "Behaviour of gaseous chlorine and alkali metals during biomass thermal utilization, Fuel 84 (2005) 841–848
- [66] E. Ferrer, "Fluidized bed combustion of refuse-derived fuel in presence of protective coal ash", Fuel Processing Technology, Volume 87, Issue 1, December 2005, Pages 33-44
- [67] Obernberger "Novel Characterisation methods for biomass fuels and their application case study straw", Fuel Quality Impacts Conference, 2012
- [68] Tarja Talonen, Chemical Equilibria of Heavy Metals in Waste Incineration: Comparison of Thermodynamic Databases, Abo Akademi, report 08-02, 2008
- [69] Davidsson, K. O., Engvall, K., Hagstrom, M., Korsgren, J. G., Lonn, B., and Pettersson, J. B. C. (2002a). A surface ionization instrument for online measurements of alkali metal components in combustion: Instrument descriptionand applications. Energy&Fuels, 16:1369–1377
- [70] Jensen, P., Frandsen, F., Dam-Johansen, K., and Sander, B. (2000b). Experimental investigation of the transformation and release to gas phase of potassium and chlorine during straw pyrolysis. Energy & Fuels, 14:1280–1285.
- [71] Lindberg, D. Backmann, R., Chrtrand, P., Hupa, M. "Towards a comprehensive thermodynamic databse for ash-forming elements in biomass and waste combustion Current situation and future developments" Fuel Processing Technology 105 (2013) 129-141
- [72] https://www.outokumpu.com/SiteCollectionDocuments/253MA % 20Hig h_Temperatu_Resistant_Tubes.pdf
- [73] http://www.kanthal.com

Appendices

- A. Determination of amounts of additives to be used in laboratory test
- B. HSC Modelling results for KME 512 Project, Thermodynamical equilibrium calculations performed by Vattenfall
- C. Fuel additives to reduce corrosion at elevated steam data in biomass boilers Laboratory experiments, Full report of results from laboratory testing performed by SP



SVENSKA ELFÖRETAGENS FORSKNINGS- OCH UTVECKLINGS - ELFORSK - AB

Elforsk AB, 101 53 Stockholm. Besöksadress: Olof Palmes Gata 31 Telefon: 08-677 25 30, Telefax: 08-677 25 35 www.elforsk.se